

Exploring the signalling mechanism of excitotoxic neuronal injury by molecular and quantitative proteomic approaches

Md Ashfaqul Hoque

Submitted in total fulfilment of the requirements of the degree of
Doctor of Philosophy

April 2016

Department of Biochemistry and Molecular Biology
Bio21 Molecular Science and Biotechnology Institute
& Cell Signalling Research Laboratories
The University of Melbourne

Abstract

Excitotoxicity caused by over-stimulation of the ionotropic glutamate receptors is a key neuronal cell death process underpinning brain damage in acute and chronic neurological disorders such as ischaemic stroke, traumatic brain injury, and neurodegenerative diseases. Exactly how neurons die in excitotoxicity still remains unclear and is an important area of research in the field of neuroscience. In my PhD study, I employed the targeted biochemical and molecular approaches and the unbiased mass spectrometry-based systems biology approaches to address this outstanding question.

The protein tyrosine kinase Src, which co-localises with and phosphorylates the ionotropic glutamate receptor, is implicated in regulation of neuronal survival in excitotoxicity. Previous study from our laboratory demonstrated that upon excitotoxic stimulation Src is cleaved by the Ca^{2+} -dependent cysteine protease calpain in the unique domain to form a ~52-kDa truncated Src fragment (Src Δ N). Lentiviral expression of this recombinant Src Δ N in cultured neurons revealed that Src Δ N is neurotoxic and its expression inhibits the Akt signalling pathway. A cell-membrane permeable fusion peptide (Tat-Src) derived from the unique domain of Src was found to prevent Src cleavage by calpain and also protects against excitotoxic neuronal death (Hossain et al., 2013). These findings indicate that calpain cleavage of Src is a key event directing neuronal death in excitotoxicity. As a logical continuation, I employed the targeted biochemical and molecular approaches to decipher the mechanism by which Src governs neuronal survival. Treatment with specific Src kinase inhibitor (A419259) and knockdown of *Src* using shRNA significantly reduced neuronal viability and caused inactivation of the pro-survival protein kinase Erk1/2, indicating that intact Src is indispensable for neuronal survival and it exerts its pro-survival function in part by activating Erk1/2. Based upon these results we conclude that intact Src performs neurotrophic function under normal physiological conditions and it is converted by calpain cleavage into a potent cell death executor in excitotoxicity. Exactly how Src Δ N exerts its neurotoxic action in excitotoxicity is not fully clear.

Next, I sought to define the neurotoxic mechanism of Src Δ N and understand how Src Δ N interplays with other neuronal signalling proteins to direct neuronal death in excitotoxicity. To this end, I employed the unbiased quantitative proteomics-based systems biology approaches to identify the neuronal proteins of which the abundance and/or phosphorylation

are significantly perturbed in excitotoxicity. Using the stable-isotope dimethyl labelling-based quantitative proteomic method, I was able to identify at least 80 neuronal proteins with significantly perturbed expression in cultured primary cortical neurons after 15 min or 4 h of glutamate-induced excitotoxicity. Most of these proteins exhibited decreased expression in excitotoxicity. Signalling network analysis using the Ingenuity Pathway Analysis (IPA) software to ascertain the potential functions of the identified neuronal proteins revealed the following canonical pathways as the top perturbed signalling pathways in excitotoxicity: (i) 14-3-3-mediated signalling, (ii) remodelling of epithelial adherens junctions, (iii) cell cycle including G2/M DNA damage checkpoint regulation, (iv) Myc-mediated apoptosis signalling, (v) PI3K/Akt signalling and (vi) Erk/MAPK signalling pathways. Additionally, I performed quantitative phosphoproteomic analysis and identified 59 neuronal proteins showing significant changes in phosphorylation in either one or more phosphorylation sites upon over-stimulation by glutamate for 15 min and 4 h. Most of the identified phosphoproteins showed decreased phosphorylation, implying that inactivation of the upstream kinases or activation of the specific phosphatases targeting those phosphorylation sites as the causes for the decreased phosphorylation. In agreement with the pathway and network analysis, Western blot analysis also confirmed that phosphorylation of Erk1/2 and Akt are perturbed in excitotoxicity. My results collectively indicate that inactivation of a number of pro-survival signalling pathways and activation of a series of pro-death signalling pathways cooperate to cause neuronal demise in excitotoxicity.

Specific types of the N-methyl-D-aspartate (NMDA) receptors, α -amino-3-hydroxy-5-methyl-4-isoxazolepropionic acid (AMPA) receptors and Kainate receptors are the ionotropic glutamate receptors from which the cytotoxic signals directing excitotoxic neuronal death originate. Among them, the extrasynaptic NMDA receptor is the major neurotoxic receptor directing excitotoxic neuronal death. Upon over-stimulation by glutamate, the extrasynaptic NMDA receptor allows massive influx of Ca^{2+} into the neuronal cytosol, where the excess Ca^{2+} over-activates a number of calcium-dependent enzymes. The calcium-dependent proteases calpains are among these over-activated enzymes. The over-activated calpains cleave a number of neuronal proteins such as Src to direct neuronal death. Since Ifenprodil, an antagonist of the extrasynaptic NMDA receptor, calpeptin, a cell-permeable pan-calpain inhibitor and Tat-Src have been shown to protect neurons against excitotoxic cell death, I therefore used them to further define the signalling

networks underpinning excitotoxic neuronal death by quantitative global proteomic and phosphoproteomic approaches. Specifically, I identified specific neuronal proteins of which perturbation of expression and/or phosphorylation induced by glutamate treatment are offset by co-treatment with Ifenprodil, calpeptin and Tat-Src. Some of these neuronal proteins are likely downstream effectors mediating the neurotoxic signals of the extrasynaptic NMDA receptors, over-activated calpains and Src Δ N. Several identified neuronal proteins were selected for validation of their perturbed expression and/or phosphorylation in excitotoxicity by Western blot and label-free full-scan precursor ions (MS1) quantitation analysis using isotopically labelled synthetic peptide standards.

In summary, my findings shed light on the molecular mechanism of excitotoxic neuronal death. The neuronal proteins involved in excitotoxic neuronal death identified in my PhD project are potential targets for the development of neuroprotectants to reduce excitotoxic brain damage in neurological disorders.

Declaration

This is to certify that:

- i. the thesis comprises only my original work towards PhD except where indicated in the *publications*,
- ii. due acknowledgement has been made in the text to all other materials used, and
- iii. the thesis is less than 100,000 words in length, exclusive of tables, figures and references.

Md Ashfaqul Hoque

April, 2016

Contents

Abstract.....	ii
Declaration.....	v
Contents	vi
List of figures.....	xiii
List of tables.....	xvi
Publications.....	xvii
Acknowledgement	xviii
Abbreviations.....	xix
Thesis outline.....	xxvii
Chapter 1.....	1
Declaration and Acknowledgements	1
Chapter 1: Excitotoxicity-the early key event for neuronal loss in acute ischaemic stroke.....	2
1.1 Overview of stroke.....	2
1.1.1 Acute ischaemic stroke	2
1.2 Cascade of cellular events leads to ischaemic brain injury.....	3
1.2.1 Excitotoxicity-a major cause of neuronal loss in ischemic stroke and chronic neurodegenerative diseases such as Alzheimer’s disease	5
1.2.2 Caspase-independent cell death underpins neuronal demise in excitotoxicity	7
1.2.3 Excessive intracellular Ca ²⁺ influx leads to excitotoxic brain injury	8
1.3 Signalling mechanisms of excitotoxic neuronal death.....	9
1.3.1 Cell surface receptors and ion channels.....	9
1.3.2 Antagonising roles of synaptic and extrasynaptic NMDA receptors.....	14
1.3.3 Neuroprotective signalling pathways of the synaptic NMDA receptors	15
1.3.3.1 Stimulation of pro-survival genes.....	15
1.3.3.2 Suppression of pro-death genes	16
1.3.3.3 Antioxidant activity	17
1.3.4 Pro-death signals from extrasynaptic NMDA receptors.....	19
1.3.5 Calpains: major executors of neuronal death.....	21

1.3.6 Calpain substrates participating in neuronal death.....	22
1.3.6.1 Metabotropic glutamate receptor α -1 (mGluR α -1).....	23
1.3.6.2 Na ⁺ /Ca ²⁺ exchanger 3 (NCX3), plasma membrane calcium ATPase (PMCA) and Transient receptor potential cation channel C6 (TRPC6).....	26
1.3.6.3 Kidins220/ARMS.....	26
1.3.6.4 Calmodulin-dependent protein kinase and phosphatase	27
1.3.6.5 Protein tyrosine kinase Src.....	27
1.3.6.6 Pro-survival and pro-apoptotic proteins.....	28
1.3.6.7 Apoptosis inducing factor (AIF).....	28
1.3.6.8 Collapsin response mediator protein 3 (CRMP3).....	29
1.3.6.9 Striatal-enriched protein tyrosine phosphatase (STEP).....	29
1.3.7 JNK3 and p38 are key mediators of neuronal demise.....	30
1.3.8 Cyclin-dependent protein kinase 5 (Cdk5)	32
1.3.9 Epigenetic modifications in neuronal death.....	32
1.3.9.1 REST, Sin3A and CoREST chromatin modifying complex.....	33
1.3.9.2 REST gene and miRNA targets	36
1.4 Pathologically activated cellular events as potential neuroprotective targets.....	37
1.4.1 Antagonists of the over-stimulated extrasynaptic NMDA receptors as neuroprotectants	38
1.4.2 Blockade of calpain cleavage of pathologically significant protein substrates..	39
1.4.3 Blockade of protein-protein interactions governing neuronal death.....	41
1.4.4 Blockade of dysregulated S-nitrosylation of specific neurotoxic proteins	42
1.4.5 Targeting chromatin-modifying epigenetic enzymes as a neuroprotective therapy.....	42
1.5 Lessons learned from the success of developing memantine and Tat-NR2B9c as clinically effective neuroprotectants	46
1.6 Mass spectrometry-based quantitative proteomic approach to investigate the mechanism of neuronal death in excitotoxicity	47
1.6.1 Quantitative phosphoproteomic approach.....	48
1.6.2 Selected or multiple reactions monitoring (SRM/MRM)	50
1.7 Aims of the study	50
Chapter 2	52
Declaration and Acknowledgements.....	52

Chapter 2: Material and Methods	53
2.1 Materials	53
2.2 Methods.....	54
2.2.1 Primary cortical neurons culture.....	54
2.2.2 Excitotoxicity model and treatment of cultured primary cortical neurons under various experimental conditions	55
2.2.3 MTT cell viability assay	55
2.2.4 Lysis of the cells	56
2.2.5 Acetone precipitation of neuronal lysates.....	56
2.2.6 In-solution trypsin digestion of proteins in neuronal lysates	56
2.2.7 Solid phase extraction clean-up of tryptic peptides	57
2.2.8 Stable isotope dimethyl labelling of tryptic peptides.....	57
2.2.9 TiO ₂ phosphopeptides enrichment.....	58
2.2.10 LC-MS/MS analysis.....	58
2.2.11 Processing and analysis of the proteomic data.....	59
2.2.12 Pathway and network analysis using IPA and FunRich	60
2.2.13 Western blotting.....	60
2.2.14 Expression and purification of recombinant nSrcH ₆ protein	61
2.2.14.1 Construction of expression vector for recombinant nSrcH ₆ production ...	61
2.2.14.2 Purification of recombinant nSrcH ₆ protein expressed in Sf9 insect cells	62
2.2.15 <i>In vitro</i> digestion of recombinant nSrcH ₆ with calpain 1.....	62
2.2.16 In-gel digestion of protein bands	63
2.2.17 Production of lentivirus containing the genes of interest.....	63
2.2.17.1 Generation of the plasmids for the lentivirus production	63
2.2.17.2 Culturing HEK293FT cells for lentivirus production.....	64
2.2.17.3 Lentivirus generation	64
2.2.17.4 Production of lentivirus of shRNA against c-Src	65
2.2.17.5 Transduction of primary cortical neurons with lentivirus.....	65
2.2.18 Immunofluorescence.....	66
2.2.19 Synthesis of isotopically labelled synthetic phosphopeptides	66
Chapter 3.....	68
Declaration and Acknowledgements	68

Chapter 3: Dual role of Src protein tyrosine kinase governing neuronal survival	69
3.1 Introduction.....	69
3.2 Methods.....	70
3.2.1 Primary cortical neurons culture and MTT cell viability assay	70
3.2.2 Assay of LDH released from damaged neurons	70
3.2.3 Monitoring neuronal survival by Calcein-AM and Ethidium homodimer-1 staining	71
3.2.4 Expression of recombinant Src-GFP, Src Δ N-GFP and GFP in primary cortical neurons	71
3.2.5 Knockdown of endogenous Src in primary cortical neurons	71
3.2.6 Immunofluorescence	72
3.2.7 Data analysis	72
3.3 Results	72
3.3.1 Expression levels of Src and NMDA receptor subunits undergo time-dependent increase in cultured primary cortical neurons	72
3.3.2 The signalling pathways governing cell death and aberrant regulation of Src are intact in cortical neurons at DIV7	76
3.3.3 Truncated fragment of Src kinase generated by calpain is neurotoxic	78
3.3.4 Treatment with SFK inhibitors induce cell death of primary cortical neurons ..	81
3.3.5 Suppression of Src expression induces cell death in cultured primary cortical neurons	83
3.3.6 Inhibition of SFK activity or knockdown of Src expression leads to decrease in Erk1/2 phosphorylation	86
3.4 Discussion	89
Chapter 4	92
Declaration and acknowledgement	92
Chapter 4: Quantitative global proteomic approach to understand the mechanism of glutamate-induced excitotoxicity	93
4.1 Introduction.....	93
4.2 Methods.....	95
4.2.1 Primary cortical neurons culture and cell viability assay.....	95
4.2.2 Experimental design.....	95
4.2.3 Proteomic data analysis.....	96
4.3 Results	100

4.3.1 The <i>in vitro</i> cell model and selection of the time points for proteomics analysis	100
4.3.2 Data processing for protein quantification and the criteria for selection of peptides exhibiting differences in abundance	102
4.3.3 Over stimulation of glutamate receptors induced changes in expression levels of over 680 neuronal proteins	103
4.3.4 Identities of the neuronal protein molecules of which the abundance were significantly perturbed by glutamate overstimulation	106
4.3.5 Data validation	110
4.3.6 Bioinformatics analysis of the differentially expressed neuronal proteins revealed cellular processes that are dysregulated in excitotoxicity	113
4.3.7 Pathway and network analysis using IPA	116
4.4 Discussion	119
Chapter 5	122
Declaration and acknowledgement	122
Chapter 5: Phosphoproteomic analysis to identify the key signalling pathways of glutamate-induced excitotoxicity in cultured primary neurons	123
5.1 Introduction	123
5.2 Methods	124
5.2.1 Experimental design	124
5.2.2 TiO ₂ phosphopeptides enrichment	125
5.2.3 Phosphoproteomic data analysis	125
5.2.4 PTEN immunofluorescence	126
5.3 Results	129
5.3.1 Data processing to identify phosphoproteins with changes in phosphorylation in glutamate-induced excitotoxicity	129
5.3.2 More than 70 significantly dysregulated phosphopeptides were identified in glutamate-induced excitotoxicity in cultured primary neurons	130
5.3.3 Gene ontology analysis of the altered phosphoproteins in excitotoxicity	136
5.3.4 Pathway and network analysis of the identified phosphoprotein molecules using IPA	139
5.3.5 Data validation by Western blot analysis	143
5.3.6 Akt and Erk1/2 are two important pro-survival pathways dysregulated in glutamate-induced excitotoxicity	145

5.3.7 Increased nuclear translocation of PTEN following glutamate-induced excitotoxicity.....	149
5.4 Discussion.....	151
Chapter 6.....	156
Declaration and acknowledgement.....	156
Chapter 6: Quantitative proteomic analysis to define how the neurotoxic signalling events originating from the NMDAR interplay to direct neuronal death.....	157
6.1 Introduction.....	157
6.2 Methods.....	160
6.2.1 Expression and purification of recombinant full-length Src protein and <i>in vitro</i> calpain digestion of recombinant nSrcH ₆ protein.....	160
6.2.2 Strategies for the calpain cleavage site determination.....	160
6.2.2.1 Dimethyl labelling of the nascent N-terminus of truncated nSrcH ₆ generated by calpain cleavage of nSrcH ₆ <i>in vitro</i>	160
6.2.2.2 Label-free MS1 quantitation of the selected peptides in tryptic digest of full-length and truncated nSrcH ₆	162
6.2.3 Primary cortical neurons culture and MTT cell viability assay.....	162
6.2.4 Experimental design for the antagonist/inhibitor study.....	162
6.2.5 Proteomic data analysis.....	163
6.2.6 Label-free quantitation using isotopically labelled synthetic phosphopeptide standards.....	163
6.2.6.1 Phosphoproteomic data analysis following label-free quantitation.....	164
6.3 Results.....	167
6.3.1 Identification of the calpain cleavage site in Src unique domain.....	167
6.3.1.1 Generation of recombinant full-length Src protein.....	167
6.3.1.2 Dimethyl labelling approach to identify N-terminus of the truncated Src fragment.....	169
6.3.1.3 Label-free time course MS1 quantitation of selected peptides derived from target regions of nSrcH ₆ and its truncated fragment.....	169
6.3.2 Selective inhibition of the extrasynaptic GluN2B receptors, calpain over-activation, or neurotoxic SrcΔN generation can protect neurons against excitotoxic cell death.....	173
6.3.3 Identification of neuronal proteins showing significant changes in abundance due to the over-activation of GluN2B receptors, calpains or SrcΔN generation.....	174

6.3.4 Identification of neuronal phosphoproteins showing significant changes in phosphorylation due to over-stimulation of GluN2B receptors, over-activation of calpains or Src Δ N generation.....	178
6.3.5 Western blot analysis to confirm that enhanced dephosphorylation of Ser-21 and Ser-9 of Gsk3 α and Gsk3 β , respectively occurs as a result of over-stimulation of the GluN2B-containing NMDA receptors	185
6.3.6 Label-free quantitation to confirm changes in phosphorylation of Mef2c, Mff, Mlf2 and Stmn1 induced by overstimulation of the GluN2B-containing extrasynaptic NMDA receptors.....	187
6.4 Discussion	192
Chapter 7: Summary and future directions	196
7.1 Summary	196
7.2 Future directions	198
7.2.1 Investigation of the mechanism by which calpain-mediated cleavage of c-Src causes neuronal loss in neurodegenerative diseases	198
7.2.2 Identification of the direct protein substrates and downstream targets of Src Δ N in neurons undergoing excitotoxic cell death	199
7.2.3 Tat-Src as a potent neuroprotectant in animal models of stroke.....	200
7.2.4 Co-treatment of Tat-Src and Tat-NR2B9c to reduce neuronal damage in acute ischaemic stroke.....	201
7.2.5 Quantitative protease proteomic approach to identify calpain or other protease substrates in neurons undergoing excitotoxic cell death.....	201
7.3 Concluding remarks	204
References.....	205
Appendix I	235

List of figures

Figure 1.1 Temporal events leading to brain damage following ischaemic stroke.....	5
Figure 1.2 Calpains, nNOS and NOX2 are key intracellular neurotoxic enzymes activated at the initial phase of excitotoxic neuronal death.....	7
Figure 1.3 Selected neurotoxic signalling pathways originating from the over-stimulated NMDA receptors.....	13
Figure 1.4 Opposing roles of synaptic and extrasynaptic NMDA receptors for governing neuronal survival.....	18
Figure 1.5 Model for REST-mediated transcriptional repression.....	35
Figure 1.6 Neuroprotective strategies to reduce neuronal loss in excitotoxicity.....	45
Figure 2.1 Search parameters used for proteomic data analysis.....	60
Figure 3.1 Expression levels of Src and NMDA receptor subunits in cultured primary cortical neurons from Day 1 to Day 7 in culture.....	75
Figure 3.2 Effects of over-stimulation of glutamate receptors on neuronal viability and Src integrity.....	77
Figure 3.3 Effects of expression of recombinant truncated Src (Src Δ N-GFP) in primary cortical neurons.....	80
Figure 3.4 Effects of treatment of SFK inhibitors on neuronal viability.....	81
Figure 3.5 Effects of treatment of the selective SFK inhibitor A419259 on neuronal viability.....	82
Figure 3.6 Knockdown of Src kinase with shRNAs decreases neuronal viability.....	85
Figure 3.7 Effect of transduction of cultured neurons with the Src shRNA at DIV1 to DIV6 on cell viability.....	86
Figure 3.8 Effects of SFK inhibitors and Src knockdown on the phosphorylation status of neuronal Erk1/2 and Akt.....	88
Figure 3.9 Src is both a promoter of neuronal survival and an executor of neuronal death.....	91
Figure 4.1 Workflow for exploring global proteome changes in glutamate excitotoxicity.....	98
Figure 4.2 Workflow for proteomic data search and analysis.....	99
Figure 4.3 Glutamate induced excitotoxic neuronal death in cultured primary cortical neurons.....	101
Figure 4.4 Venn diagram showing the numbers of the identified protein molecules in cultured cortical neurons treated with glutamate for 15 min and 4h.....	105

Figure 4.5 Volcano plots and histograms showing the fold change distributions of the identified protein molecules in neurons 15 min and 4 h after glutamate treatment.....	109
Figure 4.6 MS2 spectra and the extracted ion chromatogram (XIC) spectra used for MS1 quantification of 14-3-3 beta/alpha unique peptide and immunoblot analysis.	112
Figure 4.7 Gene Ontology (GO) analyses of the differentially expressed protein molecules in neurons in excitotoxicity.....	115
Figure 4.8 Top canonical pathways and interaction network of the identified significantly perturbed protein molecules in glutamate-induced excitotoxicity.....	118
Figure 5.1 TiO2 phosphopeptides enrichment.....	124
Figure 5.2 Workflow for exploring phosphoproteome changes in glutamate excitotoxicity.	128
Figure 5.3 Gene Ontology (GO) analyses of the differentially regulated phosphoprotein molecules in glutamate-induced excitotoxicity.	138
Figure 5.4 Interaction network analysis of the identified altered-phosphoproteins in glutamate-induced excitotoxicity.....	142
Figure 5.5	144
Figure 5.5 XIC based MS1 quantification and MS2 spectra used for the quantification of Erk2 phosphopeptide and immunoblot analysis.	145
Figure 5.6 Dysregulation of the Akt and Erk1/2 pro-survival pathways in glutamate-induced excitotoxicity in cultured primary neurons.	148
Figure 5.7 Nuclear localisation of PTEN following glutamate-induced excitotoxicity in cultured primary cortical neurons.	150
Figure 5.8 Postulated model for PTEN nuclear translocation and neuronal death in excitotoxicity.....	155
Figure 6.1 Selective inhibition of neurotoxic signals can rescue glutamate-induced excitotoxic neuronal death.	159
Figure 6.2 Workflow for calpain cleavage site determination.....	161
Figure 6.3 Workflow to define the neurotoxic signalling networks downstream of the extrasynaptic NMDAR by quantitative proteomic and phosphoproteomic analysis.....	166
Figure 6.4 Expression of recombinant full-length neuronal Src (nSrcH6) protein.....	168
Figure 6.5 Determination of calpain cleavage site in Src unique domain.	172
Figure 6.6 Ifenprodil, calpeptin and Tat-Src can reduce glutamate-induced excitotoxic neuronal death.....	173
Figure 6.7 Identification of neuronal proteins that function downstream of the GluN2B-containing extrasynaptic NMDA receptors in glutamate-induced excitotoxicity.....	177

Figure 6.8 Identification of neuronal phosphoproteins that function downstream of the GluN2B-containing extrasynaptic NMDA receptors in glutamate-induced excitotoxicity.	184
Figure 6.9 Blocking of the extrasynaptic NMDA receptor over-stimulation reduces dephosphorylation of Gsk3 α	186
Figure 6.10 Label-free quantitation using synthetic phosphopeptides to confirm changes in phosphorylation of Mef2c, Mff, Mlf2 and Stmn1 in glutamate-induced excitotoxicity... ..	189
Figure 6.11 Label-free quantitation using synthetic phosphopeptide confirms change in phosphorylation of Ser-237 of Mlf2 in glutamate-induced excitotoxicity.....	191
Figure 7.1 Neurotoxic signalling pathways leading to neuronal demise in glutamate-induced excitotoxicity.	197
Figure 7.2 Amyloid beta oligomer (A β) treatment of cultured neurons induces calpain cleavage of Src.	198
Figure 7.3 A general workflow to identify downstream substrates of Src Δ N.	200
Figure 7.4 A general workflow for protease proteomics.	203

List of tables

Table 1.1 Some of the calpain substrates that participate in regulation of neuronal survival.	24
Table 1.2 Protein-protein interactions governing some of the key pathologically activated cellular events directing excitotoxic neuronal death.....	44
Table 2.1 List of synthetic phosphopeptides.....	67
Table 4.1 Mass spectrometric data for all biological replicates following glutamate treatment of cultured primary cortical neurons for 15 min and 4 h.	104
Table 4.2 List of differentially expressed proteins in glutamate-induced excitotoxicity.	107
Table 4.3 Top upstream regulators of the potentially neurotoxic signalling pathways identified by IPA.....	116
Table 5.1 A selected list of phosphopeptides showing significant changes in phosphorylation following glutamate-induced excitotoxicity.	132
Table 5.2 Significantly dysregulatyed phosphoproteins-derived top canonical pathways identified by IPA.....	140
Table 5.3 Top upstream regulators of the phosphoproteins-derived potentially neurotoxic signalling pathways indentified by IPA.....	140
Table 6.1 A selected list of neuronal protein molecules of which the changes in abundance induced by glutamate treatment are fully or partially offset by co-treatment with Ifenprodil, calpeptin or Tat-Src.....	176
Table 6.2 A selected list of phosphopeptides of which the changes in phosphorylation induced by glutamate treatment are fully or partially offset by co-treatment with Ifenprodil, calpeptin or Tat-Src.....	180

Publications

- ✚ The literature review (Chapter 1) has been published as a review article in *Pharmacology and Therapeutics*. I contributed to 75% of the writings for this manuscript.

Hoque A, Hossain MI, Ameen SS, Ang CS, Williamson N, Ng DC, Chueh AC, Roulston C and Cheng HC (2016) A beacon of hope in stroke therapy-Blockade of pathologically activated cellular events in excitotoxic neuronal death as potential neuroprotective strategies. *Pharmacology and Therapeutics*, 160, 159–179.

- ✚ Study findings presented in Chapter 3 have been published in *Brain Research*. I am one of the equal contributing first authors of the published manuscript. I contributed to 50% of the data presented in this manuscript.

Hossain, M.I., **Hoque, A.***, Lessene, G., Kamaruddin, A., Chu, P.W., Ng, I.H., Irtegun, S., Ng, D. C., Bogoyevitch, M. A., Burgess, A.W., Hill, A.F. & Cheng, H.C. 2015. Dual role of Src kinase in governing neuronal survival. *Brain Research*, 1594, 1-14. (**Equal contribution*)

- ✚ Two more manuscripts are under preparation with data presented in Chapter 4, 5 and 6.

Acknowledgement

First of all, I like to thank Allah (SWT) for His greatness and for giving me the strength and courage to complete this thesis and my PhD project.

I am deeply grateful to my principal supervisor Assoc. Prof. Heung-Chin Cheng for giving me this excellent opportunity to join his lab, where I have learnt and explored a lot over the last four years. It was my huge pleasure to receive his continuous guidance, encouragement and support throughout my PhD career.

I would like to express my earnest gratitude to my co-supervisors Dr. Dominic Ng and Dr. Ching-Seng Ang for their continuous support and appreciation. Special thanks to Dr. Ching-Seng for teaching me all the basics of mass spectrometry and the use of proteomic software applications.

I am grateful to my colleague Dr. M Iqbal Hossain for teaching me how to perform primary neurons culture, lentivirus generation and most of the basic Biochemistry techniques. My special thanks to my respectful senior colleague Mrs. Daisy Lio for her continuous encouragement and logistic support in the lab.

I am thankful to my PhD committee members Professor Andrew Francis Hill, Dr. Nick Williamson, Dr. Carli Roulston and Assoc. Prof. Marie Bogoyevitch for their continuous support, encouragement and valuable insights in my PhD project.

I am grateful to all the present and past (since 2012) Cheng lab members for making my journey so smooth and life easier in the lab and their support and appreciation. Also, thanks to all my friends home and abroad for their continuous encouragements and appreciations.

I also like to express my gratitude for all the staff members of the Department of Biochemistry and Molecular Biology for their continuous help in last four years.

Finally, it is my parents and my wife, without their inspiration and continuous support it wouldn't have been possible for me to complete the journey. Don't know how to thank my wife who has sacrificed her own career and supported me all the way in this journey.

Thank you all, and without you guys nothing would have been possible. I am really lucky to have you all beside me.

Abbreviations

4930544G11Rik	Transforming protein RhoA
5031439G07Rik	Protein 5031439G07Rik
Abat	4-aminobutyrate aminotransferase, mitochondrial
Abcd3	ATP-binding cassette sub-family D member 3
Acat3	Acetyl-Coenzyme A acetyltransferase 3
Actc1	Actin, alpha cardiac muscle 1
Ahsa1	Activator of 90 kDa heat shock protein ATPase homolog 1
AID	Activity-regulated inhibitors of death gene
AIF	Apoptosis-inducing factor
Akt	Protein Kinase B
Akt1s1	Proline-rich AKT1 substrate 1
ALS	Amyotrophic lateral sclerosis
AMPA	α -amino-3-hydroxy-5-methyl-4-isoxazolepropionic acid
Ank2	Ankyrin 2, neuronal
Anp32a	Acidic leucine-rich nuclear phosphoprotein 32 family member A
APAF1	Apoptotic protease activating factor 1
Apba1	Amyloid beta (A4) precursor protein-binding, family A, member 1
Arf3	ADP-ribosylation factor 3
Arf4	ADP-ribosylation factor 4
Arf6	ADP-ribosylation factor 6
Arhgap35	Rho GTPase activating protein 35
Arhgap39	Rho GTPase activating protein 39
Arl3	ADP-ribosylation factor-like protein 3
Arpc3	Actin-related protein 2/3 complex subunit 3
ASICs	Acid-sensing ion channels
Atat1	Alpha-tubulin N-acetyltransferase 1
Atf3	Activating transcription factor 3
ATP	Adenosine tri phosphate
Atp5a1	ATP synthase subunit alpha, mitochondrial
BAD	Bcl-2-associated death promoter
Bax	Bcl-2-associated X-protein
Bcl-2	B-cell lymphoma 2
Bcl-XL	B-cell lymphoma-extra large
BDNF	Brain-derived neurotrophic factor
BH3	Bcl-2 homology domain 3
Bim	Bcl-2-interacting mediator of cell death
BRAG 2	Brefeldin A-resistant Arf-GEF 2
BRDs	Bromodomain proteins
BRG1/SMARCA4	ATP dependent RNA helicase
Btg2	B-cell translocation gene 2

CADTK	Calcium-dependent tyrosine kinase
CAK β	Cell adhesion kinase β
Calm1	Calmodulin
Camk2a	Calcium/calmodulin-dependent protein kinase type II subunit alpha
Camk2b	Calcium/calmodulin-dependent protein kinase type II subunit beta
CaMKII	Calcium- and calmodulin-dependent protein kinase II
CaMKIV	Calcium-calmodulin-dependent kinase IV
CaMKK	Calcium-calmodulin-dependent kinase kinase
CaMs	Calmodulins
Camsap2	Calmodulin regulated spectrin-associated protein family, member 2
CaN	Calcineurin
Canx	Calnexin
CAPN1	Calpain-1
CAPN2	Calpain-2
CAPN4	Calpain-4
CAPON	Carboxy-terminal PDZ ligand of nNOS
CBP	CREB binding protein
CD 45	Cluster of differentiation 45
CDC 42	Cell division cycle 42
Cdc42	Cell division control protein 42 homolog
Cdh2	Cadherin-2
Cdk5	Cyclin-dependent kinase 5
Cdkn1b	Cyclin-dependent kinase inhibitor 1B (p27, Kip1)
Cep170	Centrosomal protein 170kDa
CK1	Casein kinase 1
CK2	Casein kinase 2
Clca1	Ca ²⁺ -activated chloride channel regulator 1
Cnksr2	Connector enhancer of kinase suppressor of Ras 2
CNS	Central nervous system
CoREST	REST corepressor 1
Coro1a	Coronin-1A
COX-2	Cyclooxygenase -2
CP-101,606	Traxoprodil
CREB	cAMP responsive element-binding protein
Crk	Proto-oncogene c-Crk
Crmp1	Collapsin response mediator protein 1
CRMP3	Collapsin response mediator protein 3
CSF	Cerebrospinal fluid
Csl	Small muscular protein
Csnk1d	Casein kinase 1, delta
Csnk1e	Casein kinase 1, epsilon
Ctnna2	Catenin (cadherin-associated protein), alpha 2
Ctnnd2	Catenin (cadherin-associated protein), delta 2

Cxadr	Coxsackie virus and adenovirus receptor
DAPK	Death associated protein kinase
Dbn1	Drebrin 1
Dclk1	Doublecortin-like kinase 1
Dex	Doublecortin
DNA	Deoxyribonucleic acid
DNMT	DNA methyltransferase
DNMTs	DNA methyltransferases
DOT1L	Histone H3 methyltransferase also known as <i>DOTIL</i>
Dpysl3	Dihydropyrimidinase-like 3
Drp1	Dynamin1
Eef1b	Elongation factor 1-beta
EGFR	Epidermal growth factor receptor
Eif3b	Eukaryotic translation initiation factor 3, subunit B
Elavl2	ELAV-like protein 2
Epb41l3	Erythrocyte membrane protein band 4.1-like 3
Eph	Ephrins receptor
Erk1/2	Extracellular-signal regulated kinase 1/2
Erk2	Mitogen-activated protein kinase 1
Fabp3	Fatty acid-binding protein 3
Fabp5	Fatty acid-binding protein 5
FAK2	Focal adhesion kinase 2
Fasl	Fas ligand
FGFR	Fibroblast growth factor receptors
Fh1	Fumarate hydratase, mitochondrial
Fnbp1l	Formin binding protein 1-like
FOXO	Forkhead box protein O
G3bp1	Ras GTPase-activating protein-binding protein 1
G9a/EHMT2	Euchromatic histone-lysine N-methyltransferase 2, also known as <i>G9a</i>
GABA	γ -Amino butyric acid
Gadd 45b	Growth arrest and DNA-damage-inducible 45 beta
GAPDH	Glyceraldehyde-3-phosphate dehydrogenase
Gdi1	Rab GDP dissociation inhibitor alpha
GDNF	Glial cell line-derived neurotrophic factor
GEF	Guanine-nucleotide exchange factor
GFLs	GDNF family ligands
GFP	Green fluorescence protein
Git1	G protein-coupled receptor kinase interacting ArfGAP 1
Glod4	Glyoxalase domain-containing protein 4
GluN1	Glutamate (NMDA) receptor subunit 1
GluN2	Glutamate (NMDA) receptor subunit 2
GluN3	Glutamate (NMDA) receptor subunit 3
GOSPEL	GAPDH's competitor of Siah Protein Enhances Life

GPCRs	G-protein coupled receptor
Grb2	Growth factor receptor-bound protein 2
GRIA2	Glutamate Receptor, Ionotropic, AMPA 2
GRIP	Glutamate receptor interacting protein
Gsk3a	Glycogen synthase kinase 3 alpha
H ₂ O ₂	Hydrogen peroxide
HATs	Histone acetyltransferases
HDAC1	Histone deacetylase enzymes subfamily C, member 1
HDAC2	Histone deacetylase enzymes subfamily C, member 2
HDACs	Histone deacetylase enzymes subfamily C
Hdgf	Hepatoma-derived growth factor
Hmgb1	High mobility group protein B1
Hmgcs1	3-hydroxy-3-methylglutaryl-CoA synthase 1 (soluble)
Hnrnpa3	Heterogeneous nuclear ribonucleoprotein A3
HP	Heterochromatin Protein 1
Hpcal4	Hippocalcin-like protein 4
ICAM	Intercellular adhesion molecule 1
ICAT	Isotope coded affinity tags
Ifi202B	Interferon activated gene 202B
Igf2r	Insulin-like growth factor 2 receptor
IL1 β	Interleukin 1 beta
IMAC	Immobilized metal ion affinity chromatography
iTRAQ	Isobaric tags for relative absolute quantification
JNK	c-Jun N-terminal kinases
Kidins220/ARMS	Kinase D interacting substrate of 220 kDa/Ankyrin repeat-rich membrane spanning
Klc2	Kinesin light chain 2
Lamp1	Lysosome-associated membrane glycoprotein 1
Ldhb	L-lactate dehydrogenase B chain
Limch1	LIM and calponin homology domains 1
Lsamp	Limbic system-associated membrane protein (LSAMP)
LSD1/KDM1A	Histone H3K4 demethylase
LTP	Long term potentiation
MAGUK	Membrane-associated guanylate kinase
Map1b	Microtubule-associated protein 1B
Map1lc3b	Microtubule-associated proteins 1A/1B light chain 3B
Map2	Microtubule-associated protein 2
Map4	Microtubule-associated protein 4
MAPK	Mitogen-activated protein kinase
Mapk8ip3	C-Jun-amino-terminal kinase-interacting protein 3
Mapt	Microtubule-associated protein tau
MeCP2	Methyl-CpG-binding protein
Mef2c	Myocyte enhancer factor 2C

Mff	Mitochondrial fission factor
mGluR	Metabotropic glutamate receptor
mGluR α -1	Metabotropic glutamate receptor α -1
Mios	WD repeat-containing protein mio
miR-132	MicroRNA 132
Mlf2	Myeloid leukemia factor 2
MLLs	Mixed lineage leukemia proteins
mPTP	Mitochondrial permeability transition pore
Myh10	Myosin, heavy chain 10, non-muscle
nAchRs	Nicotinic acetylcholine receptors
NADH	Nicotinamide adenine dinucleotide
Napa	Alpha-soluble NSF attachment protein
NCX	Sodium-calcium exchanger
ND2	NADH dehydrogenase subunit 2
Ndfip-1	NEDD4-family interacting protein 1
NEDD4	Neural precursor cell expressed developmentally down-regulated protein 4
Nedd4l	E3 ubiquitin-protein ligase NEDD4-like
NFAT	Nuclear factor of activated T-cells
NF κ β	Nuclear Factor-Kappa β
NMDA	N-methyl-D-aspartate receptors
Nme1	Tumor metastatic process-associated protein
nNOS	Nitric oxide synthase
NO	Nitric oxide
NOS	Nitric oxide synthase
NOX2	NADPH oxidase 2
Npas4	Neuronal PAS domain protein 4
Npc2	Epididymal secretory protein E1
Nr4a1	Nuclear receptor subfamily 4, group A, member 1
Otub1	Ubiquitin thioesterase
p38	Pro-death protein kinase
panx1	Pannexin1 ion channel
PDGFR	Platelet-derived growth factor receptor
Pfdn2	Prefoldin subunit 2
Pfdn5	Prefoldin subunit 5
Pfkm	ATP-dependent 6-phosphofructokinase, muscle type
Pfn1	Profilin-1
PHLPP1	PH domain and Leucine rich repeat Protein Phosphatases 1
PHLPP1 α	PH domain and Leucine rich repeat Protein Phosphatases 1 α
PHLPP1 β	PH domain and Leucine rich repeat Protein Phosphatases 1 β
PI(3,4,5)P3	Phosphatidylinositol-3,4,5-trisphosphate
PI(4,5)P2	phosphatidylinositol-4,5-bisphosphate
PI3K	Phosphoinositide 3-kinase
PICK1	Protein interacting with PRKCA 1

Pitpna	Phosphatidylinositol transfer protein alpha isoform
PKA	Protein tyrosine kinase A
PKC	Protein tyrosine kinase C
PMCA	Plasma membrane calcium ATPase
Ppfia3	Protein tyrosine phosphatase, receptor type, f polypeptide (PTPRF), interacting protein (liprin), alpha 3
Prdx1	Peroxiredoxin-1
Prrc2a	Proline-rich coiled-coil 2A
Psap	Prosaposin
Psd3	Pleckstrin and Sec7 domain containing 3
PSD-95	Postsynaptic density protein 95
Psip1	PC4 and SFRS1 interacting protein 1
Psmb1	Proteasome subunit beta type-1
Psmc1	Proteasome 26S subunit ATPase 1
PTEN	Phosphatase and tensin homolog
PTM	Post-translational modifications
Ptn	Pleiotrophin
PTP	Protein tyrosine phosphatase
Puma	p53 upregulated modulator of apoptosis
Rab1b	Ras-related protein Rab-1B
Rab3b	Ras-related protein Rab-3B
Rad23b	UV excision repair protein RAD23 homolog B
Rbm25	RNA binding motif protein 25
Rbmx	RNA-binding motif protein, X chromosome
REST	RE1-Silencing Transcription factor,
Rnmt	RNA (guanine-7-) methyltransferase
ROS	Reactive oxygen species
Rp13	Ribosomal protein L3
Rpl7	60S ribosomal protein L7
Rps13	40S ribosomal protein S13
Rps14	40S ribosomal protein S14
Rps28	40S ribosomal protein S28
Rps4x	40S ribosomal protein S4, X isoform
rt-PA	Recombinant tissue plasminogen activator
SAP-102	Synapse associated protein 102
Serbp1	Plasminogen activator inhibitor 1 RNA-binding protein
Serpinb2	Serine protease inhibitor B2
Sfr1	SWI5-dependent recombination repair 1
Shp1	Src homology 2 domain containing tyrosine phosphatase 1
Siah1	Seven in absentia homolog 1
SILAC	Stable isotope labelling by amino acids in cell culture
Sin3A	Paired amphipathic helix protein Sin3a
siRNAs	Small interfering RNA

Snap91	Synaptosomal-associated protein, 91kDa
SrcΔN	Truncated Src fragment
Srcin1	SRC kinase signaling inhibitor 1
SRM/MRM	Single or multiple reactions monitoring
Srsf1	Serine/arginine-rich splicing factor 1
STAT-3	Signal transducer and activator of transcription 3
STEP	Striatal-enriched tyrosine phosphatase
Stip1	Stress-induced-phosphoprotein 1
Stmn1	Stathmin 1
Syn3	Synapsin III
SynGAP	Synaptic RAS-GTPase activating protein
tAIF	Truncated AIF
TAILS	Terminal Amine Isotopic Labelling of Substrates
Tardbp	TAR DNA-binding protein 43
Tat-K13	Tat-K13 short interfering peptide
TGFβ	Transforming growth factor β
Thrap3	Thyroid hormone receptor associated protein 3
TLRs	Toll-like receptors
TMT	Tandem mass tag
TNFα	Tumor necrosis factor α
Tnik	TRAF2 and NCK interacting kinase
Tom1l2	TOM1-like protein 2
Tpt1	Translationally-controlled tumor protein
Tra2b	Transformer-2 protein homolog beta
Trim2	Tripartite motif containing 2
Trk	Tropomyosin <i>receptor</i> kinase
Trk-A	TRK1-transforming tyrosine kinase protein
Trp53bp1	Tumor suppressor p53-binding protein 1
TRPC6	Transient receptor potential cation channel, subfamily C, member 6
TRPM2	Transient receptor potential cation channel, subfamily M, member 2
TRPM7	Transient receptor potential cation channel, subfamily M, member 7
Tubb3	Tubulin beta-3 chain
Tubb4b	Tubulin beta-4B chain
Tubb6	Tubulin beta-6 chain
Txnip	Thioredoxin-interacting protein
Uchl1	Ubiquitin carboxyl-terminal hydrolase isozyme L1
Usp14	Ubiquitin specific peptidase 14
Vamp2	Vesicle-associated membrane protein 2
VDCC	Voltage dependent calcium channels
XIAP	X-linked inhibitor of apoptosis protein
Yars	Tyrosine--tRNA ligase, cytoplasmic
Ybx1	Nuclease-sensitive element-binding protein 1
Ywhab	14-3-3 protein beta/alpha

Ywhae	14-3-3 protein epsilon
Ywhaq	14-3-3 protein theta
Ywhaz	14-3-3 protein zeta/delta
β -TrCP	β -transducin repeat-containing protein
γ CaMKII	γ -isoform of calcium-calmodulin-dependent kinase II

Thesis outline

This thesis consists of 7 chapters. Chapter 1 is the literature review describing the current knowledge of ischaemic stroke-induced neuronal death mechanisms. Specifically, it focuses on how the known signalling pathways interplay to mediate excitotoxic cell death. Chapter 2 lists the reagents used and some of the methods I adopted to generate the data presented in Chapters 3, 4, 5 and 6. Chapter 3 describes the data demonstrating the dual role of Src protein tyrosine kinase in governing neuronal survival. Chapter 4 outlines the data describing the changes in global neuronal proteome following glutamate-induced excitotoxicity. Chapter 5 presents the data on the changes in neuronal phosphoproteome in excitotoxicity. In Chapter 6, I present the data on defining the calpain cleavage site in Src unique domain and identification of neuronal proteins mediating the neurotoxic signals originating from the extrasynaptic NMDA receptor, calpains and Src Δ N. Chapter 7 summarises the study findings and conclusions of my studies and the experimental strategies for future investigations to bridge our knowledge gaps in understanding the excitotoxic neuronal death mechanism.

Chapter 1

Declaration and Acknowledgements

- ✚ This literature review chapter has been published as a review article in *Pharmacology and Therapeutics*. I contributed to 75% of the writings for this manuscript.

Hoque A, Hossain MI, Ameen SS, Ang CS, Williamson N, Ng DC, Chueh AC, Roulston C and Cheng HC (2016) A beacon of hope in stroke therapy-Blockade of pathologically activated cellular events in excitotoxic neuronal death as potential neuroprotective strategies. *Pharmacology and Therapeutics*, 160, 159–179.

- ✚ Thanks to all the co-authors for their valuable inputs, suggestions and contributions for the final manuscript.

Chapter 1: Excitotoxicity-the early key event for neuronal loss in acute ischaemic stroke

1.1 Overview of stroke

A stroke is the sudden loss of brain functions because of the disturbance in blood supply to the brain. Brain cells die within minutes due to the lack of oxygen and nutrient supply or sudden bleeding into and around the brain. In the immediate vicinity, brain cells die rapidly due to the interruption of the oxygen supply, whereas surrounding outer cells remain at risk and may die over hours to days (Small et al., 1999). Strokes are classified into two major categories: ischaemic and haemorrhagic stroke. An ischaemic stroke is the result of the blockage of a blood vessel in the brain, whereas a haemorrhagic stroke occurs because of blood leakage from a burst in a blood vessel. A stroke can lead to permanent neurological damage, complications and for many deaths.

Stroke is the second most common cause of death and accounts for approximately 9.7% of all deaths worldwide following ischaemic heart disease (Mathers et al., 2009); and in western countries it accounts for 10-12% of all death (Bonita, 1992). Stroke can occur at any age including childhood, however stroke incidence increases exponentially from 30 years of age (Ellekjaer et al., 1997). Most important risk factors for stroke include hypertension, heart disease, diabetes, and smoking. Others include heavy alcohol consumption, high blood cholesterol levels, illicit drug use, and genetic or congenital conditions, particularly vascular abnormalities. Atrial fibrillation and transient ischaemic attacks (TIAs) in the brain are less prevalent but are more likely to lead to stroke incidence (Donnan et al., 2008). Recent genome wide association studies are yet to correlate the susceptible genes for stroke though several loci have been identified (Hegele and Dichgans, 2010).

1.1.1 Acute ischaemic stroke

Ischaemic stroke or focal cerebral ischaemia results from occlusion of an artery in the brain mostly by thrombus (local formation of blood clot) or emboli (free-roaming clot originating elsewhere in the body) and accounts for approximately 85% of all strokes (Flynn et al., 2008). Shock mediated systemic hypoperfusion (decrease in blood supply) (Shuaib and

Hachinski, 1991) and cerebral venous thrombosis (Stam, 2005) can also result in ischaemic stroke. Brain cells die rapidly without adequate blood flow following ischaemic injury. Brain tissue requires about 60 ml of blood for 100 gm of tissue per minute to exert normal brain functions. Following an ischaemic injury, blood flow becomes 10-12 ml per 100 gm of tissue per minute or even less in the centre of the ischaemic infarct area (Heiss, 2000), this immediately affected region is referred to as the ischaemic core where irreversible damage has already occurred. The ischaemic core is surrounded by a zone of less severely affected cells referred to as the ischaemic penumbra (Astrup et al., 1981). Brain cells in the penumbra region are unable to carry out full normal functions as they receive compromised blood flow below the normal rate but which can be redeemed if blood flow is restored (reperfused) quickly. Sustained occlusion of flow results in the infarct region expanding, neuronal activities become depressed and cells die. Although reperfusion is one of the goals for most clinical therapies, their benefits are mitigated by secondary injury to the penumbra mostly because of the oxidative stress and, acute and prolonged inflammatory responses (Aronowski et al., 1997; Chan, 2001; Ritter et al., 2000).

1.2 Cascade of cellular events leads to ischaemic brain injury

Brain cells incur ischaemic attack due to the lack of energy supplies, reduction in metabolic rates, oxidative stress, alterations in brain metabolism, and potentiation of inflammatory responses. Energy crisis, acidosis, ion-influx, generation of free radicals, blood-brain barrier disruptions, oedema and inflammation are the concurrent steps in an ischaemic brain injury. During the onset of cerebral ischaemia, cells within the ischaemic core die within minutes due to the massive shortage of oxygen and glucose delivery (**Figure 1.1**). Ischaemic cells within the penumbra maintain some blood flow due to collateral vessels, however metabolic demand increases resulting in excitotoxic neuronal death, and accounts for half of neuronal loss following ischaemic attack (Broughton et al., 2009). Thus, cells within the penumbra are targeted for possible intervention following stroke (Ginsberg, 1997). Recent findings suggest that most of the neuronal cells in the penumbra region (peri-infarct zone) experience cell death several hours or even days after the onset of the ischaemic attack and thus these cells are potentially salvageable (Mehta et al., 2007; Nakka et al., 2008; Zheng and Yenari, 2004). However, these cells will also die unless therapeutic intervention is initiated (Fisher, 2004). Neuronal death in stroke may be excitotoxic (glutamate-induced

excitotoxicity), inflammatory, radical (oxidative stress and free radicals), and suicidal (apoptosis-like pathways) (Chan, 2001; Graham and Chen, 2001; Lipton, 1999). Current treatment strategies for ischaemic stroke mainly focus on reducing the size of ischaemic damage and rescuing dying cells soon after the ischaemic attack (Sahota and Savitz). Intravenous recombinant tissue plasminogen activator (rt-PA), which is a serine-protease that binds to fibrin in thrombus and converts plasminogen to plasmin and restores blood flow by initiating fibrinolysis, is the only FDA-approved drug for the treatment of acute ischaemic stroke (NINDS.(rt-PA).SSG, 1995). For patients admitted to hospital 4.5 h after the onset of ischemic stroke, rt-PA may cause haemorrhagic complications. Thus, it is used for the treatment in less than 10% of the ischemic stroke patients [reviewed in (Miller et al., 2011)]. Despite years of intensive research, therapeutics that directly protect against neuronal loss to reduce stroke-induced brain damage are not available for clinical use (O'Collins et al., 2006; Savitz and Fisher, 2007). This pessimistic scenario has been challenged by the promising clinical trial success of Tat-NR2B9c, a cell membrane permeable peptide, which effectively reduces brain damage caused by small, procedurally induced ischaemic strokes in patients undergoing treatment to repair ruptured brain blood vessel aneurysm (Hill et al., 2012). In this treatment scenario, Tat-NR2B9c was delivered after the onset of stroke. Thus, its success proves that neuroprotection to reduce brain damage in human acute ischaemic stroke is achievable. The neuroprotective effect of Tat-NR2B9c is attributed to its ability to inhibit a key pathological cellular event that directs stroke-induced neuronal death, confirming that investigation of the mechanism of stroke-induced neuronal death is one of the best avenues to develop therapeutic strategies to reduce stroke-induced brain damage.

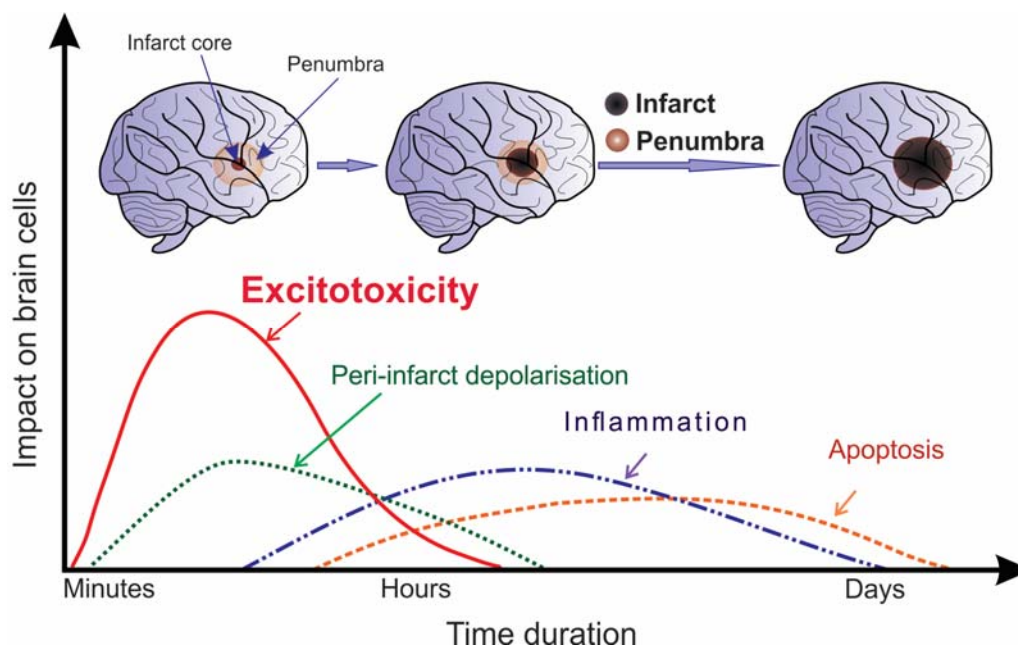


Figure 1.1 Temporal events leading to brain damage following ischaemic stroke.

Immediately after blood vessel occlusion, deficits in oxygen and glucose delivery induce neural cell death within minutes and this region is referred to as the ischaemic core (infarct). Surrounding the core is the penumbra, where cells are kept alive by the limited oxygen and nutrients supply from collateral blood flow. However, with time, cells in the penumbra will also die as a result of a series of events. The temporal events leading to neuronal demise are depicted. This figure is adapted from the review article by Dirnagl *et al.*, (1999).

1.2.1 Excitotoxicity-a major cause of neuronal loss in ischemic stroke and chronic neurodegenerative diseases such as Alzheimer's disease

Excitotoxicity, a pathological process caused by over-stimulation of ionotropic glutamate receptors, is a major cause of neuronal loss in acute neurological conditions such as ischemic stroke, traumatic brain injury, prolonged seizure in stroke and neurodegenerative diseases such as Alzheimer's and Huntington's diseases. Glutamate, the most abundant excitatory neurotransmitter is released from the injured brain cells in ischaemic core. Since the brain cells in the ischemic penumbra receive limited blood supply, they fail to generate sufficient ATP to sustain the ionic gradient essential for the reuptake of glutamate via the glutamate transporters (Zerangue and Kavanaugh, 1996). Consequently, glutamate accumulates in the extracellular space of central nervous system (CNS) (Choi and Rothman, 1990) to cause prolonged and uncontrolled activation of the ionotropic glutamate receptors including N-methyl-D-aspartate (NMDA), α -amino-3-hydroxy-5-methyl-4-isoxazolepropionic acid

(AMPA) and kainite receptors (**Figure 1.2**). These receptors are permeable to extracellular ions especially Ca^{2+} . As a result of their over-stimulation, excessive Ca^{2+} , along with Na^{+} and water enter the affected neurons; this in turn activates proteases, lipases, nucleases (Ankarcona et al., 1995). These activated enzymes produce excess nitric oxide (NO), arachidonic acid metabolites, and reactive oxygen species, which act as mediators of cell death (Dirnagl et al., 1999; Lo et al., 2003).

Excitotoxicity occurring in neurons located in ischemic penumbra in ischemic stroke as well as that in other acute neurological disorders is referred to as ‘acute excitotoxicity’ because the neurons affected are over-stimulated by acute elevation of extracellular glutamate. In contrast, the type of excitotoxicity contributing to the chronic neurodegenerative diseases such as Alzheimer’s disease is referred to as ‘slow excitotoxicity’ [reviewed in (Ong et al., 2013) and (Ferrarese, 2004)]. It differs from acute excitotoxicity in that the neurotoxic ionotropic glutamate receptors are tonically stimulated by glutamate at levels much lower than those in acute excitotoxicity. The molecular basis of slow excitotoxicity remains unclear. Ample experimental evidence suggest that it is a consequence of impaired energy metabolism caused by mitochondrial dysfunction and abnormalities of turnover and signalling of the neurotoxic ionotropic glutamate receptors [reviewed in (Ong et al., 2013)]. Alzheimer’s disease is characterised by accumulation of the extracellular neurotoxic amyloid β oligomers ($\text{A}\beta$), which induce excitotoxicity leading to neuronal loss by direct binding to astrocytes and neurons. $\text{A}\beta$ binds astrocytes and induces release of astrocytic glutamate, which in turn over-stimulates the neurotoxic ionotropic glutamate receptors in the nearby neurons (Talantova et al., 2013). $\text{A}\beta$ also binds to the nearby neurons. The binding enhances both the retention on the plasma membrane and cytotoxic signalling of the neurotoxic ionotropic glutamate receptors (Ittner et al., 2010; Larson et al., 2012; Um et al., 2013; Um and Strittmatter, 2013).

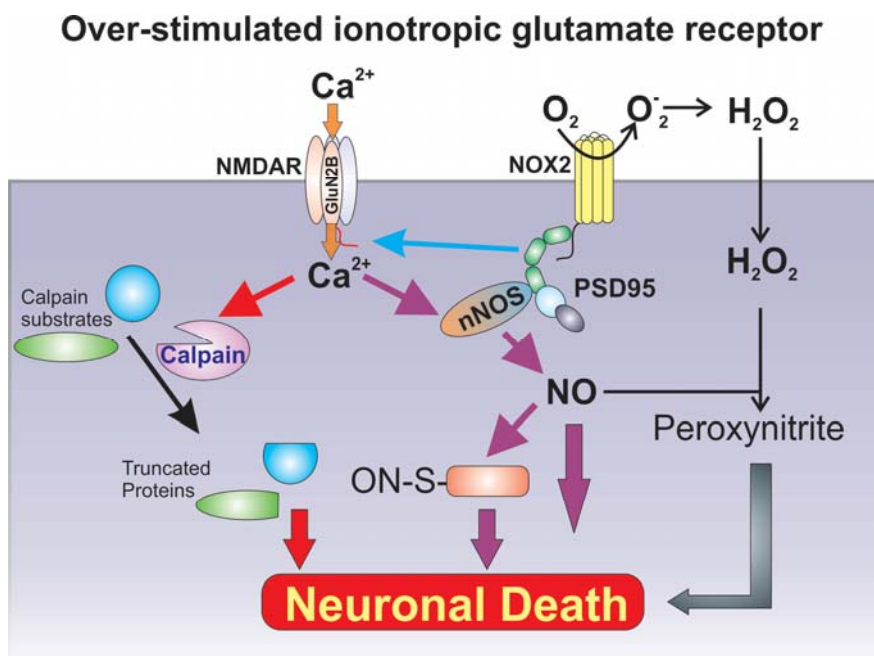


Figure 1.2 Calpains, nNOS and NOX2 are key intracellular neurotoxic enzymes activated at the initial phase of excitotoxic neuronal death. Over-stimulation of neuronal ionotropic glutamate receptors such as NMDA receptors leads to calcium overload, and enhanced interactions between NMDA receptors and the PSD95/nNOS/NOX2 complex. The excess cytosolic calcium over-activates calpains, nNOS and NOX2. Upon activation, calpains modulate the functions of selected neuronal proteins by limited proteolysis. The proteolysed proteins lose their pro-survival function and/or acquire neurotoxic function. The over-activated nNOS and NOX2 produce excessive amount of nitric oxide (NO) and reactive oxygen species such as H₂O₂, respectively. NO and H₂O₂ react to form peroxynitrite. H₂O₂, NO and peroxynitrite together cause oxidative damages and in turn contribute to neuronal death. NO also directly S-nitrosylates selected neuronal proteins. Upon S-nitrosylation, some neuronal proteins acquire neurotoxic activity and contribute to neuronal death.

1.2.2 Caspase-independent cell death underpins neuronal demise in excitotoxicity

The intrinsic pathway of apoptosis is the major contributor of neuronal death in brain development [reviewed in (Stefanis, 2005)]. In contrast, when adult neurons are exposed to high concentrations of glutamate in excitotoxicity, they adopt morphological features characteristic of necrosis and undergo caspase-independent cell death [reviewed in (Fujikawa, 2015)]. Mechanistically, the over-stimulated glutamate receptors allow an excessive influx of calcium to the cytosol that constitutively activates a number of enzymes.

Among them, neuronal nitric oxide synthase (nNOS) and the calcium-activated proteases calpains are major mediators of the cytotoxic signals emanating from the over-stimulated glutamate receptors (**Figure 1.2**). The excess NO produced by the over-activated nNOS and the over-activated calpains contribute to mitochondrial dysfunction, leading to opening of mitochondrial permeability transition pore (mPTP), release of mitochondrial calcium and pro-apoptotic regulators such as cytochrome c and apoptosis-inducing factor (AIF) to the cytosol. Owing to the high level of expression of X-linked inhibitor of apoptosis protein (XIAP) (Potts et al., 2003) and reduced expression of apoptotic protease activating factor 1 (APAF-1) (Johnson et al., 2007) in adult neurons, cytosolic cytochrome c cannot readily activate caspases to induce apoptotic cell death [reviewed in (D'Orsi et al., 2012; Moskowitz et al., 2010)]. Thus, adult neurons undergo cell death by a caspase-independent mechanism in excitotoxicity. Based upon the morphological changes and some of the biochemical events of neurons undergoing excitotoxic neuronal death, a number of terms including excitotoxic programmed necrosis, programmed necrosis and Parthanatos have been suggested for excitotoxic neuronal death (Fatokun et al., 2014; Fujikawa, 2015; Moskowitz et al., 2010). To avoid further confusion, the neuronal death process in excitotoxicity is referred to as caspase-independent cell death in this thesis.

1.2.3 Excessive intracellular Ca²⁺ influx leads to excitotoxic brain injury

Excessive intracellular accumulation of Ca²⁺ in neurons following ischaemic injury leads to the over-activation of a number of pernicious cellular enzymes and signalling processes that result in neuronal cell death (Dirnagl et al., 1999). Recent studies support 'source specificity hypothesis' that is distinct Ca²⁺ signalling pathways are linked to specific route of Ca²⁺ influx is important for Ca²⁺ neurotoxicity (Sattler et al., 1998; Tymianski et al., 1993); whereas earlier it was thought to be 'calcium overload hypothesis' where Ca²⁺ concentration exceeding a given threshold leads to neurotoxicity (Manev et al., 1989; Marcoux et al., 1990). By three mechanisms Ca²⁺ can be overloaded in the neuronal cytoplasm following ischaemic injury, these include: (i) excess Ca²⁺ entry through the plasma membrane Ca²⁺-transporters or receptors, (ii) dysfunction of the Ca²⁺ extruding ion channels in the plasma membrane and (iii) compromised internal stores (mitochondria and endoplasmic reticulum) Ca²⁺ homeostasis. Following cerebral ischaemia Ca²⁺ ions enter the neurons mostly via ionotropic NMDA glutamate receptors (Choi, 1987) and, also by GluA2 lacking AMPAR (Cull-Candy et al., 2006). Other ion channels and transporters have also been described as

routes of Ca^{2+} entry following ischaemic injury [reviewed in (Szydlowska and Tymianski, 2010)]; these include transient receptor potential (TRP) channel members TRPM2 and TRPM7 (Aarts et al., 2003; Aarts and Tymianski, 2005; Kaneko et al., 2006; Nicotera and Bano, 2003; Sun et al., 2009), bi-directional ion transporter $\text{Na}^+/\text{Ca}^{2+}$ exchanger (NCX) that can extrude Ca^{2+} by driving force from Na^+ influx (Czyz and Kiedrowski, 2002; Jeffs et al., 2007), acid sensing ion channels (ASICs) (Xiong et al., 2004), dihydropyridine-sensitive L-type voltage-dependent Ca^{2+} channels (CaV1.2) [reviewed in (Horn and Limburg, 2000)].

Disruptions in neuronal Ca^{2+} homeostasis enhance cytoplasmic Ca^{2+} accumulation. Compromised membrane potential of mitochondria and endoplasmic reticulum and, malfunction of their own ion channels following excitotoxicity releases Ca^{2+} back into the cytoplasm. On the other hand, NMDAR mediated dysfunction of membrane NCX can no longer pump out intracellular Ca^{2+} and further overloads intracellular Ca^{2+} concentration that ultimately triggers downstream neurotoxic signalling pathways. In the following sections, the pathologically activated cellular events are reviewed that occur at various subcellular localisations in neurons undergoing cell death in excitotoxicity.

1.3 Signalling mechanisms of excitotoxic neuronal death

1.3.1 Cell surface receptors and ion channels

There are two major types of glutamate receptors: the metabotropic receptors, which are G-protein coupled receptors and ionotropic glutamate receptors, which are ligand-gated ion channels. Ionotropic glutamate receptors are central players in glutamate-induced excitotoxicity. Among the three types of ionotropic glutamate receptors, NMDA receptors are highly permeable to calcium and therefore the major contributors of neuronal death (Choi, 1988a). NMDA receptors are ligand- and voltage-gated ion channels activated by depolarisation and binding of glutamate and the co-agonist glycine. They are heteromeric protein complexes with subunits encoded by three gene families: (i) GluN1 which are the obligatory subunit and contains the binding site for the glycine, (ii) GluN2 subunits which contain the binding site for glutamate, and the (iii) GluN3 subunit (Cull-Candy et al., 2001). The GluN2 subunits are further subdivided into subtypes, namely, GluN2A, GluN2B, GluN2C and GluN2D (Hollmann and Heinemann, 1994). Although the exact subunit compositions of NMDA receptors have yet to be fully defined, it is believed that a functional NMDA receptor is usually a tetramer containing either two obligatory GluN1 and two

GluN2 subunits [i.e., (GluN1)₂(GluN2)₂] or two GluN1 and one GluN2 and one GluN3 subunits [i.e. (GluN1)₂(GluN2)(GluN3)] (Cull-Candy and Leszkiewicz, 2004). At resting potential, magnesium ions enter and tightly bind to the pore of NMDA receptors, blocking the influx of extracellular calcium ions into the cytosol. Proper functioning of NMDA receptors requires binding of glutamate and the co-agonist glycine as well as concurrent membrane depolarization of the channel which removes the Mg²⁺ from the channel in a voltage-dependent manner (Erreger et al., 2004; Lynch and Guttman, 2001).

Over-stimulation of the AMPA and kainate receptors by glutamate also contributes to excitotoxic neuronal death. Similar to NMDA receptors, AMPA and kainate receptors are multimeric ion channels [(Kumar et al., 2011) and reviewed in (Gan et al., 2015)]. They contribute to the calcium influx into the excitotoxic neurons by direct and indirect mechanisms. The indirect mechanism relates to their ability to remove the Mg²⁺ block in NMDA receptors by membrane depolarisation (Courtney et al., 1990; Nowak et al., 1984). AMPA receptors can directly contribute to the increase in cytosolic calcium by acting as calcium channels. The calcium permeability of AMPA receptors are mainly governed by its subunit composition, AMPA receptors containing the GluA2 subunit encoded by the *GRIA2* gene are impermeable to calcium. Expression of the GluA2 subunit and its incorporation in the AMPA receptor involves RNA editing to replace the codon encoding glutamine-607 to arginine prior to translation (Sommer et al., 1991). Incorporation of the Q/R-edited GluA2 subunit in AMPA receptor renders the AMPA receptor impermeable to calcium ions (Burnashev et al., 1992). In the late phase of excitotoxicity, expression of the *GRIA2* gene encoding the GluA2 subunit is suppressed by epigenetic silencing, leading to the formation of calcium permeable GluA1 subunit-deficient AMPA receptor (Noh et al., 2012). The increased level of GluA1 subunit-deficient AMPA receptor allows influx of calcium and in turn directly contributes to the increase in cytosolic calcium concentration in excitotoxicity [(Noh et al., 2012) and reviewed in (Hwang et al., 2013)]. The mechanism of epigenetic silencing of *GRIA2* gene is discussed in section 1.3.9.

In addition to the ionotropic glutamate receptors, several plasma membrane-bound proteins also contribute to calcium overload in excitotoxicity. These proteins include the sodium-calcium exchanger (NCX) and several ion channels including the large pore ion channel pannexin1 (panx1), acid-sensing ion channels (ASICs) and transient receptor potential (TRP) channels (TRPM7, TRPM2 and TRPC6) [(Bano et al., 2005; Du et al., 2010) and reviewed in (Szydlowska and Tymianski, 2010)] (**Figure 1.3**). These proteins are

dysregulated as a result of the initial phase of increase in cytosolic calcium concentration caused by the influx of calcium via the over-stimulated NMDA receptors (refer to section 1.3.6 for more detail). Thus, some of them such as NCX and the three TRP channels are involved in maintaining the sustained increase in cytosolic calcium level at the later stage of excitotoxicity. The mechanisms of their dysregulation and how their dysregulation contributes to calcium overload are reviewed in this chapter. Additionally, how blockade of dysregulation of some of these proteins can be exploited as neuroprotective strategies for the treatment of stroke patients are also discussed.

In Alzheimer's disease, neuronal damages such as synaptic dysfunction and dendritic spine retraction are caused in part by a tonic activation of the extrasynaptic NMDA receptors by glutamate released by astrocytes in response to A β stimulation. Since the increase in extracellular glutamate is much smaller than that in the ischemic penumbra in ischemic stroke, excitotoxic neuronal loss is further facilitated by A β -induced aberrant Ca²⁺ homeostasis and hyperexcitability of NMDA receptors in the affected neurons (Renner et al., 2010). The aberrant neurotoxic signalling in these neurons is initiated in part by A β binding to prion complexed with the metabotropic glutamate receptor mGluR5 on the plasma membrane. A consequence of A β interaction with the prion/mGluR5 complex is activation of the Src-family protein tyrosine kinase Fyn and its recruitment to the postsynaptic density where it is located in close proximity to NMDA receptors. Using transgenic mice expressing a truncated form of tau, Ittner *et al.* demonstrated that binding of Fyn to tau is a pre-requisite for recruitment of Fyn to the postsynaptic density (Ittner et al., 2010). Following aberrant recruitment and activation of Fyn to the postsynaptic density, Fyn phosphorylates Tyr-1472 of GluN2B subunit of NMDA receptors and sensitises the NMDA receptors to deliver neurotoxic signals.

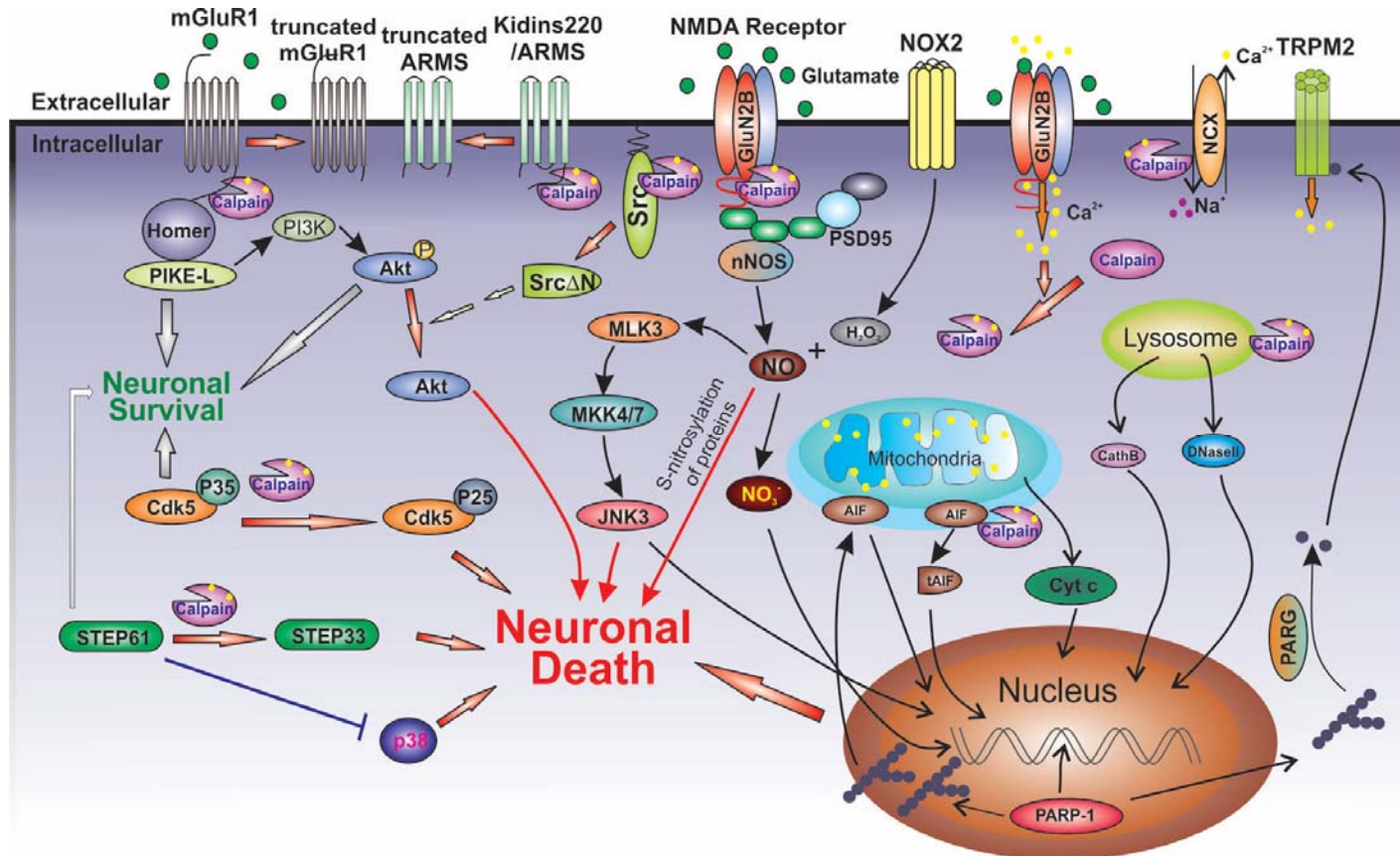


Figure 1.3

Figure 1.3 Selected neurotoxic signalling pathways originating from the over-stimulated NMDA receptors. Upon over-stimulation, NMDA receptors allow excessive Ca^{2+} influx, which activates calpains, nNOS and NOX2. The constitutively active nNOS and NOX2 produce excess NO and reactive oxygen species, which cooperate with calpains to activate pro-death signalling pathways and suppresses pro-survival signalling pathways. Calpain cleavage of specific cellular proteins directly or indirectly inactivates the pro-survival enzymes PI3K, Akt, Cdk5/p35 and STEP. Calpains, NO and reactive oxygen species aberrantly activate a number of pro-death cellular events in the plasma membrane, cytosol, mitochondria, lysosomes and nucleus. The cumulative effects of these activated pro-death events and suppression of the pro-survival enzymes govern neuronal death in excitotoxicity. *Abbreviations not listed in text: Homer, homer protein; PIKE-L, longer isoform of phosphoinositide 3 kinase (PI3K) enhancer; cathB, cathepsin B.*

1.3.2 Antagonising roles of synaptic and extrasynaptic NMDA receptors

In addition to functioning as ion channels, NMDA receptors are also hubs of signal transduction from which intracellular signals governing neuronal survival originate. The types of intracellular signals emanating from the NMDA receptors are determined by the subunit composition [reviewed in (Paoletti et al., 2013)]. The different subunits bind to specific subsets of scaffolding proteins (such as PSD-95), adapter proteins and signalling molecules to form protein complexes (Husi et al., 2000). These NMDA receptor complexes generate distinct signals to control neuronal survival and their ion channel activities. The subunit composition of NMDA receptors varies with the subcellular locations. NMDA receptors containing the GluN2A subunits are found mostly in synapses while the GluN2B subunit-containing receptors are more prevalent in extrasynaptic locations (Charton et al., 1999; Lopez de Armentia et al., 2003) (**Figure 1.4**). Compelling evidence suggests that these two different types of NMDA receptors, upon stimulation, exert opposite effects on neuronal survival. Upon stimulation by glutamate, synaptic NMDA receptors initiate neuroprotective signals while extrasynaptic NMDA receptors trigger mitochondrial dysfunction and initiate neurotoxic signalling pathways that ultimately direct neuronal death [(Hardingham and Bading, 2002; Hardingham et al., 2002) and reviewed in (Parsons and Raymond, 2014)] (**Figure 1.4**). An elegant study by Martel *et al.* revealed that the C-terminal domain of the GluN2A and GluN2B subunits contains structural determinants governing the generation of neuroprotective and neurotoxic signals, respectively (Martel et al., 2012). Thus, susceptibility of neurons to excitotoxic neuronal death is governed by the balance of these opposing signals from the synaptic and extrasynaptic NMDA receptors.

Intriguingly, increase in Ca^{2+} influx is required for initiation of both neuroprotective and neurotoxic signals originating from the synaptic and extrasynaptic NMDA receptors, respectively. How can Ca^{2+} entering neurons via the two types of NMDA receptors initiate opposing signals in neurons? The C-terminal domain of the GluN2A and GluN2B subunits determines the subset of neuronal proteins bound to the synaptic and extrasynaptic NMDA receptors. The GluN2B subunit preferentially associates with the Ca^{2+} -responsive neurotoxic signalling proteins such as nNOS, facilitating activation of these neurotoxic signalling proteins by the Ca^{2+} via the extrasynaptic NMDA receptor. In contrast, the signal from Ca^{2+} influx via the synaptic NMDA receptors is directed to nucleus where it stimulates

transcription of pro-survival genes. Ma *et al.* demonstrated that calmodulins (CaMs) are activated by Ca^{2+} influx through the L-type Ca_v1 channels. The Ca^{2+} -bound calmodulins are trapped by the γ -isoform of calcium-calmodulin-dependent kinase II (γCaMKII), which acts as a carrier shuttling $\text{Ca}^{2+}/\text{CaMs}$ from the cytosol to the nucleus (Ma *et al.*, 2014). Upon arrival at the nucleus, $\text{Ca}^{2+}/\text{CaMs}$ activate the calcium-calmodulin-dependent kinase kinase (CaMKK) and calcium-calmodulin-dependent kinase IV (CaMKIV). The activated CaMKIV phosphorylates the transcription factor cAMP responsive element-binding protein (CREB) to direct transcription of pro-survival genes (**Figure 1.4**). Future investigation should focus on determining if γCaMKII also acts as the carrier shuttling $\text{Ca}^{2+}/\text{CaMs}$ generated by calcium influx via the synaptic NMDA receptor to stimulate transcription of the pro-survival gene in neurons.

1.3.3 Neuroprotective signalling pathways of the synaptic NMDA receptors

Synaptic NMDA receptors are activated by glutamate released during low-frequency synaptic events (Harris and Pettit, 2007). Cumulative evidence suggests that survival of several types of neurons is dependent on synaptic NMDA receptor activity and function (Hardingham, 2006; Hetman and Kharebava, 2006). Synaptic NMDA receptors form signalling complexes with specific scaffolding proteins and signalling molecules such as calpain-1 and the protein phosphatase PHLPP1 (Wang *et al.*, 2013) (**Figure 1.4**). Upon stimulation by glutamate, the influx of calcium through the synaptic NMDA receptor preferentially activates calpain-1, which degrades and inactivates PHLPP1. As PHLPP1 is a major upstream inhibitor of the pro-survival protein kinases Akt and Erk1/2, its degradation by calpain-1 maintains Akt and Erk1/2 in the active state and in turn contributes to neuronal survival. Stimulation of synaptic NMDA receptors can also induce long-term neuroprotection by modulating expression of pro-survival and pro-death genes. These long-term neuroprotective mechanisms are discussed below.

1.3.3.1 Stimulation of pro-survival genes

Calcium ions entering cells via the synaptic NMDA receptors can propagate to the nucleus to regulate expression of genes that provide neuroprotection [reviewed in (Bading, 2013)]. Transcriptome analyses revealed that in hippocampal neurons nearly 200 genes are controlled by nuclear Ca^{2+} signalling. The genes directing the expression of nuclear

CaMKIV and the transcription factor CREB are two of the examples (Hardingham et al., 1997; Kwok et al., 1994). CaMKIV is an upstream regulatory kinase phosphorylating and activating CREB to promote neuronal survival, synaptic plasticity, neurogenesis, learning and memory. Being a transcription factor, CREB enhances the expression of genes that protect against apoptotic and neurotoxic insults (Mayr and Montminy, 2001). Among the genes regulated by CREB are the activity-regulated inhibitors of death (AID) genes, which provide neuroprotection in cultured neurons and in animal models of neurodegeneration (Tan et al., 2012; Zhang et al., 2009). All these CREB target genes are believed to provide neuroprotection by rendering mitochondria more resistant to cellular stress and neurotoxic insults (Lau and Bading, 2009; Leveille et al.; Zhang et al., 2011). The *Bdnf* gene encoding the neurotrophin brain-derived neurotrophic factor (BDNF) is another prominent target of synaptic NMDA receptor-stimulated nuclear Ca^{2+} -CREB signalling pathway. BDNF is neuroprotective in different neurodegenerative diseases (Caccamo et al.; Iwasaki et al., 2012). Lau *et al.* demonstrated that elevated level of BDNF enhances the intracellular neuroprotective signalling of the synaptic NMDA receptor and reduces the neurotoxic signals of the extrasynaptic NMDA receptor (Lau et al., 2015), suggesting that stimulation of *Bdnf* gene transcription is a feed forward neuroprotective signalling mechanism shielding neurons from cellular damage in neurological disorders.

1.3.3.2 Suppression of pro-death genes

Another mechanism whereby synaptic NMDA receptors mediate neuroprotection is by suppressing the expression of pro-death genes (Lau and Bading, 2009; Leveille et al.). For example, synaptic NMDA receptor activity suppresses the expression of the pro-apoptotic Bcl-2 homology domain 3 (BH3)-only member gene (*Puma*) *in vitro* and *in vivo* and provides neuroprotection (Leveille et al., 2010). Suppression of *Puma* by synaptic NMDA receptors inhibit the apoptotic cascade upstream of cytochrome c as well as apoptotic protease activating factor 1 (APAF1) and pro-caspase 9. Synaptic NMDA receptor activity also suppresses the expression and/or activity of important pro-death transcription factors such as the forkhead box protein O (FOXO) class of transcription factors (Dick and Bading, 2010). In neurons undergoing excitotoxic cell death, FOXOs are constitutively located in the nucleus where they activate pro-apoptotic genes such as the BH3-only genes *Noxa*, Bcl-2-interacting mediator of cell death (*Bim*) and *Puma*, Fas ligand (*Fasl*) and thioredoxin-

interacting protein (*Txnip*). Synaptic NMDA receptor activity promotes sustained activation of Akt, leading to the phosphorylation and nuclear export of FOXO and the subsequent inactivation of the pro-death FOXO target genes (Davila et al., 2012; Kim et al., 2014; Papadia et al., 2008; Shinoda et al., 2004).

1.3.3.3 Antioxidant activity

Synaptic NMDA receptors also provide antioxidant activity to protect neurons from detrimental effects during hypoxic condition. Stimulation of synaptic NMDA receptors can transcriptionally modulate expression of enzymes in thioredoxin–peroxiredoxin system and glutathione biosynthesis to exert the protective effects (Baxter et al., 2015; Papadia et al., 2008).

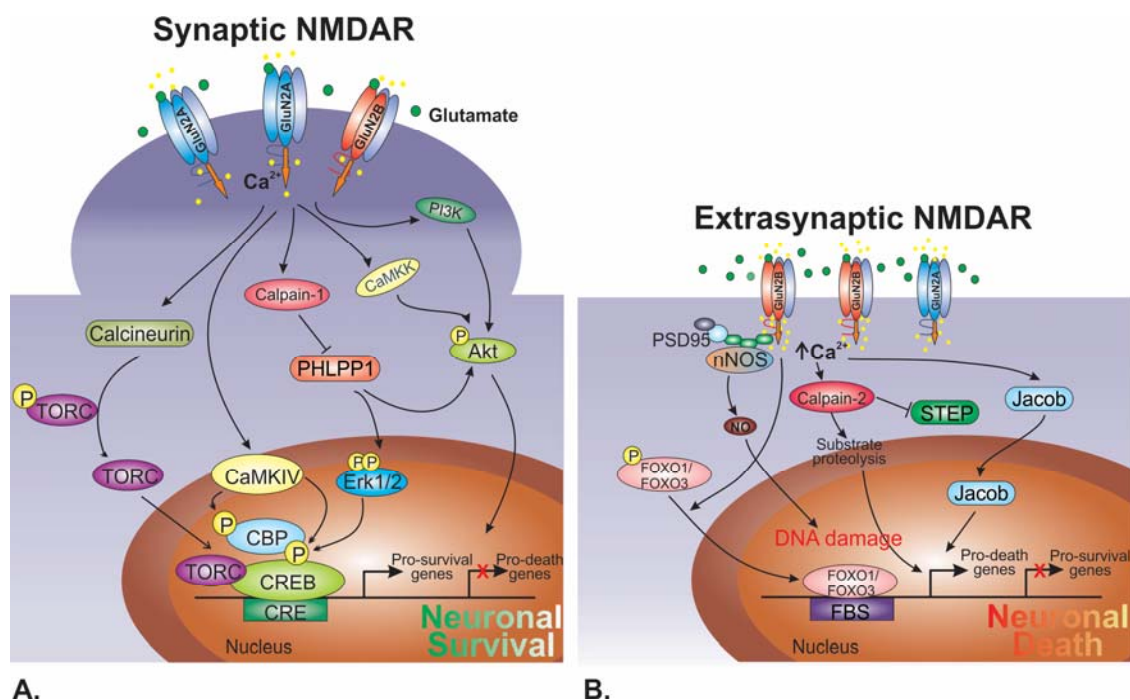


Figure 1.4 Opposing roles of synaptic and extrasynaptic NMDA receptors for governing neuronal survival. **A.** Neurotrophic signals from synaptic NMDA receptors maintain neuronal survival. Synaptic NMDAR stimulates calpain-1 that degrades PHLPP1 and activates downstream Akt and Erk1/2 pro-survival pathways. Ca^{2+} influx via the synaptic NMDA receptor also enters the nucleus where it activates CaMKIV. Both CaMKIV and Erk1/2 phosphorylate and activate CREB to induce expression of pro-survival genes. Calcineurin dependent dephosphorylation of TORC and its nuclear translocation also helps CBP to CREB binding. The pro-survival kinase Akt is activated by NMDAR induced PI3K activation or Ca^{2+} /calmodulin-dependent kinase kinase (CaMKK) activation. Akt maintains neuronal survival in part by suppression of apoptotic FOXOs by phosphorylation and in turn prevents its nuclear export. **B.** Ca^{2+} influx via the over-stimulated extrasynaptic NMDA receptors activates calpain-2, nNOS and NOX2 (not shown) to initiate the pro-death signalling pathways. Excessive NO and reactive oxygen species produced by nNOS and NOX2 leads to DNA damage and cooperate with the activated calpains to activate a number of pro-death cellular events. Some of these events include (i) stimulation of FOXO nuclear import and transcription of pro-death genes (e.g. *Foxo1*, *Txnip*, *Bim*, *Fasl* etc.), (ii) translocation of Jacob to nucleus where it enhances dephosphorylation of CREB to inhibit transcription of pro-survival genes, (iii) dephosphorylation and activation of DAPK leading to further increase in conductance of extrasynaptic NMDA receptors (not shown) and (iv) limited proteolysis of STEP to abolish its neuroprotective function. *Abbreviations not listed in text. CRE, cAMP response element; CBP, CREB binding protein; TORC, Transducer of regulated CREB activity; FOXO, forkhead box protein O; BAD, Bcl2-associated death promoter; Txnip, thioredoxin-interacting protein; Fasl, Fas ligand; Bim, Bcl2-interacting mediator of cell death; Jacob, juxta synaptic attractor of caldendrin on dendritic boutons proteins.*

1.3.4 Pro-death signals from extrasynaptic NMDA receptors

There are multiple routes of calcium entry into the cytosol of neurons. The route of entry is the major determinant governing whether the calcium influx activates the neurotoxic or neuroprotective signalling pathways. The most convincing evidence supporting this notion was provided by Sattler *et al.* who use different pharmacological agents to inhibit the different routes of calcium entry into neurons in excitotoxicity. They found that entry of calcium through the voltage dependent calcium channels (VDCC) does not confer cell death whereas entry of calcium through other receptors such as NMDA receptors stimulates the cell death cascade (Sattler *et al.*, 1998). Because of its high permeability to Ca^{2+} , NMDA receptors were found to be the major contributors to Ca^{2+} dependent neuronal death in excitotoxicity (Choi, 1987). These findings were later confirmed by Mattson who demonstrated that antagonists of NMDA receptors are neuroprotective in glutamate induced excitotoxic neuronal cell death (Mattson, 2003). It is now clear that calcium ions entering neurons through the over-stimulated extrasynaptic GluN2B subunit-containing NMDA receptors over-activate calpain-2 and nNOS to direct neuronal death (**Figures 1.2, 1.3 and 1.4**).

The over-activated calpains catalyse limited proteolysis of a selective group of neuronal proteins to irreversibly modify their biological functions [reviewed in (Hara and Snyder, 2007; Liu *et al.*, 2008)]. Calpains are unique proteases that cleave their protein substrates at one or a small number of specific sites. The resultant truncated fragments either lose some activities or may acquire new biological functions. For example, colleagues in our lab previously demonstrated that in neurons undergoing excitotoxic cell death, the over-activated calpains specifically cleave the non-receptor Src tyrosine kinase at a specific site near the N-terminus to generate a truncated Src fragment (Src Δ N) (Hossain *et al.*, 2013). Src Δ N then directs neuronal death by selectively phosphorylating unknown neuronal protein substrates (Hossain *et al.*, 2015; Hossain *et al.*, 2013). Piatkov *et al.* provided evidence that calpains cleave its substrates at specific sites such that the C-terminal segments of the resultant cleavage are short-lived and subjected to degradation by the N-end rule ubiquitin-proteasome pathway (Piatkov *et al.*, 2014). Thus, in addition to modifying the functions of their protein substrates, calpains can also modify their stability in cells.

In acute excitotoxicity occurring in neurons in ischemic penumbra, over-stimulation of the extrasynaptic NMDA receptor enhances binding of the C-terminal domain of GluN2B subunit to the scaffolding protein PSD95 (Aarts et al., 2002). As PSD95 forms protein complexes with nNOS and NADPH oxidase 2 (NOX2) (Baxter et al., 2015; Chen et al., 2015), binding of GluN2B subunit to the PSD95/nNOS/NOX2 complexes recruits nNOS to the over-stimulated extrasynaptic NMDA receptor and in turn facilitates its over-activation by the influx of calcium through the receptor. The over-activated nNOS over-produces NO, which directly contributes to neuronal death by S-nitrosylation of specific cellular proteins involved in regulation of neuronal survival or indirectly contributes to neuronal death by oxidative damages [reviewed in (Nakamura et al., 2013)]. Recruitment of PSD95/nNOS/NOX2 complex to the over-stimulated extrasynaptic NMDA receptor facilitates activation of NOX2, leading to an increase in production of reactive oxygen species (ROS) (Chen et al., 2015). ROS reacts with NO to produce the reactive peroxynitrite (NO_3^-), which causes oxidative damage to induce neuronal death (**Figures 1.2 and 1.4**).

Besides binding PSD95/nNOS/NOX2, GluN2B subunit of the over-stimulated extrasynaptic NMDA receptors also binds the death-associated protein kinase (DAPK). The binding site is mapped to C-terminal tail of GluN2B and it does not overlap with that of PSD95 (Tu et al., 2010), suggesting the extrasynaptic NMDA receptor can potentially form a pro-death signalling complex containing multiple mediators to mediate its neurotoxic signals. Upon binding to the NMDA receptors, DAPK is activated by dephosphorylation by calcineurin. The active DAPK phosphorylates Ser-1303 of the GluN2B subunit, leading to increased conductance and in turn Ca^{2+} influx of the extrasynaptic NMDA receptors (Tu et al., 2010). In addition to strengthening the neurotoxic signals of extrasynaptic NMDA receptor, DAPK can also phosphorylate or indirectly activate a number of intracellular neurotoxic proteins including tau and JNKs to exert its cytotoxic effects (Eisenberg-Lerner and Kimchi, 2007; Wu et al., 2011). Thus, DAPK binding to GluN2B subunit to activate the extrasynaptic NMDA receptor is a pathologically activated event contributing neuronal death in excitotoxicity.

Both over-activation of calpains and enhanced binding of GluN2B subunit to the PSD95/nNOS/NOX2 complex are also neurotoxic cellular events in A β -induced slow excitotoxicity in Alzheimer's disease (Ittner et al., 2010). These findings suggest that pharmacological agents blocking these events are effective in reducing excitotoxicity-induced neuronal loss in both acute and chronic neurological disorders.

1.3.5 Calpains: major executors of neuronal death

Calpains (*Calcium*-dependent protease with *papain*-like activity) are a group of calcium-dependent proteases with papain-like activity (Guroff, 1964). They are cysteine proteases activated at neutral pH by calcium in the cytoplasm (Croall and Ersfeld, 2007). Calpains contain a cysteine protease domain carrying a conserved catalytic “Cys-His-Arg” motif along with a calmodulin-like Ca^{2+} binding site (Nakagawa et al., 2001). In the human genome, as many as 15 genes (namely *CAPN1-15*) are reported to encode calpains and calpain-like proteases. Among these ubiquitous and tissue-specific isoforms, μ -calpain and m-calpain (referred to as calpain-1 and calpain-2, respectively) are abundantly expressed in the CNS (Goll et al., 2003). Both calpain-1 and calpain-2 are heterodimers consisting of a 80kDa catalytic subunit encoded by the *CAPN1* and *CAPN2* genes, respectively and a common 26 kDa regulatory subunit encoded by the *CAPN4* (also referred to as *CAPNS1*) gene [reviewed in (Campbell and Davies, 2012)]. In the absence of the regulatory subunit, the protease activity of the catalytic subunits of these two calpains is eliminated (Arthur et al., 2000).

To decipher the functional role of calpain-1 and calpain-2 in controlling neuronal survival in pathological conditions, Amini *et al.* generated a mouse model of conditional disruption of the *CAPNS1* gene, which encode the common regulatory subunit of both calpains in CNS (Amini et al., 2013). Using this mouse model, they demonstrated that elimination of the activity of calpain-1 and/or calpain-2 as a result of knock-down of *CAPNS1* gene can protect against neuronal death caused by excitotoxicity and mitochondrial toxicity, indicating that one or both of the two calpains direct neuronal death in excitotoxicity (Amini et al., 2013). The distinct functional role of calpain-1 and calpain-2 in physiological and pathological conditions were investigated by Wang *et al.* who used calpain-1- and calpain-2-specific inhibitors and siRNAs to selectively suppress the activity or expression of the two calpains in neurons (Wang et al., 2013). They demonstrated that calpain-1 is preferentially activated by the GluN2A subunit-containing synaptic NMDA receptors. The activated calpain-1 contributes to neuronal survival by selectively degrading the protein phosphatase PHLPP1 α and PHLPP1 β , which dephosphorylate and inhibit the pro-survival protein kinase Akt (**Figure 1.4**). In contrast, stimulation of the GluN2B subunit-containing extrasynaptic NMDA receptor selectively activates calpain-2, which contributes to neuronal death by

degrading the protein tyrosine phosphatase STEP. Since STEP binds to and dephosphorylates the pro-death protein kinase p38 (Deb et al., 2013), its degradation by calpain-2 is a key step in the neurotoxic signalling pathways directing neuronal death in excitotoxicity (**Figures 1.3 and 1.4**). Taken together, these results suggest that calpain-1 is functionally coupled to the synaptic GluN2A subunit-containing NMDA receptor to maintain neuronal survival while calpain-2, activated by the extrasynaptic GluN2B subunit-containing NMDA receptor, is an executor of neuronal death in excitotoxicity. The biochemical basis of specific functional coupling of the two calpains to the synaptic and extrasynaptic NMDA receptors remains unclear. Presumably, the specific functional coupling is achieved either by co-localisation and/or physical association of the two calpains with their respective NMDA receptors. Indeed, Wang *et al.* demonstrated that stimulation of the synaptic NMDA receptor recruits calpain-1 from the cytosol to a complex containing the Glu2A subunit-containing synaptic NMDA receptor and PHLPP1 (Wang et al., 2013). Since calpain-1 contains a mitochondrial targeting sequence, a portion of it is imported to the mitochondria and resides in the intermembrane space (Badugu et al., 2008), Yamada *et al.* reported that deficiency of calpain-1 could attenuate caspase 3 activation, release of AIF and mitochondrial membrane permeability of neurons induced by 6 h treatment with H₂O₂ *in vitro* (Yamada et al., 2012). They also demonstrated that calpain-1-deficient mice exhibited significantly less brain damage and neural degeneration than those of wild type mice 24-48 h after traumatic brain injury. Their results suggest that calpain-1 is involved in the late phase of neuronal death caused by mitochondrial dysfunction. Further investigation is needed to clearly define the regulation and function of these two isoforms of calpains at different stages of excitotoxic neuronal death.

1.3.6 Calpain substrates participating in neuronal death

A number of neuronal proteins have been found to be cleaved by the over-activated calpains in neurons undergoing excitotoxic cell death. The cleavage leads to their aberrant regulation or premature degradation (Vosler et al., 2008). For example, both α -fodrin and microtubule-associated protein 2 (MAP2) are two major structural proteins that undergo limited proteolysis by over-activated calpains (Bernath et al., 2006; Kieran and Greensmith, 2004; Pettigrew et al., 1996). In this literature review chapter, our discussion is focused on the calpain substrates that fulfil two criteria: (i) their cleavage occur specifically during

pathological conditions such as ischaemic stroke but not in physiological conditions and (ii) their cleavage by calpain contributes to neuronal death in excitotoxicity. Calpain substrates fulfilling these two criteria are listed in **Table 1.1**. They can be divided into four groups. The first group including NCX3, TRPC6, STEP and mGluR α -1 are receptor or receptor-like key neuroprotective signalling proteins. Their cleavage by calpains either abolishes their neuroprotective functions or leads to their early degradation. The second group contains Ca²⁺/calmodulin binding proteins or their regulatory signalling molecules such as calcineurin and cain/cabin1. Third group contains protein tyrosine kinases or phosphatases such as Src and STEP, and the fourth group contains epigenetic regulator CRMP3. They all acquire neurotoxic activities upon cleavage by calpain and they are discussed below.

1.3.6.1 Metabotropic glutamate receptors-1 (mGluR α -1)

Unlike the extrasynaptic NMDA receptor, mGluR α -1 is a neuroprotective glutamate receptor. It exerts its neuroprotective action by direct binding and activating phosphatidylinositol-3-kinase (PI3K), which catalyses the biosynthesis of the pro-survival phospholipid second messenger phosphatidylinositol-3,4,5-trisphosphate [PI(3,4,5)P₃]. PI(3,4,5)P₃ then activates Akt to maintain neuronal survival. During excitotoxicity, the over-activated calpains selectively cleave mGluR α -1 near its C-terminus. The cleavage abolishes the neuroprotective function of mGluR α -1 by removing the C-terminal domain that contains the PI3K binding motif (Xu et al., 2007). A cell permeable peptide containing the calpain cleavage site in mGluR α -1 was designed and synthesised. This peptide termed Tat-mGluR1 blocks calpain cleavage of mGluR α -1 in cultured neurons. More importantly, the blockade protects against excitotoxic neuronal death (Xu et al., 2007).

Table 1.1 Some of the calpain substrates that participate in regulation of neuronal survival.

Substrates	Functional consequences	Neuroprotective calpain inhibitory peptide	References
1. Receptor or receptor-like proteins			
Metabotropic glutamate receptor-1 (mGluR1)	Removal of the C-terminal tail that governs the binding and activation of PI3K	Tat-mGluR1	(Xu et al., 2007)
Na ⁺ /Ca ²⁺ exchanger (NCX3)	Calpain cleavage removes its C-terminus, preventing NCX3 to direct efflux of calcium from the cytosol to the extracellular compartment.	Not examined	(Bano et al., 2005)
Kidins200/ARMS – an adaptor protein mediating cross-talks of receptors TRPC6	Calpain cleavage prevents Kidins200/ARMS from coupling the NMDAR to the neuroprotective Eph receptor and Trk receptor Calpain-mediated cleavage generates the truncated TRPC6, which is incapable of activating the CREB signalling pathway to maintain neuronal survival.	Tat-K (with residues 1668-1681 of Kidins200/ARMS) Tat-C6 peptide, which blocks calpain-mediated cleavage of TRPC6, protects against ischaemic stroke-induced brain damage.	(Gamir-Morralla et al., 2015) (Du et al., 2010)
2. Calcium/CaM binding proteins and their regulators			
Calcineurin (CaN)	Calpains cleaved CaN at multiple sites. Two of the cleavage products are constitutively active The activated CaN dephosphorylate several neuronal proteins including Drp1, BAD, NFAT and huntingtin to cause neuronal death.	The authors did not design CaN-specific calpain inhibitors.	(Shioda et al., 2006; Slupe et al., 2013; Wu et al., 2004)

Table 1.1 (continued)

Substrates	Functional consequences	Neuroprotective calpain inhibitory peptide	References
Cain/Cabin1	Calpain cleavage at the Calcineurin-binding site abolishes its ability to inhibit calcineurin	The authors did not design Cain-specific calpain inhibitors.	(Kim et al., 2002)
3. Protein tyrosine kinases & phosphatases			
Src	Calpains cleave Src at the N-terminal unique domain to generate a truncated Src fragment. The truncated Src fragment generates neurotoxic signals to induce neuronal death.	A cell membrane-permeable Tat-Src peptide derived from the cleavage site in Src is neuroprotective.	(Hossain et al., 2013)
Striatal-Enriched Protein Tyrosine Phosphatase (STEP)	Calpains cleave STEP at Ser-223 in the substrate-binding domain to abolish the ability of STEP to bind and dephosphorylate its substrates	The cell membrane-permeable TAT-STEP peptide is neuroprotective.	(Deb et al., 2013; Xu et al., 2009)
4. Epigenetic regulator			
Collapsin response mediator protein 3 (CRMP3)	Calpain cleavage generates a 54 kDa truncated CRMP3, which translocates to nucleus. This truncated product deacetylates histone H4 to cause nuclear condensation and neuronal death	The authors did not design CRMP3-specific calpain inhibitors.	(Hou et al., 2013; Hou et al., 2006)

1.3.6.2 Na⁺/Ca²⁺ exchanger 3 (NCX3), plasma membrane calcium ATPase (PMCA) and Transient receptor potential cation channel C6 (TRPC6)

Over-activated calpain(s) can contribute to neuronal death during cerebral ischemia by cleaving several proteins involved in the control of calcium influx and efflux: NCX3 (Bano et al., 2005), PMCA (Pottorf et al., 2006) and TRPC6 (Du et al., 2010). NCX3, a major plasma membrane calcium extrusion system in neurons, can prevent calcium overload by facilitating efflux of calcium from the cytosol to the extracellular space. In excitotoxic conditions, calpains cleave NCX3 at several sites and the cleavage abolishes its ability to extrude calcium out of neurons and in turn contributes to calcium overload in neurons (Bano et al., 2005). Besides NCX3, calpains also cleave PMCA in neurons to enhance its internalisation in neurons. Down-regulation of PMCA further reduces the ability of neurons to extrude calcium in excitotoxicity (Pottorf et al., 2006). TRPC6, a calcium permeable non-selective cation channel, exerts its neuroprotective function by suppressing calcium load via the over-stimulated NMDA receptor in neurons in excitotoxicity (Li et al., 2012). In neurons undergoing excitotoxic cell death, calpains cleave TRPC6 at a specific site near its N-terminus to abolish its neuroprotective ability. A cell permeable synthetic peptide (Tat-C6) derived from the calpain cleavage site in TRPC6 selectively blocks truncation of TRPC6 by calpain in neurons and protects against excitotoxic neuronal death. These results indicate that TRPC6 is an important neuroprotective enzyme in neurons and its cleavage by calpains is a key event underpinning excitotoxic neuronal death (Du et al., 2010).

1.3.6.3 Kidins220/ARMS

Kidins220/ARMS (Kinase D-interacting substrate of 220 kDa/ankyrin repeat-rich membrane spanning) is a transmembrane scaffolding protein mediating cross-talks of receptors. In neurons, it couples the NMDAR to the neuroprotective Eph receptor and Trk receptor, facilitating the activation of neuroprotective protein kinase Erk1/2, whereas in neurons undergoing excitotoxic neuronal death, Kidins220/ARMS is cleaved by calpains (Gamir-Morralla et al., 2015). More importantly, cleavage of Kidins220/ARMS by calpains is a key step in excitotoxic neuronal death. Exactly how this cleavage process directs neuronal death remains unclear. A cell membrane-permeable synthetic peptide (Tat-K) derived from the calpain cleavage sequences and containing residues 1668-1681 of Kidins220/ARMS, was able to protect against excitotoxic neuronal death. The findings

suggest that cross-talk between NMDA receptor and Kidins220/ARMS is critical to neuronal survival (Gamir-Morralla et al., 2015).

1.3.6.4 Calmodulin-dependent protein kinase and phosphatase

Calpain also cleaves two important calcium/calmodulin regulated enzymes: Ca²⁺/calmodulin-dependent protein kinase type IV (CaMKIV) and the protein phosphatase calcineurin (CaN) (Jayanthi et al., 2005; Mukherjee and Soto, 2011; Shioda et al., 2007; Shioda et al., 2006; Tremper-Wells and Vallano, 2005). Calpain cleavage irreversibly activates CaN by deletion of its auto-inhibitory domain. This constitutively active truncated CaN induces neuronal death by dephosphorylating the pro-mitochondrial fission protein dynamin-related protein 1 (Drp1) (Slupe et al., 2013), Bcl-2-associated death promoter (BAD), huntingtin and nuclear factor of activated T-cells (NFAT) (Mukherjee and Soto, 2011). Among these substrates, Drp1 and BAD are directly involved in mitochondrial dysfunction in excitotoxicity. Upon dephosphorylation by CaN, Drp1 is translocated from the cytosol to the mitochondria where it directs mitochondrial fragmentation and in turn contributes to neuronal death induced by oxygen-glucose deprivation *in vitro* (Slupe et al., 2013). CaN dephosphorylates BAD to enhance its heterodimerisation with another pro-apoptotic mitochondrial protein Bcl-xl to promote neuronal death (Wang et al., 1999).

CaN activity is tightly controlled in cells. Cain (also referred to as cabin1) is a major endogenous inhibitor of CaN in neurons. The over-activated calpains can potentially cleave cain at the CaN-binding site to abolish its ability to inhibit CaN in neurons undergoing excitotoxic neuronal death (Kim et al., 2002).

CaMKIV is a major component of the neuroprotective signalling pathways originating from the synaptic NMDA receptor. Upon activation by calcium in nucleus, CaMKIV phosphorylates and activates CREB, which direct the expression of genes that promote neuronal survival (**Figure 1.4**). Calpain cleavage of CaMKIV down-regulates the CaMKIV/CREB neuroprotective signalling (Tremper-Wells and Vallano, 2005).

1.3.6.5 Protein tyrosine kinase Src

Src is an important protein tyrosine kinase critical to neuronal survival under physiological conditions (Hossain et al., 2015). In neurons undergoing excitotoxic neuronal death, Src is

selectively cleaved by the over-activated calpains to generate a neurotoxic truncated Src fragment (**Figure 1.3**) (Hossain et al., 2013). The truncated Src fragment directs neuronal death by inactivating Akt. Blockade of calpain cleavage of Src by a cell-permeable peptide inhibitor (Tat-Src) derived from the calpain cleavage site in Src could protect against excitotoxic neuronal death (Hossain et al., 2013).

1.3.6.6 Pro-survival and pro-apoptotic proteins

Several mitochondrial proteins involved in regulation of cell survival including Bcl-2-associated X-protein (Bax) and the Bcl2-interacting protein (Bid) are cleaved by calpains. Calpain cleaves Bax to generate an 18-kDa truncated fragment which is a more potent inducer of neuronal death than intact Bax (Choi et al., 2001). In cancer cells, the pro-apoptotic Bid protein is cleaved by calpain between Gly-70 and Arg-71 to generate a truncated Bid with its BH3 domain intact. This truncated Bid protein somehow induces mitochondrial cytochrome c release and apoptosis (Mandic et al., 2002). Further work is needed to establish if Bid is a substrate of calpains in neurons and whether calpain cleavage of Bid contributes to excitotoxic neuronal death.

1.3.6.7 Apoptosis inducing factor (AIF)

Mitochondrial AIF is a 62-kDa flavoprotein NADH oxidase residing in the mitochondrial-inner membrane in close proximity of complex I and the cytosolic side of the mitochondrial outer membrane (Yu et al., 2009). It is a key player of caspase-independent cell death (Loeffler et al., 2001; Susin et al., 1996). Experimental evidence suggests that AIFs residing in both mitochondrial compartments are involved in excitotoxic neuronal death. As calpain-1 contains a mitochondrial targeting sequence near its N-terminus, it can potentially enter mitochondria and reside in mitochondrial inter-membrane space where it cleaves AIF bound to the inner mitochondrial membrane to generate the truncated AIF (tAIF) (Norberg et al., 2008). Indeed, several groups of researchers demonstrated in a rat model of transient global ischemia and in isolated mitochondria, that calpain-1 cleaves AIF at the N-terminus to form a 57-kDa pro-apoptotic fragment (tAIF) (Cao et al., 2007; Polster et al., 2005). tAIF translocates to the nucleus to induce chromatin condensation and DNA fragmentation. Exactly how tAIF and intact AIF in the nucleus induce DNA fragmentation and chromatin condensation remains unclear.

Approximately 30% of the mitochondrial AIFs are loosely bound to the cytosolic side of the mitochondrial outer membrane (Yu et al., 2009). In excitotoxicity, oxidative damage of DNA by ROS and reactive nitrogen species activates the nuclear enzyme poly(ADP-ribose) (PAR) polymerase-1 (PARP-1) (Wang et al., 2009a), which generates excess PAR. PAR released from the nucleus to the cytosol can bind AIF on the mitochondrial outer membrane with high affinity to trigger their release from the mitochondria (Wang et al., 2011) (**Figure 1.3**). Unlike the release of AIFs residing in the inner mitochondrial membrane, the release of the outer membrane-bound AIFs to the cytosol is solely dependent on PAR-binding and is independent of cleavage by calpains (Wang et al., 2009b). Once they are released from the mitochondria, these intact AIFs can translocate into nucleus to exert their neurotoxic action (Wang et al., 2011). These findings suggest that PAR binding to mitochondrial AIF is a pathologically activated cellular event. Inhibitors blocking the PAR/AIF interaction are potential therapeutics to reduce excitotoxic caspase-independent neuronal death in acute and chronic neurological disorders [reviewed in (Delavallee et al., 2011)].

1.3.6.8 Collapsin response mediator protein 3 (CRMP3)

CRMP3, a novel histone H4 deacetylase is cleaved by over-activated calpain in neurons undergoing excitotoxic neuronal death (Hou et al., 2013; Hou et al., 2006). Under physiological conditions, full-length CRMP3 does not exhibit histone H4 deacetylase activity and resides in the cytosol. Upon cleavage by calpains at a site near the N-terminus, the truncated CRMP3 translocates into the nucleus where it exhibits robust histone H4 deacetylase activity, induces nuclear condensation and neuronal death (Hou et al., 2013). Exactly how histone H4 deacetylation caused by the truncated CRMP3 contributes to nuclear condensation and neuronal death remains unclear. Nevertheless, these results suggest that blockade of calpain cleavage of CRMP3 is potentially a neuroprotective mechanism.

1.3.6.9 Striatal-enriched protein tyrosine phosphatase (STEP)

STEP, a brain-specific protein tyrosine phosphatase enriched in endoplasmic reticulum and postsynaptic termini exerts both neuroprotective and neurotoxic effects by dephosphorylates protein substrates in both the pro-survival and pro-death signalling pathways. Specifically, it targets the conserved activating tyrosine phosphorylation site in the activation loop of

ERK1/2 and p38 MAPK operating in the pro-survival and pro-death signalling pathways, respectively (Xu et al., 2009). Upon over-stimulation of the extrasynaptic NMDA receptors, STEP (also referred to as STEP₆₁) is selectively cleaved by calpains at the peptide bond between Ser-224 and Leu-225 to generate a truncated STEP of 33-kDa (STEP₃₃) (**Figure 1.3**). The cleavage abolishes the ability of STEP to dephosphorylate its substrates. Since STEP₃₃ is unable to dephosphorylate and inactivate the neurotoxic p38 MAPK, calpain cleavage of STEP contributes to neuronal death. This notion is confirmed by the ability of a cell membrane-permeable Tat-STEP peptide derived from the calpain cleavage site in STEP to protect cultured neurons against excitotoxic cell death (Xu et al., 2009). In a subsequent study, Deb, *et al.* used a cell membrane-permeable Tat-STEP-myc fusion protein containing the segment from residues 173-279 to demonstrate that blockade of calpain cleavage of STEP activates p38 MAPK and reduces ischemic stroke-induced brain damage in rats (Deb et al., 2013). The results indicate that calpain cleavage is a proteolytically activated cellular event directing neuronal death in excitotoxicity.

1.3.7 JNK3 and p38 are key mediators of neuronal demise

The c-Jun N-terminal kinases (JNKs) and p38 mitogen-activated protein kinase (p38) are key mediators of the neurotoxic signals originated from the over-stimulated extrasynaptic NMDA receptors and other neurotoxic glutamate receptors [(Borsello et al., 2003; Centeno et al., 2007; Soriano et al., 2008) and reviewed in (Coffey, 2014)]. They are activated by canonical upstream protein kinases in response to stress-activated and pro-death signals originated from cell surface death receptors and intracellular oxidative stress signals such as ROS and NO [reviewed in (Bogoyevitch et al., 2010; Coffey, 2014; Lai et al., 2014)].

How neuronal JNKs and p38 are activated and how blockade of their activation protect against excitotoxic neuronal loss in acute and chronic neurological disorders? Three isoforms of JNKs (JNK1, JNK2 and JNK3) are expressed in mammalian brain cells. Gene knock-out studies revealed that JNK3 is a key mediator of neurotoxic signals in excitotoxicity (Pirianov et al., 2007; Yang et al., 1997). In comparison with wild type mice, *JNK3* knockout mice exhibited reduced excitotoxic neuronal death and seizure activity caused by over-activation of the kainate receptor (Yang et al., 1997) and reduced neuronal loss caused by hypoxic ischemic injury (Pirianov et al., 2007). The signalling pathway governing activation of neuronal JNK3 in excitotoxicity has not been clearly defined. JNK3

is activated by a canonical protein kinase cascade. Specifically, its activation requires phosphorylation of the conserved threonine and tyrosine in the activation loop by the upstream activating kinases mitogen-activated protein kinase kinase 4 (MKK4) and mitogen-activated protein kinase kinase 7 (MKK7) (Centeno et al., 2007), with MKK4 and MKK7 preferentially targeting the tyrosine and threonine, respectively (Lawler et al., 1998; Wada et al., 2001). MKK4 and MKK7 are activated by a number of upstream protein kinases in different cell types in response to cellular stress and death receptor activation. Among these upstream kinases of MKK4/7, dual leucine zipper kinase (DLK) (Pozniak et al., 2013) and mixed lineage kinase 3 (MLK3) (Hu et al., 2012) were found to be involved in activating JNK in ischemic stroke.

Using the conditional *DLK* knockout mice as the tools, Pozniak *et al.* demonstrated that DLK-deficiency significantly reduces JNK activation and neuronal loss induced by over-stimulation of the kainate receptors (Pirianov et al., 2007). They also found that DLK is targeted to the post-synaptic density and interacts with PSD95. Exactly how DLK is activated upon over-stimulation of kainate receptor remains unclear.

MLK3 is activated in mouse brain following global ischemia (Hu et al., 2012). Biochemical analysis revealed that the activation is initiated by S-nitrosylation of MLK3 at Cys-688 by NO. Upon S-nitrosylation, MLK3 undergoes dimerisation and autophosphorylation, leading to its activation. These results suggest that activation of JNK by the MLK3-MKK4/7 signalling pathway is a consequence of over-activation of nNOS bound to the extrasynaptic NMDA receptors in excitotoxicity (**Figure 1.3**). Since Tat-NR2B9c blocks binding and activation of PSD95/nNOS to the over-stimulated extrasynaptic NMDA receptors (Aarts et al., 2002), treatment with Tat-NR2B9c is expected to suppress over-production of NO, S-nitrosylation and activation of MLK3 and activation of JNKs. However, in contrast to this prediction, Tat-NR2B9c did not inhibit activation of neuronal JNK in excitotoxicity (Soriano et al., 2008). The conflicting evidence highlights the complexity of the upstream signalling mechanism in activation of JNKs in excitotoxicity. In the studies by Hu, *et al.*, significant increase in S-nitrosylation and autophosphorylation of MLK3 in the hippocampal neurons was obvious 3 h after cerebral ischemia/reperfusion, suggesting that activation of JNKs by the MLK3-MKK4/7 pathway occurs at a later stage of excitotoxicity (Hu et al., 2012). Future investigation to follow the time course of S-nitrosylation and autophosphorylation of MLK3 in cultured neurons upon over-stimulation of NMDA receptors will shed light on the role of MLK3 in mediating the activation of JNKs.

1.3.8 Cyclin-dependent protein kinase 5 (Cdk5)

The neuron-specific cyclin dependent kinase Cdk5 is a major mediator of neurotoxic signals originating from the over-stimulated extrasynaptic NMDA receptor in ischemic stroke (Meyer et al., 2014) and Alzheimer's disease (Lee et al., 2000). Structurally, active Cdk5 is a heterodimer formed by Cdk5 complexed with the 35-kDa activator protein called p35 [reviewed in (Lew and Wang, 1995)]. In neurons undergoing excitotoxic cell death p35 is cleaved by calpains to form a truncated fragment p25 of 25-kDa (Lee et al., 2000; Lew et al., 1994). Once formed, p25 confers neurotoxic function to Cdk5 by aberrant activation of its kinase activity and by directing Cdk5 to phosphorylate a particular subset of pathologically relevant protein substrates such as tau and GluN2A subunit of NMDA receptor (Lee et al., 2000; Wang et al., 2003). Intriguingly, in addition to conferring neurotoxic activity of Cdk5, p25 also binds and activates the neurotoxic protein kinase GSK3 β to induce neuronal damage (Chow et al., 2014). These findings suggest that calpain cleavage of p35 to form p25 and formation of the neurotoxic p25/Cdk5 and p25/GSK3 β complexes are pathologically activated cellular events directing neuronal death. In a recent study, a 24-residue peptide fragment (P5) derived from p35 was found to selectively inhibit the neurotoxic p25/Cdk5 but not p35/Cdk5 (Zheng et al., 2010). More importantly, a cell membrane-permeable version of P5 was effective in alleviating Alzheimer's disease pathology in a mouse model (Shukla et al., 2013).

1.3.9 Epigenetic modifications in neuronal death

In this section, the post-receptor nuclear events critically involved in ischemic stroke-induced neuronal loss are discussed. Central to these nuclear events is the REST/Sin3A/CoREST chromatin modifying complex, which functions as a key mediator controlling pro-survival and neurotoxic signalling pathways. Investigation of how dysregulation of the REST/Sin3A/CoREST complex contributes to neuronal loss will benefit the design and development of small-molecule inhibitors of this complex as neuroprotective therapeutics to reduce ischaemic stroke-induced brain damage.

1.3.9.1 REST, Sin3A and CoREST chromatin modifying complex

REST (Repressor Element 1-Silencing Transcription factor), encoded by the *REST* gene in humans, functions as a sequence-specific master transcriptional repressor of neuronal genes in pluripotent stem cells and neuronal progenitor cells in embryonic development (Ooi and Wood, 2007). However, REST is kept in the quiescent state once neuronal differentiation occurs to allowing the expression of neuron-specific proteins in neurons.

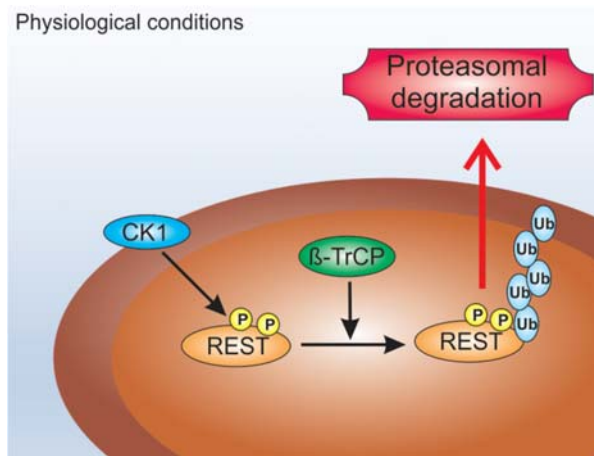
REST knockout mice displayed widespread apoptotic death, resulting in malformations of the developing nervous system and restricted growth (Chen et al., 1998). Reactivation of quiescent REST frequently occurs in vulnerable neurons after ischaemic insults (Noh et al., 2012), allowing REST to modulate expression of specific proteins that are critical to neuronal function and survival. Thus, in normal physiological conditions, the REST-mediated transcriptional repressive function is tightly controlled for proper neuronal differentiation and maintenance of cell survival. Dysregulation of REST can cause neuronal cell death.

Being a member of the Gli/Kruppel-type zinc finger transcription factor family, REST contains 8 C2H2 zinc fingers in its DNA binding domain. It directs gene repression by recruiting several chromatin-modifying enzymes to bind to Repressor Element 1 (also known as Neuron-Restrictive Silencer Element) in the target gene promoters (Chong et al., 1995; Schoenherr and Anderson, 1995). The chromatin-modifying enzymes directly associated with REST are Sin3A and CoREST, which bind to the amino- or carboxyl-terminus repressor domains of REST, respectively (Andres et al., 1999; Grimes et al., 2000). Common to both Sin3A and CoREST co-repressor complexes are the HDAC1 and HDAC2 histone deacetylase enzymes, which catalyse histone deacetylation to silence the target genes (**Figure 1.5**). In addition to binding HDAC, the CoREST/REST complexes recruit additional chromatin modifying enzymes such as histone H3K4 demethylase LSD1/KDM1A, histone H3K9 methyltransferase G9a/EHMT2, chromatin-remodelling enzyme ATP dependent RNA helicase BRG1/SMARCA4, and methyl-CpG-binding protein MeCP2 (**Figure 1.5**). It is clear that REST, together with two co-repressor complexes Sin3A and CoREST, functions in short-term transcription silencing of genes involved in the neuronal signalling. However, it is unknown how long-term gene silencing is achieved. The target chromatin modified by G9a-mediated enzymatic activity of CoREST/REST complex leads to the accumulation of histone H3 with dimethylation at lysine 9 (H3K9me2), which

acts as a signal of transcriptional silencing. H3K9me2 in the target chromatin acts as a binding pocket for Heterochromatin Protein 1 (HP1) proteins to form the high-order heterochromatin structure. MeCP2 in the REST/CoREST complex directly binds to methylated CpG to yield further compaction of the chromatin for long-term gene silencing. However, it is not known whether REST/CoREST binding is the primary or a secondary event leading to long-term gene silencing. It is plausible that DNA methylation by DNA methyltransferase (DNMT) is one of the earliest and essential steps contributing to long-term silencing of the target genes. The specific epigenetic mechanism for long term gene silencing is currently subjected to active research investigation.

Under physiological conditions, REST proteins are constantly being produced and turned over by the casein kinase 1 (CK1)-mediated β -TrCP dependent proteasome pathway in neurons (**Figure 1.5**). In this pathway, CK1 phosphorylates REST at sites in two motifs located near the C-terminus. Upon phosphorylation, REST binds the ubiquitin E3 ligase β -TrCP, which catalyses ubiquitination of REST and target REST for proteosomal degradation. In a rat model of global ischemia, CK1-mediated β -TrCP dependent proteasome pathway was significantly interfered, resulting in accumulation of REST proteins in the neuronal cells that silences REST target genes and resulting in neuronal cell death (Kaneko et al., 2014).

A.



B.

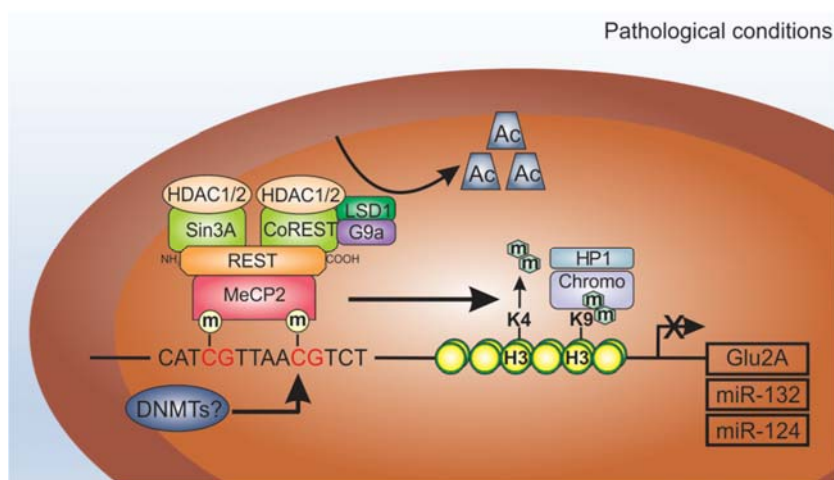


Figure 1.5 Model for REST-mediated transcriptional repression. **A.** Regulation of the abundance of REST by casein kinase I (CK1) and the ubiquitin E3 ligase β -TrCP in physiological conditions. **B.** Neurotoxic signals of REST in pathological conditions. Sin3A and CoREST are assembled into the REST corepressor complex via direct binding to the amino- or carboxyl terminus of REST respectively. REST also binds to MeCP2, which recognize the methylated CpG dinucleotides (highlighted in red) in target gene promoter. Methylation was catalyses by DNMTs. Sin3A recruits HDAC1 and HDAC2 for histone deacetylase activity. CoREST recruits HDAC1, HDAC2, LSD1 and G9A to elicit further histone deacetylase, H3K4 demethylase and H3K9 methyltransferase activity for gene silencing. Methylated H3K9 are recognized by chromodomain-containing HP1 protein, which functions in the formation of higher-order structure for chromatin compaction. Examples of key REST-regulated genes and miRNAs include Glu2A, miR-132, and miR-124. *Abbreviations:* Ac, acetyl; m, methyl; K4, lysine 4; K9, lysine 9; DNMTs, DNA methyltransferases; MeCP2, methyl CpG binding protein 2; REST, repressor element (RE)-1 silencing transcription factor; CoREST, corepressor for REST; HDAC1/2, histone deacetylases 1 and 2; LSD1, lysine (K)-specific demethylase 1A; G9a, histone-lysine 9 N-methyltransferase; HP1, heterochromatin protein 1; chromo, chromodomain.

1.3.9.2 REST gene and miRNA targets

REST targets at least 1000 neuronal specific genes, as predicted bioinformatically using RE1 consensus binding sites or based on ChIP-seq data (Rodenas-Ruano et al., 2012). The most notable one is the gene encoding the AMPA receptor Glu2A subunit, which has been implicated in ischemia. REST binding to Glu2A promoter suppresses Glu2A gene expression. As a result, AMPA receptor lacking Glu2A are permeable to calcium. Hence, REST activation contributes to excitotoxic neuronal death, in part by enhancing calcium influx through the AMPA receptor lacking the Glu2A subunit (Rodenas-Ruano et al., 2012).

In addition to the chromatin modifying activity on critical neuronal genes, REST also mediated repression of miR-132 expression in hippocampal neurons that are destined to die (Hwang et al., 2014). These findings suggest that over-expression of miR-132 can protect against ischemia-induced neuronal cell death. Future investigation focusing on defining the targets of miR-132 will shed light on its role in neuronal death. Besides miR-132, over-expression of another miRNA called miR-124 is also involved in epigenetic changes induced by focal cerebral ischemia (Doepfner et al., 2013). miR-124 has a unique expression pattern, where it is preferentially expressed in the CNS with 100 times higher abundance in the CNS than in other organs. miR-124 is negatively regulated by REST in neuronal precursor cells to allow transcription of non-neuronal genes to maintain stem cellness. During neuronal differentiation, ubiquitination and degradation of REST results in the increase expression of miR-124, which acts to repress non-neuronal transcripts to result in the acquisition of a neuronal phenotype. Cerebral ischemia resulted in the accumulation of REST-mediated miR-124 repression in cortical neurons, and that over-expression miR-124 restored REST to basal level, via the action of a novel Usp14-dependent REST degradation mechanism. In summary, the key established downstream effectors of REST undergo changes in expression levels in excitotoxicity are genes encoding Glu2A and miR124/132, which regulate calcium influx and post-translation negative feedback loop of neuronal gene expression (Doepfner et al., 2013).

Intriguingly, complete lack of REST expression enhances neuronal death induced by oxidative stress and A β stimulation (Lu et al., 2014). Furthermore, ChIP-seq analysis of REST-targets in SH-SY5Y cells reveals that REST represses expression of a number of genes involved in cell death. Examples of these genes include *p38MAPK*, *Bax* and *Bid*. Thus, in contrast to the findings by Rodenas-Ruano *et al.* which suggest that REST is

neurotoxic (Rodenas-Ruano et al., 2012), the studies by Lu, *et al.* suggest that REST is neuroprotective (Lu et al., 2014). The conflicting results from both studies imply that REST plays dual roles in controlling neuronal survival. At low expression level REST suppresses expression of apoptotic proteins to maintain neuronal survival, while at high expression level such as that in ischemic stroke it sensitises neurons to undergo excitotoxic neuronal death by suppressing the expression of Glu2A and miR124/132. Further studies are needed to clearly define the role of REST in neuronal survival in physiological and pathological conditions.

1.4 Pathologically activated cellular events as potential neuroprotective targets

Pan-antagonists directing all NMDA receptors are not suitable for use as neuroprotectants to reduce brain damage caused by excitotoxicity in acute and chronic neurological disorders because they can interfere with the normal physiological functions as well as suppress the pro-survival signals emanating from the synaptic NMDA receptors. Given that neurotoxic signals directing excitotoxic neuronal loss are originated from the over-stimulated extrasynaptic NMDA receptors, antagonists selectively targeting the extrasynaptic NMDA receptors only when they are over-stimulated are potential neuroprotectants (**Figure 1.6A**).

One of the major intracellular signalling pathways by which extrasynaptic NMDA receptors propagate their neurotoxic signals is by over-activation of calpains, which selectively cleaves specific cellular proteins to cause neuronal death (**Figure 1.6A**). **Table 1.1** lists the cellular proteins, which upon cleavage by calpains, contributes to excitotoxic neuronal death. Using cell-permeable synthetic peptides derived from the calpain cleavage sites, several neuroprotectant peptides have been developed.

Besides limited proteolysis of cellular proteins by the over-activated calpains, other post-translational modifications such as phosphorylation, S-nitrosylation and ubiquitination are involved in modifying key cellular proteins to direct neuronal death. **Table 1.2** lists the peptide inhibiting these modifications or blocking interactions of the modified proteins with the downstream targets in several known pathologically activated cellular events. The suitability of targeting these cellular events to develop neuroprotectants for the treatment of patients suffering from stroke and other neurological disorders is reviewed in the following sections.

Some of the pathologically significant cellular events in excitotoxic neuronal death involve suppression and stimulation of transcription of specific genes. The suitability of inhibitors of chromatin modifying epigenetic enzymes as potential neuroprotectants for the treatment of stroke patients is also reviewed (**Figure 1.6B**).

1.4.1 Antagonists of the over-stimulated extrasynaptic NMDA receptors as neuroprotectants

Antagonists such as Ifenprodil and CP-101,606 selectively targeting the GluN2B subunit-containing NMDA receptors were trialled as neuroprotectants in patients suffering from ischemic stroke [Reviewed in (Small, 2002)]. Owing to the wide spectrum of physiological functions of GluN2B subunit-containing NMDA receptors and/or the off-target effects of some of these antagonists, most of these antagonists were found to be unsuitable for use as neuroprotectants in clinical trials (Mony et al., 2009; Small, 2002). One well-studied antagonist termed memantine is an exception because it selectively binds to a site overlapping the Mg^{2+} -blocking site of the ion channel-forming motif of NMDA receptors only when channels are open (Chen and Lipton, 2005; Kashiwagi et al., 2002). Since the ion channel of an over-stimulated extrasynaptic GluN2B-containing NMDA receptor is tonically open in excitotoxicity, memantine preferentially binds the receptor to inhibit its ion channel activity. In contrast, the ion channels of synaptic NMDA receptors are transiently open under physiological conditions, memantine only weakly associates with these receptors. Furthermore, the bound memantine rapidly dissociates from the synaptic NMDA receptors because it rapidly dissociates from the receptors as soon as their ion channels are closed (Kotermanski et al., 2009). Owing to these properties, memantine does not affect the normal neurological function of synaptic NMDA receptors [reviewed in (Nakamura and Lipton, 2016)]. These findings suggest that memantine is a potential pathologically activated therapeutic for neuroprotective treatment of stroke patients (Lipton, 2007).

In excitotoxicity, the excessive NO produced by the over-activated nNOS associated with the over-stimulated extrasynaptic NMDA receptors can chemically modify specific cysteine residues of the receptors by the S-nitrosylation reaction. Furthermore, the hypoxic condition caused by shortage of blood supply prevents these cysteine residues in the extrasynaptic NMDA receptor in neurons of ischemic penumbra from forming disulphide bonds, further

facilitating their modification by S-nitrosylation (Takahashi et al., 2007). Biochemical analysis revealed upon poly-S-nitrosylation, the ion channel activity of the extrasynaptic NMDA receptors is significantly reduced (Takahashi et al., 2007). Based upon this observation, Lipton and co-workers developed NitroMemantines, the dual functional memantine derivatives preferentially targeting and S-nitrosylating the over-stimulated extrasynaptic NMDA receptors; their memantine moiety selectively directs them to the over-stimulated extrasynaptic NMDA receptors while their nitro group S-nitrosylates specific cysteine residues in the receptors. S-nitrosylation maintains inhibition of the extrasynaptic NMDA receptor even after the remaining memantine moiety dissociates from the modified receptor [reviewed in (Nakamura and Lipton, 2016)]. In a recent report, Takahashi, *et al.* demonstrated that NitroMemantines selectively S-nitrosylated ischemic neurons and in turn reduced brain damage in a rat model of ischemic stroke (Takahashi et al., 2015). Besides contributing to neuronal loss in acute neurological conditions, excitotoxicity also contributes to brain damage in Alzheimer's disease (Mattson, 2003; Mattson et al., 1992; Talantova et al., 2013). Memantine alone or in combination with the cholinesterase inhibitor donepezil is effective in improving cognition and alleviating behavioural problems in patients with moderate to severe Alzheimer's disease (Howard et al., 2012; Jones et al., 2009). Furthermore, memantine and NitroMemantines were effective in reducing synaptic damage *in vitro* and *in vivo* in a mouse model of Alzheimer's disease (Talentova et al., 2013). Given the clinical trial success of memantine for treatment of Alzheimer's disease patients and the proven efficacy of memantine and NitroMemantine in reducing ischemic stroke-induced brain damage in animal models, the clinical trial of memantine as a neuroprotectant in ischemic stroke patients is currently underway (refer to ClinicalTrials.gov for detail).

1.4.2 Blockade of calpain cleavage of pathologically significant protein substrates

Over-activation of calpains is an early event in excitotoxicity. Some of the cellular proteins, upon modification by calpains, acquire the ability to initiate the neurotoxic signalling pathways directing neuronal death (**Figures 1.3 and 1.6A**). Among the calpain substrates listed in **Table 1.1**, Src, CaN and CRMP3 acquire the ability to initiate neuronal death only after they are cleaved by calpains (Hossain et al., 2013; Hou et al., 2013; Shioda et al., 2006). In cultured neurons, both Src and CRMP3 were cleaved by calpains to generate the

neurotoxic truncated fragments within 30 min after glutamate over-stimulation, suggesting that their truncated fragments act as signal transduction hubs from which the cytotoxic signals directing neuronal death originate. Indeed, blockade of calpain cleavage of Src in neurons by a cell membrane permeable peptide inhibitor could protect against excitotoxic neuronal death (Hossain et al., 2013). Future investigation should focus on developing small-molecule inhibitors selectively block cleavage of Src and CRMP3 by calpains as potential neuroprotectants to reduce stroke-induced brain damage.

As a calmodulin-regulated enzyme, CaN phosphatase activity is expected to be rapidly activated by influx of calcium through the ionotropic glutamate receptors, it is unclear how truncation by calpain modulate the activity, subcellular localisation and substrate specificity of CaN. Further studies to define the calpain cleavage sites in CaN and address this question are needed. Once the calpain cleavage sites in CaN are defined, cell permeable peptide calpain inhibitors derived from these sites can be designed. These peptides will be valuable lead compounds for the development of neuroprotective small molecule inhibitors for stroke therapy.

The calpain substrates NCX3, Kidins220/ARMs, TRPC6, mGluR1, Ret and Cain are neuroprotective neuronal proteins. Calpain cleavage either abolishes their biological activity or decreases their stability. Among them, cell permeable peptide inhibitors selectively blocking calpain cleavage of mGluR1, Kidins220/ARMs and TRPC6 have been designed and they all exhibit the ability to protect against excitotoxic neuronal death (Du et al., 2010; Gamir-Morralla et al., 2015; Xu et al., 2007). Small molecule mimicking these peptide inhibitors are therefore potential neuroprotective therapeutics for the treatment of stroke patients.

It is noteworthy that some of these cell permeable peptide inhibitors are substrate-specific, i.e. they can only block calpain cleavage of the selected protein substrate. For example, the Tat-Src peptide developed by colleagues in our lab could block calpain cleavage of Src but not the other substrates (Hossain et al., 2013). Likewise the, the TatC6 peptide developed by Du, *et al.* could block calpain cleavage of TRPC6 but not the other protein substrates (Du et al., 2010). Defining the structural features in calpain governing its specific binding of these peptide inhibitors will facilitate the development of the substrate-specific small-molecule inhibitors of calpains. Since the crystal structure of calpain-2 complexed with its endogenous inhibitors has been solved (reviewed in (Campbell and Davies, 2012)),

determination of the structure of calpain-2 complexed with the substrate-specific peptide inhibitors is one of the best avenues to define these structural features.

1.4.3 Blockade of protein-protein interactions governing neuronal death

Table 1.2 lists the protein-protein interactions contributing to excitotoxic neuronal death. Among them, the binding of GluN2B subunit of the extrasynaptic NMDA receptor to PSD95 governs the over-activation of several neurotoxic enzymes including nNOS, NOX and DAPK. These over-activated enzymes initiate major neurotoxic signalling pathways governing excitotoxic neuronal death at early stage in excitotoxicity. Thus, it is not surprising the cell membrane permeable peptide inhibitor Tat-NR2B9c blocking interactions of GluN2B subunit with PSD95 is efficacious in protecting against excitotoxic neuronal death (Aarts et al., 2002) (**Figure 1.6A**).

Activation of the pro-survival kinase Akt is critical to neuronal survival. The major mechanism activating Akt in neurons involves the synthesis of PI(3,4,5)P₃ catalysed by PI3K in the plasma membrane. Phosphatase and tensin homolog (PTEN) antagonises this process by directly dephosphorylating PI(3,4,5)P₃, leading to Akt inactivation. For this reason, PTEN is generally believed to be a mediator of neurotoxic signalling pathways. Two groups of researchers independently demonstrated enhanced nuclear localisation of PTEN in neurons undergoing excitotoxic neuronal death (Howitt et al., 2012; Zhang et al., 2013). Since nuclear translocation of PTEN is governed by mono-ubiquitination of Lys-13, Zhang, *et al.* treated the cultured adult neurons with a cell-permeable peptide Tat-K13 containing the ubiquitination motif of PTEN in its sequence (Zhang et al., 2013) (**Figure 1.6A**). They found that Tat-K13 inhibited ubiquitination of PTEN and blocked nuclear translocation of neuronal PTEN. More importantly, treatment with Tat-K13 protected against ischemia-induced brain damage in a rat model of ischaemic stroke. Interestingly, using genetically modified mice that lack the ability to import PTEN into the nucleus, Howitt *et al.* obtained experimental results contradicting those reported by Zhang, *et al.* They found that these mice exhibited a high degree of ischaemic stroke-induced brain damage, suggesting that blockade of nuclear translocation of PTEN causes more ischemia-induced brain damage (Howitt et al., 2012). Further studies to clearly define the consequence of nuclear translocation are needed before the observation of nuclear translocation of PTEN can be exploited for the development of neuroprotective therapeutic strategies.

1.4.4 Blockade of dysregulated S-nitrosylation of specific neurotoxic proteins

Depending on the neuronal proteins targeted by NO for modification, dysregulated S-nitrosylation can promote or suppress neurotoxic signalling in excitotoxicity. As discussed in section 1.4.1, S-nitrosylation of extrasynaptic NMDA receptors can attenuate their ion channel activity and in turn reduce the influx of Ca^{2+} into the cytosol. Thus, S-nitrosylation of extrasynaptic NMDA receptor is neuroprotective as it suppresses the neurotoxic action of the extrasynaptic NMDA receptors over-stimulated in excitotoxicity. In contrast, S-nitrosylation of MLK3 leads to its activation, allowing the activated MLK3 to activate the neurotoxic protein kinases JNKs (Hu et al., 2012) (**Figure 1.3**). Likewise, S-nitrosylation of glyceraldehyde-3-phosphate dehydrogenase (GAPDH) abolishes its catalytic activity and enhances formation of complexes formed by the S-nitrosylated GAPDH (SNO-GAPDH) and the E3 ubiquitin ligase Siah1 (Hara et al., 2005). The SNO-GAPDH/Siah1 complex enters nucleus where SNO-GAPDH alone and SNO-GAPDH/Siah1 complex modulate the activity and abundance of specific nuclear proteins to cause cell death (Hara et al., 2005). These findings indicate that S-nitrosylation of MLK3 and GAPDH is a pathologically activated cellular event and inhibitors blocking S-nitrosylation MLK3 and GAPDH are potential neuroprotectants capable of reducing neuronal loss in acute and chronic neurological disorders. The small molecule compounds deprenyl and its derivative CGP326B can selectively bind GAPDH and prevents its S-nitrosylation. Further studies revealed that CGP326B is a neuroprotectant capable of reducing dopaminergic neuronal loss in animal models of Parkinson's disease (Hara et al., 2006).

1.4.5 Targeting chromatin-modifying epigenetic enzymes as a neuroprotective therapy

In recent years, a suite of small molecule inhibitors have been developed to specifically inhibit chromatin modifying epigenetic enzymes (such as the histone deacetylases (HDACs), histone acetyl transferases (HATs), the histone methyl transferases (MLLs) and DNA methyl transferases (DNMTs) or block the recognition interface between post-translationally modified histones and chromatin binding proteins (such as the BRDs) (**Figure 1.6B**). Although the development of epigenetic inhibitors is primarily driven by the motivation to target malignant diseases, these compounds have also been pre-clinically or

clinically tested as novel treatment options for other human diseases. In particular, Valproate, a HDAC inhibitor has been clinically approved for the treatment of epilepsy (Chateauvieux et al., 2010; Gerstner et al., 2008). Since abnormal over-expression and up-regulation of REST and its co-repressor complexes (Sin3A and CoREST) are some of the neurotoxic mechanisms directing neuronal loss in ischaemic stroke, inhibitors of the epigenetic modifying enzymes including HDACs, histone lysine N-methyl transferase G9a/EHMT2 or lysine-specific demethylase LSD1/KDM1A can potentially inhibit REST functions and in turn reduce ischaemic stroke-induced brain damage. HDAC inhibitors are the largest class of clinically approved epigenetic inhibitors. Some of them can be used to test for their efficacy to protect against excitotoxic neuronal death and reduce stroke-induced brain damage. For example, inhibitors of G9a and LSD1 have been recently developed (Feng et al., 2014; Kakizawa et al., 2015; Ma et al., 2015; Prusevich et al., 2014; Sweis et al., 2014). They can be examined for the efficacy in neuroprotection in cell-based assays and in animal models of stroke.

In addition to directly targeting the REST/CoREST/Sin3A complex, methyl-lysine mimetic small molecule inhibitors that interferes the recognition interface between methylated-lysine on histones (i.e. histone H3 lysine 9 H3K9) and chromodomain containing proteins such as heterochromatin protein 1 (HP1) can potentially inhibit REST activity (**Figure 1.6B**). Multiple acetyl-lysine mimetics small molecule inhibitors that interferes the recognition interface between acetyl-lysine on histones (H3 and H4) and its binding partners bromodomain proteins (BRDs) has been developed and are currently in late phase clinical trials (Delmore et al., 2011; Filippakopoulos and Knapp, 2014; Zhao et al., 2013). These BET (bromodomain and extra-terminal) BRD inhibitors exert their anti-tumour activity by suppressing HAT-mediated hyperacetylation-dependent transcriptional activation of key cancer-causing genes such as c-Myc (Delmore et al., 2011). Clearly, the blood-brain barrier will ultimately be a major hurdle for the development of epigenetic therapeutics to treat ischemia stroke patients. Recent efforts have demonstrated that small- molecule epigenetic inhibitors can effectively cross the blood-brain barrier and elicits potent neuroprotective activity in preclinical animal models (Abel and Zukin, 2008). Importantly, HDAC inhibitor TSA has recently been demonstrated to be efficacious in blocking neuronal cell death in a rat model of ischaemic stroke (Noh et al., 2012). TSA treatment was found to cause hyperacetylation of histones at promoter of the gene encoding the GluA2 subunit of AMPA receptor. Presumably, the treatment de-represses the GluA2 gene and facilitates the

synthesis of GluA2-subunit-containing AMPA receptor. Nevertheless, defining the role of epigenetic modifications in excitotoxic neuronal death will benefit development of target-specific epigenetic small-molecule inhibitors as therapeutics to reduce ischaemic stroke-induced brain damage.

Table 1.2 Protein-protein interactions governing some of the key pathologically activated cellular events directing excitotoxic neuronal death.

Interacting partners or modifications	Consequences	Neuroprotective peptide blocking the interactions	References
GluN2B subunit of NMDA receptor/PSD95	PSD95 acts as a scaffolding protein that anchors nNOS and NOX. Binding of PSD95 to the GluN2B subunit facilitates activation of nNOS and NOX.	Tat-NR2B9c	(Aarts et al., 2002)
GluN2B subunit of NMDA receptor/DAPK	DAPK specifically binds to the C-terminal tail of the GluN2B subunit of NMDA receptor. Upon binding, DAPK phosphorylates S1303 of GluN2B, leading to increased conductance of NMDAR.	Tat-NR2B _{CT}	(Tu et al., 2010)
Nedd4 binding and ubiquitination of PTEN	Enhanced nuclear translocation of PTEN.	Tat-K13 of PTEN	(Howitt et al., 2012; Zhang et al., 2013)

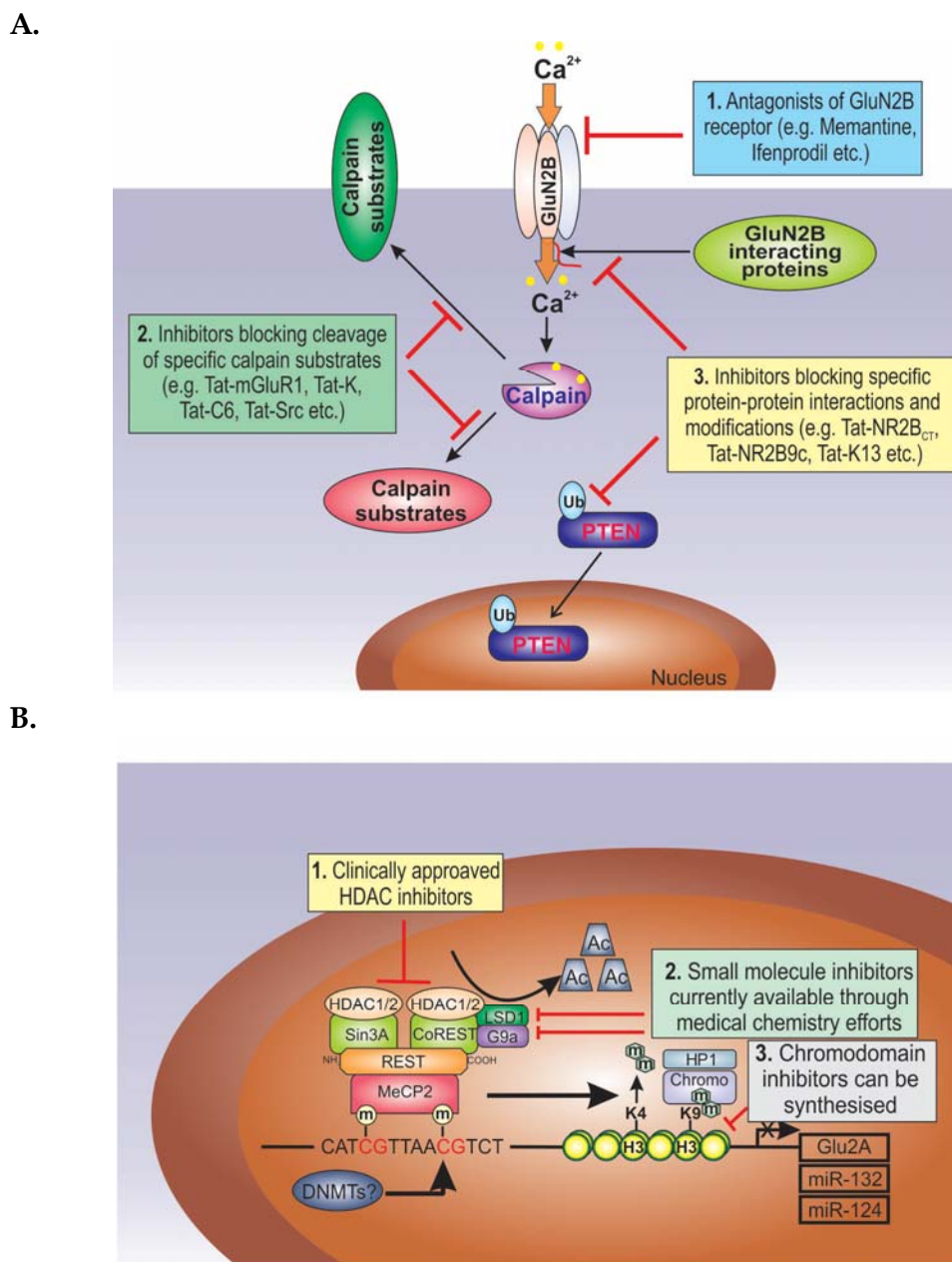


Figure 1.6 Neuroprotective strategies to reduce neuronal loss in excitotoxicity. A. Neuroprotectants targeting cellular proteins modified by pathologically activated cellular events in excitotoxicity. These neuroprotectants include: (i) Antagonists of the neurotoxic NMDA receptors, (ii) substrate-specific inhibitors of calpains and (iii) inhibitors blocking cytotoxic protein-protein interactions and protein modifications. **B.** Potential neuroprotective agents targeting chromatin-modifying epigenetic enzymes. Three main strategies utilising small molecule inhibitors that could be employed to target REST-mediated gene repression are illustrated.

1.5 Lessons learned from the success of developing memantine and Tat-NR2B9c as clinically effective neuroprotectants

Both memantine and Tat-NR2B9c are the only neuroprotective drugs proven in clinical trials to be safe and effective in reducing or delaying brain damage caused by excitotoxicity in human stroke and Alzheimer's disease patients. A few lessons can be learnt from their clinical trial success for the development of new neuroprotective therapeutics to reduce brain damage in acute and chronic neurological conditions. In a review article on the fates of the pipeline of drugs developed by the AstraZeneca's small molecule drug project, Cook *et al.* listed five determinants of project success. These determinants, which they referred to as five 'Rs', are right patients, right targets, right tissues, right safety and right commercial potential (Cook et al., 2014). Here, the first four determinants are used as the criteria to discuss the reasons behind the clinical trial success of memantine and Tat-NR2B9c.

First, memantine and Tat-NR2B9c exhibit the abilities to inhibit the right targets in the right tissues. Both drugs interfere with the pathological activated cellular events at the early phase of excitotoxic neuronal death. Memantine inhibits the ion channel activity of the over-stimulated extrasynaptic NMDA receptors which initiate the neurotoxic signals. Tat-NR2B9c prevents the activation of nNOS and NOX by blocking the interaction of the over-stimulated extrasynaptic NMDA receptor with PSD95/nNOS and PSD95/NOX complexes. Consequently, excessive synthesis of the neurotoxic molecules NO and ROS by nNOS and NOX2, respectively at the early phase of excitotoxicity is suppressed. Second, memantine and Tat-NR2B9c have little or no impact on the normal neurological processes. Memantine cannot inhibit the synaptic NMDA receptor transiently stimulated under physiological conditions (Chen and Lipton, 2005). Likewise, Tat-NR2B9c cannot interfere coupling of PSD95 to synaptic NMDA receptor and other cell surface receptors (Aarts et al., 2002). Owing to the lack of impacts on the normal neurological processes, both memantine and Tat-NR2B9c exhibited no toxicity and little side effects in clinical trials (Hill et al., 2012; Jones, 2010). Thus, they are drugs of the right safety for the treatment of Alzheimer's disease patients and patients suffering from ischemic stroke. Third, they exert neuroprotective action by binding to the right targets. They inhibit the pathologically activated cellular events initiated by over-stimulation of extrasynaptic NMDA receptors. For memantine, it preferentially blocks the tonically open ion channel motif of over-stimulated extrasynaptic neuronal NMDA receptors (Chen and Lipton, 2005). For Tat-NR2B9c, it inhibits binding of PSD95/nNOS and PSD95/NOX complexes to the GluN2B

subunit of the over-stimulated extrasynaptic NMDA receptors (Aarts et al., 2002; Chen et al., 2015). Fourth, the right patients were chosen for the clinical trials of memantine and Tat-NR2B9c. Patients with moderate to severe Alzheimer disease symptoms were chosen for clinical trials because the efficacy of memantine in delaying disease progression can be easily detected. For clinical trials of Tat-NR2B9c, only a well-defined subgroup of patients suffering from stroke was selected. These patients were scheduled to undergo the endovascular coiling procedure for ruptured aneurysm repair prior to receiving treatment with Tat-NR2B9c. Since iatrogenic stroke in these patients can be closely monitored by MRI (Hill et al., 2012), this permitted the clinicians to readily assess the efficacy of Tat-NR2B9c in these patients.

Excitotoxicity contributes to neuronal loss in a wide spectrum of acute and chronic neurological disorders (Ferrarese, 2004). However, the extent and duration of its contribution to brain damage vary in these disorders. Ideally, appropriate pharmacological agents should be available for effective treatment of all types of disorders, and at any stages after the onset of the disorders. To discover more neuroprotective pharmacological agents and to define their efficacies for treatment of these disorders, we need to clearly define the networks of signalling pathways governing excitotoxic neuronal death in each disorder and how the signalling strength of each pathway changes at different stages after the onset of the disorder. How the quantitative proteomic-based systems biology approaches can be applied to future investigation to achieve this aim is discussed in the next section.

1.6 Mass spectrometry-based quantitative proteomic approach to investigate the mechanism of neuronal death in excitotoxicity

As depicted in **Figure 1.2**, over-activation of calpains, nNOS and NOX2 are the key post-receptor cellular events directing neuronal death in excitotoxicity. The over-activated calpains, excessive nitric oxide and ROS generated modulate the structures and functions of a large number of cellular proteins by post-translational modifications including proteolysis, phosphorylation, S-nitrosylation and ubiquitination. Exactly how these modified proteins interplay spatially and temporally to cause neuronal death remains unclear. Mass spectrometry-based quantitative proteomic is one of the best approaches to address this question.

1.6.1 Quantitative phosphoproteomic approach

Protein phosphorylation is the most ubiquitous and versatile post-translational modifications (PTM) involved in regulation of cellular proteins participating in directing neuronal death in excitotoxicity. To define the changes in phosphorylation levels of cellular proteins in neurons undergoing excitotoxic neuronal death, the high throughput mass spectrometry (MS)-based phosphoproteomic approaches have been developed over a decade ago. These approaches have a number of advantages. First, they are sensitive—they are capable of detecting proteins with abundance as low as at femtomole levels. Second, prior purification of cellular proteins from the crude neuronal lysates is not required. Third, exact locations of phosphorylation sites in the cellular proteins can be readily identified (Mann and Jensen, 2003; Ozlu et al., 2010). Phosphoproteomic studies require extensive sample preparation, fractionation and phosphopeptide enrichment to maximise the number of detectable cellular proteins (Loroch et al., 2013; Ozlu et al., 2010; Polat and Ozlu, 2014; Thingholm et al., 2009). Quantitative measurement of the time-dependent changes in phosphorylation levels of multiple cellular proteins in neuron undergoing excitotoxic cell death will reveal key neurotoxic signalling events directing neuronal death. In this approach, the abundance of phosphopeptides derived from cellular proteins in two or more biological samples are quantitatively compared using the stable isotope labelling methods (metabolic and chemical) or label-free methods (Ong and Mann, 2005). For detail of the general work flow for quantitative phosphoproteomics, readers are directed to the excellent review on recent advances in quantitative neuroproteomics by George E. Craft *et al.* (Craft et al., 2013).

Metabolic labelling of cellular proteins relies on the incorporation of stable isotope labels (^{15}N or ^{13}C , or heavy amino acids Arg, Lys, Leu and Ile) in a living cell. Stable isotope labelling by amino acids in cell culture (SILAC) is the most frequently used metabolic labelling method for quantitative proteomics analyses (Ong et al., 2002). SILAC has been used to metabolically label the intracellular proteins in cultured proliferating cells. The use of SILAC approaches to metabolically label cellular proteins in primary neurons and mice has been documented (Kruger et al., 2008; Spellman et al., 2008).

Isotope coded affinity tags (ICAT), isobaric tags for relative and absolute quantification (iTRAQ), tandem mass tag (TMT) and stable-isotope dimethyl labelling are examples of chemical derivatisation techniques used to label proteins or proteolytic fragments derived

from cellular proteins extracted from the cultured cells. ICAT is used for the labelling of free sulfhydryl groups of cysteines (Gygi et al., 1999). Chemical labelling approaches (iTRAQ, TMT) are extensively used where metabolic labelling of the samples is not possible (Ross et al., 2004; Thompson et al., 2003). The iTRAQ approach was adopted by Datta *et al.* to identify proteins undergoing changes in abundance in rodent brains in response to cerebral ischemia/reperfusion injury (Datta et al., 2011). Network analysis of the identified proteins revealed that the treatment induced metabolic coupling between astrocytes and neurons, breakdown of the blood-brain barrier prior to the occurrence of serious tissue damage and spontaneous upregulation of proteins involved in neural regeneration (Datta et al., 2011). Since the authors did not perform quantitative phosphoproteomic analyses, results of the study could not reveal the dysregulated signalling mechanism governing neuronal loss and the aforementioned pathological events.

Another recent advancement in chemical labelling of cellular proteins and peptides is the stable isotope dimethyl labelling method which is used to label peptides derived from tryptic digestion of cellular proteins. This is a cost effective and robust method that has microgram to milligrams of sample labelling range and can be used for three samples simultaneously (Boersema et al., 2009). This method can also improve the phosphopeptides enrichment by preventing nonspecific binding of the phosphopeptides to the IMAC column (Polat et al., 2012). Label-free quantification method uses either precursor signal intensity or spectral counting in the absence of labels that requires multiple analysis of each sample and separate analysis for each condition thus it is time consuming and laborious (Asara et al., 2008; Old et al., 2005). On the other hand, for absolute quantification, single or multiple reactions monitoring (SRM/MRM) techniques are followed where known concentrations of internal standards are added to the protein digests. These standards are synthetic peptides containing heavy amino acids or stable isotope containing tags. Absolute quantification is achieved by comparing signals of standards and endogenous peptides (Kirkpatrick et al., 2005). Low abundance of phosphoproteins and lack of phospho-specific antibodies favour this robust targeted absolute quantification method.

Quantitative phosphoproteomics relies on the proper identification and quantification of phosphorylated proteins and the identification of phosphorylation sites (Mann and Jensen, 2003). Selective enrichment of phosphopeptides is required prior to quantitative mass spectrometric analysis. Immobilised Fe³⁺ ions are used in immobilised metal affinity chromatography (IMAC) to selectively bind phosphopeptides (Ficarro et al., 2002). Other

metals Zr^{4+} (Feng et al., 2007) and Ga^{3+} (Sykora et al., 2007) are also used with IMAC for improved coverage and specificity. Metal oxide affinity columns are also used for selective phosphopeptides enrichment e.g. TiO_2 (Pinkse et al., 2004), Fe_3O_4 (Li et al., 2008), and ZrO_2 (Zhou et al., 2007). Several other enrichment strategies include anion-exchange chromatography (Han et al., 2008) and mixed-bed chromatography (Motoyama et al., 2007).

1.6.2 Selected or multiple reactions monitoring (SRM/MRM)

For absolute quantitation of the abundance of the proteolytically modified cellular proteins at different stages of excitotoxic neuronal death, the SRM/MRM techniques can be adopted (Kirkpatrick et al., 2005). Phosphopeptides identified in quantitative phosphoproteomics analysis can be chemically synthesised with one or more ^{13}C and/or ^{15}N -labelled amino acids. These peptides are then used as internal standards for the SRM/MRM techniques. Absolute quantification of the phosphorylation changes and abundance of proteolytically modified cellular proteins is achieved by comparing signals of the standards and those of the tryptic peptides derived from the endogenous cellular proteins. With this approach, researchers are able to monitor the temporal changes in regulation of phosphorylation of signalling molecules and abundance of specific proteolytically modified cellular proteins in neurons undergoing excitotoxic cell death. Most of the phosphorylated proteins and proteolytically processed proteins involved in excitotoxicity are low abundant proteins in neurons. Furthermore, phospho-specific and cleavage-specific antibodies against these proteins are unavailable. Thus, it has been technically challenging to absolutely quantitate their changes at different stages of neuronal death. The SRM/MRM approach described here can overcome these technical challenges.

1.7 Aims of the study

The major goal of my PhD project was to explore the signalling cascades that ultimately lead to excitotoxic neuronal death. In excitotoxicity, the over-stimulated glutamate receptors allow massive influx of calcium ions into the affected neurons. The excessive cytosolic calcium ions over-activate Ca^{2+} -dependent proteases and several other calcium-dependent enzymes, which in turn modulate the expression and phosphorylation of specific neuronal proteins to direct neuronal death. Previously my colleagues discovered that the neuronal Src protein tyrosine kinase is cleaved by calpain in excitotoxicity to generate a neurotoxic

truncated Src fragment (Src Δ N) which phosphorylates specific neuronal proteins to direct neuronal death in part by downregulating the activity of the pro-survival kinase Akt (Hossain et al., 2013). The findings indicate that calpain cleavage of Src is a key pathologically activated cellular event directing neuronal death in excitotoxicity. In my PhD project, I employed targeted molecular approach to define the role of Src in governing neuronal survival. I also employed unbiased quantitative proteomic-based systems biology approaches to identify the neuronal proteins of which abundance and/or phosphorylation are significantly perturbed in excitotoxicity. Specifically, I aimed to:

- (i) define the role of Src protein tyrosine kinase in governing neuronal survival,
- (ii) optimise the stable isotope dimethyl labelling-based quantitative proteomic and phosphoproteomic approaches using neuronal lysates,
- (iii) explore the changes in global proteome following glutamate-induced excitotoxicity in cultured neurons,
- (iv) explore the changes in neuronal phosphoproteome in excitotoxicity, and
- (v) identify the neuronal proteins and phosphoproteins that operate downstream of neurotoxic GluN2B-containing NMDA receptors

Chapter 2

Declaration and Acknowledgements

- ✚ My colleague Dr. M Iqbal Hossain generated the lentivirus used for the experiments described in Chapter 3. He also contributed for several experiments described in Chapter 3.

- ✚ My colleague Daisy Lio helped me to transfect *Sf9* cells with pBacPAK9-nSrcH₆ baculovirus expression vector to generate the baculovirus directing expression of the recombinant Src.

- ✚ Dr. Ching-Seng Ang, one of my co-supervisors provided help to run the samples in Orbitrap Elite mass spectrometer. He also personally contributed to repeating the calpain dimethyl labelling and label-free MS1 quantitation experiments described in Chapter 6.

- ✚ Dr. Dominic Ng, one of my co-supervisors provided help to capture the images following immunofluorescence experiments and also trained me on how to analyse the data using LAS AF Lite software.

- ✚ My colleague Syeda S. Ameen synthesised the isotopically labelled synthetic peptides that I used for label-free quantitation experiments described in Chapter 6.

Chapter 2: Material and Methods

2.1 Materials

Neurobasal medium, Dulbecco's Modified Eagle Medium (DMEM), Opti-MEM reduced serum media, B-27 supplement, GlutaMAX-I, and RPMI 1640 medium were purchased from GIBCO (Rockville, MD, USA). Trypsin, soybean trypsin inhibitor, sodium pyruvate, L-glutamine, non-essential amino acids, glutamate, DMSO, DNAase, poly-D-lysine, Penicillin, and Streptomycin were purchased from Sigma (St Louis, MO). The two anti-Src monoclonal antibodies, mAb(327) and mAb(2-17) were purified by Dr. Jeff Bjorge of the University of Calgary and were kindly given to us by Drs. Jeff Bjorge and Donald Fujita of the University of Calgary. Calpain-1, calpain inhibitor (calpeptin) and anti-tubulin, anti-GluN2A, anti-6× His tag antibodies were purchased from Abcam. Anti-Src antibody was from Epitomics. Phospho-Src418 antibody was from Invitrogen. Anti-GluN1, anti-GluN2B, anti-Akt, phospho-Akt (S473), phospho-Akt (T308), anti-p44/42 MAPK (Erk1/2), phospho-p44/42 MAPK (Erk1/2), anti-Gsk3 $\alpha\beta$, phospho-Gsk3 $\alpha\beta$ (Ser21/9) antibodies were from Cell Signalling. Protein A-Sepharose was from Sigma (Amersham Pharmacia Biotech). The NMDA receptor antagonist MK-801 [(+)-5-methyl-10,11-dihydro-5H-dibenzo[a,d]cyclohepten-5,10-imine maleate], the GluN2B subunit-specific NMDA receptor antagonist Ifenprodil and the AMPA-receptor antagonist CNQX were purchased from Sigma-Aldrich.

For expression of the recombinant wild type c-Src and c-Src mutants, the lentiviral vectors pLVX-Tight-Puro and pLVX-Advance were purchased from Clontech. Lentivirus packaging plasmid psPAX.2 and the envelop plasmid pMD2.G were from Addgene. HEK293 FT cell line for the generation of lentivirus, Opti-prep media, Lipofectamine 2000 and 3-(4,5-Dimethylthiazol-2-yl)-2,5-diphenyltetrazolium bromide (MTT reagent) were purchased from Invitrogen (Carlsbad, CA, USA). A set of lentiviral vectors PLKO.1 containing the five genes encoding the shRNA for silencing the expression of mouse neuronal Src (Catalog Number: RMM4534-NM_001025395) and the empty PLKO.1 vector were from Open Biosystems. Cell culture dishes and plates were bought from Corning (NY, USA).

2.2 Methods

2.2.1 Primary cortical neurons culture

All experiments involving animals were approved by the University of Melbourne Animal Ethics Committee and were performed in accordance with the Prevention of Cruelty to Animals Act 1986 under the guidelines of the National Health and Medical Research Council Code of Practice for the Care and Use of Animals for Experimental Purposes in Australia. Pregnant mice (C57BL/6) were group-housed (4 mice to a cage) in the Animal Facility in Bio21 Institute at The University of Melbourne under a 12-hour light/dark cycle. All efforts were made to minimize suffering of animals. The animals were provided access to drinking water and standard chow *ad libitum* and monitored daily prior to the experiments. For primary cortical neuronal cultures the embryos were collected from pregnant mice (gestational day 15-16) after they were euthanised by CO₂ asphyxiation. The cortical region was aseptically micro-dissected out of the brains of the embryos, free of meninges and dissociated in Solution 1 (250 ml HBSS, 1.94 ml of 150 mM MgSO₄, 0.75 g BSA). The suspended tissues were subjected to trypsin digestion at 37°C for 5 min in Solution 2 (20 ml Solution 1, 80 µl DNase, 4 mg trypsin) that followed trypsin inactivation by the addition of Solution 4 (16.8 ml Solution 1 and 3.2 ml Solution 3) and centrifuged at 1000×g for 5 min at room temperature. The tissue pellet was then subjected to mechanical trituration in Solution 3 (20 ml solution 1, 80 µl DNase, 200 µl 150 mM MgSO₄ and 10.4 mg trypsin inhibitor) and allowed to stand for 0.5min. The suspension was then transferred to a new sterile 50 ml tube and centrifuged for 5 min at 1000×g at room temperature. The cell pellet was then re-suspended in warm (37°C) neurobasal medium (GIBCO, Life Technologies) supplemented with 2.5% B-27 supplement (GIBCO, Life Technologies), 0.25% GlutaMAX-I (GIBCO, Life Technologies), and 1× penicillin-streptomycin (GIBCO, Life technologies). Cells were plated to a density of 5×10^5 cells/well in 24-well plates or 1.5×10^6 cells/well in 6-well plates pre-coated with 0.1 mg/ml sterile poly-D-lysine (Sigma). The cultures were maintained at 37°C in a humidified incubator containing 5% CO₂. In the following day, the medium was replaced with fresh medium containing 2.5% B-27, 0.25% GlutaMAX-I and 1×penicillin-streptomycin. Cultures were grown for seven days (days *in vitro* 7 or DIV7) before further treatments and half of the medium was changed with fresh medium at day 5 (DIV5).

2.2.2 Excitotoxicity model and treatment of cultured primary cortical neurons under various experimental conditions

To induce excitotoxicity, the cultured primary cortical neurons were treated with 100 μM glutamate on Day 7 in culture (DIV7). Glutamate was added to the neurobasal medium as an aqueous solution (Khanna et al., 2007). Neurobasal medium without glutamate was added to the culture as the control. Cultured neurons were treated with glutamate for different time intervals before proteomics analysis to define the early signalling cascades that lead to excitotoxic neuronal death. Primary cortical neuronal cells were also treated with the NMDA receptor antagonist MK-801 (50 μM), GluN2B-subunit containing NMDA receptor antagonist Ifenprodil (20 μM), AMPA receptor antagonist CNQX (50 μM), calpain inhibitor calpeptin (20 μM) and specific Src kinase inhibitor A419259 (1 μM) along with glutamate as an aqueous solution.

2.2.3 MTT cell viability assay

The enzyme mitochondrial reductase from metabolically active cells can cleave the yellow tereazolium salt MTT [3-(4,5-dimethylthiazole-2-yl)-2,5-diphenyltetrazolium bromide] to purple formazan crystal. Primary neurons isolated from fetal mouse cortex (5×10^5 cells per well) were cultured in 24-well plates as described the previous sections. After treatment with 100 μM glutamate, the cells in each well were monitored for their viability by the MTT assay. Briefly, MTT was dissolved in RPMI medium 1640 without phenol red at a stock concentration of 5 mg/ml and filtered using 0.22 μm to remove insoluble residues as described previously (Shioda et al., 2007). MTT solution equal to 10% (v/v) of the volume of culture medium (0.5 mg/ml final concentration) was added per well of cells. After incubation at 37°C, 5% CO₂ for 30 min, the culture medium was removed by aspiration and dried for 10 min. An aliquot of 200 μl DMSO was added to dissolve the formazan crystals formed from reduction of MTT by the mitochondrial reductase of live neurons. To determine the amount of formazan formed, three aliquots (100 μl each) of the mixture from each well of cells were transferred to separate wells in a 96-well microtiter plate (Falcon) and the absorbance at 570 nm was measured using FLUOstar Optima (BMG) plate reader. Cell viability was compared as a percentage of the untreated cells (control).

2.2.4 Lysis of the cells

Cells were lysed in ice-cold RIPA buffer containing 50 mM Tris, pH 7.0, 1 mM EDTA, 5 mM EGTA, 1 mM dithiothreitol, 10% (v/v) Glycerol, 1% Triton X-100, 0.01% SDS, 150 mM NaCl, 50 mM NaF, 40 mM sodium pyrophosphate, 0.5 mM Na₃VO₄, 50 mM β-glycerol phosphate, 0.2 mg/ml benzamidine, 0.1 mg/ml phenylmethyl sulfonyl fluoride (PMSF), EDTA-free protease and phosphatase inhibitors cocktail (Roche, Indianapolis, IN, USA). After centrifugation at 12500 ×g for 10 min, supernatant was collected and total protein quantification was performed using BCA protein assay (Pierce- Thermo Scientific). The supernatant was stored at -20°C for further analysis.

2.2.5 Acetone precipitation of neuronal lysates

Neuronal lysates were mixed with freezer-cold acetone (-20°C) (1:5, v/v) in microfuge tubes and incubated at -20°C overnight to precipitate the neuronal proteins. The tubes were centrifuged at 12500 ×g for 15 min at 4°C, supernatant was removed carefully and the protein precipitates were washed with freezer-cold acetone (-20°C) and centrifuged at 12500 ×g for 5 min. The supernatant was removed and the proteins pellets were air-dried before they were resuspension in the appropriate buffer for subsequent analysis.

2.2.6 In-solution trypsin digestion of proteins in neuronal lysates

Acetone precipitated control and treated neuronal protein lysates were resuspended in 8M urea in 50 mM Triethyl Ammonium Bicarbonate (TEAB) (pH 8.0), and estimation of protein concentration was carried out using BCA assay (Pierce-Thermo Scientific) according to the manufacturer's instructions. Equal amounts of proteins from both lysates were reduced with 10 mM tris-(2-carboxyethyl)-phosphine (TCEP) for 45 min at 37°C with mixing by a bench top vortex shaker. The reduced protein samples were alkylated with 55mM iodoacetamide in the dark. Samples were diluted to 1M urea in 25 mM TEAB and digested with sequencing grade modified trypsin (1:40) (w/w) with shaking overnight at 37°C.

2.2.7 Solid phase extraction clean-up of tryptic peptides

The digested samples were acidified to 1% (v/v) with pure formic acid and for each of the samples solid phase extraction (SPE) clean-up was carried out with a 60-mg Oasis HBL cartridge (Waters). Briefly, cartridges were pre-washed with 80% acetonitrile (ACN) containing 0.1% trifluoro acetic acid (TFA) first and then equilibrated with 0.1% TFA before sample loading. After loading the trypsin digests to the pre-washed columns, the columns were washed with 0.1% TFA and the bound tryptic peptides were finally eluted with 800 μ l of 80% ACN containing 0.1% TFA. The eluted peptides were partially reduced in volume by Speedy-vac for 25 min and then freeze-dried overnight.

2.2.8 Stable isotope dimethyl labelling of tryptic peptides

Stable isotope dimethyl labelling was performed according to the protocol described earlier by Boersema *et al.* (Boersema *et al.*, 2009). In brief, the freeze-dried peptides were re-dissolved in 100 μ l of 100 mM TEAB (pH 8.0) to achieve a final concentration of 25 μ g/100 μ l. At this stage, a micro BCA quantitation assay (Pierce-Thermo Scientific) was carried out to ensure that equal amounts of dissolved digested peptides derived from control and treated lysates were used for labelling. For every 25 μ g peptides, 4 μ l of normal formaldehyde, CH₂O [4% (v/v)] (light label) and 4 μ l of deuterated formaldehyde, CD₂O [4% (v/v)] (medium label) were used for reductive amination of the α -amino group of the free N-termini and the ϵ -amino group of lysine residues of the tryptic peptides derived from control and treated neuronal lysates, respectively. To each tube 4 μ l of 0.6 M sodium cyanoborohydride (NaBH₃CN) was added to initiate the labelling reaction at room temperature and the reaction was allowed to proceed for 60 min. To stop the labelling reaction, 16 μ l of 1% (v/v) ammonia in milli-Q H₂O was added to each tube and the samples were mixed briefly. Eight (8) μ l of formic acid was used to further quench the reaction. The reaction mixtures were left on ice. At this stage, the differentially labelled samples are mixed (light: medium = 1: 1) together before a small aliquot (15 μ l) being analysed by LC-MS/MS for the total proteome changes.

2.2.9 TiO₂ phosphopeptides enrichment

The remaining mixed labelled peptides from 2.2.8 were cleaned-up by SPE and freeze-dried before titanium dioxide (TiO₂) phosphopeptides enrichment. Phosphopeptides enrichment by TiO₂ was carried out by the protocol described earlier by Thingholm *et al.* (Thingholm *et al.*, 2006). Freeze-dried samples were reconstituted with 80 μ l of DHB (2,5-dihydroxybenzoic acid) loading buffer [200 mg DHB in 1 ml of wash buffer (80% ACN, 3% TFA)]. TiO₂ loaded micro-columns were washed with 30 μ l of 100% ACN before sample loading and the columns were centrifuged at 500 \times g with adaptors. After sample loading, columns were washed sequentially with 20 μ l DHB loading buffer and 60 μ l of wash buffer. Samples were eluted in clean microfuge tubes with 80 μ l of Buffer 3 [0.5% (v/v) ammonia in milli-Q H₂O]. Elutions were continued with 2 μ l of Buffer 2 (30% ACN). Eluents were acidified with 1 μ l of pure formic acid per 10 μ l of eluent to obtain pH of 2-3. Samples were concentrated using Speedy-vac to \sim 30 μ l before they were analysed by LC-MS/MS to follow the changes in phosphoproteome associated with excitotoxicity.

2.2.10 LC-MS/MS analysis

The resultant tryptic peptides (mixed labelled peptides with and without TiO₂ enrichment) were analysed on a LTQ Orbitrap Elite (Thermo Scientific) mass spectrometer coupled to an Ultimate 3000 nano LC system (Dionex) equipped with an Acclaim Pepmap nano-trap column (Dionex – C18, 100 \AA , 75 μ m x 2 cm) and an Acclaim Pepmap analytical column (Dionex C18, 2 μ m, 100 \AA , 75 μ m x 15 cm). The peptide mixture was loaded onto the trap column isocratically with 3% (v/v) ACN in 0.1% (v/v) formic acid at a flow rate of 5 μ l/min before the enrichment column was switched in-line with the analytical column. The bound peptides were eluted by a gradient made up of Solvent A [0.1% (v/v) formic acid] and Solvent B [0.1% (v/v) formic acid in 100% ACN]. The flow gradients were (i) 3% to 12% of Solvent B for 1 min, (ii) 12% to 35% of Solvent B for 20 min, (iii) 35% to 80% of Solvent B for 2 min, and (iv) elution with 80% of Solvent B was maintained for 2 min that followed equilibration of the column with 3% of Solvent B for 7min before the next sample injection.

The LTQ Orbitrap Elite mass spectrometer was operated in the data-dependent mode with nano ESI spray voltage of +2.0 kv, capillary temperature of 250°C and S-lens RF value of 60%. The data dependent mode refers to the procedure whereby spectra were acquired first in positive mode with full scan MS spectra scanning from m/z 300-1650 in the FT mode at

240,000 resolution followed by rapid collision induced dissociation (rCID) in the ion trap. The top twenty of the most intense peptide ions with charge states ≥ 2 were isolated and fragmented using normalised collision energy of 35 and activation Q of 0.25.

2.2.11 Processing and analysis of the proteomic data

The mass spectrometric data from Xcalibur RAW data file format were processed using Proteome Discoverer 1.4 (version 1.4.0.288, Thermo Scientific) with Mascot (Matrix Science version 2.4) search algorithm against the Uniprot database (maintained at the Mass Spectrometry and Proteomics Facility at the Bio21 Institute, The University of Melbourne, Australia and currently containing 54,958,551 sequences) for the taxonomy *Mus musculus* (mouse). Search parameters were precursor mass tolerance of 10 ppm, fragment mass tolerance 0.6 Da with signal-to-noise ratio of 1.0 and mass precision of 2 ppm. Carbamidomethyl cysteine was set as fixed modification and oxidation of methionine was set as variable modifications (**Figure 2.1**). Two-plex dimethylation (C_2H_6 , $C_2H_2D_4$) was selected as the quantification method for dimethyl modification at the N-terminus of the peptide and lysine. Trypsin with a maximum of 2 missed cleavages was used as the cleavage enzyme. Results were set to reflect a maximum of 1% false discovery rate (FDR) with ≥ 2 peptides or at least one unique peptide is required for positive identifications. For phosphorylation site prediction the PhosphoRS 3.0 node in Proteome Discoverer 1.4 was used, it contains the phospho-site localisation algorithm (Taus et al., 2011). The relative expression patterns of identified proteins or the phosphorylation status of phosphoproteins were determined on the basis of the relative intensities of the reporter ions of the corresponding peptides. The significance of differential expression pattern was calculated by a permutation-based statistical test using the web-based quantitative proteomics *p*-value calculator (QPPC) and *p*-value of ≤ 0.05 was considered significant (Chen et al., 2014).

Search parameters:

- Precursor mass tolerance: 10 ppm
- Fragment mass tolerance: 0.6 Da
- Fixed modification: Carbamodomethyl of cysteine
- Variable modification: Oxidation of methionine
- Quantification method: 2-plex dimethylation (C_2H_6 , $C_2H_2D_4$)
- Enzyme: Trypsin (max 2 missed cleavage)
- False discovery rate: 1%
- Unique peptides: 2

Figure 2.1 Search parameters used for proteomic data analysis. *Abbreviations: C_2H_6 , dimethyl; $C_2H_2D_4$, deuterated dimethyl.*

2.2.12 Pathway and network analysis using IPA and FunRich

Proteomic data were analysed through the use of QIAGEN's Ingenuity Pathway Analysis (IPA, QIAGEN Redwood City, www.qiagen.com/ingenuity) for pathway and network analysis. The proteomic dataset which included accession numbers and median medium to light ratios (that was converted to fold changes by the software) was input into IPA using the core analysis platform. The core analysis matched proteins in the uploaded data set with those in the Ingenuity Knowledge base. The statistical significance of each network or list was determined by IPA using a Fisher exact test ($p < 0.05$). IPA was also used to construct network of interacting proteins. The current knowledge available on genes, proteins, normal and disease cellular processes, signalling and metabolic pathways were used from the IPA database for pathway construction. Along with IPA, Functional Enrichment Analysis Tool (FunRich v.2.1.1) was also used for Gene Ontology (GO) enrichment analysis (Pathan et al., 2015). Gene names for the significantly perturbed protein molecules were uploaded in the FunRich software, and using human background dataset, the software enriched the molecules for molecular function, cellular process, biological process, biological pathway and site of expression analysis.

2.2.13 Western blotting

Equal amount of protein was loaded in each well of a SDS-PAGE gel and separated using running buffer [25 mM Tris, 192 mM glycine, 10% (w/v) SDS] for approximately 1.2 h at

150 Volt, and then transferred onto a PVDF membrane at constant voltage (100 V) for 1 h using Western transfer buffer [25 mM Tris, 192 mM glycine, 10% (w/v) SDS, 20% (v/v) methanol]. The membrane was then blocked with 5% (w/v) non-fat dry milk in Tris buffered saline with Tween 20 (TBST) (0.2 M Tris-HCl, pH 7.4, 1.5 M NaCl, and 0.1% Tween 20). After blocking, the membrane was washed three times; 10 min each time with TBST, and then probed with primary antibodies overnight. The membrane was again washed with TBST three times before probing with horseradish peroxidase-conjugated secondary antibodies (Chemicon, Australia) for 1 h at 25°C. Protein bands were visualized using chemiluminescence (ECL, Amersham Biosciences) according to the manufacturer's instructions. Images were taken using Fuji film LAS-3000.

2.2.14 Expression and purification of recombinant nSrcH₆ protein

Recombinant full-length neuronal Src (nSrc) protein with C-terminal His₆-tag (referred to as nSrcH₆) was generated by baculovirus directing expression of the recombinant protein in *Spodoptera frugiperda* 9 (*Sf9*) insect cells. The procedures are described below.

2.2.14.1 Construction of expression vector for recombinant nSrcH₆ production

The gene of full-length neuronal Src (nSrc) (mouse neuronal Src, Uniprot ID# P05480) with C-terminal GFP tag and a GSGS (glycine rich) linker between them was synthesised and inserted in the kanamycin resistant vector pMK (GeneArt, Invitrogen). The full-length nSrc gene was PCR amplified from this parent vector pMK-nSrc-GFP (kanR). A BamH1 site was incorporated in the sense primer (5'-ATCGGGATCCGCCACCATGGGCAG-3') and six histidine (H₆) residues, an in-frame stop codon and an EcoR1 site were incorporated in the antisense primer

(5'-CGATGAATTCTTAGTGGTGGTGATGATGGTGGCTGCCAGAGCCCAGATTCTC-3').

The amplified PCR product was cloned into the pBacPAK9 (Clontech) baculoviral expression vector. The resultant plasmid pBacPAK9-nSrcH₆ was sequenced to confirm the additional sequence encoding GSGSHHHHHH at the C-terminus of the recombinant protein. This plasmid was used to co-transfect *Sf9* cells with the BacPAK6 baculoviral DNA to generate the recombinant nSrcH₆ baculovirus by following the manufacturer's (Clontech) instructions. The recombinant nSrcH₆ baculovirus was purified by the plaque purification

assay as described elsewhere (Lalumiere and Richardson, 1995). For large scale expression of nSrcH₆, 1 litre of *Sf9* insect cells were grown at 27°C to a density of 1.0×10^6 cells per ml in Grace's medium (Invitrogen) with 10% (v/v) foetal bovine serum. The *Sf9* cells were then infected with the recombinant nSrcH₆ baculovirus at a multiplicity of infection (MOI) ≥ 10 .

2.2.14.2 Purification of recombinant nSrcH₆ protein expressed in *Sf9* insect cells

All purification procedures were carried out at 4°C. Forty-eight to fifty-two hours after infection, infected *Sf9* cells were harvested by centrifugation at 1000 ×g for 5min. The cell pellet was homogenised in 20 ml of Lysis Buffer (pH 8.0) containing 50 mM Tris, 10% (v/v) glycerol, 0.2 mg/ml benzamidine, 1% (v/v) Triton X-100, 2 mM β-mercaptoethanol and EDTA-free protease and phosphatase inhibitors cocktail (Roche, Indianapolis, IN, USA) using a Dounce homogeniser. After homogenisation, the cell suspension was ultracentrifuged at 120,000 ×g for 30 min and the supernatant was saved. The pellet was homogenised again with 20 ml of Lysis Buffer, centrifuged at 120,000 ×g for 30 min and the supernatant was saved. These two supernatants were pooled and applied to a Ni-NTA column (2 ml of bed volume) (Promega) that was equilibrated with the Base Buffer (20 mM Tris pH 8.0, 10% (v/v) glycerol and 0.2 mg/ml benzamidine). The column was washed with 45 ml of Wash Buffer 1 (Base Buffer containing 5 mM β-mercaptoethanol) and followed by 40 ml of Wash Buffer 2 (Base Buffer containing 0.5 M NaCl, 20 mM Imidazole and 5 mM β-mercaptoethanol). Proteins bound to the columns were eluted with 20 ml of Elution Buffer (Base Buffer containing 250 mM Imidazole and 5 mM β-mercaptoethanol) and collected in 20 fractions with 1 ml each. The collected fractions were analysed by SDS-PAGE and Western blot analysis. The peak protein fractions were pooled, divided in 100µl aliquots and stored at -80°C.

2.2.15 *In vitro* digestion of recombinant nSrcH₆ with calpain 1

Purified recombinant nSrcH₆ protein (1 µg) was digested *in vitro* with constitutively active calpain 1 (0.5 µg) in calpain digestion buffer (50 mM Tris-HCl, pH 7.4, 2 mM DTT, 30 mM NaCl, 10 mM CaCl₂). The reaction mixtures were incubated at 25°C for different time intervals (2 min -120 min) and stopped by the addition of 4× sample buffer and was resolved in a 10% SDS-PAGE. The gel was stained with Coomassie brilliant blue and destained with

20% (v/v) methanol/10% (v/v) acetic acid solution and observed for the presence of truncated Src fragment.

2.2.16 In-gel digestion of protein bands

For in-gel protein digestion, separated protein bands in SDS-PAGE gel were stained with Coomassie brilliant blue solution for 1 h and then destained with 20% (v/v) methanol/10% (v/v) acetic acid solution overnight. Destained gel was washed 2-3 times with dH₂O before protein bands were excised from the gel. Excised bands were destained with 50mM TEAB (50%)/ACN (50%) overnight and subsequently 30min on a rotation device. Gel plugs were dehydrated for 30min with 100% ACN on a rotation device. Dehydrated gel plugs were reduced with 10mM Tris (2-Carboxyethyl) phosphine (TCEP) for 45 min at 55°C. Reduced gel pieces were then alkylated with 55 mM iodoacetamide at room temperature in the dark for 30 min. Gel pieces were then washed 3 times with 50 mM TEAB for 10 min each on a rotation device before they were dehydrated with 100% ACN. Dehydrated gel plugs were digested with trypsin (Sigma# T7575) dissolved in 25 mM TEAB at 37°C overnight. On the following day, the supernatants containing the digested tryptic peptides were transferred to clean microfuge tubes for LC-MS/MS analysis.

2.2.17 Production of lentivirus containing the genes of interest

2.2.17.1 Generation of the plasmids for the lentivirus production

The gene of full length neuronal Src (*Src-GFP*) with a glycine-Serine-Glycine-Serine (GSGS) linker and a Green Fluorescence Protein (GFP) tag linked to its C-terminal tail was synthesized and inserted in the kanamycin-resistant vector, pMK-RQ (kanR) (GeneArt, Invitrogen). The GSGS-linker was added to minimize the impact of GFP on the regulatory properties of function of Src. Sandilands *et al.* examined Src-GFP expressed in SYF^{-/-} cells and found that it could be inactivated by phosphorylation by CSK and the presence of the GSGS linker and the GFP tag did not affect its activity and function in cells (Sandilands *et al.*, 2004). To facilitate cloning of the synthetic Src-GFP gene in the pLVX-Tight-Puro vector for lentivirus production, BamHI and EcoRI restriction sites were introduced at the 5' and 3'-ends of the synthetic genes.

To generate the Src Δ N-GFP mutant, the Src Δ N-GFP cDNA was amplified from the pMK-RQ-Src-GFP plasmid. Src Δ N-GFP lacking the N-terminal segment (residues 1-75) of mouse neuronal Src Sequence (NCBI Reference Sequence: NM_009271.3) was generated with the forward primer (ATCGGGATCCGCCACCATGCAGAGAGCTGGACCTCTGGCAGG) and the reverse primer for GFP (from 5'-3' ends: ATCGGAATTCTCATTGTACAGCTCGTCCATG). The forward prime also includes the ATG sequence (underlined) as the start codon. The resultant recombinant Src mutant lacks the N-terminal fatty acid acylation motif and the unique domain and contains an additional methionine residue preceding Gln-76 of the original full-length mouse neuronal Src. The cDNAs encoding Src-GFP and Src Δ N-GFP were subcloned into the lentiviral vector, pLVX-Tight-Puro via the BamHI and EcoRI restriction sites. The resultant pLVX-Tight-Puro-Src-GFP and pLVX-Tight-Puro-Src Δ N-GFP plasmids were used for lentivirus production. Using a similar procedure, the gene encoding GFP was introduced into the pLVX-Tight-Puro vector to generate the pLVX-Tight-Puro-GFP plasmid.

2.2.17.2 Culturing HEK293FT cells for lentivirus production

The HEK293FT cells, used for the production of lentivirus, were grown at 37°C in DMEM complete media supplemented with 10% (v/v) foetal bovine serum, 2 mM L-glutamine, 1 mM sodium pyruvate, 1 mM non-essential amino acid and 100U/ml penicillin–streptomycin and incubated in the presence of 5% CO₂. Cells were maintained in Geneticin (G418) (500 µg/ml). The cultures were passaged when they reached 80% confluence.

2.2.17.3 Lentivirus generation

For expression of recombinant Src-GFP, Src Δ N-GFP and GFP, lentiviruses were generated by transfecting HEK293FT cells with mixture containing three plasmids (packaging and expression plasmids) and lipofectamine 2000. In brief, for generation of the lentivirus, 2.5 µg of pMD2.G [pCMV-VSV-G-poly(A)] and 6.5 µg of psPAX2 (pCMV-gag-pol) vectors were mixed with 3 µg of pLVX-Tight-Puro plasmid containing the gene encoding GFP-fusion protein of Src (Src-GFP) or Src mutant (Src Δ N-GFP) or GFP. For generation of the lentivirus directing the expression of the mutant Tet repressor protein (TetR), 2.5 µg of pMD2.G and 6.5 µg of psPAX2 were mixed with the 3 µg of pLVX-Tet-On Advanced plasmid. Each of the reaction mixtures was diluted in 1.5 ml Opti-MEM reduced serum

media and incubated for 5 min. In another 15-ml falcon tube 36 μ l Lipofectamine 2000 was mixed gently with 1.5 ml of Opti-MEM reduced serum media. The plasmid mixtures and diluted Lipofectamine 2000 were mixed and incubated for 20 min at room temperature. Each plasmid/Lipofectamine 2000 mixture was added to the HEK293FT cells (80% confluence) grown in a 10 cm tissue culture dish. The cells were cultured in 5% CO₂ at 37°C overnight. The original medium was replaced with fresh medium 18-20 h after transfection. The supernatant containing the first batch of the lentivirus was collected 24 h after replacement of the medium. This step was repeated and the second batch of lentivirus was collected after 48 h. The two batches of lentivirus were combined and filtered with a 0.22 μ m syringe filter. To concentrate the lentivirus, the filtrate was placed in a centrifuge tube containing OptiPrep (~4 ml) as the cushion. The sample was centrifuged at 50,000 \times g for 2 h using SW32Ti rotor (Beckman Coulter). After centrifugation, the thick layer containing the lentiviral particles located between the medium and OptiPrep was carefully collected in a 50-ml falcon tube. Culture media was added to the tube to top up the volume to 50 ml and a second centrifugation was performed at 5000 \times g overnight at 4°C. In the following day, the pellet containing the lentiviral particles was re-suspended in 20-150 μ l of ice-cold PBS (pH 7.4) and stored as 10 μ l aliquots at -80 °C.

2.2.17.4 Production of lentivirus of shRNA against c-Src

The shRNAs were supplied in the lentiviral vector pLKO.1 (Open Biosystems). Lentivirus using the shRNAs was generated using 3 μ g of pLKO.1 plasmids containing shRNAs against the mouse *Src* gene, mixing them with lentiviral packaging plasmids pMD2.G (2.5 μ g) and pSPAX2 (6.5 μ g) and by following the method described in the above section (2.2.17.3).

2.2.17.5 Transduction of primary cortical neurons with lentivirus

Primary cortical neurons were transduced with lentivirus containing plasmid of genes of interest (pLVX-Tight-Puro-*Src*-GFP or pLVX-Tight-Puro-*Src* Δ N-GFP) and regulator (pLVX-Tet-On-Advanced) at day 1 in culture (DIV1). Lentiviral expression vector pLVX-Tight-Puro allows doxycycline-controlled, tightly regulated expression of a gene of interest that requires the presence of a vector that contains tetracycline-controlled transcriptional activator (rtTA Advanced or tTA Advanced), which can be provided by either pLVX-Tet-On Advanced or pLVX-Tet-off Advanced lentiviruses. The cells were also transduced with

pLVX-tight-Puro-GFP as a control. After adding both lentiviruses at first day in culture (DIV1), media were changed on the following day and induction of the target protein was achieved by adding doxycycline (1 $\mu\text{g}/\text{ml}$) on DIV5. Subsequent experiments were performed at DIV7 (i.e. 48 h after doxycycline induction) and lentivirus transduction efficiency was found to be 70-80%.

2.2.18 Immunofluorescence

For immunofluorescence, primary cortical neuronal cells were grown on poly-D-lysine coated cover slips for seven days. Cells were washed twice with ice-cold PBS then fixed in 4% (w/v) paraformaldehyde for 30 min at room temperature. Cells were then again washed 3 \times with PBS followed by permeabilisation using 0.2% (v/v) Triton X-100 in PBS for another 20 min. Next, cells were washed with PBS four times before being blocked with 10% (v/v) foetal bovine serum in PBS for 30 min. Cells were then again washed three times with cold PBS and incubated 1 h with primary antibody at room temperature. After incubation with primary antibodies, cells were washed three times with cold PBS and incubated with the secondary antibody (Alexa Flour 488/555, 1:800 in PBS) for 1 h at room temperature. Finally, cells were washed with PBS twice before DAPI (1:10000 in PBS) was added for 5 min to stain the nucleus. After one wash cover glass was mounted with GelCode FLUROMOUNT mounting media on a glass slide and dried. Cells were visualized and the images were captured using a Leica TCS SP5 confocal microscope (Wetzlar, Hessen, Germany). Captured images were analysed using Leica LAS AF Lite software.

2.2.19 Synthesis of isotopically labelled synthetic phosphopeptides

My colleague Syeda S. Ameen provided help to synthesise isotopically labelled synthetic phosphopeptides that were used for label-free quantitation experiments. Phosphopeptides were synthesized by Fmoc [N-(-9-fluorenyl) methoxycarbonyl]-based solid phase peptide synthesis chemistry on a CEM Liberty automated microwave peptide synthesizer (North Carolina, USA). The starting resins used were Fmoc Arg(Pbf) TentaGel S PHB resin (Cat# SA1302, loading capacity 0.23 mmol/g) and Fmoc Lys(Boc) TentaGel S PHB resin (Cat# SA1317, loading capacity 0.22 mmol/g) from Rapp Polymere GmbH. Following completion of the synthesis, peptides were cleaved from the resin by treatment with TFA/triisopropylsilane/water (95:2.5:2.5) and isolated by precipitation with cold diethyl

ether. Crude peptides were purified on an Agilent Zorbax C18 reversed-phase HPLC column in 0.1% TFA/water buffer with a linear acetonitrile gradient on an Agilent 1100 HPLC equipped with an automated fraction collector. The molecular weights of all peptides were confirmed by electrospray mass spectrometry on an Agilent 6220 QTOF LC/MS instrument. The isotopically labelled synthetic peptides that were synthesised and used for label-free quantitation experiments are listed in **Table 2.1**.

Table 2.1 List of synthetic phosphopeptides.

S/L	Gene	Protein	Peptide sequence	Phosphorylation site	m/z (Heavy) (Synthetic)	m/z (Light) (Endogenous)
1	<i>Mef2c</i>	Myocyte enhancer factor 2c	NpSPGLLVSPGN <u>L</u> NK	S222	748.8827	745.3742
2	<i>Mff</i>	Mitochondrial fission factor	NDpSIVTPSP <u>P</u> QAR	S146	734.3472	731.3403
3	<i>Mlf2</i>	Myeloid leukemia factor 2	LAIQGPEDpSP <u>S</u> SR	S237	678.3154	675.3085
4	<i>Stmn1</i>	Stathmin	ESVPDFPLpSP <u>P</u> K	S38	699.8329	696.8260

Heavy amino acids (leucine or proline) are underlined and phosphorylation sites are in **red**.

Chapter 3

Declaration and Acknowledgements

- ✚ Study findings presented in this result chapter have been published in Brain Research. I am one of the equal contributing first authors of the published manuscript. I contributed to 50% of the data presented in this manuscript.

Hossain, M.I., **Hoque, A.***, Lessene, G., Kamaruddin, A., Chu, P.W., Ng, I.H., Irtegun, S., Ng, D. C., Bogoyevitch, M. A., Burgess, A.W., Hill, A.F. & Cheng, H.C. 2015. Dual role of Src kinase in governing neuronal survival. *Brain Research*, 1594, 1-14. (**Equal contribution*)

- ✚ My colleague Dr. M Iqbal Hossain generated the lentivirus used for the experiments described in this result chapter. He also contributed for the experiments described in several subsections of this chapter. Specifically, he contributed to the experiments for Figures 3.2, 3.4, 3.5 and 3.7.

Chapter 3: Dual role of Src protein tyrosine kinase governing neuronal survival

3.1 Introduction

Involvement of Src-family kinases (SFKs) in neuronal survival has been well documented (Hossain et al., 2012). Five SFK members Src, Fyn, Yes, Lyn and Lck are widely expressed in neurons (Bae et al., 2012; Lowell and Soriano, 1996; Maness, 1992; Summy et al., 2003). Among them, Src mediates neurotrophic signalling by Ret, the tyrosine kinase common to receptors of the glial cell line-derived neurotrophic factor (GDNF) (Encinas et al., 2001). In addition, Src forms complexes with phosphatidylinositol-3-kinase (PI3K) and the 3,3',5-triiodothyronine (T3) receptor in primary cortical neurons and is implicated in mediating the neuroprotective actions of the T3 receptor by activating the neurotrophic PI3K in this complex (Cao et al., 2009). Thus, Src and other neuronal SFKs are considered to be key enzymes in signalling pathways sustaining neuronal survival.

Paradoxically, Src and Fyn are known to contribute to brain damage in ischemic stroke, intracerebral haemorrhage and Alzheimer's disease (Haass and Mandelkow, 2010; Ittner et al., 2010; Liu and Sharp, 2011; Paul et al., 2001). Targeted disruption of the Src gene, and treatment with several SFK inhibitors significantly reduce brain damage in rodent models of cerebral ischemia, specifically *Src*-KO mice but not *Fyn*-KO mice showed reduced infarct size comparing to the controls ($p < 0.05$) following MCA embolism, suggesting that Src in neurons contributes to neuronal death in stroke (Paul et al., 2001). On the contrary, treatment with inhibitors of SFKs induced cell death in cortical neurons (Takadera et al., 2012), suggesting that SFK activity is critical for neuronal survival as well. Thus, these conflicting reports concerning the role of Src and other SFKs in neurons suggest that neuronal SFKs participate in maintaining neuronal survival in physiological conditions also contributes to neuronal death under pathological conditions. Presumably, neuronal SFKs are aberrantly regulated to exert their neurotoxic function. Previous study demonstrated *in vivo* in a rat model of endothelin-1 induced middle cerebral artery occlusion and in cultured primary neurons undergoing excitotoxic cell death that Src is cleaved by calpains to form a 52-kDa truncated Src fragment (Hossain et al., 2013). More importantly, the 52-kDa truncated Src fragment contributes to neuronal death, which indicates that calpain cleavage is a key step in the conversion of Src to a mediator of cell death in neurons undergoing excitotoxic neuronal death (Hossain et al., 2013). A cell membrane permeable fusion

peptide (Tat-Src) derived from the Src unique domain, covering this cleavage site was able to restrict calpain cleavage of Src and restricted neuronal death in excitotoxicity (Hossain et al., 2013).

Extending our ongoing efforts to elucidate the mechanism of these apparently conflicting functions of neuronal SFKs, we employed pharmacological and small hairpin RNA (shRNA) knockdown approaches to define the role of Src in survival of cultured primary cortical neurons. Data presented in this chapter describe the dual role of Src protein tyrosine kinase maintaining neuronal survival under normal physiological condition and its conversion to a potent executor of neuronal death in excitotoxicity. Study results suggest sustaining the neuroprotective Src/Erk1/2/Akt signalling pathways as a potential strategy to maintain neuronal survival in acute neurological conditions and chronic neurodegenerative diseases.

3.2 Methods

3.2.1 Primary cortical neurons culture and MTT cell viability assay

Primary cortical neurons were cultured from embryonic (E16) pups collected from the pregnant C57BL/6 mice as described earlier in section 2.2.1 of Chapter 2. MTT cell viability assay was performed as described in section 2.2.3 of Chapter 2.

3.2.2 Assay of LDH released from damaged neurons

The activity of LDH released from the damaged neurons to the culture medium is a measure of neuronal death. The LDH activity assay was performed in the dark according to the manufacturer's protocol. Briefly, 50 μ l of culture medium from each well of the culture plate was transferred to 96 well-microtiter plates (Falcon). 100 μ l of LDH assay mixture containing equal volume of LDH assay substrate solution, LDH Assay dye solution and LDH assay cofactor was then added to each well. The reaction was allowed to proceed at room temperature for 30 min in the dark and was stopped by adding 50 μ l of 1 mM acetic acid. The absorbance of whole mixture was measured in triplicate at a wavelength of 490 nm using FLUOstar Optima (BMG) plate reader. The release of LDH was calculated as a percentage of the untreated control.

3.2.3 Monitoring neuronal survival by Calcein-AM and Ethidium homodimer-1 staining

Calcein acetoxymethyl (Calcein-AM) and ethidium homodimer-1 (EthD-1) are used to visualize live and damaged neurons, respectively. The disrupted cell membrane of damaged neurons allows entry of EthD-1, which upon binding to nucleic acids, produces red fluorescence (excitation wavelength, ~495 nm; emission wavelength, ~635 nm). The membrane-permeable Calcein-AM enters all neurons. It is converted by the intracellular esterases of live neurons to form the intensely fluorescent Calcein (excitation wavelength, ~495 nm; emission wavelength, ~515 nm). In brief, primary cortical neurons were cultured in Neurobasal medium without phenol red. The cultured neurons were stained with Calcein-AM and EthD-1 in Neurobasal medium (final concentrations: 2 mM and 0.5 mM of Calcein-AM and EthD-1, respectively) and incubated for 30 min in a CO₂ incubator. After staining, the cells were washed twice with Neurobasal medium. Live and dead cells were visualized using a fluorescence microscope (Leica DMI6000 B).

3.2.4 Expression of recombinant Src-GFP, Src Δ N-GFP and GFP in primary cortical neurons

Lentivirus was generated for the transduction and expression of recombinant full-length Src (Src-GFP), its mutant (truncated Src lacking unique domain, Src Δ N-GFP) and only GFP in primary cortical neurons. The details procedure for lentivirus generation and recombinant target protein expression is described in section 2.2.17 of Chapter 2

3.2.5 Knockdown of endogenous Src in primary cortical neurons

For knockdown of endogenous Src neurons were treated with lentivirus containing shRNA targeting c-Src. For transduction, cultured neurons (0.5×10^6 cells) at DIV1 to DIV6 were incubated with each of the 5 shRNA lentiviruses at a multiplicity of infection (MOI) ≥ 20 . The Neurobasal media was changed after 24 hours. As a control, cells were also transduced with the lentivirus generated by the pLKO.1 plasmid containing non-silencing shRNA (ns shRNA). Experiments to analyse the effects of knockdown of the endogenous Src on the signalling mechanism and survival of the transduced neurons were performed at DIV7.

3.2.6 Immunofluorescence

For immunofluorescence of endogenous Src and three subunits of NMDA receptor primary cortical neurons were grown on poly-D-lysine coated coverslips for seven days. Src (1:200) and subunit specific NMDAR antibodies (1:250) were used as primary antibodies and anti-rabbit FITC-green for the NMDA receptor subunits and anti-mouse Cy3 red for Src were used as secondary antibodies. A detail of this procedure is described in section 2.2.18 of Chapter 2. Images were captured using Leica TCS SP2 confocal microscope with a 100 x 1.35 NA objective (Wetzler, Hessen, Germany).

3.2.7 Data analysis

Densitometry analyses for the quantification of the protein bands on Western blots were done using Image J software (<http://rsb.info.nih.gov/ij/>). Statistical analyses were performed with the GraphPad Prism version 5 software (La Jolla, CA). The data was reported as the mean \pm SD and the statistical significance was determined by parametric procedure as Student's t-test (two-tailed), $p < 0.05$ was considered statistically significant for all experiments.

3.3 Results

3.3.1 Expression levels of Src and NMDA receptor subunits undergo time-dependent increase in cultured primary cortical neurons

Both extrasynaptic and synaptic NMDA receptors play important roles in governing neuronal survival (Hardingham and Bading, 2010), and Src is an important upstream regulatory kinase controlling NMDA receptor activity by forming protein complexes with NMDA receptor and phosphorylating receptor subunits (Kaufman et al., 2012; Salter and Kalia, 2004; Zhang et al., 2007). Since both Src and NMDA receptors interplay to regulate neuronal survival (Hossain et al., 2013), we first analysed the expression levels of Src and the various subunit of NMDA receptors in primary cortical neurons and the morphology of the neurons at different times after they were cultured *in vitro*. As shown in **Figure 3.1A**, Src and NMDA receptor subunits GluN1, GluN2A and GluN2B are detectable as early as day 1 *in vitro* (DIV1). Their expression levels undergo a time-dependent increase from DIV1 to DIV7. At DIV7, extensive neurite outgrowths and many synapses between neighbouring neurons have been formed, features that are typical of differentiated neurons.

Immunofluorescence analysis of the endogenous Src and the various NMDA receptor subunits in neurons at DIV7 shows that Src is distributed in cell bodies and neurite extensions, while the subunits of the NMDA receptors are present in cell bodies and dendrites (**Figure 3.1B**). These data indicate that at DIV7, the cortical neurons are differentiated and suitable for mechanistic studies for neuronal survival.

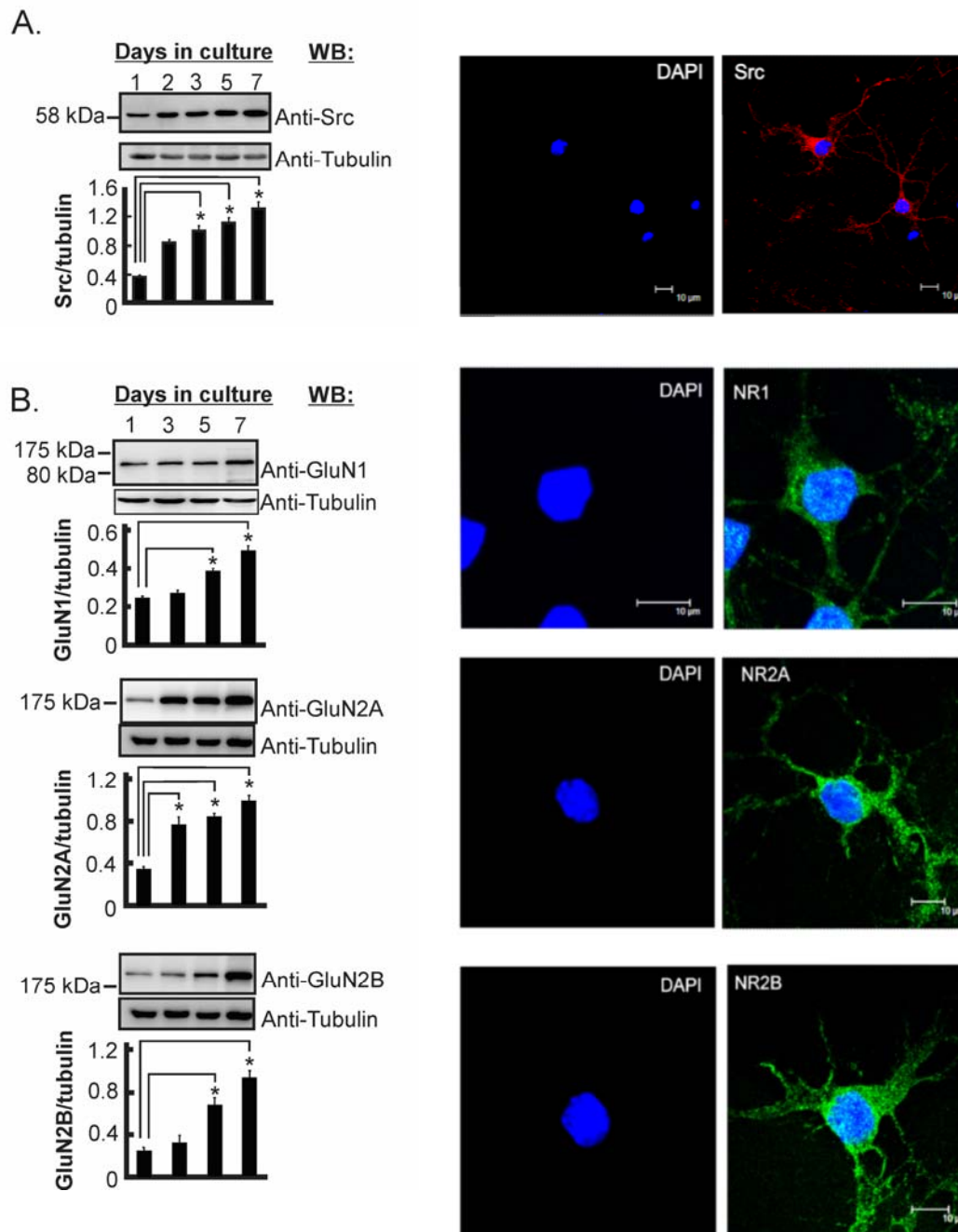


Figure 3.1

Figure 3.1 Expression levels of Src and NMDA receptor subunits in cultured primary cortical neurons from Day 1 to Day 7 in culture. Expression levels of Src, and GluN1, GluN2A and GluN2B subunits of NMDA receptor in cultured cortical neurons were monitored by Western blotting and immunofluorescence. Expression levels of Src, GluN1, GluN2A and GluN2B at different days of culture *in vitro* (DIV) were determined by Western blotting. The anti-Tubulin Western blots were used as the loading controls. The ratio of densitometric units of anti-Src, anti-GluN1, anti-GluN2A and anti-GluN2B to anti-Tubulin signals at different DIV (Data are represented as mean \pm SD and the p values were calculated by Student's t-test; $n = 5$, $*p < 0.05$). **A.** Expression of Src in neurons. Left: Western blots showing the time-dependent changes of expression level of Src and Tubulin. The ratio of densitometric units of anti-Src to anti-Tubulin signals is shown below the blots. Right: Immunofluorescence of Src in neurons at DIV7. **B.** Expression of NMDA receptor subunits in neurons. Western blots showing the time-dependent changes of expression level of GluN1, GluN2A and GluN2B and Tubulin. The ratio of densitometric units of anti-GluN1, anti-GluN2A and anti-GluN2B to anti-Tubulin signals is shown below the blots. Right: Immunofluorescence of NMDA receptor subunits GluN1, GluN2A and GluN2B in neurons at DIV7. The images of GluN1, GluN2A and GluN2B are merged with the DAPI-stained images.

3.3.2 The signalling pathways governing cell death and aberrant regulation of Src are intact in cortical neurons at DIV7

Over-stimulation of the cultured neurons at DIV7 with 100 μ M of glutamate induces cell death (**Figure 3.2A**), indicating that the signalling pathways mediating the excitotoxic signals originating from glutamate receptors are functional. The neurotoxic effect of glutamate was blocked by the NMDA receptor antagonist MK801 but not by the AMPA and kainate receptor antagonist 6-cyno-7-nitroquinoxaline-2,3-dine (CNQX) (**Figure 3.2A**), suggesting that the neurotoxic effect of glutamate is mediated by NMDA receptor. In agreement with this, over-stimulation by NMDA induces neuronal death. There are two major types of NMDA receptors: (i) the extrasynaptic NMDA receptors which are enriched in GluN2B subunit and (ii) the synaptic NMDA receptors enriched in GluN2A subunit. Previous studies revealed that signals emanating from the over-stimulated extrasynaptic NMDA receptors are neurotoxic (Hardingham and Bading, 2010; Karpova et al., 2013; Kaufman et al., 2012; Milnerwood et al., 2010; Okamoto et al., 2009; Rusconi et al., 2011; Zhang et al., 2011; Zhou et al., 2013). In agreement with these findings, the neurotoxic effect of glutamate was suppressed by the GluN2B-containing NMDA receptor antagonist Ifenprodil (**Figure 3.2A**). In a previous study, colleagues from our lab discovered that over-stimulation of glutamate receptors leads to sustained activation of calpains which catalyse the cleavage of Src to form a neurotoxic truncated Src fragment of 52-kDa (Hossain et al., 2013). As shown in **Figure 3.2B**, stimulation of cultured cortical neurons with glutamate and NMDA induces the formation of a 52-kDa truncated Src fragment. The formation of this fragment is suppressed when the cells were treated with glutamate and the calpain inhibitor calpeptin, indicating that formation of the Src fragment by limited proteolysis of Src by calpains in neurons over-stimulated by glutamate and NMDA. Furthermore, formation of this truncated fragment was abolished in neurons treated with glutamate in the presence of MK801 or Ifenprodil but not in those treated with glutamate and CNQX, suggesting that the generation of truncated Src fragment is induced in response to over-stimulation of the extrasynaptic NMDA receptors of the cultured cortical neurons.

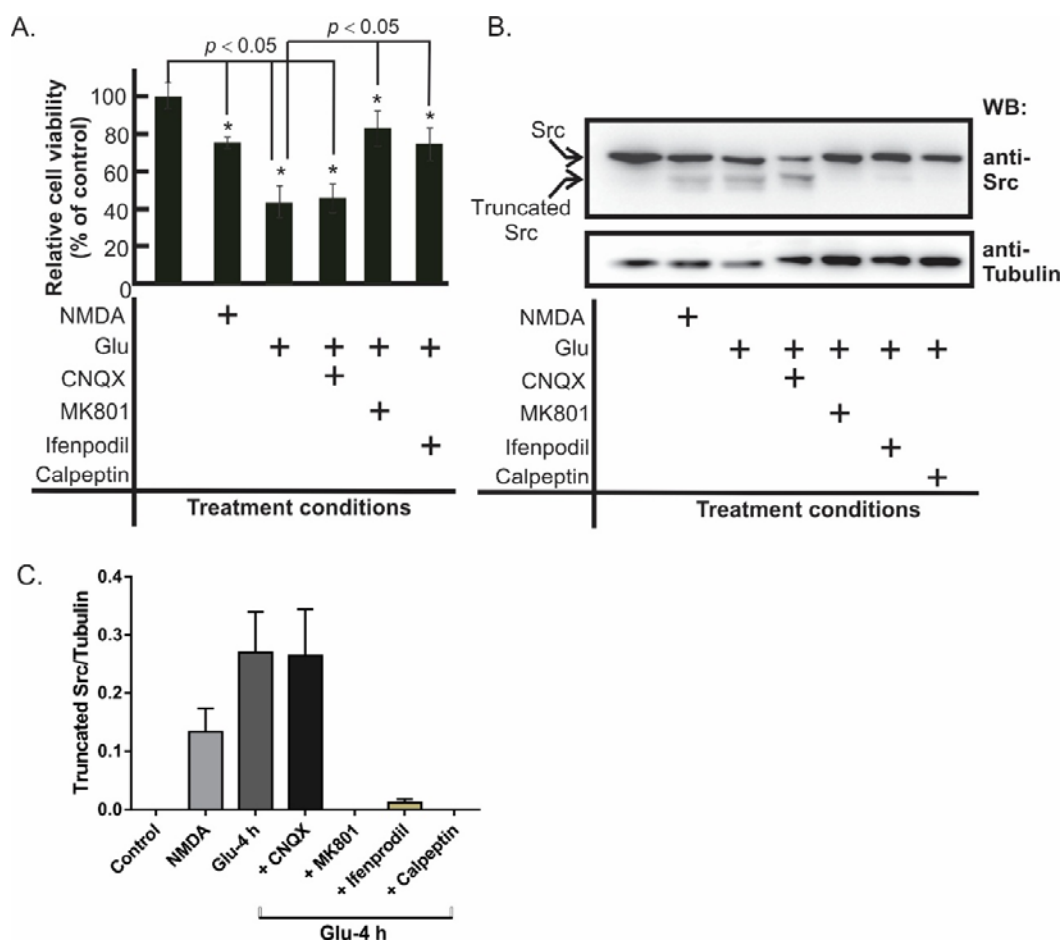
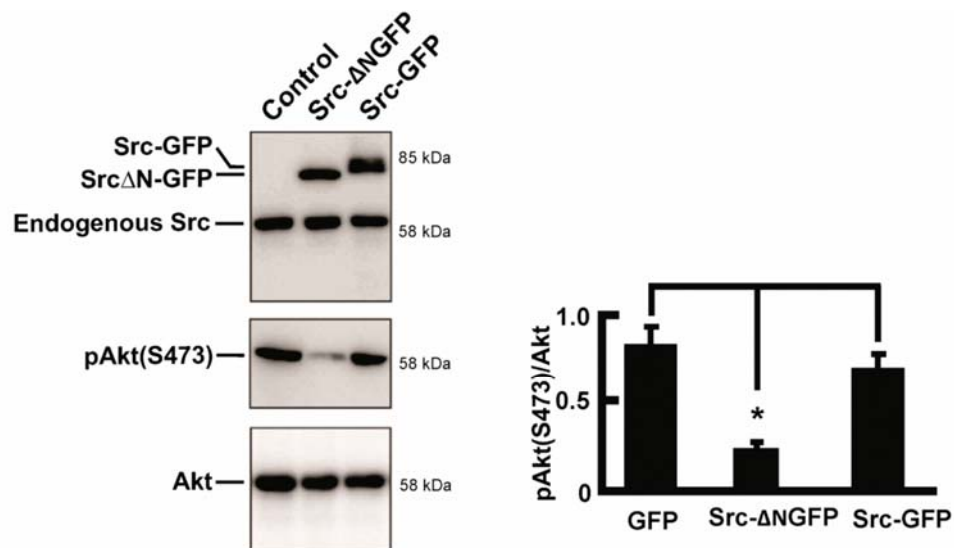


Figure 3.2 Effects of over-stimulation of glutamate receptors on neuronal viability and Src integrity. Cultured cortical neurons at DIV7 were treated with NMDA (100 μ M) alone for 4 h, glutamate (100 μ M) alone or in the presence of CNQX (50 μ M), MK801 (50 μ M) or Ifenprodil (20 μ M) for 4 h. **A.** Neuronal viability was determined by MTT assay. The viability of untreated cultured neurons was assigned as 100 %. (Data are represented as mean \pm SD, $n=5$ different cultures, * $p < 0.05$, Student's t test). **B.** Western blots of Src and Tubulin in untreated cultured neurons and neurons subjected to different treatment conditions: (i) NMDA for 4 h, (ii) glutamate for 4 h, (iii) glutamate and CNQX for 4 h, (iv) glutamate and MK801 for 4 h, glutamate and Ifenprodil for 4 h and (v) glutamate and calpeptin (20 μ M) for 4 h. **C.** Relative abundance of Src Δ N following different treatments. Proteolysis of Src is observed in neurons treated with NMDA and glutamate. NMDA receptor antagonists MK801 and Ifenprodil, and calpain inhibitor calpeptin can block Src cleavage following glutamate treatment.

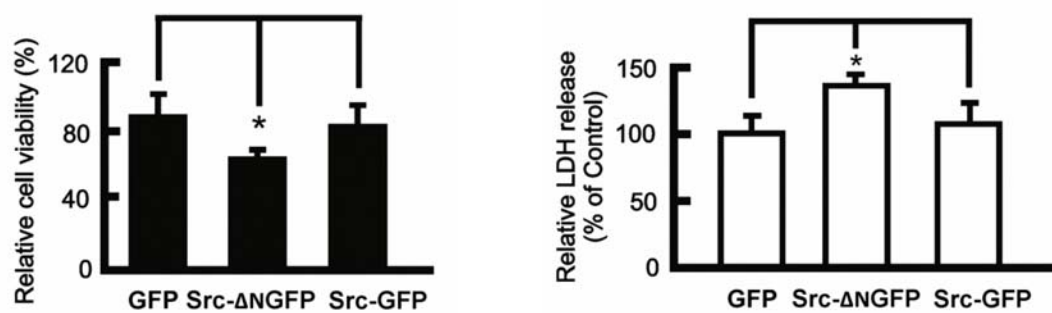
3.3.3 Truncated fragment of Src kinase generated by calpain is neurotoxic

To determine the function of the truncated Src fragment (Src Δ N), we utilised lentivirus-directed expression of GFP-tagged truncated Src (referred to as Src Δ N-GFP) under the control of doxycycline in neurons as shown in **Figure 3.3A**. For the control experiments, we transduced neurons with lentivirus expressing GFP or GFP fusion proteins of full-length Src (Src-GFP). Previously, it has been demonstrated that PI3K/Akt signalling pathway is essential in maintaining neuronal survival (Luo et al., 2003). Akt activation is shown to be a multi-step process (Bellacosa et al., 1998). Upon membrane recruitment and binding to phosphatidylinositol (3,4,5)-trisphosphate (PIP3) via PH domain, Akt is phosphorylated by the upstream kinases phosphoinositide-dependent kinase-1 (PDK1) at Thr-308 and mammalian target of rapamycin (mTOR) complex 2 (mTORC2) at Ser-473 (Datta et al., 1995; Stephens et al., 1998). Phosphorylation of Ser-473 by mTORC2 leads to full activation of Akt and its catalytic activity increases by approximately 10 fold (Alessi et al., 1996). We therefore monitored phosphorylation level of Akt at Ser-473 upon transduction of Src Δ N-GFP in primary cortical neurons. Immunoblot data revealed that Src Δ N-GFP significantly reduced phosphorylation of Akt at Ser-473 (**Figure 3.3A**) and subsequently decreased neuronal viability and survival (**Figures 3.3B** and **3.3C**). Staining of dead cells with EthD-1 further demonstrated that Src Δ N-GFP significantly increased number of dead cells compared to that of both GFP and Src-GFP transduced primary cortical neurons (**Figure 3.3D**). These results demonstrated that the signalling pathways mediating the neurotoxic action of the truncated Src fragment are intact in the cultured neurons we used in our study.

A.



B.



D.

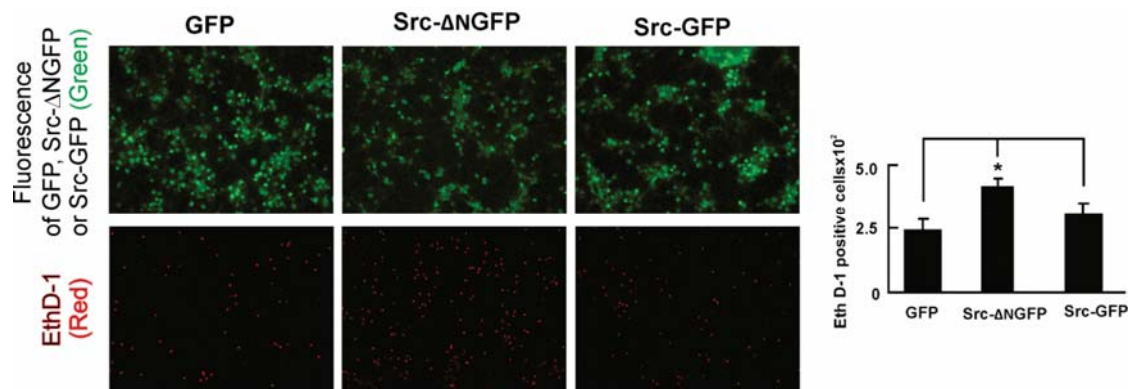


Figure 3.3

Figure 3.3 Effects of expression of recombinant truncated Src (SrcΔN-GFP) in primary cortical neurons. Primary cortical neurons were transduced with lentivirus directing expression of either GFP or SrcΔN-GFP or Src-GFP at DIV1. Expressions of the recombinant proteins were induced by doxycycline at DIV5. Effects of their expression were monitored at DIV7. **A.** Representative immunoblot showing expression of endogenous and recombinant Src and their effects on the phosphorylation level of Akt at Ser-473. Quantification data at right panel indicates densitometry of Akt and p-Akt level (Data are represented as mean ± SD, Student's t-test, n=5 different culture * $p < 0.05$). **B.** MTT assay to monitor the viability of the cultured neurons (mean ± SD, n= 5; * $p < 0.05$, Student's t-test). **C.** The activity of LDH released from the damaged neurons to the culture medium was monitored as a measure of the extent of neuronal cell death (mean ± SD, n= 5; * $p < 0.05$, Student's t-test). **D.** The effect of expression of GFP, SrcΔN-GFP and Src-GFP on neuronal survival is monitored by staining with Calcein-AM (green) and Ethidium homodimer-1 (EthD-1; red fluorescence), which stain live (intact) and damaged neurons, respectively. *Inset*, numbers of EthD-1-positive cells in the control (GFP) and neurons transduced with either SrcΔN-GFP or Src-GFP (mean ± SD, n = 5; * $p < 0.05$, Student's t-test).

3.3.4 Treatment with SFK inhibitors induce cell death of primary cortical neurons

For the pharmacological inhibition of SFKs, we first used two established chemical inhibitors of SFKs, PP2 and SU6656 to treat primary cortical neurons and examined their effects on neuronal viability. Treatment with the inhibitors decreases Src kinase activity in primary cortical neurons as suggested by decreased phosphorylation at Src-pY416 (**Figure 3.4A**). We further found that treatment of cortical neurons with SU6656 or PP2 for 8 h induced a significant reduction in cell viability as assed by an MTT assay (**Figure 3.4B**). This decrease in cell viability correlated with the increase in LDH released from damaged neurons as a result of SFK inhibitor treatment (**Figure 3.4C**).

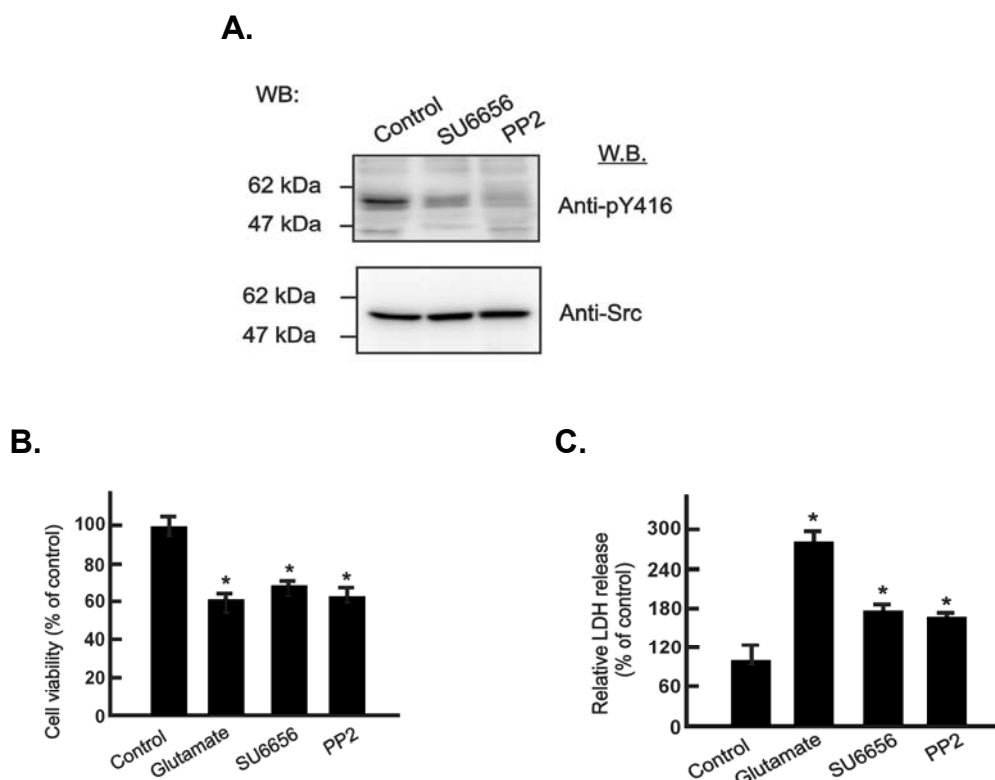


Figure 3.4 Effects of treatment of SFK inhibitors on neuronal viability. **A.** Autophosphorylation status of Src kinase in primary cortical neurons treated with SU6656 (10 μ M) and PP2 (20 μ M) for 8 h. Cultured neurons were treated with glutamate (100 μ M), SU6656 (10 μ M) and PP2 (20 μ M) for 8 h. Their viability and integrity were assessed by MTT assay (**B**) and LDH assay (**C**). Data are represented as mean \pm SD; n = 5, * $p \leq 0.05$.

As both SU6656 and PP2 are broad spectrum protein kinase inhibitors (Bain et al., 2007), their neurotoxic effects as depicted in **Figure 3.4** could be caused by inhibition of SFKs as well as inhibition of other protein kinases in neurons. To further ascertain the role of SFKs in neuronal survival, we examined the effect of treatment of neurons with a more selective SFK inhibitor A419259 on their survival. A419259 shows 1,000-fold selectivity for SFKs with IC₅₀ values for Src, Lck, Lyn, and Hck of 9, 3, 3, and 0.43 nM, respectively (Meyn et al., 2006; Pene-Dumitrescu et al., 2008; Wilson et al., 2002). **Figures 3.5A** and **3.5B** shows that treatment of neurons with 0.3–5 μ M of A419259 for 24 h significantly reduced neuronal survival. Since the treatment also led to significant reduction in autophosphorylation of neuronal Src, the reduction in neuronal viability was likely a result of inhibition of SFKs in neurons.

Taken together, our results of treatment of neurons with the chemically distinct SFK inhibitors suggest that the activity of one or more of the neuronal SFKs is critical for maintenance of neuronal survival. Since treatment of SFK inhibitors did not cause the formation of the neurotoxic 52-kDa truncated Src fragment (**Figures 3.5C** and **Figure 3.4A**), our data suggest that the SFK inhibitors induced neuronal death through inhibiting the activity of intact SFKs in neurons.

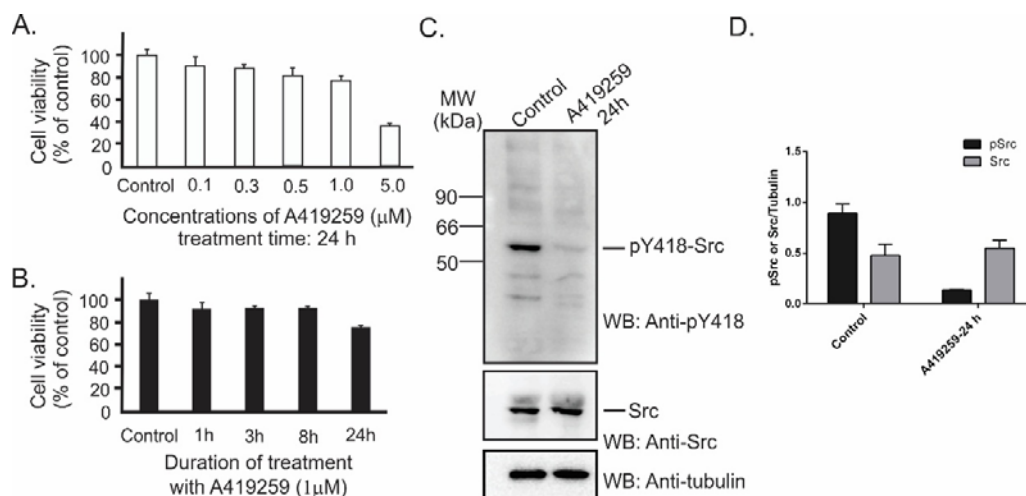


Figure 3.5 Effects of treatment of the selective SFK inhibitor A419259 on neuronal viability. **A.** Effect of treatment of cultured neurons with varying concentrations (0.1–5 μ M) for 24 h on neuronal viability monitored by MTT assay. **B.** Effect of treating the neurons with 1 μ M of A419259 for varying durations (1 – 24 h) on cell viability. **C.** Autophosphorylation status of Src kinase in primary cortical neurons treated with 1 μ M of A419259 for 24 h. **D.** Densitometry showing relative abundance of pY418 and total Src over tubulin. Data are represented as mean \pm SD; n = 3.

3.3.5 Suppression of Src expression induces cell death in cultured primary cortical neurons

In addition to Src, other SFKs co-expressed in neurons may be inhibited upon treatment of the neurons by the cell membrane-permeable SFK inhibitors. Among the SFKs co-expressed in neurons, Src has been implicated in mediating the pro-survival signalling pathways emanating from glial cell line-derived neurotrophic factor receptor Ret and the nuclear receptor of thyroid hormone 3,3',5'-tri-iodothyronine (TR1 α) (Encinas et al., 2004; Encinas et al., 2001). These observations prompted us to investigate the effect of knockdown of Src expression on the viability of primary cortical neurons. As shown in **Figure 3.6A**, neuronal Src expression was suppressed by ~70% in neurons transduced with lentivirus directing the expression of two *Src*-specific small hairpin RNAs, shRNA1 and shRNA2. In contrast, the non-silencing shRNA (ns shRNA) had no effect on Src expression. Transduction with the shRNA1- or shRNA2-lentivirus also led to significant changes in the phenotypes of the neurons with reduced intact cell bodies and the degree of axonal connections (**Figure 3.6B**). Results of both MTT and LDH assays demonstrated that the reduced expression of Src is associated with reduced cell survival (**Figure 3.6C**). This was further confirmed by the results of live/dead cell staining of the neurons with Calcein-AM and Ethidium homodimer-1 (EthD-1), namely that the transduction with the shRNA1- or shRNA2-lentivirus leads to a significant increase in the number of dead cells (stained by EthD-1) and reduction in the number of live cells stained by Calcein-AM (**Figures 3.6D** and **3.6E**). Taken together, our results indicate that Src is essential for survival of the cultured primary cortical neurons.

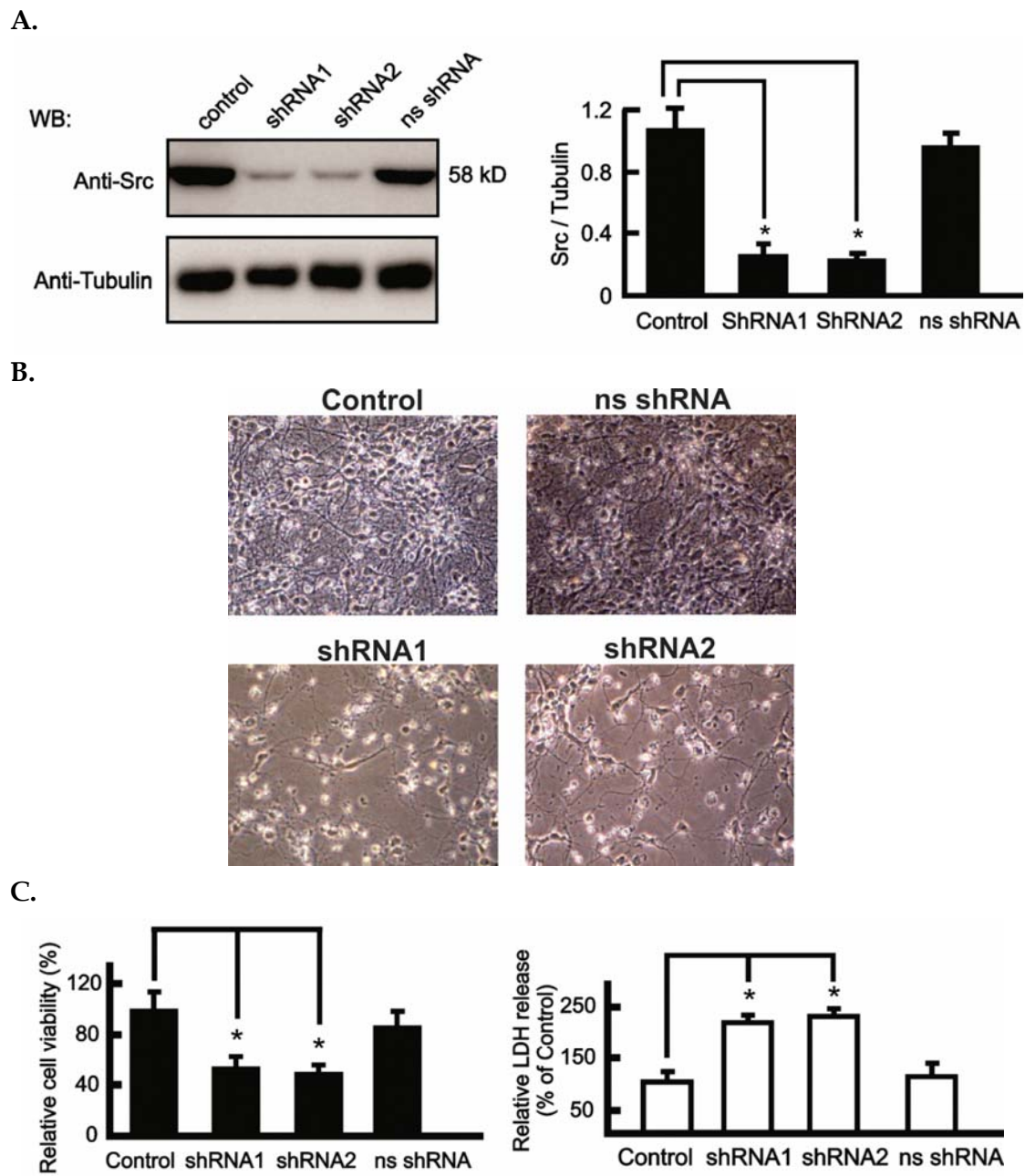


Figure 3.6

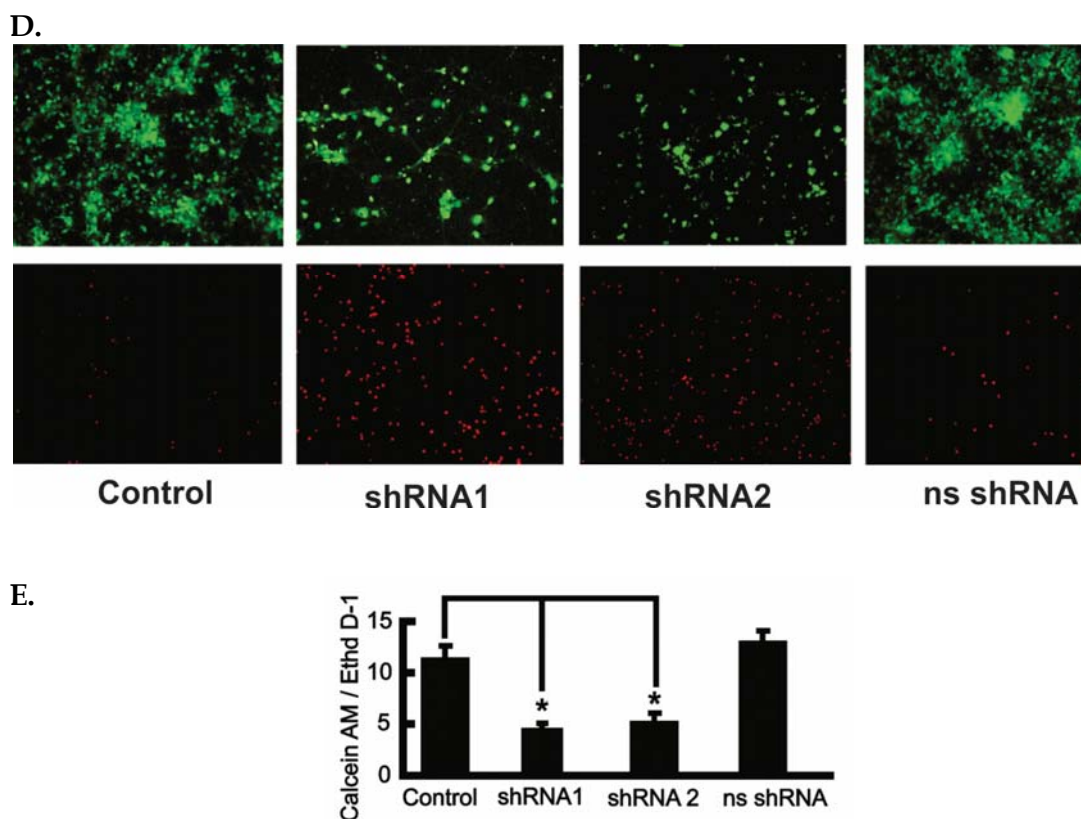


Figure 3.6 Knockdown of Src kinase with shRNAs decreases neuronal viability. Primary cortical neurons at DIV1 were transduced with lentivirus encoding shRNA1 or shRNA2 which can specifically knockdown the expression of Src in cells. The untransduced neurons were used as the control. Neurons transduced with the lentivirus encoding the non-silencing shRNA (ns shRNA) were used as the negative control. At DIV7, the neurons were harvested and analysed for the expression of Src and Tubulin, and cell morphology. **A.** Western blots of the crude lysates of the untransduced neurons (control) and the transduced neurons probed with the anti-Src mAb327 antibody and anti-Tubulin antibody. Right Panel: Ratios of Src/Tubulin level in the untransduced and transduced cells. Data are presented as mean \pm SD, $n = 3$ $*p < 0.05$, Student's t-test. **B.** Phase contrast photomicrographs of the untransduced and transduced neurons showing improper neuronal differentiation and death in shRNA1 and shRNA2 treated neurons. **C.** Left: Cell viability determined by the MTT assay (data are presented as mean \pm SD, $n = 5$ $*p \leq 0.001$, Student's t-test). Right: Assay of the activity of lactate dehydrogenase (LDH) released from the control and transduced neurons (Data presented as mean \pm SD, $n = 5$, $*p \leq 0.001$, Student's t-test). **D.** Staining of the control and shRNA transduced neurons with Calcein-AM and Ethidium homodimer-1 (EthD-1) which stain live and dead cells, respectively. **E.** Quantification of live and dead cells in control and Src knockdown primary cortical neurons. (Data are presented as mean \pm SD, $n = 5$ $*p \leq 0.001$, Student's t-test).

3.3.6 Inhibition of SFK activity or knockdown of Src expression leads to decrease in Erk1/2 phosphorylation

It is well documented that stimulation of synaptic NMDA receptor can initiate neuroprotective signals that protect neurons against apoptosis (Hardingham et al., 2001; Hardingham and Bading, 2010; Wu et al., 2001). Erk1/2 are key mediators of the synaptic NMDA receptor neuroprotective signalling pathway. To test a prediction that Src maintains neuronal survival at least in part by sustaining Erk1/2 in the active state, we examined the effect of treatment with SFK inhibitors and knockdown of Src expression on the Erk1/2 activation state in neurons.

We initially intended to monitor the phosphorylation status of Erk1/2 in neurons at DIV1 after their transduction with the Src shRNA lentivirus at DIV1. Since the majority of the transduced neurons were dead and degraded (**Figure 3.6**), they were not suitable for use for Western blots. In light of this, we examined the time course of the change in cell viability of neurons transduced by the Src shRNA2 at DIV1 to DIV6. Our results revealed significant reduction in cell viability in all transduction conditions with neurons transduced at DIV1 exhibiting the lowest level of cell viability (**Figure 3.7**).

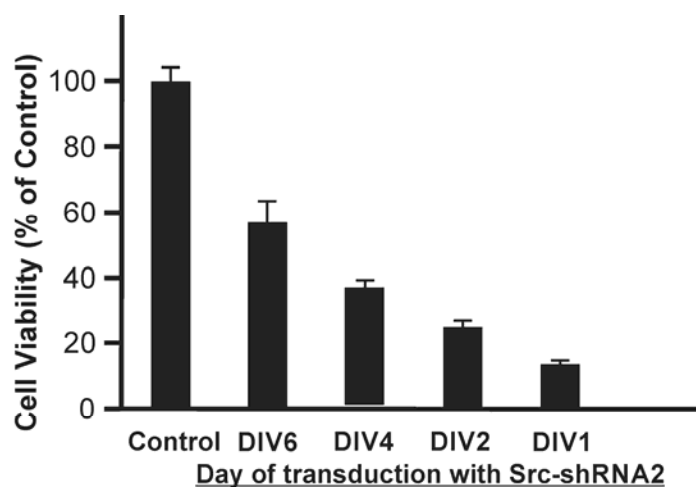


Figure 3.7 Effect of transduction of cultured neurons with the Src shRNA at DIV1 to DIV6 on cell viability. Neurons were transduced with shRNA2 lentivirus at DIV1, DIV2, DIV4 and DIV6. At DIV 7, the transduced neurons were harvested for analysis with MTT assay to monitor cell viability and compared with untransduced control neurons. Data are presented as mean \pm SD, n = 3.

Figure 3.8 shows the effects of down-regulation of Src in neurons transduced with the lentivirus expressing the Src-shRNA2 at DIV2. **Figure 3.8A** shows that the transduced neurons expressing the Src-shRNA exhibited a significant reduction in expression of neuronal Src. However, transduction of the neurons with lentivirus expressing the non-silencing shRNA and treatment of the neurons with 1 μ M A419259 for 24 h did not alter the Src expression level. **Figure 3.8B** reveals that inhibition of Src kinase activity or knockdown of Src kinase protein reduces phosphorylation of neuronal Erk1/2 at Thr-183 and Tyr-185 in the activation loop. From the ratios of the densitometric unit of the anti-pErk1/2 (T202/Y204 corresponding mouse T183/Y185) signal to that of anti-Erk signal, it is obvious that treatment with either SFK inhibitors or knockdown of Src expression significantly decreases neuronal Erk1/2 phosphorylation at these sites (**Figure 3.8B**). Since Erk1/2 activated by phosphorylation of Thr-183 and Tyr-185 by their upstream kinase MEK, our results indicate that Src is involved in the maintenance of the active state of Erk1/2. More importantly, our results suggest Erk1/2 operates down-stream of Src to mediate the pro-survival signals of intact Src in neurons (**Figure 3.9**).

PI3K and its downstream effector kinase Akt play significant roles in protecting neurons against cell death induced by ischemic stroke (Baba et al., 2009; Chan et al., 1999; Miyawaki et al., 2009; Namikawa et al., 2000; Yamaguchi et al., 2001), suggesting that PI3K and Akt are key enzymes maintaining neuronal survival. We therefore examined the effect of knockdown of Src expression and treatment with the SFK inhibitor A419259 on Akt phosphorylation. **Figure 3.8C** shows that down-regulation of Src from DIV2 to DIV7 and treatment with A419259 for 24h did not cause inactivation of Akt, suggesting that under the conditions we performed our experiments; Akt is not involved in the neuroprotective signalling mechanism of intact Src and other neuronal SFKs.

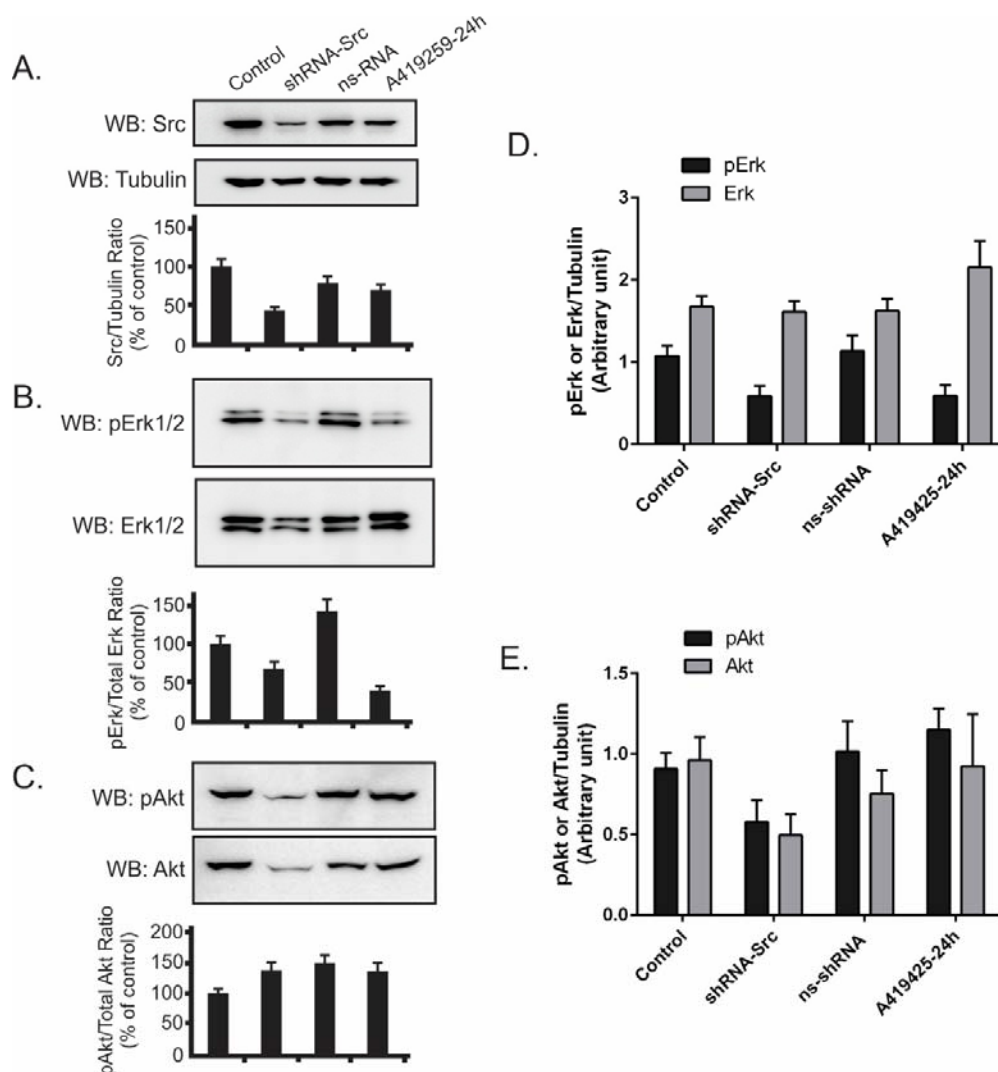


Figure 3.8 Effects of SFK inhibitors and Src knockdown on the phosphorylation status of neuronal Erk1/2 and Akt. A-C. Representative Western blots to monitor the levels of Src, Erk1/2, pErk1/2 (T183/Y185), Akt and pAkt (S473) in lysates of control neurons, neurons treated with the SFK inhibitors and neurons in which expression of Src was suppressed by shRNA. For Src knockdown, neurons were transduced with shRNA2 lentivirus at DIV2. At DIV7, the transduced neurons were harvested for analysis. For SFK inhibitors, neurons at DIV7 were treated with 1 μ M A419259 for 24 h. **B & D.** Ratios of the immunoreactive signals of Erk1/2 and pErk1/2. **C & E.** Ratios of the immunoreactive signals of Akt and pAkt (S473) (Data are presented as mean \pm SD; n = 3).

3.4 Discussion

Src family kinases (SFKs) are at the centre point of many cell-surface signalling events, such as the pathways activated by receptor tyrosine kinases (PDGFR, EGFR, and FGFR etc.), G-protein coupled receptors (GPCRs), cytokines, immune cell receptors as well as integrins and other cell adhesion molecules (Parsons and Parsons, 2004). Thus, they are important for transmitting a diverse range of cellular signals. Furthermore, SFKs not only play important role in proliferation and differentiation of neuronal cells (Ingraham et al., 1989; Maness et al., 1990), but also act as critical regulators in synaptic transmissions (Grant et al., 1992; Umemori et al., 2003; Zhao et al., 2000), axonal movement (Morse et al., 1998), and modulation of synaptic plasticity (Takasu et al., 2002). In developing CNS, SFKs are responsible for neuronal differentiation and neurite outgrowth (Beggs et al., 1994; Ignelzi et al., 1994), while in developed CNS they are mainly involved in regulating the activity of ionotropic glutamate receptors, such as the NMDA and AMPA receptors, as well as voltage-gated ion channels, including potassium channels and calcium channels. Although targeted deletion of the *Src* gene causes osteoporosis in mice, the *Src*-deficient mice did not exhibit obvious neurological abnormalities and the effect of knockdown of *Src* on neuronal survival has not been studied in detail (Soriano et al., 1991). In spite of the lack of obvious neurological abnormalities in the *Src*-deficient mice, Ignelzi *et al.* reported that cerebellar neurons derived from these mice exhibited impaired neurite outgrowth in response to stimulation by the neural cell adhesion molecule L1 (Ignelzi et al., 1994), suggesting that Src performs a specific and non-redundant function in the L1-dependent neurite outgrowth process.

Src family kinases participate in a wide array of signalling events in CNS through their interactions with many cellular proteins. Src is implicated to mediate the pro-survival action of the thyroid hormone T3 receptor TR1 α and GDNF receptor by activating phosphatidylinositol-3 kinase (PI3K) to maintain neuronal survival (Cao et al., 2009; Encinas et al., 2004; Encinas et al., 2001). In these previous studies, the authors employed SFK inhibitors capable of inhibiting all SFKs as well as a number of non-SFK kinases to define the roles of Src. Although these results suggest the significance of Src in neuronal survival, more detailed mechanistic studies using more specific approaches to inhibit Src and the SFKs are required to confirm this. In our study, in addition to using two commercially available and widely used SFK inhibitors, we employed two specific shRNAs against *Src* to address the functional role of full length Src protein in neuronal survival, and

demonstrated that suppression of Src expression significantly reduces neuronal survival. Together, our data indicates that among SFKs, Src itself plays a critical role in maintenance of neuronal survival.

In search of possible signalling mechanism of neuronal death upon Src inhibition or Src knockdown, we found a significant decrease of phosphorylation of Erk1/2. In addition to cooperating with Erk1/2, Src also maintains neuronal survival by regulating mitochondrial function. Src is targeted to the mitochondria where it phosphorylates NADH dehydrogenase [ubiquinone] flavoprotein 2 (NDUFV2) of the mitochondrial respiratory complex I, and the phosphorylation contributes to neuronal survival (Ogura et al., 2012). Thus, future investigations of the neuroprotective mechanism of Src should include defining how phosphorylation of this complex I protein cooperates with activation of Erk1/2 to mediate the pro-survival signals of Src in neurons.

If Src is a physiological pro-survival enzyme in neurons, how could Src and other neuronal SFKs contribute to ischemic stroke-induced neuronal death and brain damage in animal models? We postulate that Src is aberrantly regulated under pathological conditions and this aberrantly regulated form of Src loses its pro-survival function and gains neurotoxic activity (Hossain et al., 2012; Hossain et al., 2013). Src undergoes limited proteolysis by calpain at the unique domain to form a 52-kDa truncated product in platelets and neurons (Feder and Bishop, 1990; Hossain et al., 2013; Oda et al., 1993), and undergoes activation and S-nitrosylation of Cys-498 in rat brain after cerebral ischemia and reperfusion (Akhand et al., 1999; Rahman et al., 2010; Tang et al., 2012). A major event leading to neuronal death in ischemic stroke and neurodegeneration is excitotoxicity, in which NMDA receptors of neurons were over-stimulated by excessive concentration of glutamate. The over-stimulated NMDA receptors allow a massive influx of calcium into neurons, which causes over-activation of calpains. We demonstrated that Src in neurons over-stimulated by glutamate is cleaved by calpains to form a 52-kDa fragment. More importantly, this truncated Src fragment induces neuronal death in part by inhibiting Akt, and a cell membrane permeable fusion peptide (Tat-Src) derived from the Src unique domain that also cover the calpain cleavage site, not only restrict Src cleavage by calpain but also maintain neuronal survival in excitotoxicity (Hossain et al., 2013). Thus, our previous results and results presented in this chapter indicate that Src is a key regulator of neuronal survival and also a mediator of neuronal death (**Figure 3.10**). In neurons undergoing excitotoxic cell death, calpain cleavage converts Src from a promoter of neuronal survival to a mediator of neuronal death.

Src kinase inhibitors were shown to reduce brain damage in mouse models of ischemic and haemorrhagic stroke (Hou et al., 2007; Liu and Sharp, 2011), presumably by inhibiting the kinase activity of the neurotoxic truncated Src fragment generated by calpain cleavage. However, the use of these inhibitors may also induce adverse effects by suppressing the pro-survival signals of intact Src and other neuronal SFKs. Nevertheless, results of our studies indicate that further investigation into pro-survival signalling mechanism of intact Src and the neurotoxic mechanism of the truncated Src fragment may benefit development of therapeutic strategies for treatment of stroke patients.

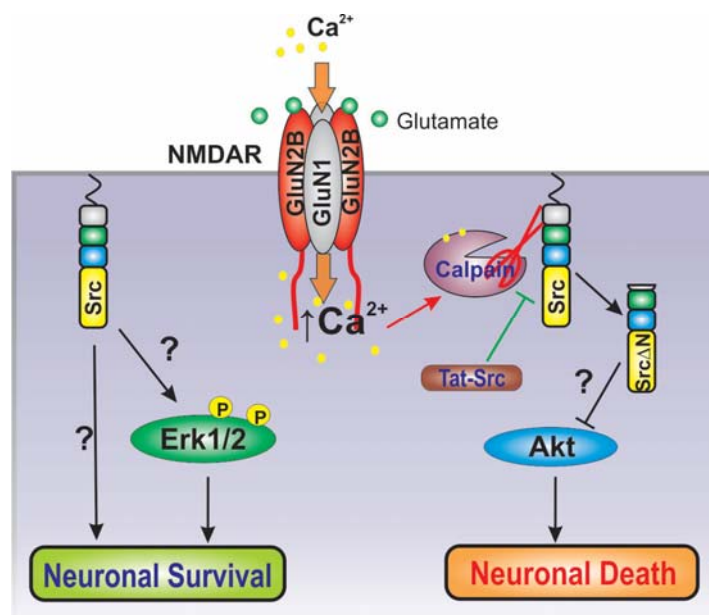


Figure 3.9 Src is both a promoter of neuronal survival and an executor of neuronal death. Under normal physiological conditions, intact Src promotes neuronal survival. It exerts its neurotrophic effect in part by activating the pro-survival kinase Erk1/2. Under excitotoxic conditions, over-stimulation of NMDA receptor by glutamate leads to massive influx of calcium into the cytosol. The sustained increase in cytosolic calcium concentration causes over-activation of calpains which cleaves Src to form the truncated Src fragment (Src Δ N). The Src fragment induces neuronal death in part by inhibiting Akt. A cell membrane permeable fusion peptide (Tat-Src) can block calpain cleavage of Src and restrict neuronal death in excitotoxicity. The question marks (?) indicate yet unknown mechanisms.

Chapter 4

Declaration and acknowledgement

- ✚ Dr. Ching-Seng Ang, one of my co-supervisors provided help to run the proteomic samples in Orbitrap Elite mass spectrometer and to search the Mascot algorithm using the Xcalibur raw files to generate msf files. I am responsible for analysing and generating all the data presented in this chapter.

Chapter 4: Quantitative global proteomic approach to understand the mechanism of glutamate-induced excitotoxicity

4.1 Introduction

Neuronal excitotoxicity is a prominent pathological process by which neurons are damaged and killed by the over-activation of receptors for the excitatory neurotransmitter glutamate, such as the NMDA (N-methyl-D-aspartate) receptor and AMPA [2-amino-3-(5-methyl-3-oxo-1,2-oxazol-4-yl) propanoic acid] receptor. These glutamate receptors under normal physiological condition maintain neural development, survival and synaptic plasticity (Hsu et al., 2003). However, excitotoxicity due to excessive extracellular glutamate results in both acute cerebral ischaemia and traumatic brain injury, and chronic neurological diseases, such as Huntington's and Alzheimer's disease (Hardingham and Bading, 2010). Glutamate can be increased up to the concentration of 1 mM in the synaptic cleft but decreases rapidly in the lapse of milliseconds (Clements et al., 1992). When the brain cells fail to generate sufficient ATP due to oxygen or glucose deprivation, energy failure occurs and ionic gradients are lost and glutamate reuptake processes become impaired. Glutamate accumulates in the extracellular space of the CNS (Choi and Rothman, 1990). This excitatory neurotransmitter binds and leads to the prolonged and uncontrolled stimulation of the ionotropic glutamate receptors, such as NMDA and AMPA receptors. These receptors being highly permeable to extracellular ions especially Ca^{2+} , allow excessive Ca^{2+} along with Na^+ and water to enter the affected neuronal cells, which in turn activate proteases, phospholipases and endonucleases (Ankarcrona et al., 1995; Choi, 1988b). These molecules also initiate the production of nitric oxide (NO), arachidonic acid metabolites, and reactive oxygen species (ROS) that act as additional triggers for cell death (Dirnagl et al., 1999; Lo et al., 2003). Excitotoxicity is the key mechanism for neuronal cell death following cerebral ischaemia and chronic neurodegenerative diseases. However, the overall molecular mechanism and signalling pathways involved in this cell death process are yet to be fully understood. Full understanding of this mechanism entails identification of the key cellular events directing neuronal death and elucidation of how they interplay spatially and temporally to direct neuronal death.

The high throughput mass spectrometry (MS) based proteomic approach has become an essential tool for examining brain cell-specific molecular pathways to understand distinct brain functions under normal physiological as well as pathological conditions, which in the past relied mostly on descriptive analysis of macroscopic and microscopic observations (Mann et al., 2001; Plum et al., 2015). Using quantitative proteomic approaches, researchers can quantitatively compare changes in total proteomes in two or more biological samples using the stable isotope labelling (metabolic or chemical) methods (Bantscheff et al., 2007) or label-free methods (Ong and Mann, 2005). Most of the previous neuroproteomic studies were carried out on traditional in-gel proteomics that followed iTRAQ labelling approach for relative and absolute quantification of the identified proteomes (Datta et al., 2011; Gygi et al., 1999; Merali et al., 2014). One of the aims of my PhD project is to identify neuronal proteins of which the abundances undergo changes in response to the treatment with cytotoxic dose (100 μ M) of glutamate. Operationally, I aim to follow the relative changes of specific neuronal proteins in neurons before and after glutamate treatment. The method I employed for quantitative proteomic analysis involved few steps, (i) in-solution (i.e. gel-free) trypsin digestion followed by stable isotope dimethyl labelling of tryptic fragments of neuronal proteins, (ii) LC-MS/MS analysis of the mixed (control: treatment, 1:1) labelled tryptic fragments and (iii) identification of the tryptic fragments (i.e. proteins) exhibiting significant differences in their abundance. Dimethyl labelling covalently attaches a dimethyl group at the N-terminal amino group and ϵ -amino group of lysine side chain. This is a robust and cost effective method capable of labelling microgram to milligrams of cellular proteins. Using a combination of deuterated and ^{13}C labelled reagents, up to three samples can be simultaneously labelled and compared (Boersema et al., 2009; Hsu et al., 2003). This chapter describes the data on global changes of the abundance of neuronal proteins following glutamate-induced excitotoxicity in cultured primary cortical neurons.

4.2 Methods

4.2.1 Primary cortical neurons culture and cell viability assay

Primary cortical neurons were cultured from embryonic (E16) pups collected from the pregnant C57BL/6 mice. At seventh days *in vitro* (DIV7), 100 μ M glutamate was added to the cultured primary neurons for different time points to induce excitotoxicity as described in the previous study (Hossain et al., 2013). Neuronal viability following glutamate excitotoxicity was checked by the MTT cell viability assay. Detailed procedures are explained in Chapter 2.

4.2.2 Experimental design

Figure 4.1 shows the workflow of the experiments. First, I collected embryos (6-8 per mouse) from C57BL/6 pregnant mice (E16), separated the brain cortices and cultured the trypsinised brain cells in poly-D lysine coated cell culture plates with neurobasal medium in presence of B-27 supplement that restricts the growth of astrocytes and glia and promotes the growth of neuronal cells. At DIV7, 100 μ M of glutamate was added to these matured neurons to induce excitotoxicity. At 15 min and 4 h (selected time points, section 4.3.1), the treated neurons and untreated control neurons were lysed using ice cold RIPA buffer. Total proteins from lysates of the untreated and treated neurons were precipitated using freezer-cold acetone (-20°C) and resuspended in 8 M urea solution (in 50 mM TEAB). A BCA protein quantitation assay was performed for the neuronal lysates to take equal amount of control (2 aliquots) and treated lysates (1 aliquot of 15 min and 1 aliquot of 4 h) to start the proteomic experiment. Before in-solution (gel-free) trypsin digestion, these samples were reduced and alkylated with 10 mM TCEP and 55 mM iodoacetamide, respectively at 37°C . Samples were then digested with trypsin (1:40) overnight at 37°C . Digested tryptic peptides were purified by solid phase extraction (SPE) clean-up method (described in Chapter 2) and purified peptides were freeze-dried overnight. Freeze-dried peptides were resuspended in 100 mM TEAB. At this stage, a micro BCA quantitation assay was carried out to ensure that equal amounts of dissolved digested peptides derived from the control lysates (2 aliquots) and 15 min and 4 h glutamate treated lysates (1 aliquot each) were used for labelling. Formaldehyde (CH_2O , light) and deuterated formaldehyde (CD_2O , medium) were used to label the control and glutamate-treated peptides, respectively in presence of 0.6 M sodium cyanoborohydride (NaBH_3CN) for the labelling reaction to occur for 60 min at room

temperature. The reaction was stopped with 1% NH₃ followed by acidification with 100% formic acid before equal amount of labelled peptides were mixed (control: treatment = 1:1) together and samples were run on LTQ Orbitrap Elite mass spectrometer for LC-MS/MS analysis (detail procedure in Chapter 2). This experiment was repeated three times with three biological replicates before data analysis.

4.2.3 Proteomic data analysis

Mass spectrometric data were analysed using Proteome Discoverer 1.4 (Thermo Scientific, v.1.4.0.288) software with Mascot as the search engine. Strategies for proteomic data analysis are outlined as a workflow in **Figure 4.2** and detailed methods are described in Chapter 2.

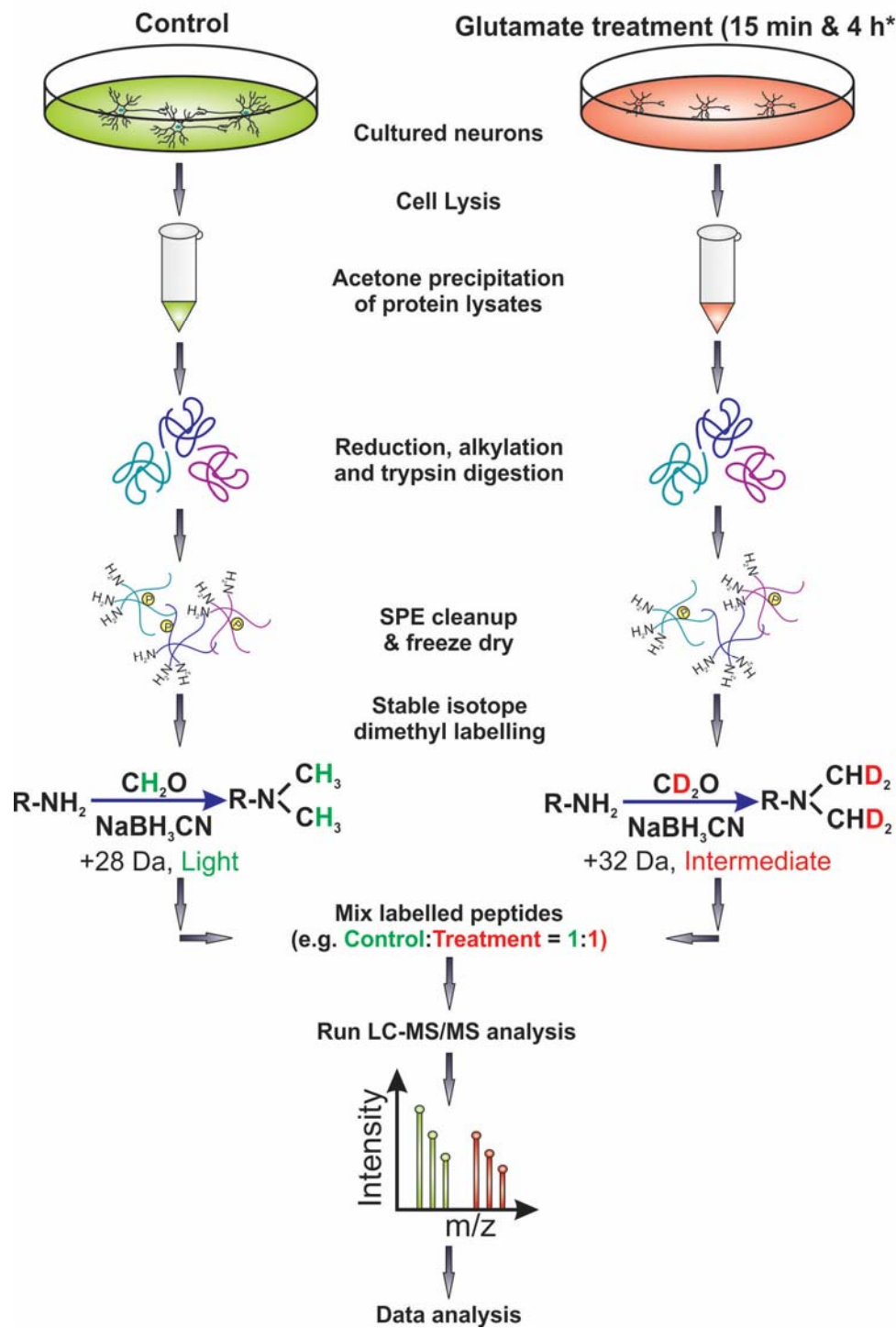
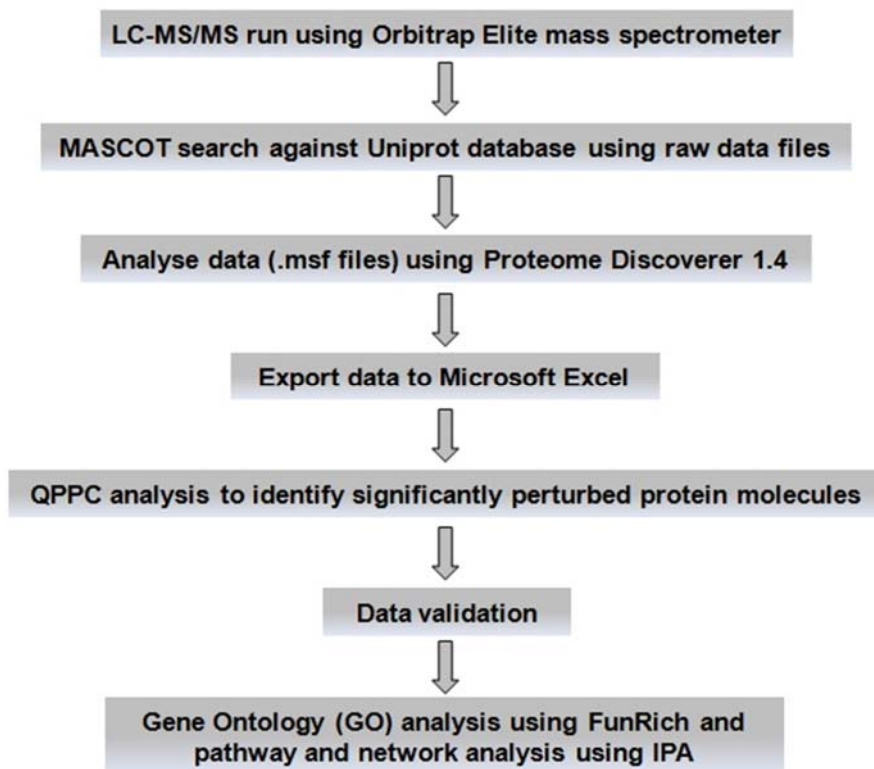


Figure 4.1

Figure 4.1 Workflow for exploring global proteome changes in glutamate excitotoxicity. The cultured primary cortical neurons were treated with glutamate (100 μ M) for 15 min and 4 h at day 7 in culture before they were lysed using RIPA buffer along with untreated (control) neurons. Total proteins from these neuronal lysates were precipitated using freezer-cold acetone (-20°C) and equal amount of control and treated lysates were reduced with 10 mM TCEP and alkylated with 55 mM iodoacetamide before they were digested with trypsin (1:40) overnight. Purified tryptic digests were dimethyl labelled with formaldehyde (CH₂O, light label) for peptides derived from the control neurons and deuterated formaldehyde (CD₂O, medium label) for peptides derived from the treated neuronal lysates in presence of sodium cyanoborohodride (NaBH₃CN). Equal amount of the labelled peptides were mixed (control: treatment, 1:1) and run on LTQ Orbitrap Elite mass spectrometer for LC-MS/MS analysis. *n = 3 for 15 min time point and n = 6 for 4 h, as this time point was repeated for inhibitor study described in Chapter 6. *Abbreviations: SPE, solid phase extraction; TCEP, tris-(2-carboxyethyl)-phosphine.*

A.



B.

Search parameters:

- Precursor mass tolerance: 10 ppm
- Fragment mass tolerance: 0.6 Da
- Fixed modification: Carbamodomethyl of cysteine
- Variable modification: Oxidation of methionine
- Quantification method: 2-plex dimethylation (C₂H₆, C₂H₂D₄)
- Enzyme: Trypsin (max 2 missed cleavage)
- False discovery rate: 1%
- Unique peptides: 2

Figure 4.2 Workflow for proteomic data search and analysis. **A.** Workflow showing different steps in proteomic data analysis those are explained in Chapter 2. **B.** Parameters that were used for Mascot search. *Abbreviations: QPPC, Quantitative Proteomics p-value Calculator; FunRich, Functional Enrichment Analysis Tool; IPA, Ingenuity Pathway Analysis.*

4.3 Results

4.3.1 The *in vitro* cell model and selection of the time points for proteomics analysis

Embryonic cultured neurons have been extensively used as an important experimental model for the study of the molecular mechanisms underlying excitotoxicity (Choi et al., 1987). To mimic excitotoxicity, the condition that leads to neuronal death in acute neurological disorders such as ischaemic stroke and traumatic brain injury, cultured primary cortical neurons were treated with 100 μ M glutamate (Hossain et al., 2013; Khanna et al., 2007) and biochemical changes in neurons in responses to the treatment were then investigated by proteomics analysis. Neurons at DIV7 were matured fully by developing dendrites and synapses, and all the subunits of NMDA receptors were fully expressed (Hossain et al., 2013). Overstimulation of these NMDA receptors by glutamate allows excessive Ca^{2+} influx inside the cells that leads to the activation of different cell death pathways ultimately leading to neuronal demise (Manev et al., 1989).

To confirm that the concentration of glutamate used is cytotoxic and to select the time points for further proteomics analysis, I performed the MTT cell viability assay for different time points after glutamate treatment. Viability data (from three independent experiments) indicated that the neurons underwent a time-dependent decrease in viability (**Figure 4.3**). No significant change in cell viability was detected up to 1 h glutamate treatment and starting from 4 h, viability decreased significantly. Eight hours (8 h) after treatment cell viability decreased to ~50% of the untreated control.

My major goal is to identify the key cellular events mediating the excitotoxic signals emanating from the over-stimulated ionotropic glutamate receptors. Since these events occur at the initial phase of the cytotoxic signalling pathway, we need to collect neurons within minutes after the glutamate treatment. Neurons that are destined to excitotoxic cell death without showing signs of cellular damage are most suitable for the study to identify the key neurotoxic cellular events at the early phase of the pro-death signalling pathway. **Figure 4.3** shows that neurons are viable after 15 min glutamate treatment. Thus we used these neurons for proteomic analysis. Again, we also need to use neurons in which the cellular events at all stages of cytotoxic signalling pathway are fully activated. Proteomics analysis of these neurons will unveil these events. **Figure 4.3** shows that neurons exhibited significant cell death 4 h after glutamate treatment. We therefore chose these neurons as another time point for our study. Quantitative proteomics analysis of the untreated neurons

and neurons at 15 min and 4 h after glutamate treatment will identify the early cellular events associated with excitotoxicity and reveal which of these events persist up to 4 h post glutamate treatment. These cellular events are likely the driver events directing neuronal death in excitotoxicity.

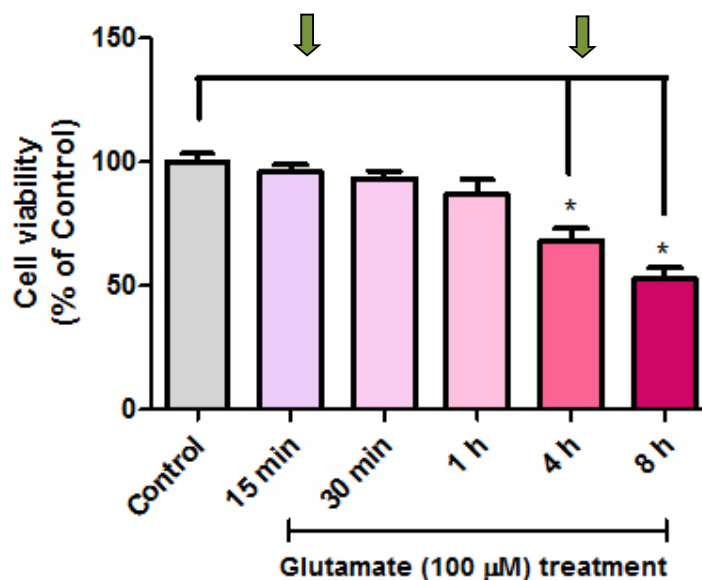


Figure 4.3 Glutamate induced excitotoxic neuronal death in cultured primary cortical neurons. MTT cell viability assay showing the time-dependent changes in cell viability of cultured neurons treated with 100 μM glutamate. Viability of glutamate treated neurons is around 50% of the untreated control after 8 hours. Data indicates that cell viability is significantly reduced from 4 h to 8 h after treatment in comparison to the control cells (mean \pm SD, $n = 3$ * $p < 0.05$, Student's t -test). Arrows indicate the selected time points used for quantitative proteomics analysis.

4.3.2 Data processing for protein quantification and the criteria for selection of peptides exhibiting differences in abundance

The mass spectrometric raw data (Xcalibur file format) were processed using Proteome Discoverer 1.4 (PD 1.4) with Mascot search algorithm against Uniprot database (detailed in chapter 2). All identified peptides were above the identity threshold score, which represents a confidence level of $p < 0.05$. The inbuilt quantitation node on PD 1.4 allows us to measure the relative abundance of the identified peptides (medium/light ratios) and corresponding protein group based on the extracted ion chromatogram (XIC) intensities from the MS1 scans. Results were filtered with high peptide confidence to reflect a maximum of 1% false discovery rate (FDR). For relative protein quantification, peptide ratios (medium/light) were calculated from the isotopic clusters for the identified peptides in both light and medium quantification (quan) channels or from a single isotopic cluster identified in either of the quan channels (light and/or medium) using the accurate mass feature of the mass spectrometer (< 2 ppm) to define the corresponding light or medium labelled peptide. For peptide ratios with any missing quantification channel were avoided to minimise protein quantitation error. To facilitate further analysis, an MS Excel file was exported from PD with protein group accession numbers, protein names, coverage, peptides, unique peptides, peptide spectrum matches (PSMs), areas, average median medium/light ratios and details of all the identified peptides. Using the MS Excel file, the exported data for 15 min glutamate treatment from all three biological replicates were analysed considering average median medium/light ratios and calculating mean and standard deviations. These ratios reflect the relative expression pattern of a given protein induced by excitotoxicity. The web-based quantitative proteomics p -value calculator (permutation based) was used to identify proteins that exhibit statistically significant ($p \leq 0.05$) perturbation in abundance induced by excitotoxicity (Chen et al., 2014). The data for 4 h glutamate treatment from six (3+3, as I repeated 4 h treatment during inhibitor study as described in Chapter 6) biological replicates were also processed and analysed in the same way as for analysis of the 15 min data. The proteins exhibiting changes in abundance after glutamate treatment for 15 min and/or 4 h were analysed by the Functional Enrichment Analysis Tool (FunRich) for Gene Ontology (GO) analysis and also by the Ingenuity Pathway Analysis (IPA) software to predict how the intracellular signalling networks are perturbed in neurons undergoing excitotoxic cell death.

4.3.3 Over stimulation of glutamate receptors induced changes in expression levels of over 680 neuronal proteins

We were able to identify a total of 13827 peptides from a total of 9 LC-MS/MS runs (3 biological replicates for 15 min and 6 for 4 h glutamate treatment). This led to the identification of 1119 proteins at 1% false discovery rate at the peptide level. **Table 4.1** describes findings for individual biological replicates. All of these 1119 proteins had at least one unique peptide and 593 (53%) were identified with 2 or more unique peptides. A total of 852 and 957 protein molecules were identified from the 15 min and 4 h glutamate treated samples, respectively. A total of 681 of these proteins were common molecules identified for these two time points (**Figure 4.4**). Among these 681 neuronal proteins exhibiting sustained perturbation of their expression levels for up to 4 h, some are executors of neuronal death and some are protector against neuronal death.

Table 4.1 Mass spectrometric data for all biological replicates following glutamate treatment of cultured primary cortical neurons for 15 min and 4 h.

Descriptions	Biological replicate 1	Biological replicate 2	Biological replicate 3	Biological replicate 4	Biological replicate 5	Biological replicate 6
Glutamate (15 min)						
(Total protein groups = 852)						
# Peptides	943	1803	1765			
# Merged proteins	1895	2692	2662	-	-	-
# Protein groups	444	691	676			
FDR value	0.0097	0.0097	0.0098			
Glutamate (4 h)						
(Total protein groups = 957)						
# Peptides	691	1763	2016	1598	1250	1998
# Merged proteins	1519	2614	2950	2533	2128	3181
# Protein groups	343	673	743	649	536	802
FDR value	0.0093	0.0098	0.0098	0.0061	0.0065	0.0075

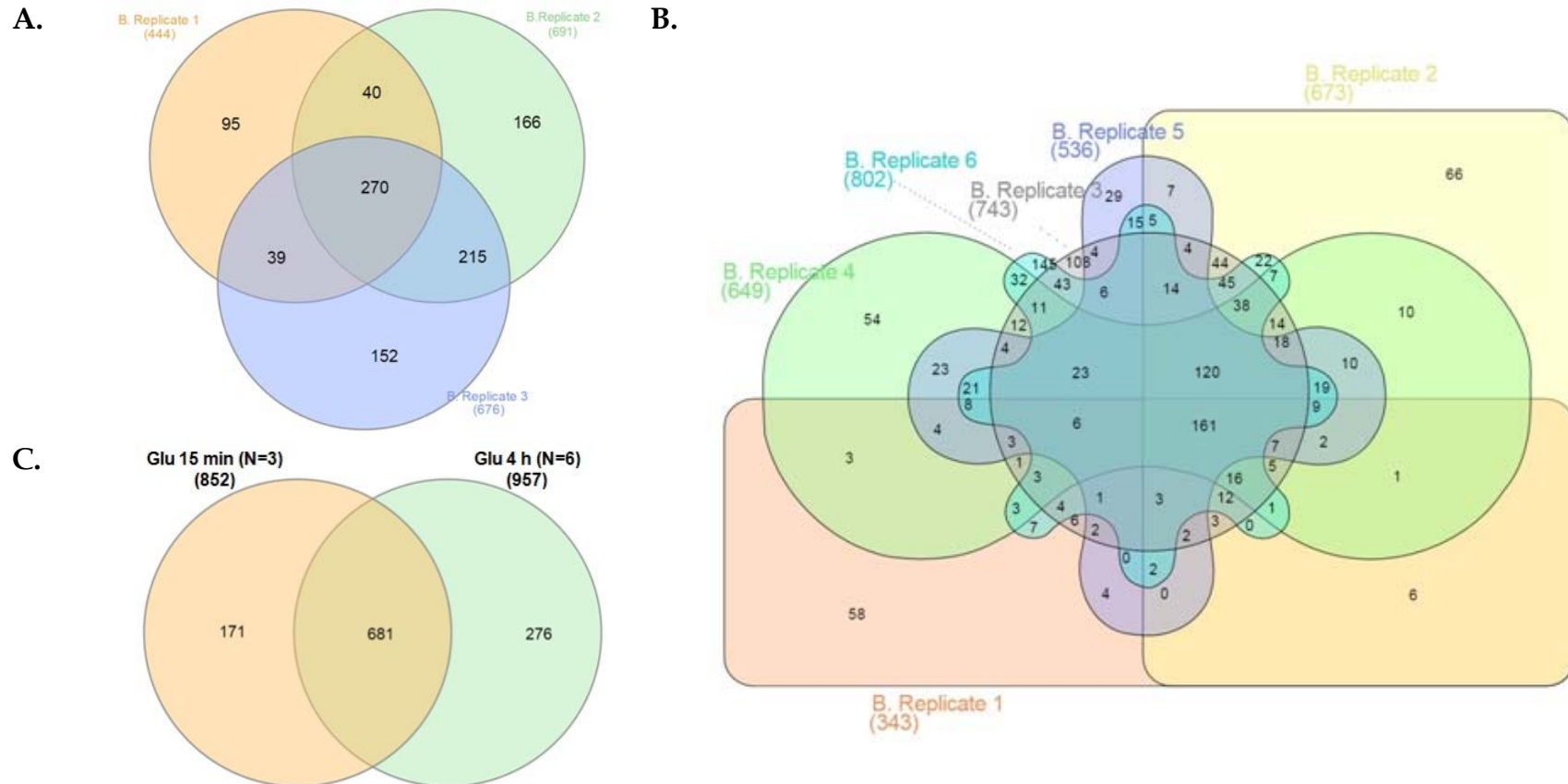


Figure 4.4 Venn diagram showing the numbers of the identified protein molecules in cultured cortical neurons treated with glutamate for 15 min and 4 h. Data represents the distribution of identified protein molecules among the biological replicates following 15 min (A) and 4 h (B) glutamate (100 μ M) treatment. C. From all these biological replicates, 681 common protein molecules were identified.

4.3.4 Identities of the neuronal protein molecules of which the abundance were significantly perturbed by glutamate overstimulation

After protein identification and quantitation, I was interested to explore the biological functions of the neuronal proteins whose abundance were significantly perturbed in excitotoxicity. To this end, the data from all 3 biological replicates for the 15 min and all 6 biological replicates for the 4 h treatment time points were exported in MS Excel files. The Quantitative Proteomics *p*-value Calculator (QPPC), an online permutation based statistical analysis software was used to identify proteins molecules of which the abundance was significantly perturbed (Chen et al., 2014). The accession numbers, protein names and medium/light ratios of all the identified proteins from all biological replicates of the 15 min glutamate excitotoxicity was used as an input for the QPCC stage 1 computation. 1000 permutations calculation was selected and 100 as a threshold were used for outlier removal, i.e. peptides with ratios of more than 100 and its inverse were removed as outliers (if any). QPPC processed input data to remove outliers, negative or missing ratio values (if any) and ratios coming out from single observations. After stage 1 computation, QPPC generated an output csv file containing mean medium/light ratio, the standard deviation (SD), the number of observations, and the *p*-value for each of the identified proteins. This file was used further in the stage 2 computations for determining significantly altered protein molecules. At stage 2, 'median' was used for normalisation that considered median value for overall quantified protein average log-ratios to normalise the data counteracting known biases such as unequal loading of the samples and incomplete labelling of the peptides (Chen et al., 2014). I chose 0.05 as *p*-value cut-off and 2 as fold change cut-off for computing and identifying the protein molecules of which the abundance was significantly perturbed in excitotoxicity. After stage 2 computation, QPPC generated one output file (csv file format) with proteins significant under either one or both criteria i.e. $p\text{-value} \leq 0.05$ and/or $\text{fold change} > \log(2)$ or $< -\log(2)$. A volcano plot was generated that visualised the proteins deemed significant under the criteria and a histogram of protein log ratios was also generated by QPPC, and as expected for a 1:1 mixture most of the identified protein molecules showed medium/light ratio within the $\log(2)$ (cut off) range (**Figure 4.5**). The analysis was repeated with protein molecules identified in the 4 h glutamate treated neurons from all six biological replicates. The significantly perturbed protein molecules in excitotoxicity are listed in **Table 4.2** and most of these proteins showed decrease in expression following glutamate exposure. The trends

of the change in expression levels of these proteins were similar for neurons at both the early (15 min) and late (4 h) stage of excitotoxicity.

Table 4.2 List of differentially expressed proteins in glutamate-induced excitotoxicity.

S/L	Accession	Gene	Protein name	Σ# Unique Peptides	Σ# PSMs	15 min (N=3)				4 h (N=6)			
						Medium /Light	SD	n	QPPC p-value	Medium /Light	SD	n	QPPC p-value
1	C0IQA7_MOUSE	4930544G 11Rik	Transforming protein RhoA	1	76	0.243	0.127	2	0.009*	0.431	0.217	5	0.006
2	Q3V1S0_MOUSE	Abat	4-aminobutyrate aminotransferase, mitochondrial	2	33	0.34	0.123	2	0.029	0.82	0.598	3	0.194
3	Q3U645_MOUSE	Abcd3	ATP-binding cassette sub-family D member 3	1	23	1.22	0.44	3	0.913	0.488	0.035	3	0.048
4	Q80X81_MOUSE	Acat3	Acetyl-Coenzyme A acetyltransferase 3	1	101	0.196	0.028	2	0.003	0.407	0.23	2	0.033
5	ACTC_MOUSE	Actc1	Actin, alpha cardiac muscle 1	2	332	0.142	-	1	-	0.204	0.065	2	0.001
6	Q3TL79_MOUSE	Ahsa1	Activator of 90 kDa heat shock protein ATPase homolog 1	1	9	0.542	-	1	-	0.43	0.373	3	0.004
7	F6UFG6_MOUSE	Anp32a	Acidic leucine-rich nuclear phosphoprotein 32 family member A	2	38	0.29	0.141	3	0.003	0.694	0.407	5	0.078
8	ARF3_MOUSE	Arf3	ADP-ribosylation factor 3	4	121	0.399	0.166	3	0.016	0.756	0.973	6	0.013
9	ARF4_MOUSE	Arf4	ADP-ribosylation factor 4	2	60	0.384	-	1	-	0.426	0.215	4	0.011
10	ARL3_MOUSE	Arl3	ADP-ribosylation factor-like protein 3	4	61	0.42	0.208	3	0.024	0.697	0.306	4	0.161
11	H7BWZ3_MOUSE	Arpc3	Actin-related protein 2/3 complex subunit 3	2	23	0.371	0.32	2	0.011	0.677	0.633	5	0.016
12	F6RPX5_MOUSE	Atat1	Alpha-tubulin N-acetyltransferase 1	1	14	1.489	0.43	2	0.798	0.587	0.125	3	0.002
13	D6RJ16_MOUSE	Atp5a1	ATP synthase subunit alpha, mitochondrial	1	78	0.177	0.05	2	0.003	0.423	0.09	4	0.013
14	Q3UKW2_MOUSE E	Calm1	Calmodulin	3	31	0.464	0.172	2	0.001	2.092	2.737	3	0.744
15	Q80TN1_MOUSE	Camk2a	Calcium/calmodulin-dependent protein kinase type II subunit alpha	3	100	-	-	0	-	0.35	0.162	3	0.004
16	Q5SVI0_MOUSE	Camk2b	Calcium/calmodulin-dependent protein kinase type II subunit beta	4	162	0.927	0.406	3	0.538	0.406	0.22	5	0.005
17	CALX_MOUSE	Canx	Calnexin	4	88	0.384	0.049	3	0.032	0.791	0.366	6	0.213
18	Q3UL78_MOUSE	Cdc42	Cell division control protein 42 homolog	2	9	0.273	-	1	-	0.384	0.228	2	0.019
19	D3YYT0_MOUSE	Cdh2	Cadherin-2	3	39	0.934	0.791	2	0.268	0.507	0.253	5	0.008
20	COR1A_MOUSE	Coro1a	Coronin-1A	4	36	0.451	0.124	3	0.041	0.626	0.249	5	0.094
21	Q8JZR2_MOUSE	Crk	Proto-oncogene c-Crk	2	19	-	-	0	-	0.493	0.334	4	0.017
22	A0FF48_MUSCR	Csl	Small muscular protein	1	59	0.194	0.032	2	0.003	0.691	0.394	4	0.094
23	G3UX43_MOUSE	Eef1b	Elongation factor 1-beta	2	44	0.291	0.164	3	0.003	0.856	0.72	5	0.049
24	B1AXZ0_MOUSE	Elavl2	ELAV-like protein 2	3	37	0.306	0.179	3	0.002	0.547	0.205	5	0.048
25	FABPH_MOUSE	Fabp3	Fatty acid-binding protein 3	2	25	0.316	0.115	2	0.023	0.999	0.436	4	0.598
26	FABP5_MOUSE	Fabp5	Fatty acid-binding protein 5	6	140	0.381	0.066	3	0.029	0.651	0.152	6	0.136
27	H3BKG7_MOUSE	Fh1	Fumarate hydratase, mitochondrial	1	24	0.216	0.026	2	0.004	1.018	0.472	2	0.908
28	Q571F9_MOUSE	G3bp1	Ras GTPase-activating protein-binding protein 1	1	108	0.368	0.007	2	0.034	0.671	0.161	4	0.007
29	B7FAU8_MOUSE	Gdi1	Rab GDP dissociation inhibitor alpha	3	66	0.339	0.061	3	0.015	1.094	0.69	5	0.215
30	F6ZTG3_MOUSE	Glod4	Glyoxalase domain-containing protein 4	4	37	0.258	0.096	3	0.002	0.842	0.246	4	0.532
31	GRB2_MOUSE	Grb2	Growth factor receptor-bound protein 2	3	13	-	-	0	-	0.469	0.171	2	0.039
32	E0CYW7_MOUSE	Hdgf	Hepatoma-derived growth factor	1	49	0.294	0.058	2	0.014	0.764	0.398	5	0.155
33	D3YZ18_MOUSE	Hmgb1	High mobility group protein B1	2	28	-	-	0	-	0.425	0.231	4	0.011
34	F2Z3Z1_MOUSE	Hpcal4	Hippocalcin-like protein 4	1	5	-	-	0	-	0.337	0.309	2	0.01
35	LAMP1_MOUSE	Lamp1	Lysosome-associated membrane glycoprotein 1	1	9	-	-	0	-	0.334	0.222	3	0.003
36	D3Z7F0_MOUSE	Ldhb	L-lactate dehydrogenase B chain	5	111	0.554	0.141	3	0.126	0.514	0.231	5	0.016
37	Q3TYE5_MOUSE	Lsamp	Limbic system-associated membrane protein (LSAMP)	1	39	0.474	0.25	3	0.029	0.778	0.378	5	0.235
38	Q2TBF9_MOUSE	Map1lc3b	Microtubule-associated proteins 1A/1B light chain 3B	2	32	0.471	-	1	-	0.525	0.153	5	0.036
39	Q3URJ7_MOUSE	Map2	Microtubule-associated protein 2	18	306	0.498	0.249	3	0.045	0.431	0.251	6	0.003
40	Q9CXX1_MOUSE	Napa	Alpha-soluble NSF attachment protein	3	26	0.427	0.084	2	0.036	0.591	0.18	4	0.094

Table 4.2 (continued)

S/L	Accession	Gene	Protein name	Σ# Unique Peptides	Σ# PSMs	15 min (N=3)				4 h (N=6)			
						Medium /Light	SD	n	QPPC p-value	Medium /Light	SD	n	QPPC p-value
41	NDKA_MOUSE	Nme1	Tumor metastatic process-associated protein	1	171	0.211	0.032	2	0.004	0.664	0.444	5	0.027
42	Q3TXQ4_MOUSE	Npc2	Epididymal secretory protein E1	1	25	0.327	0.006	2	0.038	0.967	0.684	5	0.103
43	D3YWF6_MOUSE	Otub1	Ubiquitin thioesterase	2	35	0.288	0.239	2	0.006	0.563	0.213	5	0.04
44	F8WJ30_MOUSE	Pfdn2	Prefoldin subunit 2	1	21	-	-	0	-	0.224	0.036	3	0.001
45	H7BW1_MOUSE	Pfdn5	Prefoldin subunit 5	1	37	0.381	0.01	2	0.046	0.711	0.261	5	0.224
46	Q1LZL7_MOUSE	Pfkm	ATP-dependent 6-phosphofructokinase, muscle type	1	3	-	-	0	-	0.233	0.053	2	0.007
47	PROF1_MOUSE	Pfn1	Profilin-1	5	144	0.308	0.036	3	0.008	0.552	0.192	6	0.035
48	J3QQ30_MOUSE	Pitpna	Phosphatidylinositol transfer protein alpha isoform	3	49	0.324	0.039	3	0.011	0.568	0.277	5	0.018
49	B1AXW5_MOUSE	Prdx1	Peroxiredoxin-1	6	94	0.386	0.206	2	0.03	0.724	0.477	5	0.085
50	Q3TWM9_MOUSE	Psap	Prosaposin	9	168	0.348	0.083	3	0.012	0.598	0.239	6	0.042
51	PSB1_MOUSE	Psmb1	Proteasome subunit beta type-1	4	32	0.834	0.115	2	0.011	0.456	0.432	5	0.006
52	PRS4_MOUSE	Psmc1	Proteasome 26S subunit ATPase 1	3	30	1.198	-	1	-	0.535	0.154	5	0.036
53	B0LAE3_MOUSE	Ptn	Pleiotrophin	1	35	0.689	0.182	2	0.329	0.452	0.218	5	0.004
54	RAB1B_MOUSE	Rab1b	Ras-related protein Rab-1B	3	67	0.432	-	1	-	0.383	0.132	2	0.024
55	RAB3B_MOUSE	Rab3b	Ras-related protein Rab-3B	1	49	0.5	0.217	2	0.122	0.426	0.177	4	0.008
56	Q3UQN3_MOUSE	Rad23b	UV excision repair protein RAD23 homolog B	4	92	0.447	0.16	3	0.04	0.753	0.258	6	0.185
57	A2AFI4_MOUSE	Rbmx	RNA-binding motif protein, X chromosome	2	55	0.369	0.099	2	0.025	0.81	0.262	5	0.469
58	Q99N25_MOUSE	Rp13	Ribosomal protein L3	1	19	0.269	0.043	2	0.016	0.405	0.148	3	0.018
59	Q3UBI6_MOUSE	Rpl7	60S ribosomal protein L7	3	56	0.375	0.167	3	0.011	0.622	0.192	4	0.101
60	Q921R2_MOUSE	Rps13	40S ribosomal protein S13	4	68	0.418	0.104	3	0.041	0.898	0.52	5	0.29
61	O70569_MOUSE	Rps14	40S ribosomal protein S14	1	33	0.339	0.047	3	0.012	0.732	0.354	5	0.174
62	G3UYV7_MOUSE	Rps28	40S ribosomal protein S28	2	47	0.164	0.064	3	0.001	0.46	0.287	6	0.002
63	Q545F8_MOUSE	Rps4x	40S ribosomal protein S4, X isoform	5	69	0.273	0.104	3	0.006	0.705	0.401	5	0.086
64	Q3UEI6_MOUSE	Serbp1	Plasminogen activator inhibitor 1 RNA-binding protein	1	41	0.318	0.14	2	0.013	0.66	0.179	4	0.188
65	H7BX95_MOUSE	Srsf1	Serine/arginine-rich splicing factor 1	4	59	0.342	0.103	2	0.029	0.732	0.387	6	0.102
66	Q3THQ5_MOUSE	Stip1	Stress-induced-phosphoprotein 1	4	47	0.398	0.128	3	0.023	0.639	0.234	5	0.116
67	Q8BUM1_MOUSE	Tardbp	TAR DNA-binding protein 43	3	136	1.427	0.134	3	0.733	0.534	0.151	6	0.03
68	D3YU75_MOUSE	Tpt1	Translationally-controlled tumor protein	1	8	0.487	0.295	3	0.035	1.118	0.713	2	0.533
69	F8WJG3_MOUSE	Tra2b	Transformer-2 protein homolog beta	3	82	0.561	0.167	3	0.112	0.531	0.283	5	0.021
70	Q9CRT0_MOUSE	Tubb3	Tubulin beta-3 chain	2	470	0.268	0.068	3	0.004	0.417	0.142	6	0.005
71	Q9CVR0_MOUSE	Tubb4b	Tubulin beta-4B chain	3	805	0.444	0.209	3	0.032	0.706	0.477	5	0.079
72	TBB6_MOUSE	Tubb6	Tubulin beta-6 chain	5	627	0.378	0.081	2	0.036	0.398	0.082	4	0.005
73	Q3TCH2_MOUSE	Uchl1	Ubiquitin carboxyl-terminal hydrolase isozyme L1	5	82	0.387	0.233	3	0.012	0.779	0.162	5	0.412
74	Q35619_MOUSE	Vamp2	Vesicle-associated membrane protein 2	1	23	1.356	0.272	2	0.436	0.423	0.19	5	0.004
75	A2A7S7_MOUSE	Yars	Tyrosine--tRNA ligase, cytoplasmic	4	61	0.402	0.143	3	0.024	0.851	0.208	4	0.591
76	Q71V06_MOUSE	Ybx1	Nuclease-sensitive element-binding protein 1	3	45	0.427	0.351	2	0.034	0.644	0.243	4	0.103
77	1433B_MOUSE	Ywhab	14-3-3 protein beta/alpha	6	152	0.29	0.123	3	0.004	0.888	0.653	6	0.092
78	1433E_MOUSE	Ywhae	14-3-3 protein epsilon	8	268	0.282	0.066	3	0.008	0.702	0.214	6	0.196
79	1433T_MOUSE	Ywhaq	14-3-3 protein theta	6	189	0.361	0.22	3	0.009	1.127	0.83	6	0.771
80	Q3UA58_MOUSE	Ywhaz	14-3-3 protein zeta/delta	3	248	0.204	0.028	3	0.002	0.525	0.325	6	0.006

*Quantitative Proteomics *p*-value Calculator (QPPC) derived permutation *p*-values ≤ 0.05 are in 'red-bold'.

Only protein molecules with significant *p*-value ($p \leq 0.05$) identified either from 15 min or 4 h glutamate treated samples are listed in the above table.

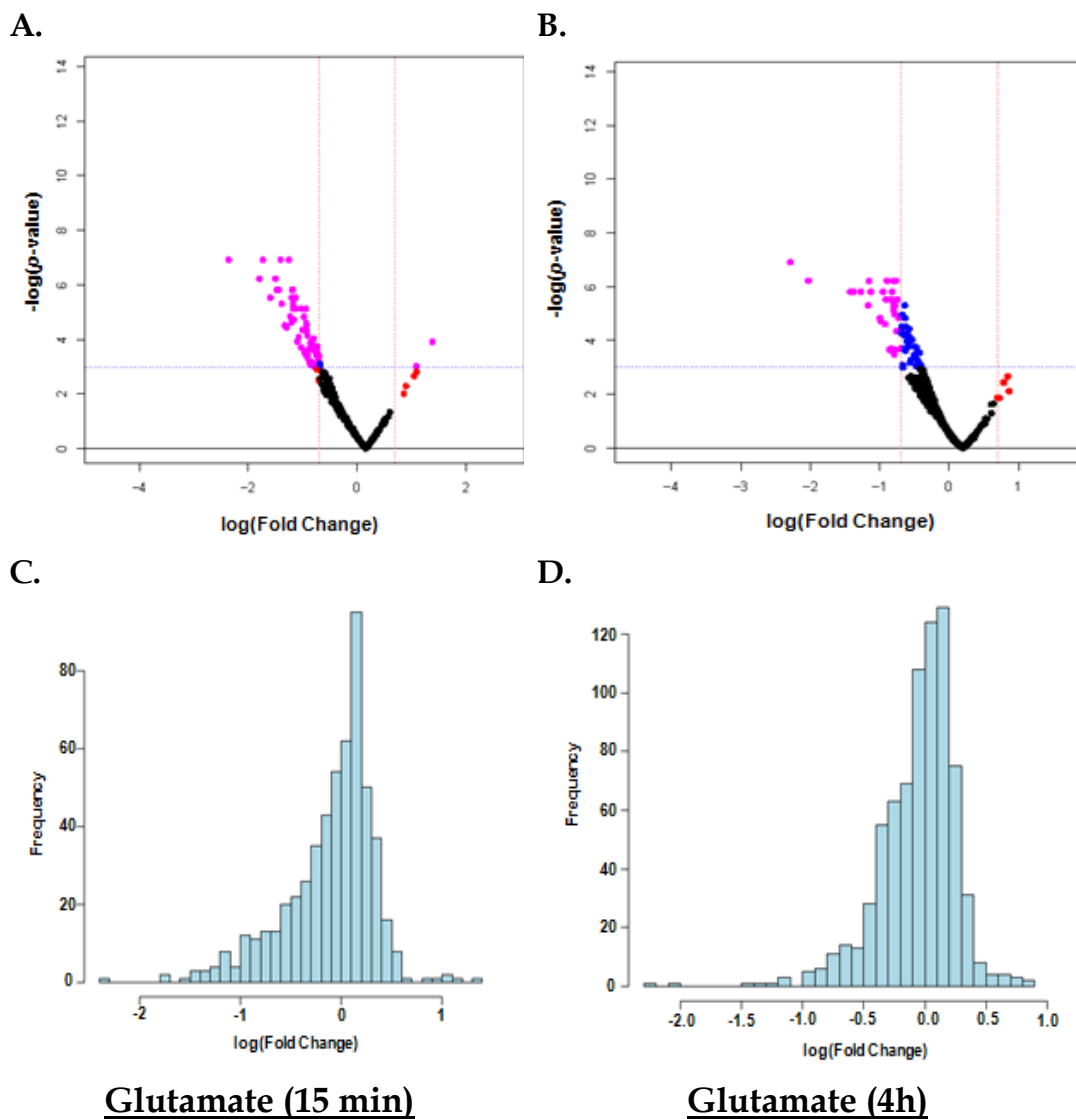


Figure 4.5 Volcano plots and histograms showing the fold change distributions of the identified protein molecules in neurons 15 min and 4 h after glutamate treatment. Identified protein molecules and their corresponding medium to light ratios for 15 min (3 biological replicates) and 4 h (6 biological replicates) glutamate excitotoxicity were used to calculate the p -values for their differential expression using Quantitative Proteomics p -value Calculator (QPCC). **A&B.** Volcano plots for 15 min and 4 h respectively. Red dots represent protein molecules significant under criterion [fold change $> \log(2)$ or $< -\log(2)$], blue dots represent protein molecules significant under p -value ($p \leq 0.05$) and pink dots for those significant under both. **C & D.** QPCC-generated histograms showing the frequency distribution of the identified protein molecules with their corresponding fold changes (log value) in excitotoxicity.

4.3.5 Data validation

Global proteomics data revealed differential expression levels for several 14-3-3 isoforms. These 14-3-3 protein molecules are molecular adaptors that interact with key signalling molecules to regulate cell cycle, transcriptional control, signal transduction by interacting with receptors and protein kinases and apoptosis (Kleppe et al., 2011; Yaffe, 2002). Identified 14-3-3 protein molecules showed decrease in expression following excitotoxic stimulation. Examination of the MS/MS spectra of the unique peptides, spectra used for quantification and quan channel values revealed that 14-3-3 β/α exhibited an approximate of 2.8-fold decrease in expression 4 h after the glutamate treatment. Western blot analysis also revealed that glutamate treatment for 4 h induced significant reduction of 14-3-3 β/α expression level in neurons (**Figure 4.6**).

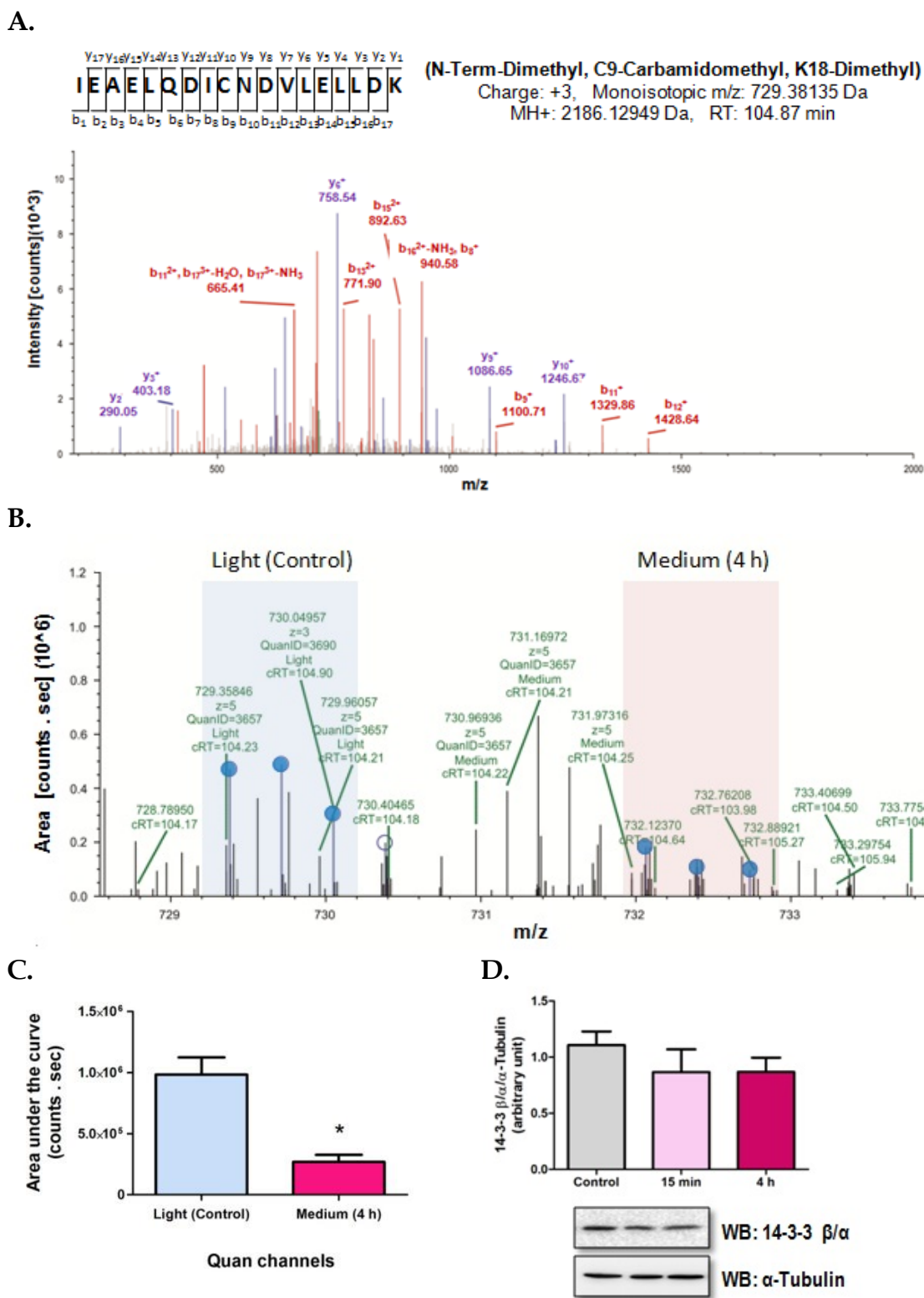


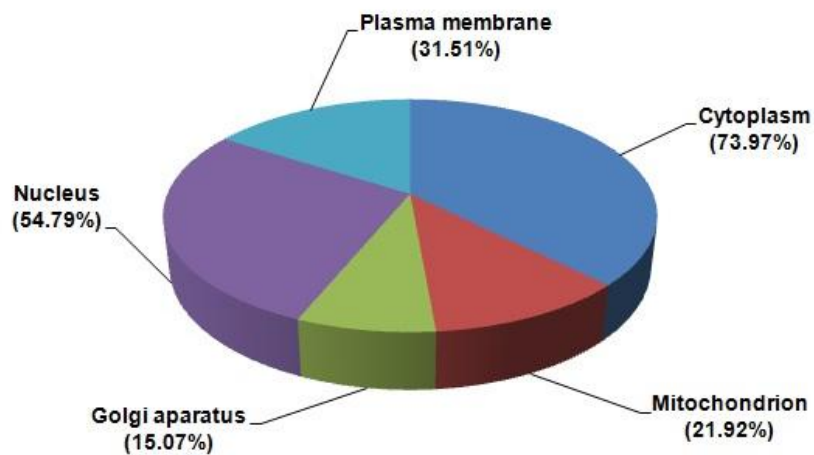
Figure 4.6

Figure 4.6 MS2 spectra and the extracted ion chromatogram (XIC) spectra used for MS1 quantification of 14-3-3 beta/alpha unique peptide and immunoblot analysis. **A.** Labelled (N-terminal dimethyl) triply charged unique tryptic peptide ($^{86}\text{IEAELQDICNDVLELLDK}^{103}$) from 14-3-3 beta/alpha was identified with range of b and y ions. **B.** Chromatogram showing isotopic clusters used for quantification. **C.** From a 1:1 mixture, medium (4 h glutamate) and light (Control) quan channel values showed significant difference in three biological replicates (Student's t-tests, mean \pm SD, $*p < 0.05$, $n = 3$). **D.** Western blot analysis also showed a similar trend of changes i.e. decrease in expression after glutamate treatment for 4 h. Data are presented as mean \pm SD, ($n = 3$ biological replicates).

4.3.6 Bioinformatics analysis of the differentially expressed neuronal proteins revealed cellular processes that are dysregulated in excitotoxicity

To explore the biological and molecular functions of the differentially expressed protein molecules identified in proteomic analysis, Functional Enrichment Analysis Tool (FunRich v.2.1.2) was used for Gene Ontology (GO) enrichment analysis. Gene names for 80 significantly perturbed ($p \leq 0.05$) protein molecules in excitotoxicity (both 15 min and 4 hr) (**Table 4.2**) were uploaded as a data set for GO analysis. The software using FunRich background database was able to map 74 genes (except *4930544G11Rik*, *Acat3*, *Csl*, *Eef1b*, *Fhl1* and *Rp13*) and generated the outputs for molecular function, cellular process, biological process, biological pathway, site of expression etc. Identified molecules represented different cellular origins (cytoplasm, plasma membrane, nucleus, mitochondria, Golgi apparatus etc.) and significantly (Bonferroni corrected p -value ≤ 0.05) enriched top molecular functions include receptor signalling complex scaffold activity (10.8%, $p < 0.001$), RNA binding (8.1%, $p < 0.01$), cytoskeletal protein binding (5.4%, $p = 0.01$), Chaperon activity (4.1%, $p = 0.01$), ATP binding (1.4%, $p = 0.02$), transporter activity (8.1%, $p = 0.03$) and Ca^{2+} ion binding (4.1%, $p = 0.04$) (**Figure 4.7**). Again, top enriched biological pathways with these significantly perturbed protein molecules include insulin-mediated glucose transport (11.8%, $p < 0.001$), neurotrophic factor-mediated Trk receptor signalling (15.7%, $p < 0.001$), protein folding (9.8%, $p < 0.001$), N-cadherin signalling events (21.6%, $p < 0.001$), metabolism of proteins (21.6%, $p < 0.001$), $\alpha 6\beta 1$ and $\alpha 6\beta 4$ integrin signalling (9.8%, $p < 0.001$), Trk receptor signalling mediated by PI3K and PLC-gamma (11.8%, $p < 0.001$), stabilisation and expansion of the E-cadherin adherences junction (21.6%, $p < 0.001$), E-cadherin signalling in the nascent adherences junction (21.6%, $p < 0.001$) etc. Also, protein metabolism (16.2%, $p < 0.01$), regulation of cell cycle (2.7%, $p = 0.02$) and cell growth and/or maintenance (12.2%, $p = 0.04$) were identified as top biological processes enriched with the identified protein molecules (**Figure 4.7**).

A.



B. Molecular functions

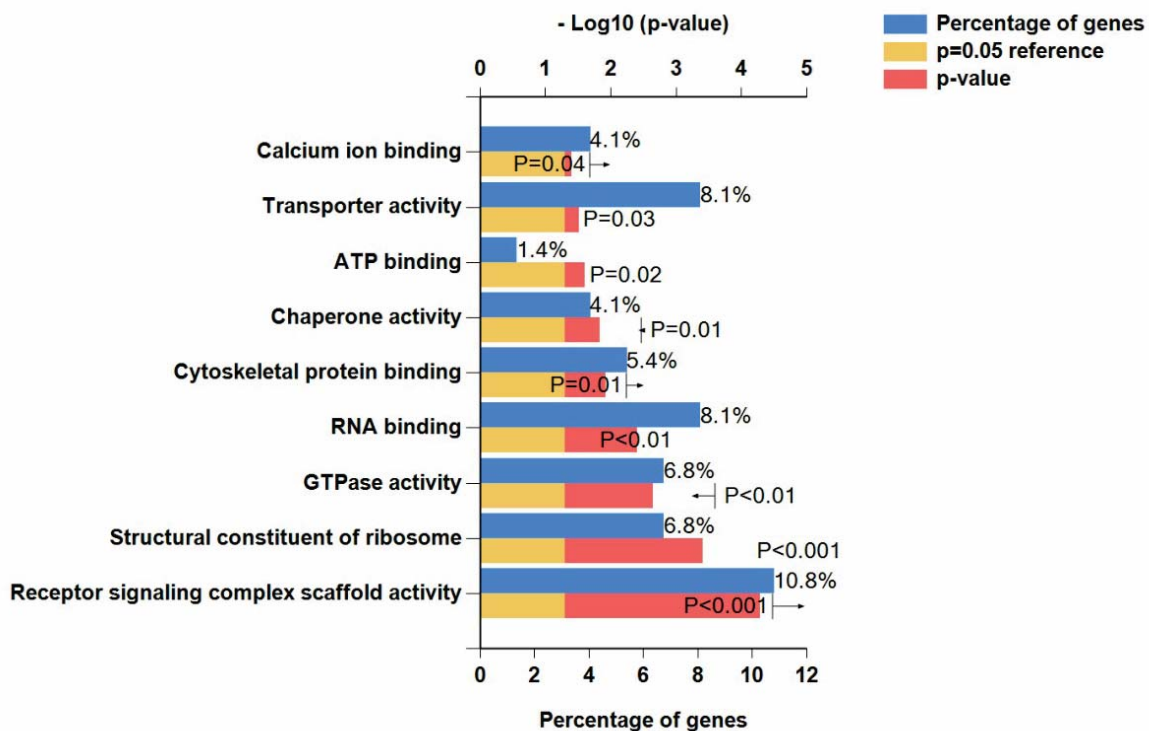
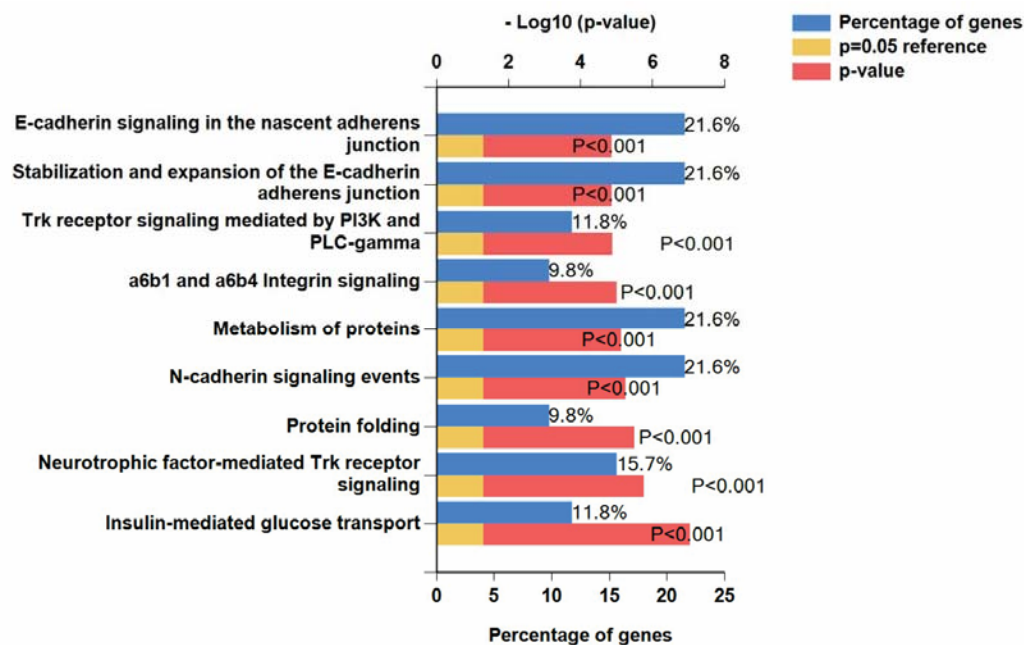


Figure 4.7

C. Biological pathways



D. Biological processes

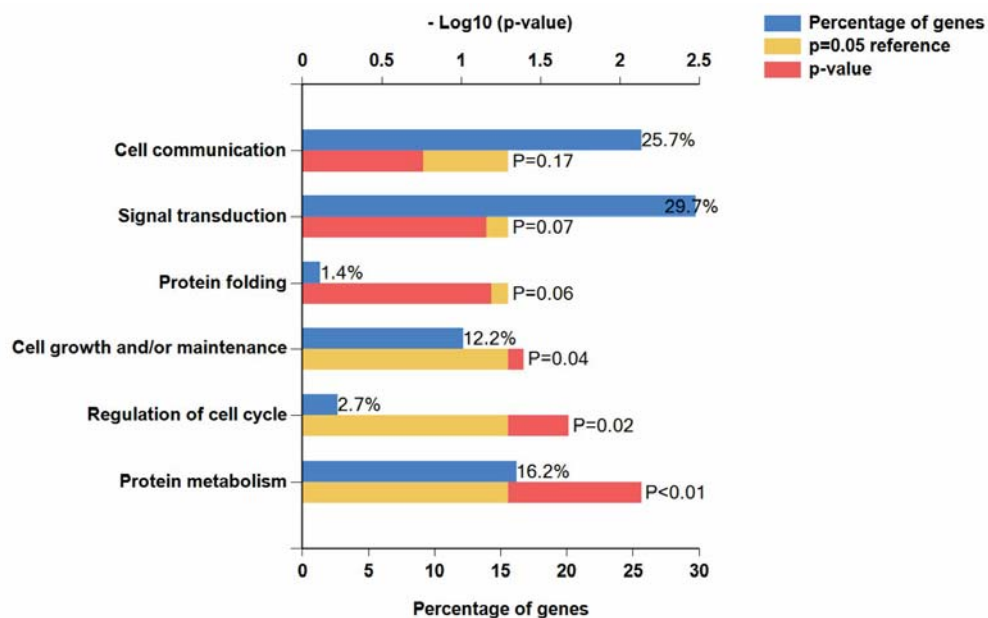


Figure 4.7 Gene Ontology (GO) analyses of the differentially expressed protein molecules in neurons in excitotoxicity. FunRich analysis showing expression site (A), and top enriched molecular functions (B), biological pathways (C) and biological processes (D).

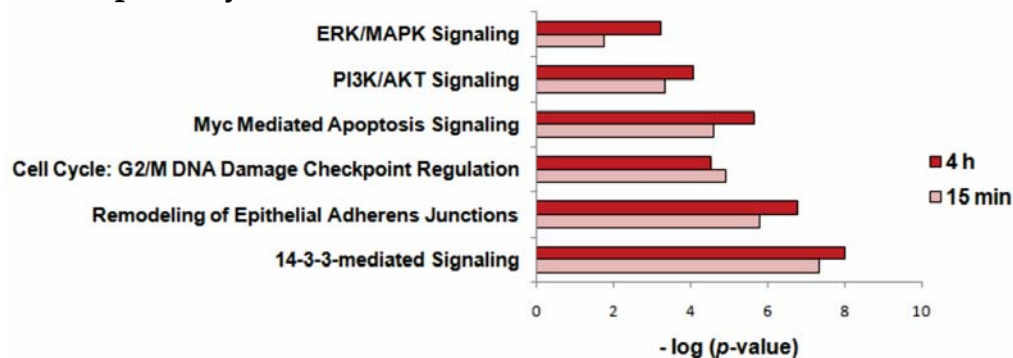
4.3.7 Pathway and network analysis using IPA

To further define the putative functions of the identified differentially expressed proteins, Ingenuity Pathway Analysis (IPA) software was used to perform the network and pathway analysis to ascertain how these protein molecules interact with each other in cells. The lists of proteins showing differential expression level after 15 min and 4 h of glutamate treatment were uploaded with corresponding medium to light ratios. Core analysis platform was used to analyse the data that matched proteins in the uploaded data set with those in the Ingenuity Knowledge base. The statistical significance of each network or list was determined by IPA using a Fisher exact test ($p < 0.05$). The top identified canonical pathways are (i) 14-3-3 mediated signalling, (ii) remodelling of epithelial adherens junctions, (iii) cell cycle including G2/M DNA damage checkpoint regulation, (iv) Myc mediated apoptosis signalling, (v) PI3K/Akt signalling (vi) Erk/MAPK signalling (**Figure 4.8**). The interacting networks of these molecules were built with IPA software. It is clear from the top canonical pathways derived from these networks that these pathways can potentially interplay to cause cell death in neurons (**Figure 4.8**). It is obvious from the analysis that the top upstream regulators of these potentially neurotoxic signalling pathways include microtubule-associated protein tau (MAPT), presenilin 1 (PSEN1), amyloid precursor protein (APP), Myc proto-oncogene protein (MYC) and retinoids (**Table 4.3**). Predicted activation of the retinoids and inhibition of Myc proto-oncogene demonstrate that the cell death signalling pathways are active in both early (15 min) and late (4 h) glutamate-induced excitotoxicity.

Table 4.3 Top upstream regulators of the potentially neurotoxic signalling pathways identified by IPA.

Molecules	Full name	Glutamate (15 min)		Glutamate (4 h)	
		<i>p</i> -value overlap	Predicted activation	<i>p</i> -value overlap	Predicted activation
MAPT	Microtubule-associated protein tau	1.47×10^{-16}		1.94×10^{-16}	
PSEN1	Presenilin 1	2.63×10^{-15}		5.99×10^{-15}	
APP	Amyloid precursor protein	4.20×10^{-14}		3.45×10^{-15}	
CD437	Retinoid CD437	7.35×10^{-8}	Activated	4.09×10^{-7}	Activated
STI926	Retinoid STI926	4.93×10^{-10}	Activated	3.58×10^{-9}	Activated
MYC	Myc proto-oncogene protein	7.25×10^{-5}	Inhibited	5.79×10^{-6}	Inhibited

A. Canonical pathways



B. Interaction network

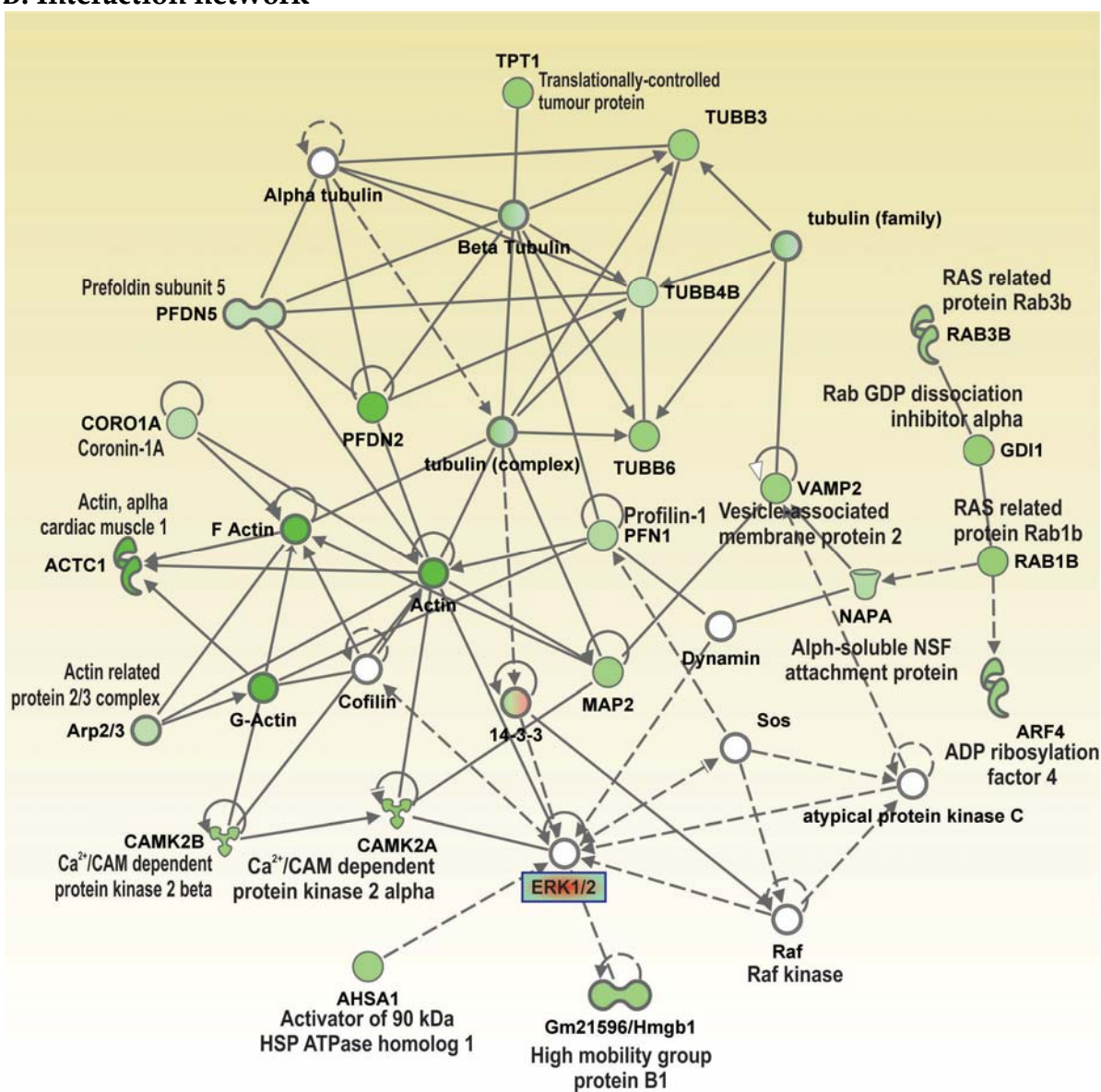


Figure 4.8

Figure 4.8 Top canonical pathways and interaction network of the identified significantly perturbed protein molecules in glutamate-induced excitotoxicity. Ingenuity pathway Analysis (IPA) was used for network and pathway analysis. **A.** Top canonical pathways identified by IPA with significantly perturbed protein molecules following 15 min and 4 h of glutamate treatment. **B.** ‘Neurological disease, cell to cell signalling and interaction’ was identified as one of the top interaction networks with an IPA network score of 44. Intermolecular interactions with the identified protein molecules showing either increase (**red**) or decrease (**green**) in expression in glutamate-induced excitotoxicity. Protein molecules that are absent (colourless) in the significant list (**Table 4.2**) or are identified after phosphoproteome analysis (boxed, □) described in Chapter 5, are also shown in the interaction network. The legend for IPA molecule shapes and relationships is presented in appendix I.

4.4 Discussion

I optimised the stable isotope dimethyl labelling based quantitative proteomic approach for in-solution tryptic digests derived from neuronal lysates. Key findings on the global proteome changes in excitotoxicity are described in this result chapter. I identified a number of significantly perturbed protein molecules in excitotoxicity as listed in **Table 4.2**. Most of these molecules showed decrease in expression in excitotoxicity. Common down regulated molecules showing decrease in expression at both 15 min and 4 h glutamate-induced excitotoxicity include transforming protein RhoA (4930544G11Rik), acetyl-Coenzyme A acetyltransferase 3 (Acat3), ADP-ribosylation factor 3 (Arf3), actin-related protein 2/3 complex subunit 3 (Arpc3), ATP synthase subunit alpha, mitochondrial (Atp5a1), elongation factor 1-beta (Eef1b), ELAV-like protein 2 (Elavl2), Ras GTPase-activating protein-binding protein 1 (G3bp1), microtubule-associated protein 2 (Map2), tumor metastatic process-associated protein (Nme1), ubiquitin thioesterase (Otub1), profilin-1 (Pfn1), phosphatidylinositol transfer protein alpha isoforms (Pitpna), prosaposin (Psap), proteasome subunit beta type-1 (Psmb1), ribosomal protein L3 (Rp13), 40S ribosomal protein S28 (Rps28), tubulin beta-3 chain (Tubb3), tubulin beta-6 chain (Tubb6) and 14-3-3 isoform zeta/delta (Ywhaz). For most of these molecules involvement in excitotoxicity are yet to be confirmed.

Previous neuroproteomic studies mainly depended on 2D-gel-based approaches (2D-GE-MS/MS) (Datta et al., 2011). In a rat model of ischaemic stroke, Chen *et al.* reported upregulation of dihydropyrimidinase-related protein 2 (DRP-2), spectrin α II chain, heat shock cognate protein 70 pseudogene 1 (HCS70-ps1) and tropomodulin 2 (Tmod2) (Chen et al., 2007). Using 2-D gel electrophoresis and subsequent proteomic analysis of human stroke brain samples, Cuadrado *et al.* identified decreased expression of ATP synthase and Rab GDP-dissociation inhibitor alpha (Gdi1) in the ischaemic core region (Cuadrado et al., 2010). Also, in support of our current study, glutamate induced excitotoxicity in cultured human cerebral endothelial cells resulted in decrease expression of ADP ribosylation factor-like 3, Rho GDP-dissociation inhibitor 1 and 14-3-3 isoform epsilon (Ywhae).

14-3-3 protein molecules are widely expressed in mammalian brains (Boston et al., 1982). These molecules are involved in maintaining cell survival via both Akt and mitogen-activated protein kinase (MAPK) pathways. Receptor induced PI3K activates Akt that phosphorylates Bad pro-apoptotic protein molecule, 14-3-3 proteins bind to phosphorylated Bad causing dissociation of Bad/BclxL complex allowing cell to survive (Berg et al., 2003). Again, 14-3-3 proteins regulate rapid transition of inactive Raf1 serine/threonine protein kinase to activation

by mediating coactivator such as Bcr, PKC and kinase repressor of Ras (KSR) binding (Brasemann and McCormick, 1995; Xing et al., 1997; Yip-Schneider et al., 2000). Active Raf1 phosphorylates MAP kinase kinase (MEK) that ultimately leads to the transcription of cell survival genes via MAPK pathway (Fu et al., 2000). Decrease in several 14-3-3 isoforms in excitotoxicity might perturb both Akt and MAPK pro-survival pathways. Unsurprisingly, PI3K/Akt and Erk/MAPK signalling pathways were also identified by IPA as top canonical pathways (**Figure 4.8**) derived from the significantly dysregulated protein lists (**Table 4.2**).

Previous studies have demonstrated that reactive oxygen species damage cellular macromolecules, such as lipids, proteins and nucleic acids, and initiates cellular death in neurological disorders such as ischaemia, trauma and degenerative disorders (Chan, 2001). In addition to exerting cellular damage, these reactive oxygen species also plays critical role in cell death/survival processes (Drose et al., 2016). For ischemic injury, a general consensus is that apoptosis is important in mediating cell death in-vitro after hypoxia (White et al., 2000). Recently, many studies involving in-vivo ischaemic models have also demonstrated that apoptosis is the prominent neuronal death process in cerebral ischaemia. Myc mediated apoptosis signalling obtained from pathway analysis of altered proteins are therefore supports previous findings and thus validates our present study. Myc is an integral part of HIF-1 α pathway and plays a critical role in attenuating cellular death during oxidative stress (Koshiji et al., 2004; Liu et al., 2006). Myc promotes adult neurogenesis during stroke through Sonic hedgehog (Shh) pathway (Liu et al., 2013). In support, using our identified global proteome data, IPA upstream regulator analysis also identified Myc as one of the upstream regulator with predicted inhibition at early (15 min) and late (4 h) excitotoxicity (**Table 4.3**).

The G2/M DNA damage checkpoint prevents the cell from entering mitosis with damaged DNA. The cells with defective G2/M DNA damage checkpoint entering mitosis without repairing their DNA espouse death after cell division (Cuddihy and O'Connell, 2003). DNA damage has been documented as a trigger of neuronal apoptosis in many neurodegenerative diseases, including ischaemic stroke and traumatic brain injuries (Gabbita et al., 1998; Mattson, 2000). Down regulation of this cell cycle check point in glutamate treated neurons suggests higher sensitivity of neurons to DNA damage and thus apoptosis during excitotoxicity. In summary our findings demonstrate apoptotic neuronal death in glutamate treated neurons. It would be interesting to investigate the effect of manipulation of these pathways in the prevention of neuronal death during excitotoxicity.

It is clear from our study and study results by others that inactivation of a number of cell survival pathways and simultaneously activation of a series of cell death pathways ultimately leads to neuronal demise in excitotoxicity. Also, the activity and function of signalling molecules does not depend only on expression level, in fact several post translational modifications namely phosphorylation status actually determines the activity and cellular function of these molecules. Hence, I was interested to explore the changes in phosphorylation level for the important signalling molecules in excitotoxicity. The following chapter describes the method and outcome of the quantitative phosphoproteomic analysis in excitotoxicity.

Chapter 5

Declaration and acknowledgement

- ✚ Dr. Ching-Seng Ang, one of my co-supervisors provided help to run the proteomic samples in Orbitrap Elite mass spectrometer and to search Mascot with Xcalibur raw files to generate msf files. I am responsible for generating and analysing rest of the data presented in this chapter.
- ✚ Dr. Dominic Ng, one of my co-supervisors provided help to capture the images following PTEN immunofluorescence experiments and also trained me to analyse the data using LAS AF Lite software.

Chapter 5: Phosphoproteomic analysis to identify the key signalling pathways of glutamate-induced excitotoxicity in cultured primary neurons

5.1 Introduction

Phosphoproteomic analysis is the key for mechanistic understanding of the neuronal signalling networks. Phosphorylation of proteins is the most ubiquitous and versatile post translational modification (PTM) that occurs in more than one-thirds of all cellular proteins (Cohen, 2001). Protein phosphorylation regulates signal transduction and lies at the heart of the signalling pathways, and is governed by approximately 500 different kinases and 150 protein phosphatases in human proteome (Manning et al., 2002). Advances in mass spectrometry-based quantitative phosphoproteomic analysis over the last ten years has made it an important tool to understand signalling mechanism in complex biological systems (Ozlu et al., 2010). Quantitative phosphoproteomic analysis relies on the proper identification and quantification of phosphorylated proteins and the identification of the phosphorylation sites (Mann and Jensen, 2003). Selective enrichment of phosphopeptides is the key step prior to quantitative mass spectrometric analysis. Immobilised metal affinity chromatography (IMAC) and TiO₂ phosphopeptides enrichment are widely used for selective binding of phosphopeptides prior to LC-MS/MS analysis (Ficarro et al., 2002; Pinkse et al., 2004; Thingholm et al., 2006).

Even though protein phosphorylation and dephosphorylation play a significant role in governing the relay of the neurotoxic signals from the over-stimulated NMDA receptors to direct neuronal death in excitotoxicity, the signalling networks by which these phosphorylated proteins are organised to relay the neurotoxic signals have not been clearly defined. We decided to use mass spectrometry-based quantitative phosphoproteomic approach to map these networks. Specifically, I aimed to identify the key signalling molecules that direct neuronal death in glutamate-induced excitotoxicity in cultured primary neurons. I monitored the changes in phosphorylation of the signalling phosphoproteins. To this end, I employed TiO₂ phosphopeptide enrichment method (Thingholm et al., 2006) prior to LC-MS/MS analysis. In brief, following stable isotope dimethyl labelling, mixed (1:1) labelled (light label for control and medium label for treated peptides) peptides were passed through a TiO₂ micro-column chromatography to enrich the phosphopeptides. At low pH (< 2), acidic amino acids are positively charged and allow the negatively charged phosphate groups to interact with the positively charged TiO₂ beads in the micro-columns. This process allows us to selectively

capture the phosphorylated peptides to enrich them from the crude peptides mixture (**Figure 5.1**). The enriched phosphopeptides were subjected to LC-MS/MS analysis followed by identification using the Mascot search engine. PhosphoRS 3.0 node in Proteome Discoverer 1.4, which it is able to efficiently localise the phosphorylation sites with high sensitivity was used to identify the phosphorylation sites of the identified phosphopeptides (Taus et al., 2011). The results presented here describe the data on global changes in phosphorylation of the signalling phosphoproteins following glutamate-induced excitotoxicity in cultured primary neurons.

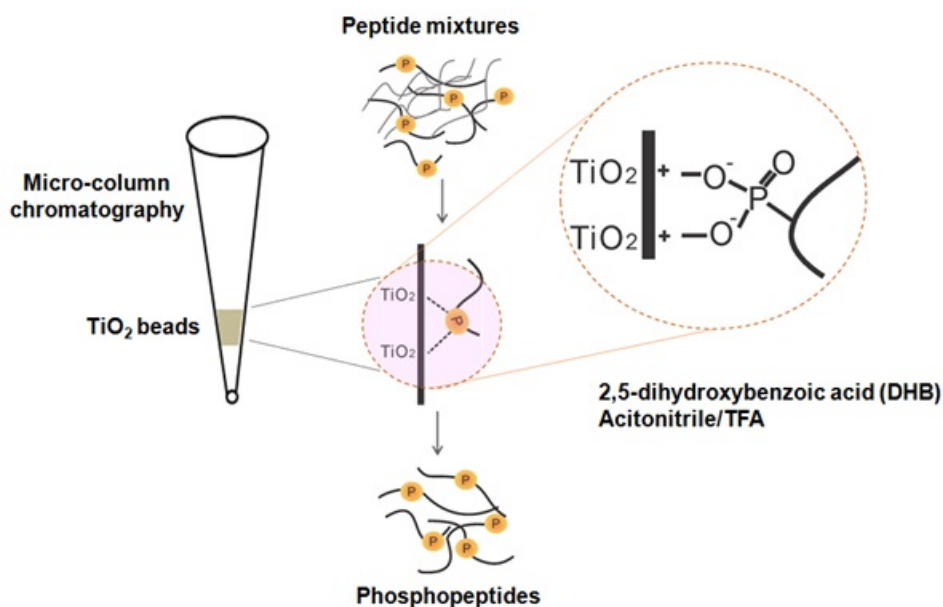


Figure 5.1 TiO_2 phosphopeptides enrichment. TiO_2 micro-column selectively enriches phosphorylated peptides from the tryptic digests of neuronal proteins.

5.2 Methods

5.2.1 Experimental design

Figure 5.2 shows the workflow of the experiments. Primary cortical neurons were cultured as described earlier (Chapter 2). At seventh days in culture (DIV7), $100 \mu\text{M}$ of glutamate was added for 15 min and 4 h to these matured neurons to induce excitotoxicity. Neuronal lysates were precipitated with acetone (-20°C) and resuspended in 8 M urea solution (in 50 mM TEAB). Equal amount of control and treated lysates were reduced with 10 mM TCEP,

alkylated with 55 mM iodoacetamide, and digested with trypsin (1:40) overnight at 37°C. The resulted tryptic peptides were purified by solid phase extraction (SPE) (Oasis HBL cartridge, Waters) clean up. Equal amounts of peptides from the control and treatment lysates were stable isotope dimethyl labelled using formaldehyde (CH₂O) (light label for control) and deuterated formaldehyde (CD₂O) (medium label for treatments) in the presence of sodium cyanoborohydride (NaBH₃CN). Equal amounts of labelled peptides were mixed (control: treatment, 1:1) together and purified using the SPE clean-up and freeze-dried overnight before TiO₂ phosphopeptides enrichment.

5.2.2 TiO₂ phosphopeptides enrichment

TiO₂ micro-column in the presence of 2,5-dihydroxybenzoic acid (DHB) solution specifically captures phosphorylated peptides and enriches them as described by Thingholm *et al.* (Thingholm *et al.*, 2006). Briefly, the freeze-dried samples were reconstituted with 80 µl of DHB loading buffer [200 mg DHB in 1 ml of wash buffer (80% ACN, 3% TFA)]. The TiO₂ loaded micro-columns were pre-washed with 30 µl of 100% ACN before sample loading and the columns were centrifuged at 500 ×g with adaptors. After sample loading, the columns were washed sequentially with 20 µl DHB loading buffer and 60 µl of wash buffer. Samples were eluted in microfuge tubes with 80 µl of Buffer 3 (0.5% ammonia solution). Elutions were continued with 2 µl of Buffer 2 (30% ACN). Eluents were acidified with 1 µl of pure formic acid per 10 µl of eluent to obtain pH of 2-3. Samples were concentrated using Speedy-vac to ~30 µl before they were run on LTQ OrbiTrap Elite mass spectrometer for LC-MS/MS analysis. This experiment was repeated 3 times with three biological replicates for the 15 min glutamate treatment and 6 times with six biological replicates for 4 h glutamate treatment before phosphoproteomics analysis.

5.2.3 Phosphoproteomic data analysis

Data analysis was carried out using Proteome Discoverer (Thermo Scientific version 1.4) with the Mascot search engine against the Uniprot database. Fixed modification was Carbamylation of Cysteine (+57.021) and variable modifications were phospho-Serine/Threonine/Tyrosine (+79.966). A false discovery rate threshold of 1% was applied and phosphopeptide identification was further validated with PhosphoRS 3.0 node in PD 1.4, requiring at least 95% confidence (Taus *et al.*, 2011). Two-plex dimethylation (C₂H₆, C₂H₂D₄) was selected as the

quantification method, and phosphopeptide quantification was carried out using the Quantitation node from Proteome Discoverer.

5.2.4 PTEN immunofluorescence

For PTEN immunofluorescence, primary cortical neuronal cells were grown on poly-D-lysine coated cover slips for seven days. Following glutamate (100 μ M) treatment for 4 h and 7 h, cells (control and treatments) were washed twice with ice-cold PBS then fixed in 4% (w/v) paraformaldehyde for 30 min at room temperature. Cells were then again washed 3 \times with PBS followed by permeabilisation using 0.2% (v/v) Triton X-100 in PBS for another 20 min. Next, cells were washed with PBS four times before being blocked with 10% (v/v) foetal bovine serum in PBS for 30 min. Cells were then again washed three times with cold PBS and incubated 1 h with anti α -PTEN (1:100) (in-house generated), anti α -tubulin (1:200) primary antibodies at room temperature. After incubation with primary antibodies, cells were washed three times with cold PBS and incubated with the secondary antibody (Alexa Flour 488/555, 1:800 in PBS) for 1 h at room temperature. Finally, cells were washed with PBS twice before DAPI (1:10000 in PBS) was added for 5 min to stain the nucleus. After one wash cover glass was mounted with GelCode FLUROMOUNT mounting media on a glass slide and dried. Cells were visualized and the images were captured using a Leica TCS SP5 confocal microscope (Wetzler, Hessen, Germany). Captured images were analysed using Leica LAS AF Lite software.

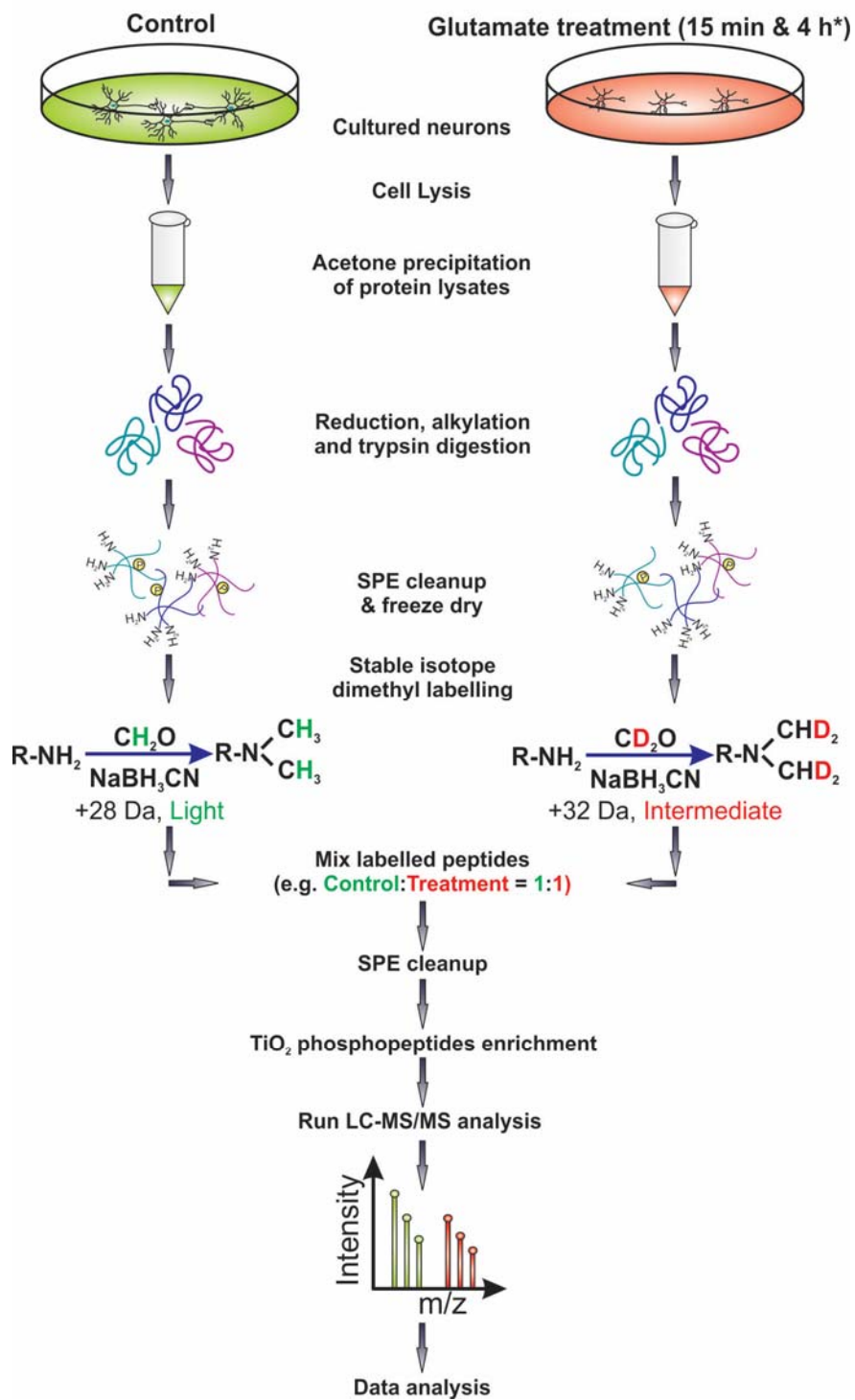


Figure 5.2

Figure 5.2 Workflow for exploring phosphoproteome changes in glutamate excitotoxicity.

Following glutamate (100 μ M) treatment for 15 min and 4 h, neuronal lysates were precipitated with acetone (-20°C). Equal amounts of proteins in the control and treated lysates were reduced with 10 mM TCEP and alkylated with 55 mM iodoacetamide before they were digested with trypsin. Purified tryptic digests were dimethyl labelled with formaldehyde (CH_2O , light label) for peptides derived from the control neurons and deuterated formaldehyde (CD_2O , medium label) for peptides derived from the treated lysates in the presence of sodium cyanoborohydride (NaBH_3CN). Equal amount of labelled peptides were mixed (control: treatment, 1:1) and cleaned up by SPE cartridge before the phosphopeptides were enriched using TiO_2 micro-columns. Enriched phosphopeptides were run on LTQ Orbitrap Elite mass spectrometer for LC-MS/MS analysis. *n = 3 for 15 min glutamate treatment and n = 6 for 4 h glutamate treatment, as this time point was repeated for inhibitor study described in Chapter 6. *Abbreviations: SPE, solid phase extraction; TCEP, tris-(2-carboxyethyl)-phosphine.*

5.3 Results

5.3.1 Data processing to identify phosphoproteins with changes in phosphorylation in glutamate-induced excitotoxicity

Similar to what was done to analyse the global proteome (Section 4.3.2, Chapter 4), the mass spectrometric raw data (Xcalibur file format) for the phosphoproteome were processed using Proteome Discoverer 1.4 (PD 1.4) with Mascot search algorithm against the Uniprot database. All identified peptides were above the identity threshold score, which represents a confidence level of $p < 0.05$. The inbuilt quantitation node on PD 1.4 allows us to measure the relative phosphorylation changes (medium/light ratios) based on the extracted ion chromatogram (XIC) intensities from the MS1 scans. Phosphosite identification probability was further calculated with the PhosphoRS 3.0 node in PD 1.4. Results were filtered with high peptide confidence to reflect a maximum of 1% false discovery rate (FDR). For phosphopeptide quantification, peptide ratio was calculated from the isotopic clusters for the identified peptide in both light and medium quantification (quan) channels or from a single isotopic cluster identified in either of the quan channels (light and/or medium) using the accurate mass feature of the mass spectrometer (< 2 ppm) to define the corresponding light or medium labelled peptide. For phosphopeptide ratios with any missing quantification channel, values were replaced with a minimum intensity (maximum and minimum fold change = 100 and 0.01, respectively). To facilitate further analysis, an MS Excel file was exported from PD with phosphopeptide sequences, modifications, phosphosite probabilities, protein group accession numbers, protein names, coverage, peptides, unique peptides, PSMs (peptide spectrum matches), areas, average median medium/light ratios, precursor ions, retention time and details of all the identified phosphopeptides. Using the MS Excel file, the exported data for 15 min glutamate treatment from all three biological replicates were analysed considering average median medium/light ratios of the identified phosphopeptides and calculating the mean and standard deviations. These ratios reflect the changes in the phosphorylation level of identified phosphopeptides in excitotoxicity. The web-based quantitative proteomics p -value calculator (permutation based) was used to identify phosphopeptides that exhibit statistically significant ($p < 0.05$) changes in phosphorylation in excitotoxicity (Chen et al., 2014). The data for 4 h glutamate treatment from six (3+3, as I repeated 4 h treatment during inhibitor study as described in Chapter 6) biological replicates were also processed and analysed in the same way as for analysis of the 15 min data. Signalling phosphoprotein molecules with selected lists of phosphopeptides showing significant changes in phosphorylation after glutamate treatment for 15 min and/or 4 h were

analysed by the Functional Enrichment Analysis Tool (FunRich) for Gene Ontology (GO) analysis and also by the Ingenuity Pathway Analysis (IPA) software to predict how the intracellular signalling networks are perturbed in neurons undergoing excitotoxic cell death.

5.3.2 More than 70 significantly dysregulated phosphopeptides were identified in glutamate-induced excitotoxicity in cultured primary neurons

Following phosphoproteomic data analysis (all data points), a total of 299 phosphopeptides (with 553 different phosphorylation stoichiometry) were identified that correspond to 230 phosphoproteins from all of the biological replicates from 15 min and 4 h time points. Approximately, 72% (299/417) of the peptides after TiO₂ enrichment were identified as phosphopeptides. For 15 min glutamate treatment data point, identified phosphopeptides with corresponding average median medium to light ratios from 3 biological replicates were imported in quantitative proteomics *p*-value calculator (QPPC) for permutation *p*-values calculation. A *p*-value of ≤ 0.05 was considered statistically significant i.e. there was a significant change in phosphorylation (either increase or decrease) following glutamate treatment. During the QPPC stage 1 computation, 1000 permutations calculations were selected and 100 was set as a threshold for outlier removal. In the stage 2 computation, median value for all quantified phosphopeptides average log-ratios was used to normalise the data counteracting known biases such as unequal loading of the samples and incomplete labelling of the peptides (Chen et al., 2014). To identify significant changes in phosphopeptides, 0.05 was set as the *p*-value cut-off and 2 as the fold change cut-off. After stage 2 computation, QPPC generated one output (.csv) file with proteins significant under either one or both criteria i.e. *p*-value ≤ 0.05 and/or fold change $> \log(2)$ or $< -\log(2)$. This analysis was repeated for phosphopeptides identified in neurons 4 h after glutamate treatment from all six biological replicates.

The criteria used to consider a phosphopeptide in the final list showing significant changes in phosphorylation include (i) QPPC *p*-value ≤ 0.05 for the changes in phosphorylation, or (ii) mean medium/light (treatment/control) ratio + standard deviation (SD) < 0.7 , or (iii) mean medium/light (treatment/control) ratio - standard deviation (SD) < 1.3 identified from either 15 min or 4 h glutamate treated neurons. A total of 73 phosphopeptides (with a total of 81 different phosphorylation stoichiometries) that are annotated to 59 phosphoproteins showed significant

changes in phosphorylation at either 15 min or 4 h after the onset of glutamate-induced excitotoxic neuronal death (**Table 5.1**).

Table 5.1 A selected list of phosphopeptides showing significant changes in phosphorylation following glutamate-induced excitotoxicity.

S/L	Protein group accession	Protein name	Gene*	Phosphopeptide sequence	Phosphosite	15 min (N=3)				4 h (N=6)			
						Medium/Light	SD	n	QPPC p-value	Medium/Light	SD	n	QPPC p-value
1	B1APX2_MOUSE	Protein 5031439G07Rik	5031439G07 Rik	VTSF p STPP p TPER	S289/T293	0.093	-#	1	-	0.211	0.203	3	0.218
2	E9QK15_MOUSE	Proline-rich AKT1 substrate 1	Akt1s1	LN p TSD F QK	T247	0.712	0.231	2	0.744	0.828	0.423	4	0.981
3	S4R2D0_MOUSE	Ankyrin 2, neuronal	Ank2	QP P p SPT S K	S1936	0.201	-	1	-	0.013	0.004	2	0.022
4	Q3UH26_MOUSE	Amyloid beta (A4) precursor protein-binding, family A, member 1	Apba1	SA p ST E p SGFHNHTDTAEGDV LAAAR	S84/S87	0.522	-	1	-	0.368	0.106	3	0.721
5	Q5U612_MOUSE	Rho GTPase activating protein 35	Arhgap35	TSFSV G p SDDEL G PIR	S1179	0.634	0.195	3	0.720	0.190	0.164	5	0.189
6	Q6PAT3_MOUSE	Rho GTPase activating protein 39	Arhgap39	AF p SEDEAL A QQ D SK	S597	0.451	-	1	-	0.011	0.001	2	0.014
7	B2RRE3_MOUSE	Calmodulin regulated spectrin-associated protein family, member 2	Camsap2	SV p SNEGLTLNNSR	S439	0.370	-	1	-	0.497	0.120	3	0.839
8	Q4FJM2_MOUSE	Cyclin-dependent kinase inhibitor 1B (p27, Kip1)	Cdkn1b	VLAQ E p SQDVSGSR	S106	0.094	0.119	2	0.013	0.441	0.385	3	0.444
9	H7BX26_MOUSE	Centrosomal protein 170kDa	Cep170	LGE A p SDSEL A DADK	S1102	0.161	0.033	2	0.155	0.049	0.053	2	0.063
10	Q3URG0_MOUSE	Connector enhancer of kinase suppressor of Ras 2	Cnksr2	GSE p SPNSFLDQ E YR	S390	0.456	0.231	3	0.456	0.135	0.141	3	0.201
11	Q3TXY0_MOUSE	Collapsin response mediator protein 1	Crmp1	NLHQSNFSL p SGAQIDDNNPR	S542	0.158	-	1	-	0.663	0.034	3	0.935
12	Q3UBT6_MOUSE	Casein kinase 1, delta	Csnk1d	GAPVNV p SSSDLTGR	S382	0.141	0.088	3	0.040	0.379	0.331	5	0.475
13	Q8CBH9_MOUSE	Casein kinase 1, epsilon	Csnk1e	GAPAN p SSSDLTGR	S389	0.050	0.033	2	0.012	0.235	0.272	6	0.065
14				LAA p SQT p SVPF D H L GK	S405/S408	-	-	-	-	0.317	0.276	3	0.305
15	E0CXB9_MOUSE	Catenin (cadherin-associated protein), alpha 2	Ctnna2	TPEE L DD p SDFEQEDYDVR	S640	2.441	0.742	3	0.507	3.549	1.951	5	0.735
16				QVQEAIAGISSAAQATSP p TDEAK	T264	0.515	0.092	3	0.616	0.691	0.212	6	0.989
17	B7ZNF6_MOUSE	Catenin (cadherin-associated protein), delta 2	Ctnnd2	GG S PLTTT Q GG p SPTK	S273	0.189	0.033	3	0.125	0.201	0.212	6	0.083
18				GG p SPLTTT Q GG p SPTK	S264/S273	0.204	-	1	-	0.345	0.249	5	0.558
19	Q3TV22_MOUSE	Coxsackie virus and adenovirus receptor	Cxadr	AP Q p SPTL A PAK	S332	0.212	0.057	3	0.124	0.194	0.228	6	0.104
20	F7CPL2_MOUSE	Drebrin 1	Dbn1	LS p SPVLHR	S142	0.629	0.156	3	0.727	0.117	0.111	2	0.260
21	Q1EDH1_MOUSE	Doublecortin-like kinase 1	Dclk1	ISQHGG p SS T p SLS S TK	S352/S355	0.224	0.064	3	0.164	0.178	0.230	5	0.034

Table 5.1 (Continued)

S/L	Protein group accession	Protein name	Gene	Phosphopeptide sequence	Phosphosite	15 min (N=3)				4 h (N=6)			
						Medium/Light	SD	n	QPPC p-value	Medium/Light	SD	n	QPPC p-value
22	Q9CXL6_MOUSE	Doublecortin	Dcx	QSPISTPTSPG p SLR	S342	0.062	0.008	2	0.023	0.298	0.396	5	0.135
23	Q3TT92_MOUSE	Dihydropyrimidinase-like 3	Dpysl3	NLHQSGFSL p SGTQVDEGVR	S541	0.367	0.275	3	0.274	0.425	0.351	5	0.658
24	Q8CIJ3_MOUSE	Eukaryotic translation initiation factor 3, subunit B	Eif3b	GHPSAGAEIEGG p SDG p SAAEAEPR	S120/S123	1.311	-	1	-	0.588	0.117	6	0.971
25	A7MCX4_MOUSE	Erythrocyte membrane protein band 4.1-like 3	Epb41I3	VESTSVGS l pSPGGAK	S804	0.112	0.017	3	0.032	0.174	0.232	5	0.042
26	O35558_MOUSE	Mitogen-activated protein kinase 1	Erk2	VADPDHDHTGFL p TEpYVATR	T183/Y185	4.132	3.081	2	0.278	1.716	0.872	4	0.942
27	E9PUK3_MOUSE	Formin binding protein 1-like	Fnbp1l	T l pSDGTISA A K	S295	0.300	0.092	3	0.252	0.255	0.368	5	0.079
28	Q3UR88_MOUSE	GTPase activating protein (SH3 domain) binding protein 1	G3bp1	ST p SPAPADVAPAQEDLR	S231	0.254	0.062	3	0.199	0.318	0.205	5	0.644
29	Q5F258_MOUSE	G protein-coupled receptor kinase interacting ArfGAP 1	Git1	SL S pSPTDNLELSAR	S371	1.061	0.070	3	0.972	0.332	0.172	6	0.745
30	D3Z7E5_MOUSE	Glycogen synthase kinase 3 alpha	Gsk3a	T S pSFAEPGGGGGGGGGGP GGASGPGGTGGGK	S21	0.631	0.175	2	0.705	0.481	0.493	4	0.491
31				GEPNV S pYICSR	Y279	-	-	-	-	0.662	0.151	3	0.938
32	Q3UJQ2_MOUSE	3-hydroxy-3-methylglutaryl-CoA synthase 1 (soluble)	Hmgcs1	LPATSAESES A V l pSDGEH	S516	0.949	0.039	2	0.963	0.552	0.162	6	0.958
33	A2AL13_MOUSE	Heterogeneous nuclear ribonucleoprotein A3	Hnrnpa3	SSG p SPYGGGYSGGGGSGG YGSR	S359	0.901	0.163	3	0.939	0.480	0.200	5	0.867
34	Q4L138_MUSMM	Insulin-like growth factor 2 receptor	Igf2r	AEALSSLHGDDQD p SEDEVL TVPEVK	S2401	0.420	0.182	2	0.430	0.291	0.151	2	0.553
35	D3YXZ3_MOUSE	Kinesin light chain 2	Klc2	A S p SLNFLNK	S575	0.826	0.020	3	0.900	0.401	0.230	4	0.758
36	Q8CGB7_MOUSE	LIM and calponin homology domains 1	Limch1	TSVPESIASAGT G pSPSK	S523	0.096	-	1	-	0.230	0.161	4	0.314
37	B2RQQ5_MOUSE	Microtubule-associated protein 1B	Map1b	ESSPLY p SPGFSDSTSA A K	S1793	0.293	0.212	3	0.202	0.012	0.002	2	0.022
38				SPSL p SPSP p SP l EP K	S1255/S1260	0.208	0.177	3	0.077	0.272	0.510	5	0.035
39				ES p SPLY p SPGFSDSTSA A K	S1789/S1793	0.453	0.253	3	0.462	0.301	0.347	6	0.197
40				TLEV V p SPSQSVTGSAGHTP YYQSPTDEK	S1317	0.314	0.101	2	0.293	0.140	0.135	3	0.222
41				SPSLSPSP p SP l EP K	S1260	0.245	0.109	3	0.166	0.416	0.431	5	0.225
42				SV p SPGV T QAVVEEHCA p SP EEK	S1293/S1307	-	-	-	-	0.329	0.137	3	0.642

Table 5.1 (Continued)

S/L	Protein group accession	Protein name	Gene	Phosphopeptide sequence	Phosphosite	15 min (N=3)				4 h (N=6)			
						Medium/Light	SD	n	QPPC p-value	Medium/Light	SD	n	QPPC p-value
43	Q3URJ7_MOUSE	Microtubule-associated protein 2	Map2	ETpSPETSLIQDEVALK	S1161	0.133	0.051	3	0.050	0.010	0.000	2	0.001
44				VDHGAEIITQpSPSR	S1782	0.114	0.023	3	0.038	0.157	0.143	6	0.137
45				TPGpTPGpTPSYPR	T1620/T1623	0.085	0.053	3	0.010	0.268	0.275	6	0.206
46				LApSVSADAEVAR	S823	0.044	0.028	3	0.001	0.653	0.488	4	0.812
47				TPGTGPpTPSYPR	T1623	0.056	0.046	3	0.003	0.811		1	
48	E9PWC0_MOUSE	Microtubule-associated protein 4	Map4	ATpSPSTLVSTGPPSR	S785	0.772	0.135	3	0.880	0.264	0.246	6	0.380
49	D3YWH6_MOUSE	C-Jun-amino-terminal kinase-interacting protein 3	Mapk8ip3	TGSpSPTQGIVNK	S366	1.046	0.151	3	0.985	0.496	0.154	6	0.930
50	Q3V1B5_MOUSE	Myocyte enhancer factor 2C	Mef2c	NpSPGLLVSPGNLTK	S222	0.023	0.022	3	0.001	0.177	0.289	3	0.054
51	F7BC60_MOUSE	Mitochondrial fission factor	Mff	NDpSIVTPSPQAR	S146	0.017	0.010	3	0.001	0.496	0.685	4	0.191
52	Q8BV62_MOUSE	WD repeat-containing protein mio	Mios	GFSQYGVSGpSPTK	S766	0.452	0.333	2	0.409	0.395	0.064	2	0.681
53	MLF2_MOUSE	Myeloid leukemia factor 2	Mlf2	LAIQGPEDSPSR	S237	0.371	0.063	3	0.402	0.321	0.249	5	0.481
54	Q6PB65_MOUSE	Myosin, heavy chain 10, non-muscle	Myh10	GGPISFSSpSR	S1939	0.354	0.288	3	0.258	0.415	0.356	5	0.441
55				QLHIEGASLELpSDDDTESK	S1956	0.235	0.050	3	0.172	0.444	0.325	4	0.773
56	G3X9H8_MOUSE	E3 ubiquitin-protein ligase NEDD4-like	Nedd4l	SLpSSPTVTLAPLEGAK	S477	0.739	0.158	3	0.839	0.137	0.079	2	0.360
57	B8QI35_MOUSE	Protein tyrosine phosphatase, receptor type, f polypeptide (PTPRF), interacting protein (liprin), alpha 3	Ppfia3	QAQpSPGGVSSEVEVLK	S142	1.088	0.077	2	0.951	0.408	0.114	4	0.803
58	Q5DTJ4_MOUSE	Proline-rich coiled-coil 2A	Prrc2a	ETPPGGNLpSPAPR	S1002	0.101	0.129	2	0.008	0.246	0.279	5	0.115
59	E9PUC5_MOUSE	Pleckstrin and Sec7 domain containing 3	Psd3	SHpSpSPSLNPDApSPVTAK	S1000/S1001/S1009	0.523	0.121	3	0.597	0.135	0.155	6	0.022
60				ISNpSSEFSAK	S44 (rat)	0.411	0.072	3	0.454	0.241	0.220	6	0.360
61				SHpSPSLNPDApSPVTAK	S1000/S1009	1.637	0.162	3	0.716	0.319	0.260	6	0.450
62	A2BI12_MOUSE	PC4 and SFRS1 interacting protein 1	Psp1	NLAKPGVTSTpSDpSEDEDDQEGEK	S272/S274	0.216	0.028	3	0.140	0.243	0.290	4	0.373
63	Q8BU35_MOUSE	RNA binding motif protein 25	Rbm25	LGASNpSPGQPNSVK	S672	0.489	0.063	2	0.555	0.290	0.216	5	0.563
64	D3Z4K1_MOUSE	RNA (guanine-7-) methyltransferase	Rnmt	EFGEDLVEQNSSYVQDpSPSK	S64	0.094	0.020	2	0.062	0.091	0.126	4	0.034

Table 5.1 (Continued)

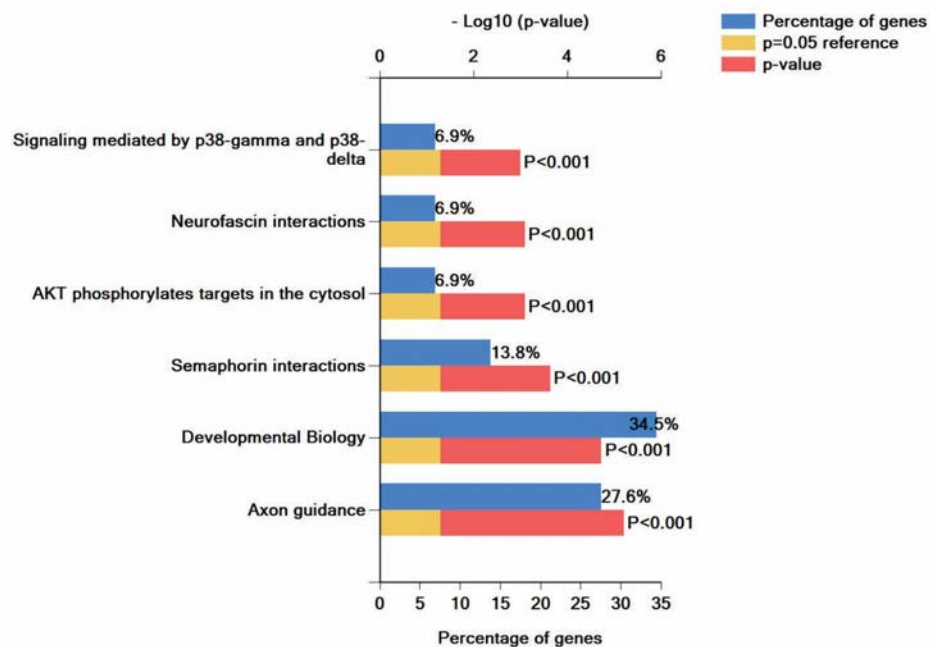
S/L	Protein group accession	Protein name	Gene	Phosphopeptide sequence	Phosphosite	15 min (N=3)				4 h (N=6)			
						Medium/Light	SD	n	QPPC p-value	Medium/Light	SD	n	QPPC p-value
65	E3WH30_MOUSE	SWI5-dependent recombination repair 1	Sfr1	ENPP p SPPTSPAAPQPR	S67	1.319	0.208	3	0.875	1.725	0.283	3	0.881
66				ENPP p SPPT p SPAAPQPR	S67/S71	1.039	0.126	2	0.969	0.610	0.104	3	0.910
67	Q3TWS4_MOUSE	Synaptosomal-associated protein, 91kDa	Snap91	SSPATTV Tp SPNSTPAK	S313	1.398	0.456	3	0.857	0.219	0.141	5	0.440
68	B1AQX6_MOUSE	SRC kinase signaling inhibitor 1	Srcin1	DSGSSSVFAE p SPGGK	S588	0.514	0.163	3	0.596	0.214	0.136	6	0.445
69	D3Z1Z8_MOUSE	Stathmin 1	Stmn1	ASGQAFELIL p SPR	S25	0.453	-	1	-	0.384	0.353	6	0.581
70	D3Z1Z8_MOUSE	Stathmin 1		ESVPDFPL p SPPK	S38	0.115	0.023	3	0.033	0.416	0.427	6	0.592
71	Q3KN99_MOUSE	Synapsin III	Syn3	SQ p SLTNSLSTSDTSHR	S540	0.535	0.199	3	0.597	0.083	0.102	4	0.029
72	Q547J4_MOUSE	Microtubule-associated protein tau	Mapt	SGY p SpSPG p SPGTPGSR	S490/S491/S494	1.080	0.791	3	0.971	0.052	0.084	4	0.005
73				SGY p SPGSPGTPGSR	S491	1.334	-	1	-	0.261	0.217	6	0.448
74				SPVVS GDTp SPR	S696	0.239	0.133	2	0.188	0.383	0.356	5	0.485
75				IG p SLDNITHVPGGGNK	S648	0.394	0.036	3	0.431	0.398	0.286	4	0.554
76				SGYSSPG p SPGTPGSR	S494	1.348	0.240	3	0.856	0.412	0.269	6	0.769
77	Q8BZN7_MOUSE	Thyroid hormone receptor associated protein 3	Thrap3	ASVSDL p SPR	S243	0.301	0.017	3	0.285	0.399	0.302	6	0.727
78	E0CZF8_MOUSE	TRAF2 and NCK interacting kinase	Tnik	Q Np SDPTSENPLPTR	S611	0.314	0.209	3	0.228	0.531	0.474	3	0.467
79	F6RBX1_MOUSE	TOM1-like protein 2	Tom1l2	AAE p TVPDLPSPTTEAPAPASNTSTR	T473	0.713	0.064	3	0.835	0.472	0.167	2	0.736
80	Q8CA33_MOUSE	Tripartite motif containing 2	Trim2	SADV p SPTTEGVK	S428	0.838	0.198	3	0.903	0.490	0.183	5	0.920
81	Q3UG49_MOUSE	Tumor suppressor p53-binding protein 1	Trp53bp1	SEDR p SpSPQVSVAAVETK	S262	0.705	0.069	3	0.816	0.255	0.211	6	0.355

*This table is arranged with gene names in an ascending order, #SD and p-value is missing if the phosphopeptide was identified from only one biological replicate and denoted with a dash (-). Data represents average (from 3 biological replicates for 15 min and 6 biological replicates for 4 h glutamate treatment) median medium to light (M/L) ratios of the phosphopeptides and corresponding p-values. Significant p-values (≤ 0.05) are in 'red' and corresponding phosphoprotein molecules are 'bold'. Only phosphopeptides identified with average M/L ratio + standard deviation (SD) < 0.7 (for decrease in phosphorylation) or average M/L ratio - standard deviation (SD) > 1.3 (for increase in phosphorylation) from either 15 min or 4 h glutamate treatment are listed in this table.

5.3.3 Gene ontology analysis of the altered phosphoproteins in excitotoxicity

Gene names for phosphoprotein molecules (59) that correspond to the listed phosphopeptides (81) in **Table 5.1** were uploaded in FunRich software for Gene Ontology (GO) enrichment analysis. The FunRich software was able to map 56 phosphoproteins (except 5031439G07Rik, Csnk1e and Trp53bp1) using background FunRich database and generated the outputs for biological pathways, biological processes, molecular functions etc. Top enriched biological pathways are axon guidance (27%, $p < 0.001$), developmental biology (34.5%, $p < 0.001$), semaphorin interactions (13.8%, $p < 0.001$), Akt phosphorylates targets in the cytosol (6.9%, $p < 0.001$), neurofascin interaction (6.9%, $p < 0.001$), signalling mediate by p38-gamma and p38-delta (6.9%, $p < 0.001$) etc. (**Figure 5.3A**). Top biological processes are identified as cell growth and/or maintenance (23.2%, $p < 0.001$), signal transduction (39.3%, $p < 0.01$), neurotransmitter transport (1.8%, $p < 0.01$), cell communication (32.1%, $p = 0.03$) and cell-cell signalling (1.8%, $p = 0.05$) (**Figure 5.3B**). Additionally, top molecular functions include cytoskeletal protein binding (12.5%, $p < 0.001$), protein serine/threonine kinase activity (8.9%, $p < 0.01$), Co-A-ligase activity (1.8%, $p < 0.01$), structural molecule activity (7.1%, $p < 0.01$), neurotransmitter transporter activity (1.8%, $p = 0.01$), RNA methyltransferase activity (1.8%, $p = 0.04$) etc. (**Figure 5.3C**).

A. Biological pathways



B. Biological processes

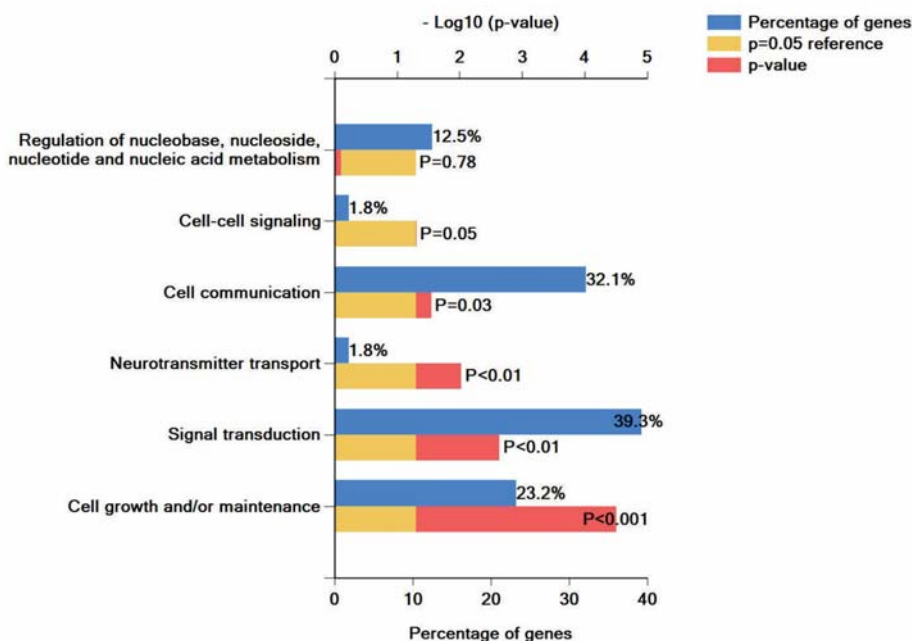


Figure 5.3

C. Molecular functions

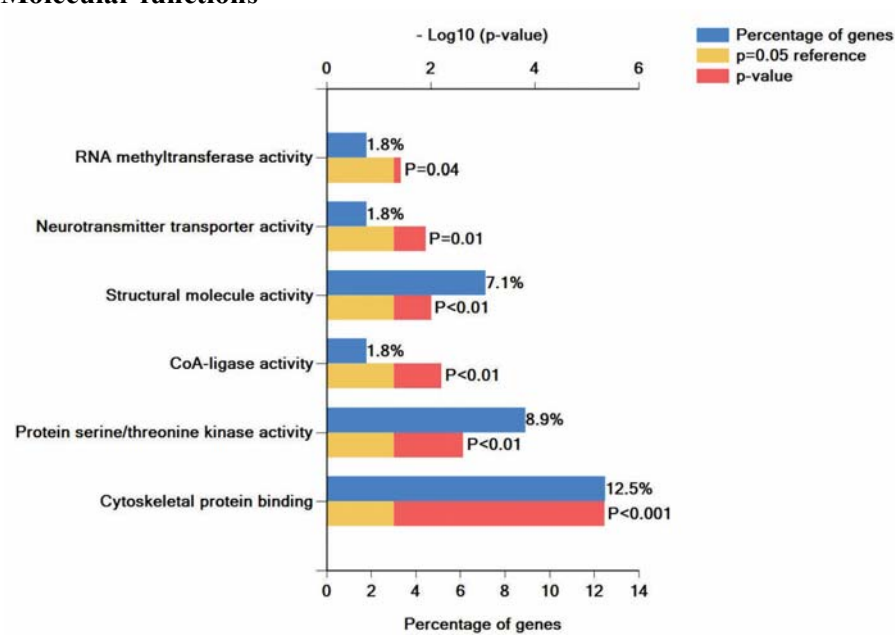


Figure 5.3 Gene Ontology (GO) analyses of the differentially regulated phosphoprotein molecules in glutamate-induced excitotoxicity. FunRich analysis showing the enriched biological pathways (A), biological processes (B) and molecular functions (C).

5.3.4 Pathway and network analysis of the identified phosphoprotein molecules using IPA

Ingenuity Pathway Analysis (IPA) was used to further ascertain the putative functions of the identified phosphoprotein molecules that showed significant changes in phosphorylation in glutamate-induced excitotoxicity and how these protein molecules interact with each other in cells. The list of the phosphoprotein molecules (59) that correspond to the significantly perturbed phosphopeptides (**Table 5.1**) in the 15 min and 4 h treatment experiments were uploaded in IPA. The core analysis platform was used to analyse these phosphoprotein molecules based on Ingenuity Knowledge base. The statistical significance of the identified pathways and networks were determined by IPA using a Fisher exact test ($p < 0.05$). The top five identified canonical pathways are (i) amyloid processing, (ii) 14-3-3 mediated signalling, (iii) role of NFAT in regulation of the immune response, (iv) PTEN signalling and (v) semaphoring signalling in neurons (**Table 5.2**), which is also identified as one of the top biological pathways by FunRich GO analysis (**Figure 5.3 A**). The two other top canonical pathways i.e. 14-3-3 mediated signalling and PTEN signalling and the previously identified Akt phosphorylates targets in the cytosol by FunRich, clearly demonstrate the involvement of Akt pro-survival pathway in glutamate-induced excitotoxicity. Indeed, it was found to be true after Western blot data analysis (in the later section). The interacting networks of these phosphoprotein molecules were generated with the IPA software and top associated network functions were identified as cell morphology, cellular assembly and organisation, cellular development (network score of 55) and organismal injury and abnormalities (network score of 32) (**Figure 5.4**). It is clear from the top scored networks that the identified pathways can potentially interplay to cause neuronal death. The propensity of calpain substrates found to undergo changes in phosphorylation implies that the changes in phosphorylation of these proteins may occur as the cause or consequence of calpain cleavage (**Figure 5.4**). The top upstream regulators of these potentially neurotoxic signalling pathways identified by IPA include MAP kinase-interacting serine/threonine-protein kinase 1 (MKNK1), brain-derived neurotrophic factor (BDNF), agrin (AGRN), microtubule-associated protein tau (MAPT) and dystonin (Dst) (**Table 5.3**). Notably, MAPT was previously (Chapter 4) also identified as one of the upstream regulators for the significantly perturbed protein molecules showing differential expression level in glutamate-induced excitotoxicity.

Table 5.2 Significantly dysregulated phosphoproteins-derived top canonical pathways identified by IPA.

Canonical pathway	<i>p</i> -value	Overlap
Amyloid processing	1.36×10^{-5}	7.8%
14-3-3 mediated signalling	2.11×10^{-5}	4.3%
Role of NFAT in regulation of the immune response	1.29×10^{-4}	2.9%
PTEN signalling	3.63×10^{-4}	3.4%
Semaphorin signalling in neurons	4.70×10^{-4}	5.7%

Table 5.3 Top upstream regulators of the phosphoproteins-derived potentially neurotoxic signalling pathways identified by IPA.

Molecules	Full name	<i>p</i> -value overlap	Predicted activation
MKNK1	MAP kinase-interacting serine/threonine-protein kinase 1	1.60×10^{-10}	-
BDNF	Brain-derived neurotrophic factor	8.66×10^{-7}	-
AGRN	Agrin	1.32×10^{-6}	-
MAPT	Microtubule-associated protein tau	3.60×10^{-6}	-
Dst	Dystonin	6.44×10^{-6}	-

A.

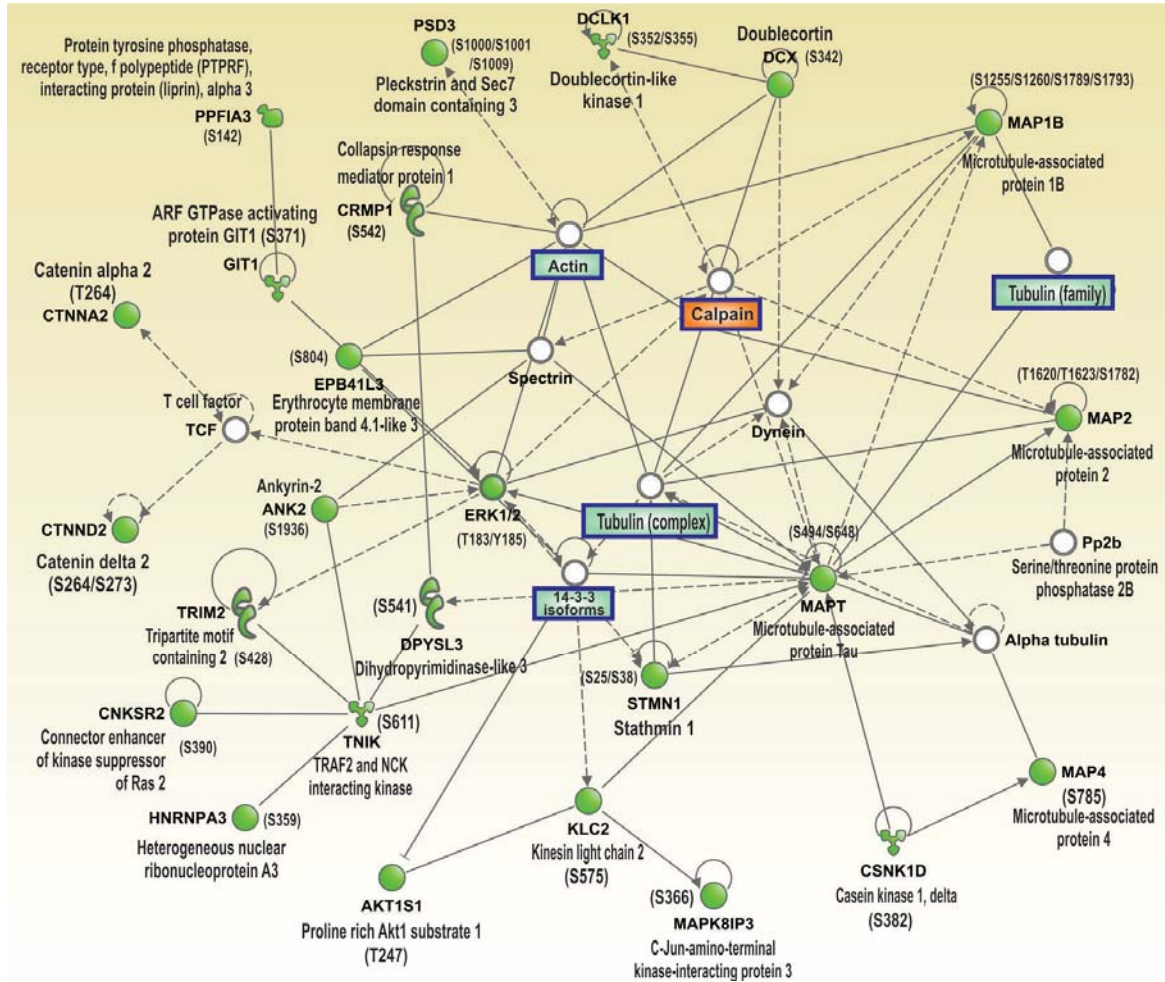


Figure 5.4

B.

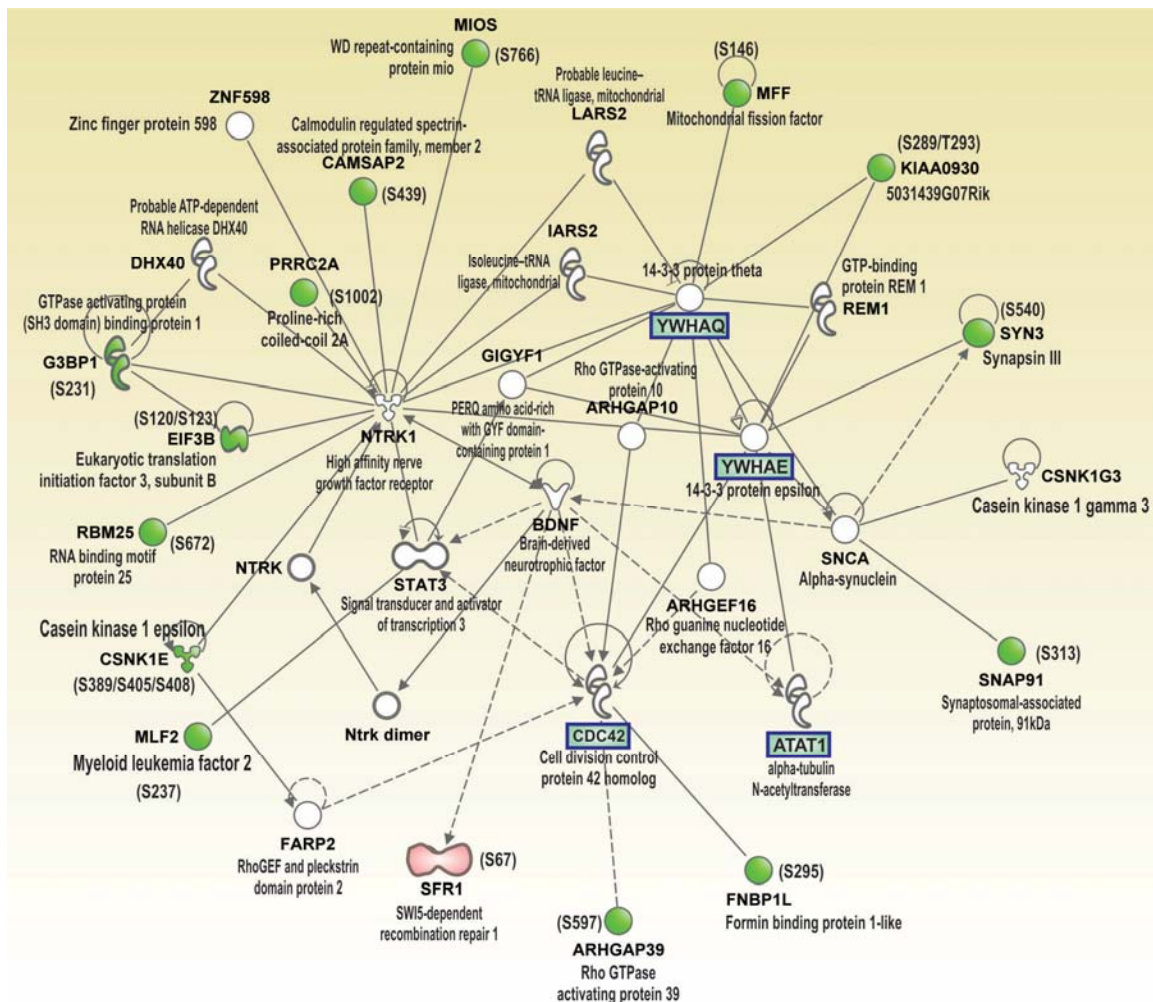


Figure 5.4 Interaction network analysis of the identified altered-phosphoproteins in glutamate-induced excitotoxicity. The intermolecular interaction networks of the identified phosphoprotein molecules were generated through the use of QIAGEN's Ingenuity Pathway Analysis (IPA, QIAGEN Redwood City, www.qiagen.com/ingenuity). Identified phosphoprotein molecules showing increase (red) or decrease (green) in phosphorylation are indicated with their corresponding phosphorylation sites. Boxed (\square) protein molecules are identified in the global proteome data showing either increase (red) or decrease (green) in expression levels. Protein/phosphoprotein molecules (colourless) that are absent in the significant list-containing tables (**Table 4.2** for global proteome and **Table 5.1** for phosphoproteome) but are known to interact with the identified proteins are also listed in the above networks. **A.** 'Cell morphology, cellular assembly and organisation, cellular development' was identified as one of the top networks with a score of 55. Calpain is identified as one of the interacting molecules and previous study clearly demonstrated the over-activation of calpain in glutamate-induced excitotoxicity (Hossain et al., 2013) and activated calpain can degrade and cleave a number of cellular proteins such as Src (described in Chapter 3) to modulate their normal physiological function **B.** 'Organismal injuries and abnormalities' network with a network score of 32. The legend for IPA molecule shapes and relationships is presented in appendix I.

5.3.5 Data validation by Western blot analysis

Phosphoproteomics data revealed changes in phosphorylation for a number of phosphoproteins listed in **Table 5.1**. One of the identified phosphopeptide ($^{171}\text{VADPDHDHTGFLpTEpYVATR}^{189}$) of mitogen-activated protein kinase 1 (Erk2) showed ~3-fold increase in phosphorylation at threonine 183 and tyrosine 185 (that correspond to Thr-185 and Tyr-187 of human isoform respectively) after 15 min glutamate treatment in cultured neurons. Western blot analysis using total (#9101, Cell Signalling) and phospho specific antibodies (#9102, Cell Signalling, specifically recognise T202/Y204 and T185/Y187 of human Erk1 and Erk2, respectively) also revealed that there was a significant increase in phosphorylation at 5 min and 15 min of glutamate treatment in neurons for the same phosphorylation sites identified using quantitative phosphoproteomic analysis (**Figure 5.5**). Phosphorylation of these two sites T202/Y204 and T185/Y187 in the activation loop by upstream kinases MEK1 and MEK2 fully activate Erk1/2 kinases that are the key pro-survival molecules in neurons maintaining cell survival (Hetman and Gozdz, 2004).

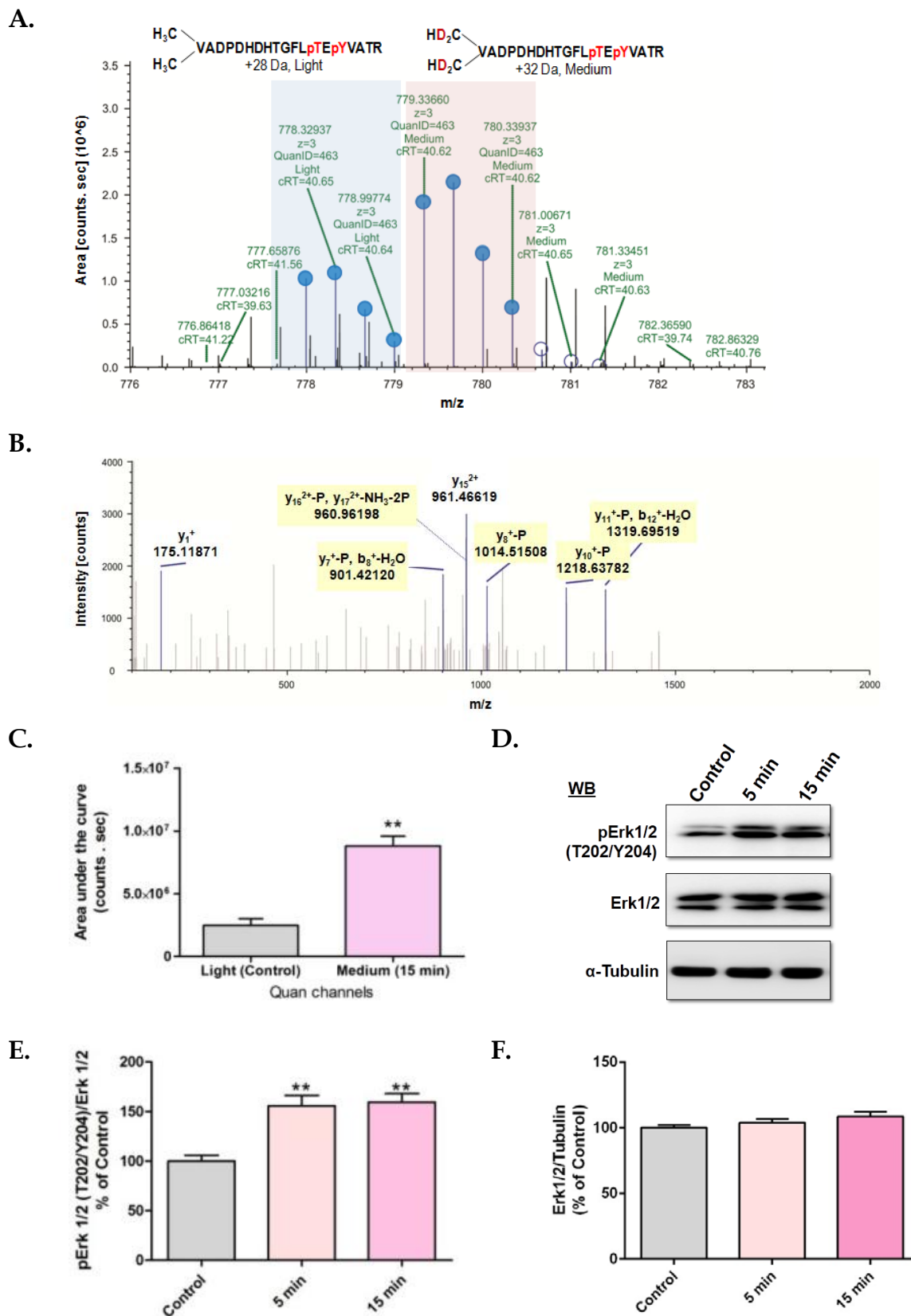


Figure 5.5

Figure 5.5 XIC based MS1 quantification and MS2 spectra used for the quantification of Erk2 phosphopeptide and immunoblot analysis. An increase in phosphorylation (T183/Y185 of the identified phosphopeptide that correspond to T202/Y204 and T185/Y187 of human Erk1 and Erk2 respectively) for one of the Erk2 (MAPK1) phosphopeptides was observed after 15 min glutamate treatment. **A.** Chromatogram showing isotopic clusters used for the quantification of labelled (N-terminal dimethyl) triply charged unique tryptic phosphopeptide ($^{171}\text{VADPDHDHTGFLpTEpYVATR}^{189}$) from Erk2. **B.** The corresponding MS2 spectra used for the identification of this unique phosphopeptide with Mascot ion score of 53. **C.** Average median medium/light ratio from three biological replicates was 3.1. **D.** This mass spectrometric data was further validated by Western blot analysis using phospho-specific antibodies. Following 5 min and 15 min glutamate treatment there was a sharp increase in phosphorylation for Erk1/2, which was evident by the mass spectrometric results beforehand. **E & F.** Densitometric data showing relative abundance of Erk1/2 and phosphorylation changes upon glutamate treatment. Data are presented as mean \pm SD, (Student's t-tests, $**p < 0.01$, $n = 3$ biological replicates).

5.3.6 Akt and Erk1/2 are two important pro-survival pathways dysregulated in glutamate-induced excitotoxicity

Akt is the key pro-survival pathway maintaining neuronal viability. Akt becomes activated by at least two mechanisms. The first mechanism is a PI3K-dependent mechanism. In brief, PI3K phosphorylates phosphatidylinositol (4,5)-bisphosphate (PIP2) to form phosphatidylinositol (3,4,5)-trisphosphate (PIP3), which binds to the pleckstrin homology (PH) domain of Akt and subsequently leads to dimerisation and activation by phosphorylation by the upstream kinases phosphoinositide-dependent kinase-1 (PDK1) at T308 and mammalian target of rapamycin (mTOR) complex 2 (mTORC2) at S473 (Datta et al., 1995; Franke et al., 1997; Franke et al., 1995; Stephens et al., 1998; Stokoe et al., 1997). The second mechanism is the PI3K-independent mechanism. In this mechanism, calcium signals from the synaptic NMDA receptors activate Akt by activating Ca^{2+} -calmodulin dependent protein kinase kinase (CaM-KK) (Yano et al., 1998). Active Akt then phosphorylates and inactivates a number of pro-death signalling proteins including glycogen synthase kinase 3 (Gsk3) (Cross et al., 1995), Bcl-2 family member BAD (Datta

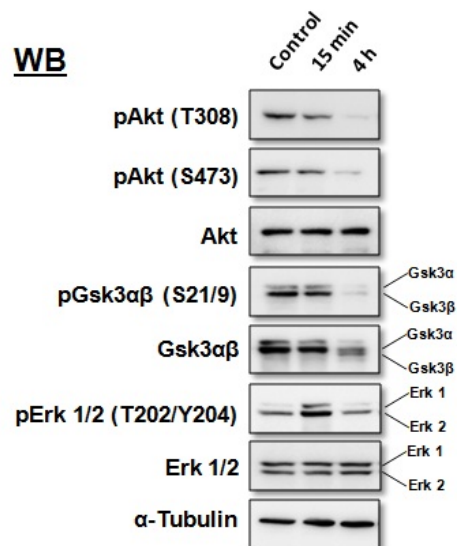
et al., 1997), forkhead transcription factor FKHR (Nakae et al., 2000) and proline rich Akt substrate (PRAS) (Kovacina et al., 2003), and ultimately contributes to neuronal survival.

Given the important role of Akt in neuronal survival, its inhibition is expected to contribute to excitotoxic neuronal death. Since (i) FunRich GO analysis suggests Akt signalling as one of the key biological processes (**Figure 5.3 A**), (ii) decrease in expression of 14-3-3 isoforms (results described in the previous global proteome analysis chapter), (iii) identification of 14-3-3 mediated signalling and PTEN signalling as top canonical pathways by IPA (**Table 5.2**) that are downstream and upstream of Akt signalling, respectively, and (iv) more importantly, the decrease in phosphorylation at Thr-247 of Akt1 substrate 1 (Akt1s1), Ser-477 of E3 ubiquitin-protein ligase NEDD4-like (Nedd4l) and Ser-21 of Gsk3 α , that are direct substrates of Akt (**Table 5.1**); I therefore examined the activation state of Akt by monitoring its phosphorylation levels at both Ser-473 and Thr-308. Western blot analysis of the glutamate treated neuronal lysates revealed a significant decrease in Akt phosphorylation at both sites at 4 h after glutamate treatment (**Figure 5.6**). This result nicely correlated to the decrease in phosphorylation of its downstream substrate Gsk3, which also exhibited a sharp decrease in Ser-21 and Ser-9 phosphorylation of the Gsk3 α and Gsk3 β isoforms, respectively. Inactivation of Akt pro-survival pathway and simultaneously activation of Gsk3 pro-death signalling ultimately contribute to neuronal death in excitotoxicity.

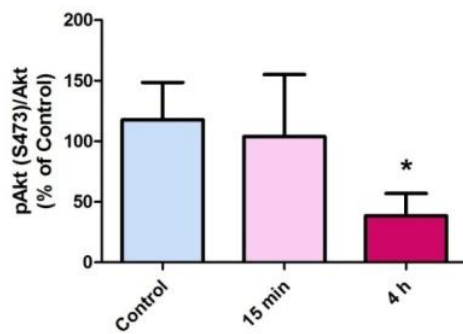
On the other hand, Western blot analysis also revealed a transient increase in Erk1/2 phosphorylation (T183/Y185 in the activation loop) at 15 min glutamate treatment (**Figure 5.6**), that was actually initiated at 5 min of glutamate treatment (**Figure 5.5 D**). Erk1/2 activity came down to the basal level after 4 h of glutamate treatment (**Figure 5.6**).

Mitogen-activated protein kinases Erk1 and Erk2 are well known for their pro-survival functions and contribute to cellular proliferation and differentiation (Johnson and Lapadat, 2002). However, growing evidence suggests that transient Erk activation is neurotoxic but the underlying molecular mechanism is not fully understood (Alessandrini et al., 1999; Subramaniam and Unsicker, 2010; Vauzour et al., 2014; Zhuang and Schnellmann, 2006). To elucidate the exact role of transient Erk activation and its downstream pro-death signalling to induce neuronal death, further investigation is warranted. Taken together, phosphoproteomics data and subsequent Western blot analysis confirm the dysregulation of two known pro-survival pathways i.e. Akt and Erk1/2 signalling pathways in neurons.

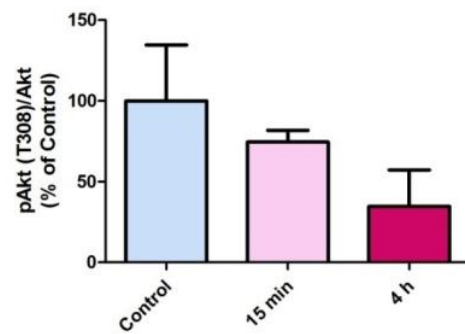
A.



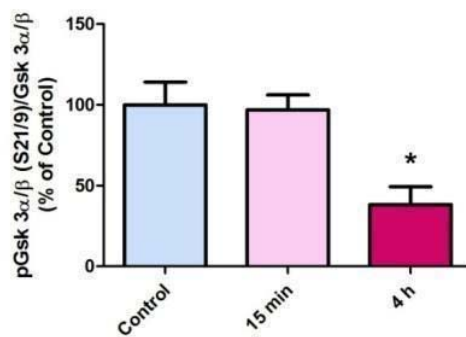
B.



C.



D.



E.

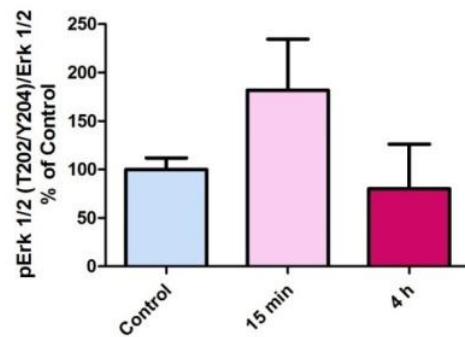


Figure 5.6

Figure 5.6 Dysregulation of the Akt and Erk1/2 pro-survival pathways in glutamate-induced excitotoxicity in cultured primary neurons. **A.** Western blots analysis of the neuronal lysates following glutamate treatment (15 min and 4 h). Glutamate excitotoxicity leads to the dephosphorylation of Akt (at both Ser-473 and Thr-308) and downstream Gsk3 $\alpha\beta$ (Ser-21 and Ser-9 of α and β isoforms, respectively). Simultaneously, there was a transient increase in Erk1/2 phosphorylation after 15 min of glutamate treatment. **B & C.** Quantitative analysis of the relative phosphorylation changes in Ser-473 and Thr-308 of Akt. **D.** Quantitative analysis of the S21/9 phosphorylation changes in Gsk3 $\alpha\beta$, which are the direct phosphorylation site of Akt. **E.** Quantitative analysis of the T183/Y185 (T202/Y204 human isoform) phosphorylation changes in neuronal lysates derived from mouse cortical neurons after glutamate treatment for 15 min and 4 h. Data are presented as mean + SD from three biological replicates (Student's t-tests, * $p < 0.05$).

5.3.7 Increased nuclear translocation of PTEN following glutamate-induced excitotoxicity

How might overstimulation by glutamate induces decrease in phosphorylation and inactivation of Akt? Phosphatase and tensin homolog (PTEN), which is a dual lipid and protein phosphatase, acts as a potent upstream inhibitor of Akt. By dephosphorylating PIP3 to PIP2, PTEN blocks phosphorylation of both S473 and T308, thereby inactivates Akt and suppress its neuroprotective function (Gao et al., 2010; Luo et al., 2003; Trotman et al., 2007). PTEN can shuttle between cytoplasm and nucleus and regulates many pathological and physiological functions including cell cycle arrest (Chung and Eng, 2005), antagonise PI3K/Akt pro-survival pathways (Vivanco and Sawyers, 2002), cooperate with p53 (Li et al., 2006), and also maintain chromosomal integrity (Shen et al., 2007). As Akt pathway was inactivated in excitotoxicity and PTEN signalling was identified as one of the top canonical pathways by IPA (**Table 5.2**), I examined the role of PTEN in excitotoxic neuronal death. Specifically, I examined how glutamate stimulation affects subcellular location of PTEN. An immunostaining experiment was performed using polyclonal anti α -PTEN primary antibody (1:100) (in-house generated) that recognise full-length PTEN. For this experiment, primary neurons were cultured on poly-D-lysine coated cover glass for 7 days before glutamate (100 μ M) was treated for 4 h and 7 h to induce excitotoxicity. Following glutamate treatment, cells were washed with PBS and immunostaining procedure was followed as described earlier (section 5.2.4). Anti α -tubulin antibody (1:200) was also used for microtubules staining and DAPI was used for nuclear staining. Following immunostaining procedure 12-18 images were captured for each of the slides (control and treatments). This experiment was repeated 3 times (three biological replicates) and the data were analysed using LAS AF Lite software (Leica Microsystem, Wetzlar, Germany). It was evident from the data that there was a significant increase in nuclear PTEN comparing to cytoplasm following glutamate-induced excitotoxicity (**Figure 5.7**). PTEN also showed a time-dependent increase in nuclear localisation after 4 h to 7 h of glutamate treatment (**Figure 5.7**). In support of these data, recent study findings also demonstrated that NMDA-induced nuclear translocation of PTEN exacerbates excitotoxic (in vitro) and ischaemic (in vivo) neuronal death and blockade of nuclear translocation of PTEN by a membrane permeable peptide (K-13) can rescue ischaemic brain damage (Zhang et al., 2013). Intriguingly, in another study Howitt *et al.* demonstrated that blockade of nuclear translocation of PTEN by Ndfip-1 deletion, exacerbates brain damage in a rat model of

stroke (Howitt et al., 2012). Thus further studies are required to clearly define the role of increased nuclear PTEN in excitotoxicity.

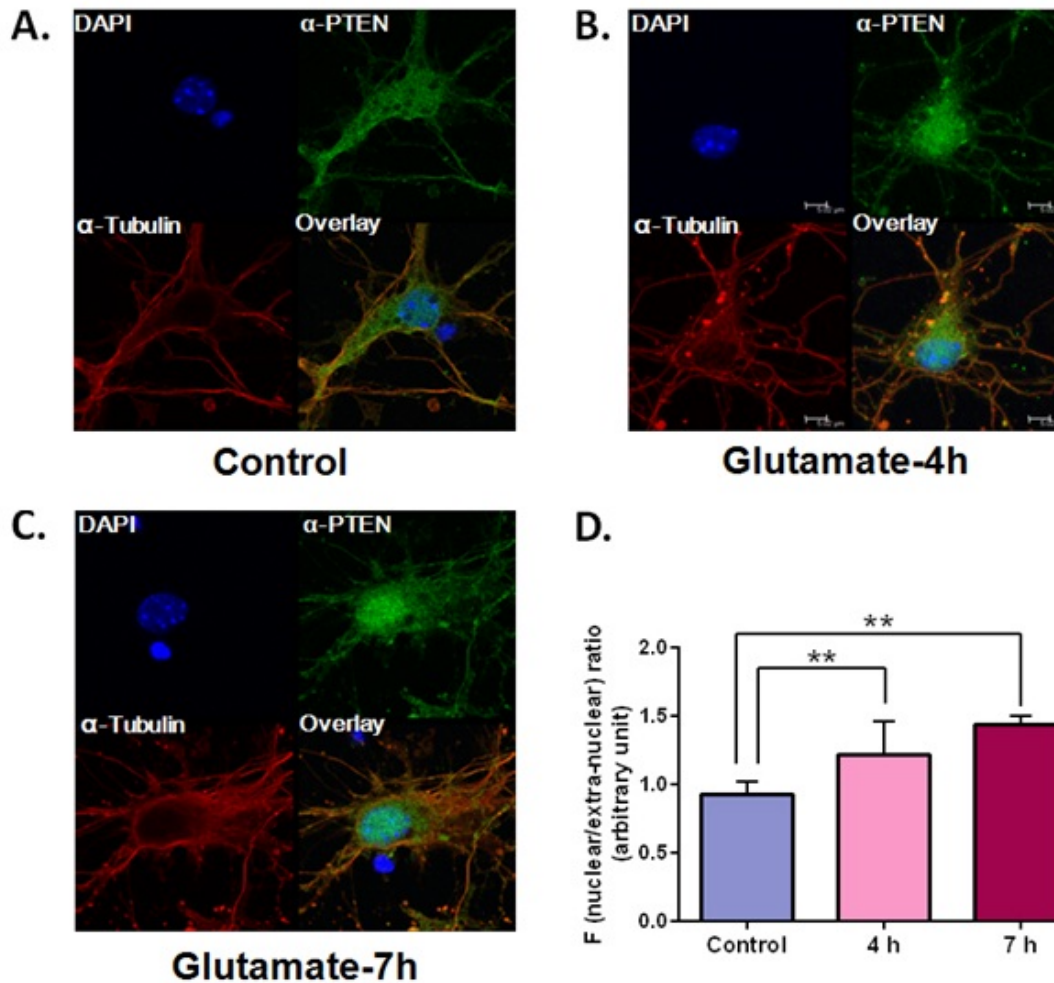


Figure 5.7 Nuclear localisation of PTEN following glutamate-induced excitotoxicity in cultured primary cortical neurons. Immunostaining of cultured neuron (DIV 7) for α -PTEN and α -Tubulin in control slides (A), and 4 h (B) and 7 h (C) glutamate (100 μ M) treated slides. **D.** Bar graph showing increased nuclear translocation of PTEN following glutamate treatment. Data represents mean \pm SD, $**p < 0.01$, $n = 3$ independent experiments, 12-18 images were captured and analysed for each time point.

5.4 Discussion

This chapter describes the findings of the changes of neuronal phosphoproteome induced by glutamate-induced excitotoxicity. A total of 59 phosphoprotein molecules showed significant changes in phosphorylation in either one or more phosphorylation sites. Most of them showed a decrease in phosphorylation upon excitotoxic glutamate stimulation for 15 min and 4 h except for T183/Y185 of Erk2 and Ser-67 of Swi5-dependent recombination DNA repair protein 1 homolog (Sfr1). It is important to note that decrease in phosphorylation for a particular phosphoprotein could be due to the decrease in expression of that particular phosphoprotein. For example, global proteome study (Chapter 4) identified that expression of Ras GTPase-activating protein-binding protein 1 (G3bp1) and microtubule-associated protein 2 (Map2) was significantly decreased in glutamate-induced excitotoxicity, thus the decrease in phosphorylation at Ser-231 of G3bp1 and Ser-823, Ser-1161, Ser-1782, Thr-1620 or Thr-1623 of Map2 listed in **Table 5.1** might be due to the decreased expression of the total protein molecules. Thus, further investigation is needed to establish whether the changes in phosphorylation levels of these proteins are results of modulation of the activities of the upstream kinases and phosphatases and/or turnover of their expression levels. Relevant to this, we have established that the changes in phosphorylation of Erk1/2 and Gsk3 α/β detected by the proteomic approach were not resulted from reduction of their expression; instead they were caused by changes in phosphorylation and/or dephosphorylation by their upstream kinases and phosphatases, respectively (**Figure 5.6**).

There is a dearth of information on phosphoproteomic analysis of neuronal proteins in excitotoxicity in ischaemic stroke animal models or cultured primary neurons. There are only few published manuscripts on proteomic analysis of cultured primary neurons and animal models of stroke (Datta et al., 2011; Liao et al., 2008). However, the study by Liao *et al.* only describes the changes in neuronal proteome caused by deletion of the *fragile X mental retardation 1 (Fmr1)* gene (Liao et al., 2008), while the one by Datta *et al.* did not reveal whether the proteomic changes induced by ischaemic stroke are due to changes in neurons or other brain cells (Datta et al., 2011). The most relevant published study of the changes in phosphoproteome in excitotoxicity was the one conducted by Kang *et al.* using the cultured mouse hippocampal cell line HT22 (Kang et al., 2007). Using 2D gel electrophoresis, Pro-Q staining for phosphoproteins and subsequent mass spectrometric analysis of the selected spots, Kang *et al.* identified 17 phosphoprotein molecules showing

significant changes upon glutamate-induced oxidative stress in HT22 cells. Among them, the authors identified splicing factor 2, peroxiredoxin 2, S100 calcium binding protein A11, and purine nucleoside phosphorylase as the proteins of which phosphorylation levels either increased or decreased in response to glutamate treatment. Intriguingly, phosphorylation of the tyrosine phosphatase CDC25A, the pro-apoptotic protease caspase-8, and the sterol 14 demethylase CYP51 was detected only in HT22 cells undergoing cell study was not conducted in primary neurons, cautions should be taken in extrapolating their findings to changes in neuronal phosphoproteome induced by glutamate excitotoxicity. Additionally, these proteins were detected by fluorescent phosphoprotein-selective Pro-Q diamond staining of neuronal proteins after separation by 2D electrophoresis prior to their identification by mass spectrometry. However, the authors did not identify the phosphorylation site (Kang et al., 2007). Thus, our study represents the first documented comprehensive analysis of how excitotoxicity affects the neuronal phosphoproteome. Our data not only identify the cellular proteins undergoing changes in phosphorylation but also define the phosphorylation sites in these proteins. The functions of many cellular proteins are regulated by phosphorylation at multiple sites. For example, our data revealed five phosphorylation sites including Ser-490, Ser-491, Ser-494, Ser-648 and Ser-696 undergoing changes to different extents in tau induced by excitotoxicity (**Table 5.1**). Our results therefore have provided valuable information for future investigation of the roles of these sites in modulating the function of tau in neuronal death.

Intriguingly, with the exception of a few proteins such as tau and Erk1/2 listed in **Table 5.1** (Hossain et al., 2015; Ittner et al., 2010), the involvement of most of the identified phosphoproteins in excitotoxic neuronal death has yet to be confirmed. In light of this, I sought to use other methods to validate the findings we made in mass spectrometry-based proteomic analysis. Representative phosphoproteomic data were validated by Western blot (e.g. Thr-183/Tyr-185 phosphorylation of Erk1/2). It is clear from the data presented in **Figure 5.5** and **Figure 5.6** that either activation of the upstream phosphatases or inactivation of the upstream kinases were responsible for the dephosphorylation of many of the identified phosphoproteins. Presumably, reduction in the phosphorylation levels of some of the identified neuronal proteins ultimately contributes to neuronal death in excitotoxicity by activation of a number of cell death processes and inactivation or perturbation of pro-survival pathways. Indeed, in our study settings, Akt and Erk1/2 pro-survival pathways were found to be dysregulated (**Figure 5.6**) and IPA analysis of the neuronal phosphoproteins

dysregulated in excitotoxicity identifies the related PTEN signalling pathway as one of the top perturbed signalling pathways in response to over-stimulation by glutamate (**Table 5.2**).

Serine/threonine protein kinase Akt (also known as protein kinase B) maintains neuronal survival. Under normal physiological conditions, binding of the neurotrophic growth factors such as BDNF to their corresponding receptors, recruits and activates phosphatidylinositol-3-kinase (PI3K) to the plasma membrane receptor complexes; the activated PI3K then phosphorylates phosphatidylinositol-4,5-bisphosphate (PIP2) to phosphatidylinositol-3,4,5-trisphosphate (PIP3) (Osaki et al., 2004). PIP3 enables recruitment of the PH (pleckstrin homology) domain-containing Akt to the plasma membrane where it is activated by phosphorylation by the phosphatidylinositol-3,4,5-trisphosphate-dependent protein kinase 1 (PDK1) (Franke et al., 1997) and mammalian target of rapamycin complex 2 (mTORC2) at S473 (Franke et al., 1995). The activated Akt emanates the pro-survival signals by phosphorylating a number of downstream cellular proteins to maintain neuronal survival (Dudek et al., 1997). For example, the activated Akt phosphorylates Ser-21 or Ser-9 near in the N-terminal segment of the α - and β -isoforms of glycogen synthase kinase 3 (Gsk3 α and Gsk3 β), respectively, to inactivate their kinase activity and in turn their pro-death signalling pathways. This neuroprotective mechanism was found to be perturbed in a rat model of cerebral ischaemia (Zhao et al., 2005). Of relevance, several studies reported that activation of Gsk3 contributes to neuronal death caused by treatment by cytotoxic agents, such as staurosporine, and apoptosis of the neuron-like SH-SY5Y cells in response to heat shock (Bijur et al., 1999). Furthermore, treatment with the small molecule inhibitors of Gsk3 SB-415286 and SB-216763 was found to protect cerebellar granule neurons against cell death caused by inhibition of the PI3K signalling pathway or potassium deprivation (Cross et al., 2001). Mechanistically, Gsk3 was found to control the Bax-mediated neuronal apoptosis (Linseman et al., 2004) and p53 mediated apoptosis (Pap and Cooper, 1998). In excitotoxicity, Akt is inactivated and therefore can no longer phosphorylate and inhibit Gsk3 $\alpha\beta$, allowing the active Gsk3 to initiate the pro-death signalling network (**Figure 5.7**). How neuronal Akt is inactivated in excitotoxicity is a topic of active investigation. Akt is inactivated by two major mechanisms: (i) dephosphorylation of the upstream activator second messenger PIP3 by the dual lipid and protein phosphatase PTEN (Maehama and Dixon, 1998; 1999), and (ii) dephosphorylation of Thr-308 and Ser-473 of Akt by the upstream phosphatases Protein Phosphatase 2A (PP2A) and PH domain and Leucine rich repeat Protein Phosphatase (PHLPP) (Jackson et al., 2010; Newton and Trotman, 2014).

Indeed, we found that PTEN exhibited a time dependent increase in nuclear translocation following glutamate-induced excitotoxicity (**Figure 5.7**). In agreement to our findings, other recent studies also demonstrated increased nuclear localisation in excitotoxicity (Zhang et al., 2013) and cerebral ischaemia (Howitt et al., 2012) but the exact role of nuclear translocation of PTEN in neuronal demise still needs further investigation.

Our phosphoproteomic data have provided further insights into the mechanism directs PTEN nuclear translocation induced by over-stimulation of the glutamate receptors in cultured primary neurons. Our analysis revealed a significant drop in phosphorylation of E3 ubiquitin-protein ligase NEDD4-like (Nedd4l or Nedd4-2) at Ser-477 4 h after glutamate treatment. The sequence around pSer-477 (IRRPRSLpSSPTVTL^SAPLEGAK) is very similar to the optimal phosphorylation sequence of Akt (RKRxRTYSFG, where S is the target phosphorylation site) (Obata et al., 2000). Indeed, Akt is known to directly phosphorylate Nedd4-2 (Lee et al., 2007). Our results show that Akt phosphorylation significantly decreased 4 h after glutamate treatment (**Figure 5.6**). Under normal physiological condition, Akt phosphorylates Ser-477 of Nedd4-2. One possible outcome of this phosphorylation event is binding of 14-3-3 protein to the phosphorylated Nedd4-2 to suppress its E3 ubiquitin ligase activity (Lee et al. 2007; Nagaki et al. 2006). Nedd4-2 is known to co-localise with PTEN by binding to the protein scaffold Ndfip1 and ubiquitinate PTEN at Lys-13 to direct its nuclear translocation. Since Akt activity is reduced in excitotoxicity, this may decrease the binding of 14-3-3 to Nedd4-2 to inhibit ubiquitination and nuclear translocation of PTEN. Relevant to this, we found that PTEN migration to the nucleus is significant at 4h and longer after the onset of glutamate induced excitotoxicity (**Figures 5.7 and 5.8**).

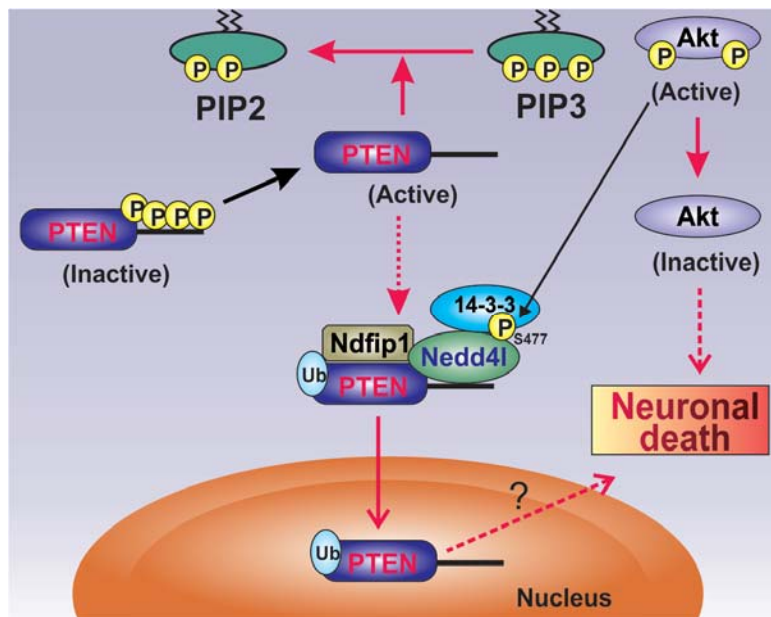


Figure 5.8 Postulated model for PTEN nuclear translocation and neuronal death in excitotoxicity. Under normal physiological condition, active Akt phosphorylates S477 of E3 ubiquitin-protein ligase NEDD4-like (Nedd41 or Nedd4-2) results in binding of 14-3-3 proteins and subsequent Nedd41 inactivation that no longer can ubiquitinate PTEN and PTEN reside mostly in the cytosol. However, following 4 h of glutamate treatment, Akt activity is significantly reduced that can no longer phosphorylate S477 of Nedd41 and also there is decrease in abundance of 14-3-3 isoforms. Nedd41 can bind to PTEN in the cytoplasm via Ndfip1 and monoubiquitinate PTEN at lysine 13 (K-13). PTEN then migrates to nucleus and leads to neuronal death via yet to be discovered mechanism.

Chapter 6

Declaration and acknowledgement

- ✚ Dr. Ching-Seng Ang, one of my co-supervisors provided help to run the proteomic samples in Orbitrap Elite mass spectrometer and to search Mascot with Xcalibur raw files to generate msf files. He also personally contributed to repeating the calpain dimethyl labelling and label-free MS1 quantitation experiments described in this chapter. I am responsible for generating and analysing rest of the data presented in this chapter.

- ✚ My colleague Daisy Lio helped me to transfect *Sf9* cells with pBacPAK9-nSrcH₆baculovirus expression vector to generate the baculovirus directing expression of the recombinant Src.

- ✚ My colleague Dr. M Aizuddin Kamaruddin synthesised the Tat-Src peptide used in antagonist/inhibitor experiments described in this chapter.

- ✚ Syeda S. Ameen provided help to synthesise the isotopically labelled synthetic phosphopeptide standards used for the label-free quantitation experiments.

Chapter 6: Quantitative proteomic analysis to define how the neurotoxic signalling events originating from the NMDAR interplay to direct neuronal death

6.1 Introduction

The type of intracellular signals emanating from the NMDA receptors is governed by the subunit composition of the receptors (Paoletti et al., 2013). The subunit composition of NMDA receptors varies with the subcellular locations. NMDA receptors containing the GluN2A subunits are found mostly in synapses while the GluN2B subunit-containing receptors are more prevalent in extrasynaptic locations (Charton et al., 1999; Lopez de Armentia et al., 2003). The C-terminal domain of the GluN2A and GluN2B subunits of the receptors contains structural determinants that govern the generation of neuroprotective and neurotoxic signals, respectively (Martel et al., 2012). Mounting evidence suggests that these two different types of NMDA receptors, upon stimulation, exert opposite effects on neuronal survival. Upon stimulation by glutamate, the synaptic NMDA receptors initiate neuroprotective signals while the extrasynaptic NMDA receptors trigger mitochondrial dysfunction and initiate neurotoxic signalling pathways that ultimately lead to neuronal death (Hardingham and Bading, 2010; Parsons and Raymond, 2014).

Ca²⁺ can enter the neurons via multiple routes and the route of Ca²⁺ entry into the cytosol of neurons is the major determinant of neuroprotective or neurotoxic signalling pathways. Sattler *et al.* demonstrated that entry of Ca²⁺ through the NMDA receptors but not voltage-dependent Ca²⁺ channels (VDCC) stimulates cell death cascade (Sattler et al., 1998). NMDA receptors are highly permeable to Ca²⁺ and over-stimulated GluN2B containing extrasynaptic NMDA receptors over-activate calpains (mainly calpain-2) and other cell death pathways (Bever and Neumar, 2008; Wang et al., 2013) (**Figure 6.1A**). The over-activated calpains catalyse limited proteolysis of a group of neuronal proteins and irreversibly modify their physiological functions leading to neuronal death (Hara and Snyder, 2007; Liu et al., 2008). While a number of neuronal proteins have been identified as calpain substrates, how proteolytic processing of these proteins by calpain affects neuronal survival remains unclear. Relevant to this, the previous study in our laboratory demonstrated that in neurons undergoing excitotoxic cell death, the over-activated calpains specifically cleave Src kinase in the unique domain to generate a truncated Src fragment (Src Δ N) (Hossain et al., 2013). Src Δ N then directs neuronal

death by selectively phosphorylating unknown neuronal protein substrates (Hossain et al., 2013).

In the previous study, a membrane-permeable TAT-fusion peptide derived from the Src unique domain (Gly₄₉ - Ala₇₉) (referred to as Tat-Src) (**Figure 6.1C**) was designed and found to be capable of blocking calpain cleavage of Src *in vitro* and *in situ* in cultured primary neurons undergoing excitotoxic cell death (Hossain et al., 2013). However, the exact calpain cleavage site and the mechanism by which Tat-Src inhibits calpain cleavage of Src remain unknown (Hossain et al., 2013). We postulate that the Src fragment in Tat-Src contains the calpain cleavage site and it functions as a competitive inhibitor to restrict calpain cleavage of Src. To further define the mechanism by which calpains aberrantly regulate Src, I aimed to identify the calpain cleavage site in Src. I employed two mass spectrometric approaches to achieve my goal. The first approach involves dimethyl labelling of the native Src and nascent N-terminus of the truncated Src fragment after *in vitro* calpain digestion. The second approach uses the label-free quantitation of selected tryptic peptides covering different domains in the sequences derived from both full-length and truncated Src to identify the calpain cleavage site in Src.

Further, to define how the neurotoxic signalling events originating from the over-activated NMDA receptors interplay to direct neuronal death, mass spectrometry based quantitative proteomic and phosphoproteomic analysis was performed. Experimentally, I used 3 inhibitors/antagonists in my studies; they include (i) Ifenprodil, a specific GluN2B-containing extrasynaptic NMDA receptor antagonist (Reynolds and Miller, 1989), (ii) calpeptin, a generic calpain inhibitor (Tsujioka et al., 1988) and (iii) Tat-Src, a peptide inhibitor that selectively blocks calpain cleavage of Src (Hossain et al., 2013). They were used to co-treat neurons with glutamate for 4 h before the neuronal lysates were subjected to quantitative proteomic and phosphoproteomic analysis (**Figure 6.1B**). These experiments allowed us to define the neurotoxic signals operating downstream of (i) Glu2B-containing extrasynaptic NMDA receptors (Ifenprodil) (ii) the over-activated calpain (calpeptin) or (iii) the neurotoxic truncated Src fragment (Src Δ N) (Tat-Src). Stable isotope dimethyl labelling approach was adopted to compare the proteomes and phosphoproteomes of control neurons, glutamate-treated neurons, and neurons co-treated with glutamate and one of the inhibitors/antagonist. TiO₂ micro-columns were used to enrich the phosphopeptides prior to analysis by LC-MS/MS. This chapter describes the findings of our analysis.

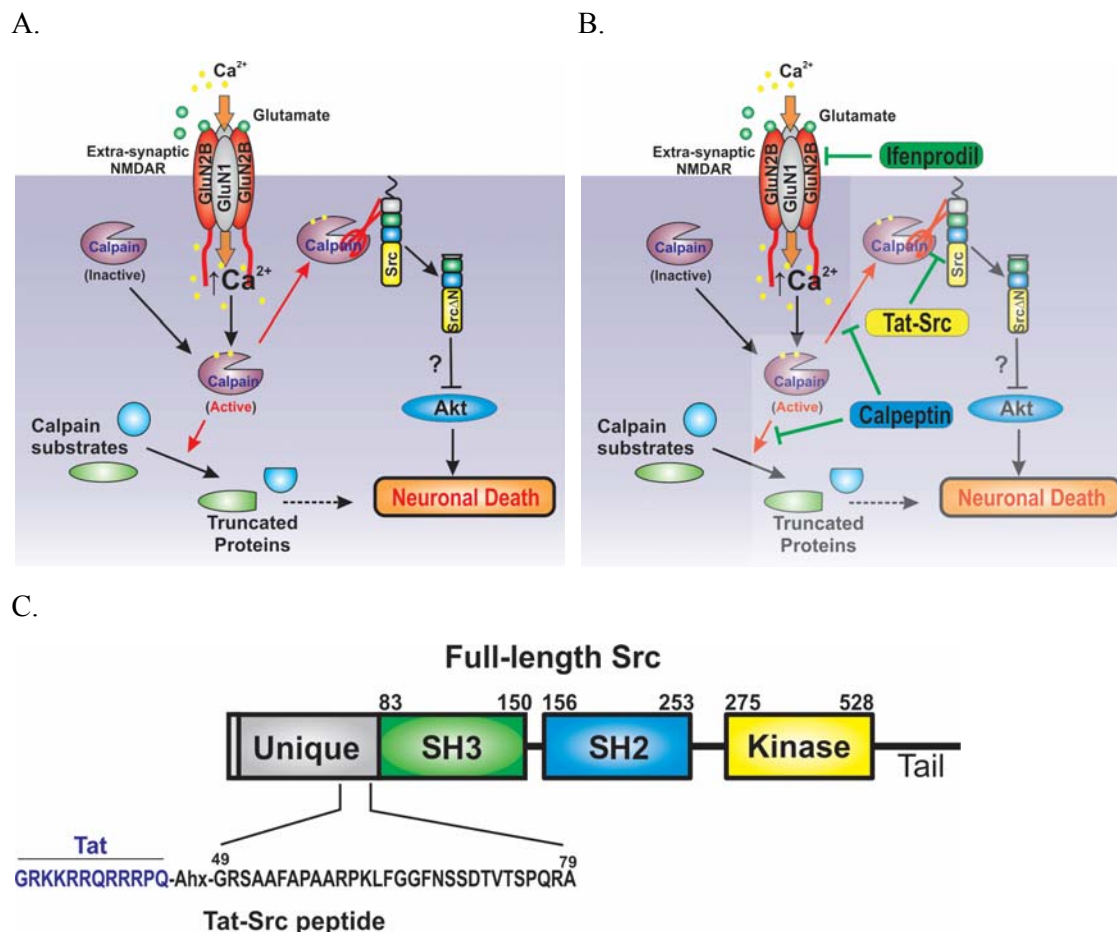


Figure 6.1 Selective inhibition of neurotoxic signals can rescue glutamate-induced excitotoxic neuronal death. **A.** Over-stimulation of GluN2B-containing extrasynaptic NMDA receptors allows a massive calcium influx inside the cell. Excess intracellular Ca^{2+} over-activates a number of enzymes including in them Ca^{2+} -dependent cysteine protease calpain. Active calpains initiate limited proteolysis of multiple neuronal proteins. Among them, Src tyrosine kinase is proteolysed to form truncated Src fragment (Src Δ N) that ultimately lead to neuronal death via several cell death mechanisms. **B.** Ifenprodil, a GluN2B receptor antagonist, can selectively block extrasynaptic NMDA receptors overstimulation and its downstream neurotoxic signals. Calpeptin is a cell-permeable pan-calpain inhibitor that inhibits calpain (both calpain 1 and calpain 2) activity and restricts neuronal death. Tat-Src is a cell-permeable fusion peptide derived from the Src unique domain (TAT-ahx-Src₄₉₋₇₉). It selectively blocks calpain cleavage of Src in excitotoxicity and in turn mitigates neuronal death by inhibiting neurotoxic signals that are downstream of Src Δ N. **C.** The sequence of Tat-Src peptide contains a membrane-permeable Tat sequence attached to the Src (G₄₉-A₇₉) sequence by a 6-aminohexanoic acid (Ahx) linker. The design and characterisation of Tat-ahx-Src₄₉₋₇₉ were presented in the manuscript by my colleagues (Hossain et al., 2013).

6.2 Methods

6.2.1 Expression and purification of recombinant full-length Src protein and *in vitro* calpain digestion of recombinant nSrcH₆ protein

To define the calpain cleavage site in Src unique domain, we utilised purified full-length Src protein for the *in vitro* calpain digestion experiment. Recombinant full-length Src with C-terminal 6 histidine residues (nSrcH₆) protein was expressed using Baculovirus-infected insect cell expression system, and purified using Ni²⁺-NTA column chromatography as described in section 2.2.14 of Chapter 2. Purified recombinant nSrcH₆ protein (1 µg) was digested *in vitro* with the calpain 1 (0.5 µg) in the calpain digestion buffer (50 mM Tris-HCl, pH 7.4, 2 mM DTT, 30 mM NaCl, 10 mM CaCl₂). The reaction mixtures were incubated at 25°C for different time intervals (2 min up to 2 h) and stopped by the addition of 4× SDS sample loading buffer, boiled at 95°C and was resolved in a 10% SDS-PAGE. The gel was stained with Coomassie brilliant blue and destained with 20% (v/v) methanol/10% (v/v) acetic acid solution and observed for truncated Src fragment.

6.2.2 Strategies for the calpain cleavage site determination

To determine the calpain cleavage site in Src unique domain, 2 strategies were followed after *in vitro* calpain digestion: (i) dimethyl labelling of the native Src and nascent N-terminus of the truncated Src fragment after calpain digestion and (ii) label-free quantitation of selected tryptic peptides covering the unique domain in Src sequence derived from both full-length and truncated nSrcH₆ generated by calpain cleavage *in vitro*. These procedural workflows are detailed below and outlined in **Figure 6.2**.

6.2.2.1 Dimethyl labelling of the nascent N-terminus of truncated nSrcH₆ generated by calpain cleavage of nSrcH₆ *in vitro*

After *in vitro* calpain digestion for 20 min, the reaction mixture was dimethyl labelled prior to resolving by SDS-PAGE. Deuterated formaldehyde (CD₂O) was used in the presence of sodium cyanoborohydride (NaBH₃CN) to label the free N-terminus generated by calpain cleavage. After labelling, the proteins in the mixture were separated by SDS-PAGE. This step enables us to visualise and isolate the truncated Src fragment and at the same time remove any residual formaldehyde. The gel was subsequently stained with Coomassie brilliant blue and

destained with 20% (v/v) methanol/10% (v/v) acetic acid solution. The truncated nSrcH₆ fragment was excised from the gel and subjected to in-gel tryptic digestion as described in section 2.2.16 of Chapter 2. The digested peptides were extracted and applied to the Orbitrap Elite mass spectrometer for LC/MS-MS analysis. The intact full-length recombinant nSrcH₆ is N-terminally blocked with its N-terminal residue covalently linked to the myristoyl group via the N^α-amino group. Thus, nSrcH₆ cannot react with CD₂O/NaBH₃CN at its N-terminus. In contrast, CD₂O/NaBH₃CN react with the nascent free N-terminus generated by calpain cleavage in the truncated Src fragment and for these reasons, only the tryptic fragment derived from the N-terminus of the truncated Src fragment would contain the dimethyl label at the N^α-amino group.

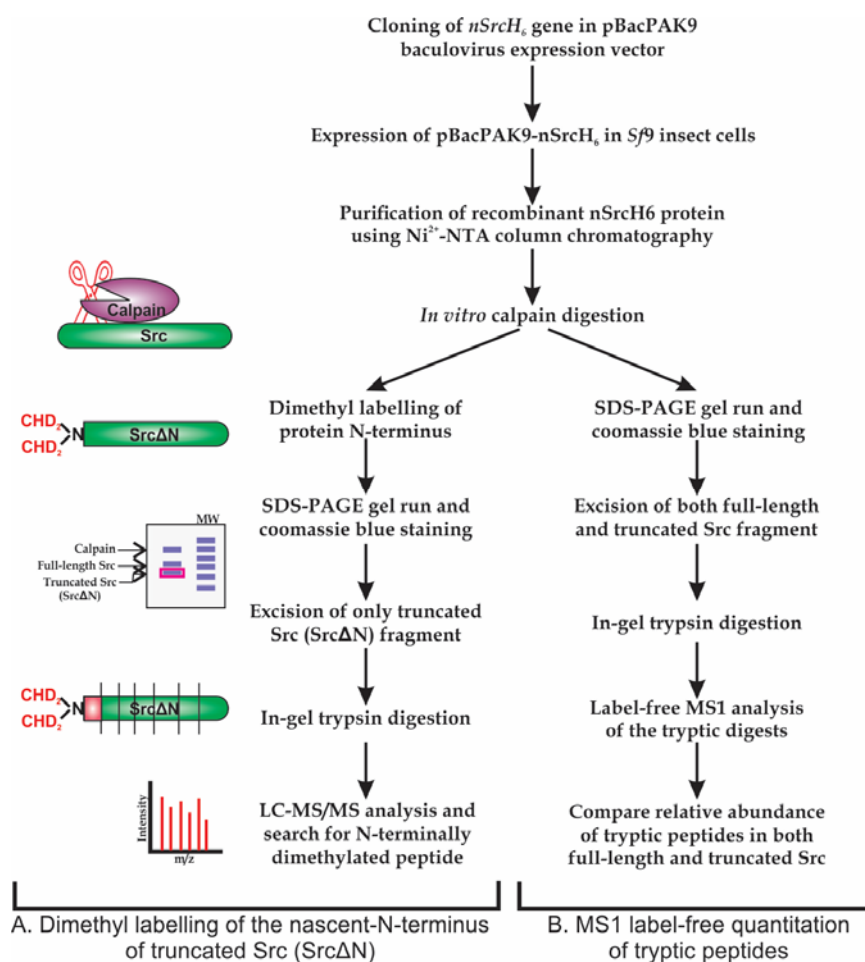


Figure 6.2 Workflow for calpain cleavage site determination. Dimethyl labelling (A) and label-free MS1 quantitation (B) methods were used for the determination of the calpain cleavage site in Src.

6.2.2.2 Label-free MS1 quantitation of the selected peptides in tryptic digest of full-length and truncated nSrcH₆

Recombinant nSrcH₆ was incubated with calpain *in vitro*. At timed intervals ranging from 2 to 120 min after the incubation, aliquots of the reaction mixture were removed and analysed by SDS-PAGE. The protein bands corresponding to full-length and truncated nSrcH₆ were excised and digested with trypsin before the digests were run for LC-MS/MS analysis. Since my colleagues in the previous study have mapped the site of calpain cleavage of Src to the unique domain (Hossain et al., 2013), specific peptide fragments derived from the unique domain of Src (listed in **Figure 6.5**) were selected for label-free MS1 quantitation. Two tryptic peptides mapped to other regions of the neuronal Src sequence were used as controls. The experiment was repeated three times before data analysis. Abundance of each peptide was determined from full scan mass spectral data (MS1) extracted ion chromatograms (XIC) as described by Schilling *et al.* in a previous study (Schilling et al., 2012).

6.2.3 Primary cortical neurons culture and MTT cell viability assay

Primary cortical neurons were cultured from the embryonic (E16) pups collected from the pregnant C57BL/6 mice as described earlier (section 2.2.1 of Chapter 2). At seventh days *in vitro* (DIV7), 100 μ M glutamate with or without Ifenprodil (20 μ M), calpeptin (20 μ M) and Tat-Src peptide (20 μ M) were added to the cultured neurons for 4 h. Following the treatments, neuronal viability was determined by the MTT cell viability assay as described in section 2.2.3 of Chapter 2.

6.2.4 Experimental design for the antagonist/inhibitor study

Figure 6.3 shows the workflow of the experiment to define the neurotoxic signalling networks that are downstream of the extrasynaptic NMDA receptors. At DIV7, cultured primary cortical neurons were treated with glutamate or other specific antagonists/inhibitors (Ifenprodil, calpeptin and Tat-Src peptide) in conjunction with glutamate for 4 h. Treated neurons were lysed with cold (4°C) RIPA buffer and proteins from the neuronal lysates were precipitated with freezer-cold acetone (-20°C). In-solution trypsin digestion and stable isotope dimethyl labelling experiments were performed as described earlier (section 2.2.6 and section 2.2.8 of Chapter 2). Tryptic peptides derived from the neuronal proteins in the control (untreated) cell

lysates were labelled with formaldehyde (CH₂O) and those from the treated neurons were labelled with deuterated formaldehyde (CD₂O) in the presence of sodium cyanoborohydride for the light and medium label, respectively. The labelled peptides were mixed (control: treatment = 1: 1) and a small aliquot (15 µl) of the mixture was analysed by LC-MS/MS to monitor the changes in global proteome of neurons before and after experimental treatments. The remaining mixed labelled peptides were cleaned up by SPE cartridges before enrichment of the phosphopeptides by TiO₂ micro-columns as described in section 2.2.7 and 2.2.9 of Chapter 2. The enriched phosphopeptides were analysed by LC-MS/MS for phosphoproteomic changes. This experiment was repeated for 6 times with six biological replicates for the 4 h glutamate only treatment group and 3 times with three biological replicates for the group with 4 h glutamate treatment in the presence of one of the three antagonist/inhibitors (Ifenprodil, calpeptin or Tat-Src).

6.2.5 Proteomic data analysis

Proteomic data were analysed by Proteome Discoverer (Thermo Scientific version 1.4) with the Mascot search engine against the Uniprot database as described in section 2.2.11 of Chapter 2.

6.2.6 Label-free quantitation using isotopically labelled synthetic phosphopeptide standards

Isotopically labelled synthetic phosphopeptides were used to confirm identity of the identified phosphopeptide (and phosphorylation site) and label-free quantitation. Four isotopically labelled synthetic phosphopeptides were synthesised (**Table 2.1** in Chapter 2) based on the findings of phosphoproteomic data analysis. My colleague Syeda S. Ameen synthesised those peptides as described in section 2.2.19 of Chapter 2. These phosphopeptides are identical to those of endogenous tryptic phosphopeptides from Mef2c, Mff, Mlf2 and Stmn1 identified in phosphoproteome analysis and contain a heavy (¹³C¹⁵N) amino acid, either Proline or Leucine in the sequence. They were synthesised by the Fmoc-based chemistry, purified by reverse phase HPLC and their identities were confirmed by ESI-MS analysis. In the label-free quantitation experiment, these synthetic phosphopeptide standards would elute with the endogenous phosphopeptides at the same HPLC retention time and would have similar fragmentation

efficiencies and patterns. The only difference is the extra mass of 6 Da from ^{13}C and ^{15}N atoms of the heavy amino acids that can be easily detected on the mass spectrometer.

Briefly, tryptic digests from the control and glutamate treatment derived neuronal lysates were purified by the SPE clean-up cartridges and freeze-dried overnight before the quantitation experiment. Tryptic digests from whole cell lysates were spiked with a known amount of synthetic isotopically labelled synthetic phosphopeptides with sequences identical to the endogenous phosphopeptides. The spiked samples were enriched for the phosphopeptides using TiO_2 micro-columns as described in section 2.2.9 of Chapter 2.

The enriched phosphopeptides were run on an LTQ Orbitrap Elite (Thermo Scientific) mass spectrometer coupled to an Ultimate 3000 RSLC nano system (Dionex) for LC-MS/MS analysis. The LC system was equipped with an Acclaim Pepmap nano-trap column (Dinoex-C₁₈, 100 Å, 75 µm x 2 cm) and an Acclaim Pepmap RSLC analytical column (Dinoex-C₁₈, 100 Å, 75 µm x 15 cm). The tryptic peptides were injected into the enrichment column isocratically with 3% (v/v) acetonitrile (ACN) containing 0.1% (v/v) formic acid at a flow rate of 5 µl/min for 5 min before the enrichment column was switched in-line with the analytical column. The elution buffers were 0.1% (v/v) formic acid (Solvent A) and 0.1% (v/v) formic acid in 100% ACN (Solvent B). The flow gradients were (i) 0-5min at 3% Solvent B, (ii) 5-65 min, 3-20% Solvent B, (iii) 65-75 min, 20-40% Solvent B, (iv) 75-80 min, 40-80% Solvent B, (v) 80-85 min, maintained at 80% and (vi) 85-86min, 80-3% Solvent B followed by equilibration for 6min at 3% Solvent B. The LTQ Orbitrap Elite spectrometer was operated in the data-dependent mode with nanoESI spray voltage of 1.8kV, capillary temperature of 250°C and S-lens RF value of 55%. All spectra were acquired in positive mode with full scan MS spectra scanning from m/z 300-1650 in the FT mode at 240,000 resolutions after accumulating to a target value of 1.0×10^6 . Lock mass of 445.120025 was used. The top 20 most intense precursors were subjected to collision induced dissociation (CID) with normalized collision energy of 30 and activation q of 0.25. Alternatively, for high energy collision (HCD), normalised collision energy of 35 and activation time of 0.1ms was used for the top 10 most intense precursors. Dynamic exclusion with of 45 sec was applied for repeated precursors.

6.2.6.1 Phosphoproteomic data analysis following label-free quantitation

Data analysis was carried out using Proteome Discoverer (Thermo Scientific version 1.4) with the Mascot search engine against the Uniprot database. Fixed modification was Carbamylation

of Cysteine (+57.021) and variable modifications were phospho-Serine/Threonine/Tyrosine (+79.966) and Heavy Proline or Leucine (+6.013). A false discovery rate threshold of 1% was applied and phosphopeptide identification was further validated with PhosphoRS 3.0 node in PD 1.4, requiring at least 95% confidence in the phosphorylated site (Taus et al., 2011). Quantitation was carried out using the Quantitation node from Proteome Discoverer, Xcalibur (Thermo Scientific 2.2) and Skyline (MacLean et al., 2010). Both the endogenous and heavy labelled synthetic peptides were identified by PD1.4 using MS2 spectra. For relative quantification, raw Xcalibur files were uploaded in the Skyline software. Peptide sequences were copied and appropriate modifications (e.g. position of phosphorylation and heavy amino acids) were selected in the peptide settings. In the transition settings, precursor ions with charges 2 and 3 were selected. Using full scan filter setting Skyline then generated the MS1 ion chromatograms (extracted ion chromatograms, XIC). Using automated peak integration, Skyline also generated peptide trees with three extracted molecular ion isotope peaks M, M+1, and M+2, corresponding retention times obtained from each MS acquisition are also shown in the peptide tree. From the results grid, areas under the curve for light (endogenous) and heavy (synthetic) peptides are counted for control and glutamate treated lysates and relative phosphorylation changes were calculated.

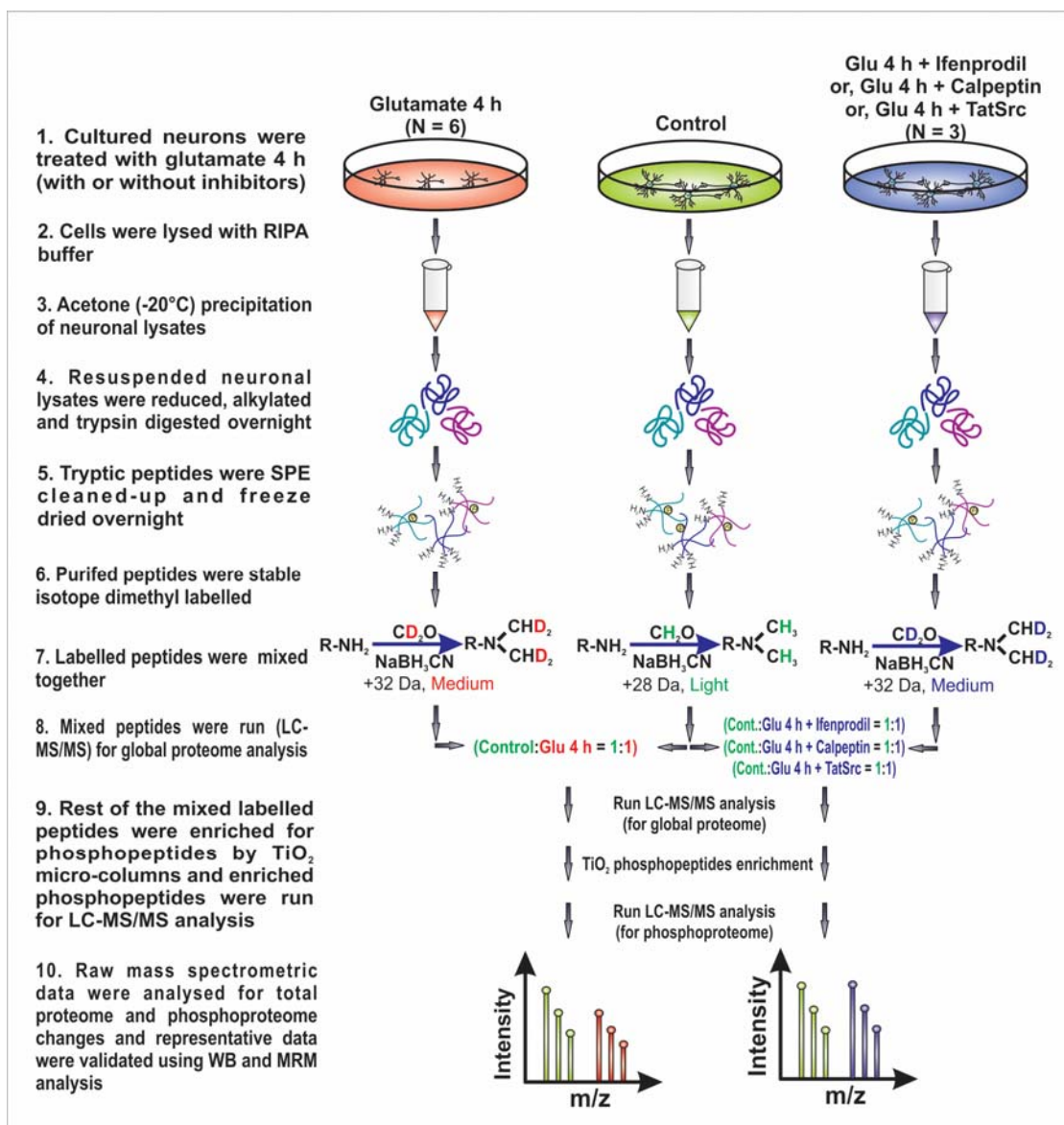


Figure 6.3 Workflow to define the neurotoxic signalling networks downstream of the extrasynaptic NMDAR by quantitative proteomic and phosphoproteomic analysis. At seventh day *in vitro* (DIV7), cultured primary cortical neurons were treated with glutamate for 4 h in the presence or absence of Ifenprodil, calpeptin and Tat-Src. In-solution trypsin digestion and subsequent stable isotope dimethyl labelling approach was followed for the relative quantitative proteomic and phosphoproteomic analysis. Comparison analysis identifies the neurotoxic signals (significant changes in abundance of neuronal proteins or changes in phosphorylation of neuronal phosphoproteins) that are originated from the Glu2B-containing extrasynaptic NMDA receptors, calpains over-activation or Src Δ N generation.

6.3 Results

6.3.1 Identification of the calpain cleavage site in Src unique domain

Previous study results from our lab indicated that the 52-kDa Src fragment generated by limited proteolysis by calpain contains the intact SH3, SH2, kinase domains and the C-terminal tail but lacks the N-terminal segment containing fatty acid acylation motif and unique domain (Hossain et al., 2013). To clearly define the calpain cleavage site in Src unique domain, I needed to generate sufficient amount of purified recombinant neuronal Src to determine the N-terminal amino acid sequence of the truncated Src fragment. To this end, I generated recombinant baculovirus expressing recombinant neuronal Src (referred to as nSrcH₆) with a linker (Gly-Ser-Gly-Ser) and a 6×His-tag at the C-terminus. We then adopted two proteomic approaches as described in section 6.2.2 to determine the calpain cleavage site in nSrcH₆ after calpain treatment.

6.3.1.1 Generation of recombinant full-length Src protein

Recombinant nSrcH₆ was generated by the procedure described in section 2.2.14 in Chapter 2. Expressed protein in the crude cell lysate was purified using Ni-NTA column chromatography and its purity and authenticity were confirmed by Western blot, SDS-PAGE and mass spectrometric analysis. Three different primary antibodies, namely anti-Src 327 (that recognise SH3 domain of Src), anti-Src antibody from epitomics (that recognises full-length c-Src by interacting with a segment in the N-terminal unique domain of Src) and anti-His tag antibody to detect C-terminus of the expressed protein were used to identify the expressed full-length protein (**Figure 6.4B**). Again this protein was run on SDS-PAGE gel, and after Coomassie staining the full-length Src band was excised from the gel. In-gel trypsin digestion method was carried out before the tryptic peptides were extracted and subjected to LC-MS/MS analysis. We determined the sequence coverage of our proteomic dataset and found a high degree of sequence coverage (80%) for mouse neuronal Src protein (**Figure 6.4C**). In addition, tryptic peptides were identified from all the domains (**Figure 6.4C**). These results suggest that the generated purified nSrcH₆ was intact and therefore suitable for use to determine the calpain cleavage site.

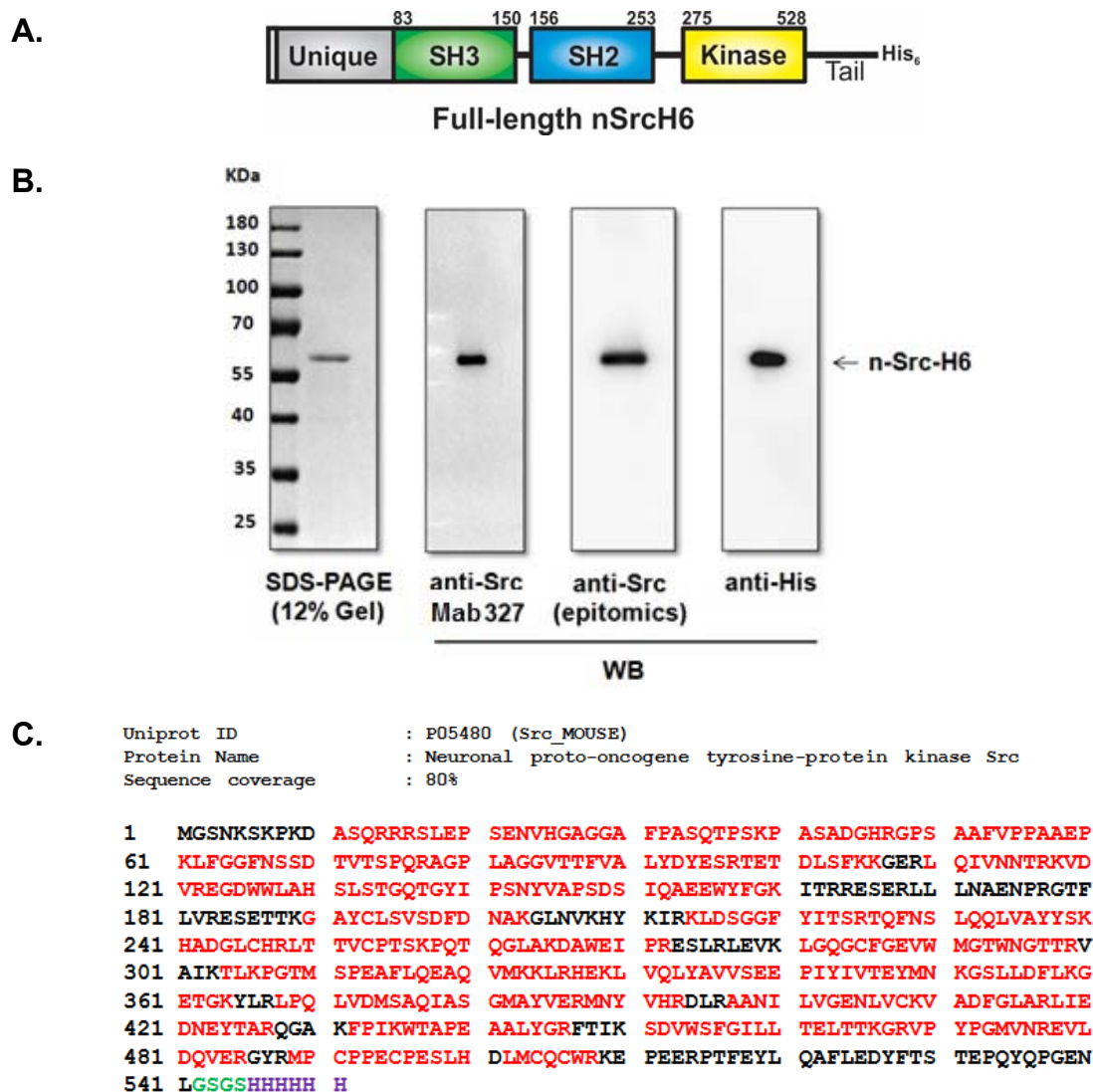


Figure 6.4 Expression of recombinant full-length neuronal Src (nSrcH6) protein. Recombinant nSrcH₆ (C-terminally His-tagged) protein was expressed in baculovirus-infected *Sf9* insect cell expression system. The expressed protein in the crude cell lysate was purified with Ni²⁺-NTA column chromatography. **A.** Schematic representation of full-length nSrcH₆. **B.** SDS-PAGE and Western Blot analysis of the purified nSrcH₆ protein preparation using the mouse Mab327 anti-Src, the rabbit Mab anti-Src from epitomics and anti-poly His antibodies. **C.** Mass spectrometric sequencing data confirming the authenticity of the purified full-length recombinant nSrcH₆. Identified peptide sequences are in red.

6.3.1.2 Dimethyl labelling approach to identify N-terminus of the truncated Src fragment

Following *in vitro* calpain digestion of recombinant nSrcH₆, protein mixture was dimethyl labelled with deuterated formaldehyde (CD₂O) in the presence of NaBH₃CN as described in section 6.2.2.1. Alpha-amino group of the nascent N-terminus of the newly formed truncated nSrcH₆ was converted to dimethylamine and also gave rise to a 32 Da mass increase that can be detected by the mass spectrometer. After labelling protein mixture was resolved in a SDS-PAGE. In-gel tryptic digestion of the truncated Src fragment and subsequent LC-MS/MS analysis identified the peptide containing the deuterated dimethyl moiety at the N-terminus. This peptide identification procedure revealed Gly-64 as the nascent N-terminus of truncated nSrcH₆ generated by calpain treatment *in vitro* (**Figure 6.5A**). This result was further confirmed using the label-free MS1 quantitation approach (**Figures 6.5C** and **6.5E**) described in the next section.

6.3.1.3 Label-free time course MS1 quantitation of selected peptides derived from target regions of nSrcH₆ and its truncated fragment

The idea of label-free quantitation of the tryptic fragments derived from full-length and truncated nSrcH₆ is to monitor unique peptides present only in full-length nSrcH₆ but not in truncated nSrcH₆. Calpain was allowed to digest recombinant Src for 2 min to 120 min *in vitro* in calpain digestion buffer. Proteins in the digestion mixtures were separated by SDS-PAGE and stained with Coomassie-blue (**Figure 6.5D**). Both full-length and truncated nSrcH₆ bands were excised from the gel and digested with trypsin. The resultant tryptic and semi-tryptic peptides were identified by their accurate molecular mass (i.e. no MS/MS fragmentation) and the isotopic dot product as described by Schilling *et al.* in a previous study (Schilling *et al.*, 2012). Four trypsin derived fragments (referred to as peptides I to IV) derived from the unique domain of the Src sequence were selected for the quantitative analysis (**Figure 6.5C**). It was evident that out of 4 fragments selected (**Figure 6.5C**) peptide I and II were most abundant in the digest of full-length Src (**Figure 6.5E**). However, peptide III with Gly-64 as the N-terminal residue and is two amino acids shorter than peptide II, was present only in the digest of truncated nSrcH₆. The abundance of peptide II was highest in the truncated nSrcH₆ generated after 20-40 min treatment with calpain. In addition to peptide II, peptide IV with Thr-87 as the N-terminal amino acid is also present in the tryptic digest of truncated nSrcH₆. Since the residue located immediately at the N-terminal side of Thr-87 is Thr-86, which is not a basic amino acid

residue targeted by trypsin, calpain rather than trypsin is likely the protease catalysing cleavage of the Thr-86/Thr-87 peptide bond. **Figure 6.5E** shows that the abundance of peptide IV is highest 2 min after incubation with calpain and its abundance decreased to a negligible level at 90 min after calpain treatment even though detectable amount of truncated nSrcH₆ was still present. This data suggests that calpain cleaves full-length nSrcH₆ at the Phe-63/Gly-64 and Thr-86/Thr-87 peptide bonds. However, its efficiency of cleaving the Thr-86/Thr-87 was significantly decreased after the Phe-63/Gly-64 bond has been cleaved (**Figures 6.5E** and **6.5C**).

Taken together, results obtained in this study with both approaches indicate that the Phe-63/Gly-64 peptide bond in the unique domain of Src is a major calpain cleavage site. Additionally, the data shown in **Figure 6.5E** suggests that Thr-86/Thr-87 bond is also a calpain cleavage site. Since the amount of peptide IV dropped steadily to a negligible level at 90 min after calpain treatment (**Figure 6.5E**), the Thr-86/Thr-87 appears to be is only a minor cleavage site of calpain and is dependent on the integrity of the full length Src protein. In agreement with this notion, the dimethyl labelled tryptic fragments with Thr-87 as the N-terminal residue was not detectable in the tryptic digests of the dimethyl labelled truncated nSrcH₆; further confirming that Thr-86/Thr-87 peptide bond is a minor calpain cleavage site of Src.

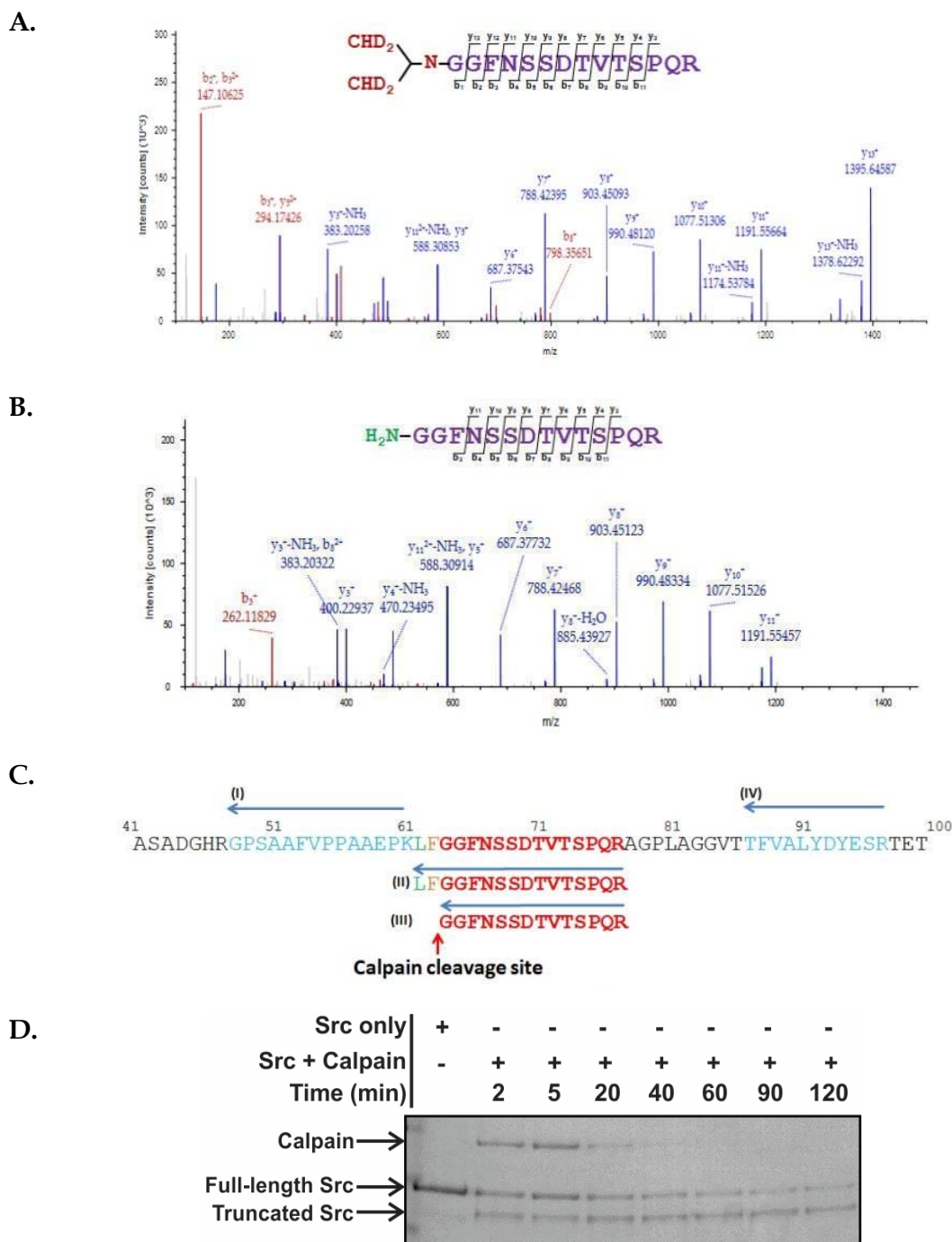


Figure 6.5

E.

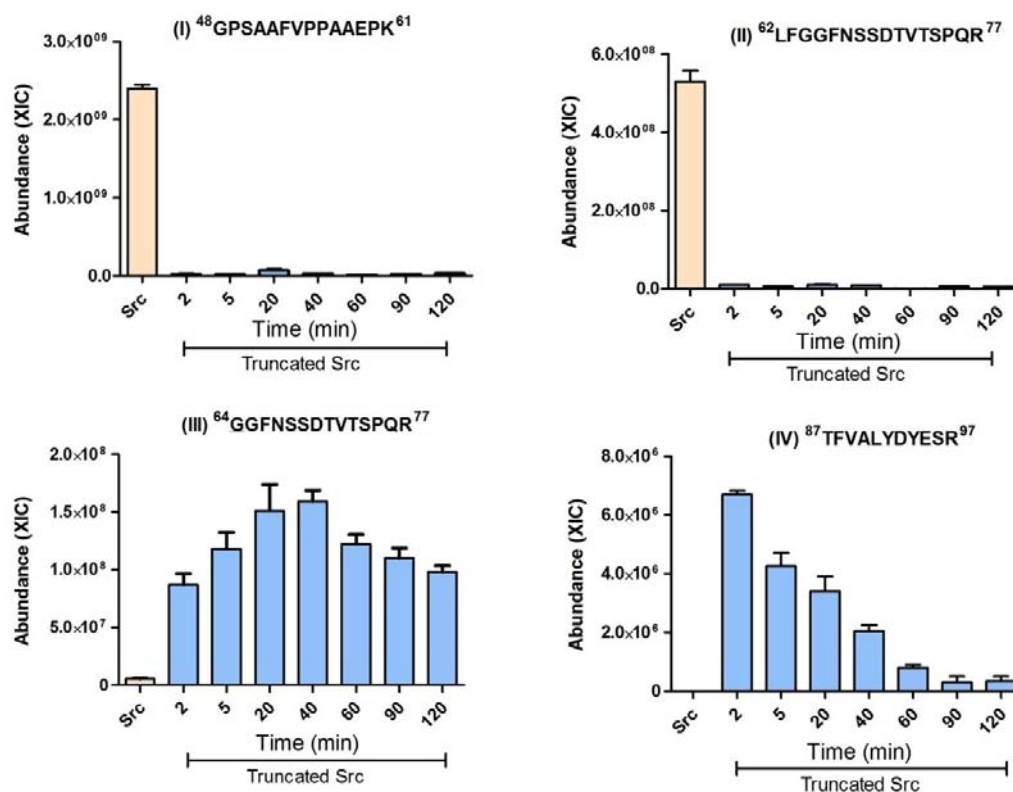


Figure 6.5 Determination of calpain cleavage site in Src unique domain. Identification of the newly formed N-terminal peptide generated by calpain cleavage of nSrcH₆ using N-terminal dimethyl labelling approach. **A.** MS/MS spectrum of the newly formed peptide containing the N-terminally labelled deuterated dimethyl moiety. **B.** MS/MS spectrum of the same unlabelled peptide. **C.** Four peptide fragments mapped to the unique domain of Src were selected for MS1 extracted ion chromatogram (XIC) analysis to determine their abundance in the digests of full-length and truncated nSrcH₆ generated at different time points after calpain treatment. **D.** Coomassie blue-stained gel showing the time course of changes of both nSrcH₆ and its truncated fragment generated by calpain cleavage used for quantitation. **E.** Quantitation of the time-dependent changes in abundance of the selected peptides using the label-free MS1-quantitation method (n = 3). Note the presence of peptides I and II exclusively in tryptic digest of full-length nSrcH₆ but not in that of truncated nSrcH₆.

6.3.2 Selective inhibition of the extrasynaptic GluN2B receptors, calpain over-activation, or neurotoxic Src Δ N generation can protect neurons against excitotoxic cell death

Before the proteomic and phosphoproteomic analysis, MTT assay was performed to check the viability of the cultured neurons following glutamate (100 μ M) treatment for 4 h in the presence or absence of Ifenprodil, calpeptin or Tat-Src. At DIV7, glutamate treatment for 4 h reduced neuronal viability. Co-treatment of the antagonists/inhibitors (Ifenprodil, calpeptin or Tat-Src) with glutamate for 4 h mitigates the neurotoxic effect of glutamate to a significant extent (**Figure 6.6**). Thus, the same conditions were used for subsequent proteomic and phosphoproteomic analyses to define the neurotoxic signals that are operating downstream of the extrasynaptic NMDA receptors, calpain and the Src Δ N generated by calpain cleavage.

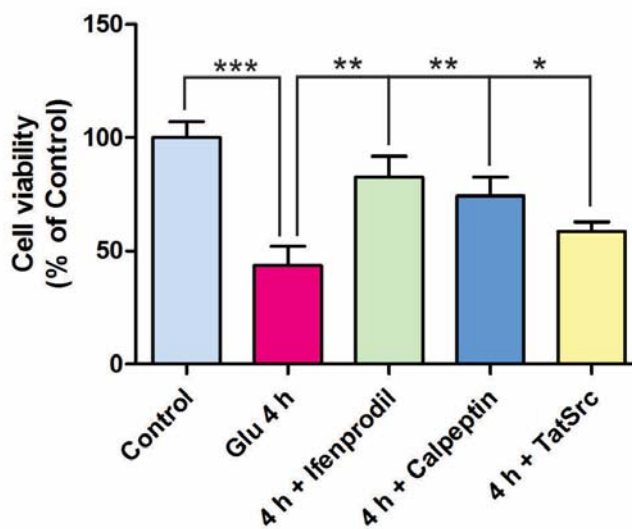


Figure 6.6 Ifenprodil, calpeptin and Tat-Src can reduce glutamate-induced excitotoxic neuronal death. At seventh days in culture, glutamate (100 μ M) treatment for 4 h significantly reduced neuronal viability. Co-treatment of Ifenprodil (20 μ M), calpeptin (20 μ M) or Tat-Src (20 μ M) with glutamate for 4 h significantly reduced neuronal death. Data are presented as mean \pm SD, * p < 0.05, ** p < 0.01 and *** p < 0.001, Student's t-test, n = 3.

6.3.3 Identification of neuronal proteins showing significant changes in abundance due to the over-activation of GluN2B receptors, calpains or SrcΔN generation

To identify neuronal proteins showing significant changes in abundance due to over-activation of the extrasynaptic GluN2B-containing NMDA receptors in excitotoxicity, global quantitative proteomic analysis was performed using neuronal lysates after treatment with glutamate (100 μ M) in the presence or absence of Ifenprodil (20 μ M) for 4 h as described in section 6.2.4. Proteomic data were processed and analysed as reported in section 4.3.2 of Chapter 4. Briefly, proteomic data analysis was carried out using Proteome Discoverer 1.4 (PD 1.4) to search Mascot against the Uniprot database. All identified peptides were above the identity threshold score, which represents a confidence level of $p < 0.05$. The inbuilt quantitation node on PD 1.4 allows us to measure the relative abundance of the identified peptides (medium/light ratios) and corresponding protein group based on the extracted ion chromatogram (XIC) intensities from the MS1 scans. Results were filtered with high peptide confidence to reflect a maximum of 1% false discovery rate (FDR). For relative protein quantification, peptide ratios [(medium/light i.e. glutamate 4 h/control and (glutamate 4 h + Ifenprodil)/control)] were calculated from the isotopic clusters for the identified peptides in both light and medium quantification (quan) channels or from a single isotopic cluster identified in either of the quan channels (light and/or medium) using the accurate mass feature of the mass spectrometer (< 2 ppm) to define the corresponding light or medium labelled peptide. For peptide ratios with either a heavy or light missing quantification channel were avoided to minimise protein quantitation error. To facilitate further analysis, an MS Excel file was exported from PD with protein group accession numbers, protein names, coverage, peptides, unique peptides, PSMs (peptide spectrum matches), areas, average median medium/light ratios etc. Using the MS Excel file, the exported data for 4 h glutamate ($n = 6$) and 4 h glutamate + Ifenprodil ($n = 3$) treatment from all biological replicates were analysed by considering the average median medium/light ratios of the identified proteins and by calculating the mean and standard deviations. These ratios reflect the relative abundance of the identified proteins in the study condition i.e. a medium to light ratio of 0.50 for a particular protein in 4 h glutamate/control indicates an ~ 2 -fold decrease in expression at 4 h of glutamate treatment; a medium to light ratio of 1.00 for the same protein in (4 h glutamate + Ifenprodil)/control indicates that the glutamate-induced decrease in expression for this protein was offset by Ifenprodil co-treatment. These results suggest that the decrease in abundance of this protein was a consequence of over-activation of the extrasynaptic GluN2B-containing NMDA receptors; Ifenprodil was able to

block the downstream signals that lead to the decrease in expression for this protein. Using GraphPad Prism 6.0 software multiple t-tests were performed for all the identified proteins in 4 h of glutamate and 4 h glutamate + Ifenprodil treatments. The analysis takes into consideration their average medium/light ratios, standard deviations (SD) and number of times (n) they were identified in the biological replicates. At least 12 protein molecules showed significant differences ($p \leq 0.05$) in their average medium/light ratios after 4 h of glutamate treatment in the presence and absence of Ifenprodil (**Table 6.1**). All of them showed decrease in expression after 4 h of glutamate treatment, and co-treatment with Ifenprodil significantly offset the perturbation to their expression induced by glutamate treatment (**Table 6.1** and **Figure 6.7**).

Proteomic data obtained from neurons co-treated with glutamate and calpeptin or Tat-Src were also processed in a similar way as described above. A selected list of proteins that show significant differences in expression due to calpain over-activation and/or generation of Src Δ N in glutamate-induced excitotoxicity are listed in **Table 6.1** and shown in **Figure 6.7**.

Table 6.1 A selected list of neuronal protein molecules of which the changes in abundance induced by glutamate treatment are fully or partially offset by co-treatment with Ifenprodil, calpeptin or Tat-Src.

S/L	Protein group accession	Gene	Protein name	Σ# Unique peptides	Σ# PSMs	4 h (N=6)			4 h + Ifenprodil (N=3)				4 h + Calpeptin (N=3)				4 h + TatSrc (N=3)			
						Medium/L ight	SD	n	Medium/L ight	SD	n	p-value	Medium/L ight	SD	n	p-value	Medium/L ight	SD	n	p-value
1	C0IQA7_MOUSE	4930544G1 1Rik	Transforming protein RhoA	1	76	0.431	0.217	5	0.682	0.232	3	0.220	0.824	0.052	3	0.024	0.625	0.306	3	0.330
2	F6UFG6_MOUSE	Anp32a	Acidic leucine-rich nuclear phosphoprotein 32 family member A	2	38	0.694	0.407	5	1.040	0.380	3	0.132	1.225	0.368	3	0.030	1.216	0.320	3	0.035
3	DC1L1_MOUSE	Dync1i1	Cytoplasmic dynein 1 light intermediate chain 1	5	65	0.700	0.045	4	1.064	0.398	3	0.029	1.215	0.657	3	0.308	1.466	0.429	2	0.015
4	B1AXZ0_MOUSE	Elavl2	ELAV-like protein 2	3	37	0.547	0.205	5	1.788	0.184	2	0.012	1.237	0.246	3	0.007	0.804	0.083	3	0.128
5	B8JK33_MOUSE	Hnrnpm	Heterogeneous nuclear ribonucleoprotein M	4	50	0.614	0.094	5	0.926	0.193	3	0.019	1.082	0.153	2	0.003	0.843	0.174	3	0.048
6	Q3TVV6_MOUSE	Hnrnpu	Heterogeneous nuclear ribonucleoprotein U	1	140	0.575	0.080	5	0.852	0.084	3	0.006	0.913	0.057	3	0.002	0.761	0.082	3	0.030
7	Q45VK5_MOUSE	Ilf3	Interleukin enhancer-binding factor 3	3	22	0.580	0.085	2	1.399	-	1	-	0.953	0.017	2	0.026	1.185	-	1	-
8	Q3URJ7_MOUSE	Map2	Microtubule-associated protein 2	18	306	0.431	0.251	6	1.041	0.302	3	0.018	1.113	0.507	3	0.024	0.743	0.226	3	0.126
9	MATR3_MOUSE	Matr3	Matrin-3	9	246	0.616	0.109	6	0.886	0.054	3	0.007	0.803	0.116	3	0.051	0.739	0.125	3	0.168
10	D3YWF6_MOUSE	Otub1	Ubiquitin thioesterase	2	35	0.563	0.213	5	0.877	0.018	2	0.106	1.243	0.340	3	0.016	0.829	0.179	3	0.122
11	F8WJ30_MOUSE	Pfdn2	Prefoldin subunit 2	1	21	0.224	0.036	3	0.360	0.018	2	0.009	0.404	0.181	3	0.142	0.368	0.042	2	0.027
12	H7BWX1_MOUSE	Pfdn5	Prefoldin subunit 5	1	37	0.711	0.261	5	0.842	0.179	3	0.480	1.200	0.240	3	0.039	0.759	0.228	2	0.830
13	PRS4_MOUSE	Psmc1	Proteasome 26S subunit ATPase 1	3	30	0.535	0.154	5	0.975	0.354	3	0.043	0.848	0.090	2	0.045	0.669	0.107	2	0.354
14	Q3UQN3_MOUSE	Rad23b	UV excision repair protein RAD23 homolog B	4	92	0.753	0.258	6	1.067	0.457	3	0.316	1.319	0.162	3	0.039	1.016	0.161	3	0.104
15	RS27A_MOUSE	Rps27a	Ubiquitin-40S ribosomal protein S27a	4	61	0.666	0.091	6	0.921	0.028	3	0.002	0.786	0.125	3	0.119	0.698	0.128	3	0.620
16	G3UYV7_MOUSE	Rps28	40S ribosomal protein S28	2	47	0.460	0.287	6	1.006	0.337	3	0.038	1.078	0.393	3	0.037	1.092	0.315	3	0.025
17	Q8BUM1_MOUSE	Tardbp	TAR DNA-binding protein 43	3	136	0.534	0.151	6	0.973	0.240	3	0.007	0.943	0.017	3	0.003	0.725	0.091	3	0.102
18	Q80ZV2_MOUSE	Tubb5	Tubulin beta-5 chain	2	550	0.599	0.156	6	0.874	0.092	3	0.026	1.083	0.562	3	0.056	0.742	0.131	3	0.202

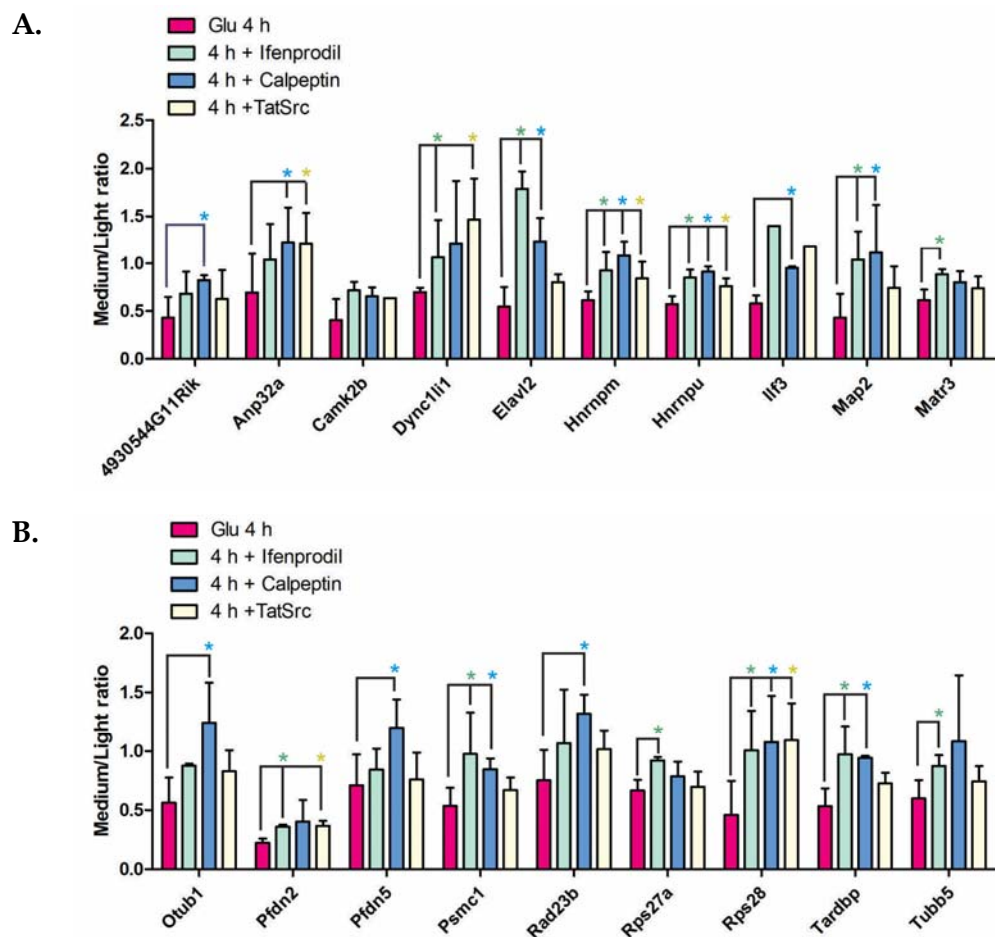


Figure 6.7 Identification of neuronal proteins that function downstream of the GluN2B-containing extrasynaptic NMDA receptors in glutamate-induced excitotoxicity. At day *in vitro* 7 (DIV7), cultured neurons were treated with glutamate for 4 h in presence or absence of Ifenprodil, calpeptin or Tat-Src. Quantitative global proteomic analysis was performed using neuronal lysates derived from these treated and untreated control neurons. Antagonist/inhibitors co-treatments with glutamate for 4 h identified a number of neuronal proteins of which the perturbations of expression levels were offset completely or partially by the antagonist and/or the two inhibitors. These proteins are likely neuronal proteins that exhibit decreased expression due to over-activation of the extrasynaptic GluN2B-containing NMDA receptors, calpain activation or truncated Src (Src Δ N) generation in glutamate-induced excitotoxicity (A&B). Data are presented as average medium/light ratios \pm SD of the identified neuronal proteins, $n = 6$ for 4 h of glutamate and $n = 3$ for 4 h glutamate + Ifenprodil/calpeptin/Tat-Src, Multiple t-tests, $*p \leq 0.05$.

6.3.4 Identification of neuronal phosphoproteins showing significant changes in phosphorylation due to over-stimulation of GluN2B receptors, over-activation of calpains or Src Δ N generation

To identify neuronal phosphoproteins showing significant changes in phosphorylation due to the over-activation of the extrasynaptic GluN2B-containing NMDA receptors in excitotoxicity, global relative quantitative phosphoproteomic analysis was performed using neuronal lysates after 4 h treatment with glutamate (100 μ M) in the presence or absence of Ifenprodil (20 μ M) as described in section 6.2.4. Proteomic data were processed and analysed as reported in section 5.3.1 of Chapter 5. Briefly, proteomic data analysis was carried out using Proteome Discoverer 1.4 (PD 1.4) to search Mascot against the Uniprot database. All identified peptides were above the identity threshold score, which represents a confidence level of $p < 0.05$. The inbuilt quantitation node on PD 1.4 allows us to measure the relative phosphorylation changes (medium/light ratios) based on the extracted ion chromatogram (XIC) intensities from the MS1 scans. Phosphosite identification probability was further calculated with the PhosphoRS 3.0 node in PD 1.4. Results were filtered with high peptide confidence to reflect a maximum of 1% false discovery rate (FDR). For phosphopeptide quantification, peptide ratio was calculated from the isotopic clusters for the identified peptide in both light and medium quantification (quan) channels or from a single isotopic cluster identified in either of the quan channels (light and/or medium) using the accurate mass feature of the mass spectrometer (< 2 ppm) to define the corresponding light or medium labelled peptide. For phosphopeptide ratios with any missing quantification channel, values were replaced with a minimum intensity (maximum and minimum fold change = 100 and 0.01, respectively). To facilitate further analysis, an MS Excel file was exported from PD with phosphopeptide sequences, modifications, phosphosite probabilities, protein group accession numbers, protein names, coverage, peptides, unique peptides, PSMs (peptide spectrum matches), areas, average median medium/light ratios, precursor ions, retention time and details of all the identified phosphopeptides. Using the MS Excel file, the exported data for 4 h glutamate treatment ($n = 6$) and 4 h glutamate + Ifenprodil co-treatment ($n = 3$) from all biological replicates were analysed taking in consideration the average median medium/light ratios of the identified phosphopeptides and calculating the mean and standard deviations. These ratios reflect the relative phosphorylation changes of the identified phosphopeptides in the chosen studied condition. For example, a medium to light ratio (glutamate treatment/control) of 0.50 for a particular phosphopeptide indicates an~2-fold

decrease in phosphorylation at the identified phosphorylation site at 4 h after glutamate treatment. A medium to light ratio of 1.00 for the same phosphopeptide in 4 h glutamate + Ifenprodil co-treatment versus control indicates that the glutamate-induced decrease in phosphorylation was offset by blocking the over-stimulation of the extrasynaptic GluN2B-containing NMDA receptors. This finding would imply that the protein phosphatase(s) and/or protein kinase(s) targeting the phosphorylation site(s) in the identified neuronal protein are operating downstream of the neurotoxic GluN2B-containing NMDA receptors. Using GraphPad Prism 6.0 software multiple t-tests were performed for all the identified phosphopeptides in the 4 h of glutamate and 4 h glutamate + Ifenprodil co-treatment data sets. The analysis takes into consideration their average medium/light ratios, standard deviations (SD) and number of times (n) they were identified in the biological replicates to trace out the downstream signals of GluN2B receptors that lead to increase or decrease in phosphorylation of the identified phosphopeptides. A list of phosphopeptides showing significant differences ($p \leq 0.05$) in changes in phosphorylation after 4 h of glutamate treatment in presence and absence of Ifenprodil are listed in **Table 6.2**. All of identified phosphopeptides showed a decrease in phosphorylation after 4 h of glutamate treatment and co-treatment with Ifenprodil significantly offset the changes in phosphorylation induced by the glutamate treatment (**Table 6.2** and **Figure 6.8**).

Likewise, phosphoproteomic data derived from neurons co-treated with glutamate and calpeptin or Tat-Src were also processed in a similar way as described above. **Table 6.2** and **Figure 6.8** show the phosphopeptides of which their glutamate treatment-induced perturbation was offset by co-treatment with Ifenprodil, calpeptin or Tat-Src.

Table 6.2 A selected list of phosphopeptides of which the changes in phosphorylation induced by glutamate treatment are fully or partially offset by co-treatment with Ifenprodil, calpeptin or Tat-Src.

S/L	Accession	Gene	Protein name	Phosphopeptide sequence	Phosphosite	Glu 4 h (N=6)			4 h + Ifenprodil (N=3)				4 h + Calpeptin (N=3)				4 h + TatSrc (N=3)			
						Medium/Light	SD	n	Medium/Light	SD	n	p-value	Medium/Light	SD	n	p-value	Medium/Light	SD	n	p-value
1	B1APX2_MOUSE	5031439G07Rik	Protein 5031439G07Rik	VTSFpSTPPPpTPER	S289/T293	0.211	0.203	3	0.838	0.007	2	0.026	0.533	0.019	2	0.124	0.395	0.268	2	0.440
2	Q3UH26_MOUSE	Apba1	Amyloid beta (A4) precursor protein-binding, family A, member 1	SAPSTEpSGFHNHTDTAEGDVLAAAR	S84/S87	0.368	0.106	3	0.790	0.107	3	0.008	0.715	0.148	3	0.030	0.418	0.277	2	0.782
3	Q5U612_MOUSE	Arhgap35	Rho GTPase activating protein 35	TSFSVGPpSDELGPIR	S1179	0.190	0.164	5	0.722	0.318	2	0.026	0.627	0.087	3	0.006	0.455	0.177	3	0.075
4	Q6PAT3_MOUSE	Arhgap39	Rho GTPase activating protein 39	AFpSEDEALAQQDSK	S597	0.011	0.001	2	0.865	-	1	-	0.632	0.054	2	0.004	0.525	-	1	-
5	H7BX26_MOUSE	Cep170	Centrosomal protein 170kDa	LGEApSDESELADADK	S1102	0.049	0.053	2	-	-	-	-	0.575	0.091	2	0.019	0.460	-	1	-
6	Q3URG0_MOUSE	Cnksr2	Connector enhancer of kinase suppressor of Ras 2	GSEpSPNSFLDQEYR	S390	0.135	0.141	3	0.670	0.034	2	0.015	-	-	-	-	0.316	0.223	2	0.334
7	Q3TXY0_MOUSE	Crmp1	Collapsin response mediator protein 1	NLHQSNFSLpSGAQIDNNPR	S542	0.663	0.034	3	0.437	0.048	2	0.008	0.950	0.105	3	0.011	0.847	0.285	3	0.329
8	Q8CBH9_MOUSE	Csnk1e	Casein kinase 1, epsilon	LAApSQTpSPVDFHLGK	S405/S408	0.317	0.276	3	1.070	0.021	2	0.035	-	-	-	-	0.530	0.255	2	0.451
9	B7ZNF6_MOUSE	Ctnd2	Catenin (cadherin-associated protein), delta 2	GGpSPLTTTQGpSPTK	S264/S273	0.345	0.249	5	0.927	0.347	3	0.032	0.604	0.099	3	0.146	0.541	0.250	3	0.324
10				GGSPLTTTQGpSPTK	S273	0.201	0.212	6	0.721	-	1	-	0.755	0.093	2	0.014	0.531	0.261	3	0.078
11	Q3TV22_MOUSE	Cxadr	Coxsackie virus and adenovirus receptor	APQpSPTLAPAK	S332	0.194	0.228	6	0.726	0.264	3	0.016	0.478	0.009	2	0.146	0.421	0.267	3	0.222
12	F7CPL2_MOUSE	Dnb1	Drebrin 1	LSpSPVLHR	S142	0.117	0.111	2	0.946	0.055	2	0.011	0.442	0.013	2	0.054	-	-	-	-
13	Q1EDH1_MOUSE	Dclk1	Doublecortin-like kinase 1	ISQHGpSSTpSLSSTK	S352/S355	0.178	0.230	5	0.953	0.135	2	0.008	0.630	0.099	2	0.050	0.489	0.346	3	0.171
14	Q3UR88_MOUSE	G3bp1	GTPase activating protein (SH3 domain) binding protein 1	STpSPADVAPAQEDLR	S231	0.318	0.205	5	0.865	0.372	3	0.033	0.527	0.048	3	0.142	0.490	0.172	3	0.272
15	Q5F258_MOUSE	Git1	G protein-coupled receptor kinase interacting ArfGAP 1	SLSpSPTDNLELSAR	S371	0.332	0.172	6	0.918	0.130	3	0.001	0.709	0.107	3	0.011	0.552	0.182	3	0.119
16	D3Z7E5_MOUSE	Gsk3a1	Glycogen synthase kinase 3 alpha	TSpSFAEPGGGGGGGGGGGGGSA SGPGGTGGGK	S21	0.481	0.493	4	-	-	-	-	0.720	-	1	-	-	-	-	-
17	A2AL13_MOUSE	Hnrnpa3	Heterogeneous nuclear ribonucleoprotein A3	SSGpSPYGGGYGSGGGGGYGS R	S359	0.480	0.200	5	1.046	0.073	2	0.014	1.086	-	1	-	0.913	-	1	-
18	D3YXZ3_MOUSE	Klc2	Kinesin light chain 2	ASpSLNFLNK	S575	0.401	0.230	4	1.025	0.147	3	0.010	0.809	0.125	3	0.041	0.713	0.354	3	0.213
19	Q8CGB7_MOUSE	Limch1	LIM and calponin homology domains 1	TSVPESIASAGTgpSPSK	S523	0.230	0.161	4	0.685	0.157	2	0.031	0.439	0.106	3	0.112	0.384	0.223	3	0.334
20	B2RQQ5_MOUSE	Map1b	Microtubule-associated protein 1B	SVpSPGVTAQVVEEHCApSPEEK	S1293/S1307	0.329	0.137	3	0.791	0.006	2	0.020	0.486	0.029	3	0.124	0.362	0.183	3	0.813
21				TLEVvpSPSQSVTGSAGHTPYQQS PTDEK	S1317	0.140	0.135	3	1.636	-	1	-	-	-	-	-	1.639	0.018	2	0.001
22				ESpSPLYpSPGFSDSTSAAK	S1789/S1793	0.301	0.347	6	1.347	0.108	2	0.007	0.829	0.334	3	0.067	0.746	0.682	2	0.244
23	Q80X35_MOUSE	Map2	Microtubule-associated protein 2	VDHGAEITQpSPSR	S1782	0.157	0.143	6	0.628	0.149	3	0.002	0.538	0.089	3	0.004	0.454	0.121	3	0.018

Table 6.2 (continued)

S/L	Accession	Gene	Protein name	Phosphopeptide sequence	Phosphosite	Glu 4 h (N=6)			4 h + Ifenprodil (N=3)				4 h + Calpeptin (N=3)				4 h + TatSrc (N=3)			
						Medium/Light	SD	n	Medium/Light	SD	n	p-value	Medium/Light	SD	n	p-value	Medium/Light	SD	n	p-value
24				TPGpTPGpTPSYPR	T1620/T1623	0.268	0.275	6	0.764	0.063	3	0.020	0.833	0.189	3	0.016	0.718	0.202	3	0.042
25	E9PWC0_MOUSE	Map4	Microtubule-associated protein 4	ATpSPSTLVSTGPSSR	S785	0.264	0.246	6	1.090	0.281	3	0.003	0.757	0.154	2	0.041	0.602	0.240	3	0.091
26	D3YWH6_MOUSE	Mapk8ip3	C-Jun-amino-terminal kinase-interacting protein 3	TGSpSPTQGVNK	S366	0.496	0.154	6	0.777	0.234	3	0.064	0.762	0.092	3	0.031	0.600	0.173	3	0.387
27	Q3V1B5_MOUSE	Mef2c [#]	Myocyte enhancer factor 2C	NpSPGLLVSPGNLNK	S222	0.177	0.289	3	0.870	0.197	2	0.063	0.340	-	1	-	0.327	0.316	2	0.621
28	F7BC60_MOUSE	Mff [#]	Mitochondrial fission factor	NDpSIVTPSPPPQAR	S146	0.496	0.685	4	0.585	-	1	-	0.921	-	1	-	0.860	-	1	-
29	MLF2_MOUSE	Mlf2 [#]	Myeloid leukemia factor 2	LAIQGPEDpSPSR	S237	0.321	0.249	5	0.757	0.211	3	0.045	0.705	0.111	3	0.049	0.651	0.216	3	0.108
30	G3X9H8_MOUSE	Nedd4l	E3 ubiquitin-protein ligase NEDD4-like	SLpSSPTVLSAPLEGAK	S477	0.137	0.079	2	1.000	-	1	-	-	-	-	-	-	-	-	-
31	B8QI35_MOUSE	Ppfia3	Protein tyrosine phosphatase, receptor type, f polypeptide (PTPRF), interacting protein (liprin), alpha 3	QAQpSPGGVSSEVEVLK	S142	0.408	0.114	4	0.980	0.022	2	0.003	0.775	0.155	2	0.028	0.542	0.210	3	0.320
32	Q5DTJ4_MOUSE	Prrc2a	Proline-rich coiled-coil 2A	ETPPGGNLpSPAPR	S1002	0.246	0.279	5	1.118	0.143	2	0.010	0.824	0.065	2	0.040	0.683	0.084	2	0.093
33	E9PUC5_MOUSE	Psd3	Pleckstrin and Sec7 domain containing 3	SHpSPpSLNPDASPVTAK	S1000/S1001/S1009	0.135	0.155	6	0.816	0.152	3	0.000	0.496	0.071	3	0.007	0.372	0.230	3	0.104
34				SHpSSPSLNPdapSPVTAK	S1000/S1009	0.319	0.260	6	0.985	0.050	3	0.004	0.857	0.190	3	0.016	0.674	0.320	3	0.115
35				ISNpSSEFSAK	S44 (rat)	0.241	0.220	6	0.867	0.145	3	0.003	0.637	0.120	3	0.025	0.495	0.274	3	0.172
36	A2B112_MOUSE	Psip1	PC4 and SFRS1 interacting protein 1	NLAKPGVTSTpSDpSEDEDDQEGEK	S272/S274	0.243	0.290	4	0.916	0.417	3	0.052	0.731	0.105	3	0.041	-	-	-	-
37	Q8BU35_MOUSE	Rbm25	RNA binding motif protein 25	LGASnpSPGQPNSVK	S672	0.290	0.216	5	0.846	0.064	2	0.019	0.655	0.077	3	0.034	0.537	0.172	3	0.147
38	Q3TWS4_MOUSE	Snap91	Synaptosomal-associated protein, 91kDa	SSPATTVTpSPNSTPAK	S313	0.219	0.141	5	0.777	0.267	3	0.007	0.641	0.217	3	0.015	0.595	0.263	2	0.048
39	B1AQX6_MOUSE	Srcin1	SRC kinase signaling inhibitor 1	DSGSSSVFAEpSPGGK	S588	0.214	0.136	6	0.658	0.300	2	0.021	0.539	0.022	3	0.005	0.447	0.119	3	0.040
40	D3Z1Z8_MOUSE	Stmn1 [#]	Stathmin 1	ESVPDFPLpSPPK	S38	0.416	0.427	6	1.619	0.658	2	0.021	0.758	0.224	3	0.243	0.786	0.334	3	0.234
41	Q547J4_MOUSE	Mapt	Microtubule-associated protein tau	SGYSpSPGSPGTPGSR	S491	0.261	0.217	6	0.627	0.005	2	0.064	0.666	0.047	3	0.017	0.576	0.212	3	0.077
42				SGYSSpGpSPGTPGSR	S494	0.412	0.269	6	1.213	0.255	3	0.004	0.884	0.318	3	0.051	0.775	0.354	3	0.127
43				IGpSLDNITHVPGGGNK	S648	0.398	0.286	4	0.961	0.207	3	0.035	0.919	0.130	3	0.035	0.755	0.297	3	0.169
44	Q8CA33_MOUSE	Trim2	Tripartite motif containing 2	SADVpSPTTEGVK	S428	0.490	0.183	5	0.915	0.131	2	0.033	0.736	0.062	3	0.071	0.665	0.158	3	0.220
45	Q3UG49_MOUSE	Trp53bp1	Tumor suppressor p53-binding protein 1	SEDRPpSPQVSVAAVETK	S262	0.255	0.211	6	0.821	0.131	3	0.004	0.669	0.096	3	0.016	0.510	0.248	3	0.148

This table is arranged with gene names in an ascending order. Data are presented as average median medium to light (M/L) ratios of the phosphopeptides and standard deviations (SD). Multiple t-tests (two-tailed) were performed using GraphPad Prism 6 software for Glutamate 4 h vs Glu 4 h + Ifenprodil / Glu 4 h + Calpeptin / Glu 4 h + Tat-Source and significant *p*-values (≤ 0.05) are in **red**. Gene names for the validated phosphoprotein molecules are in **bold**.

*Western blot analysis confirmed that Gsk3 α (Ser-21/9) dephosphorylation is a downstream result of GluN2B receptor over-activation i.e. the changes in phosphorylation can be offset by the co-treatment with Ifenprodil.

[#]Label-free quantitation experiments confirmed that Mef2c (S222), Mff (S146) and Mlf2 (S237) dephosphorylation is a result of the over-stimulated GluN2B receptor signals i.e. co-treatment of Ifenprodil with glutamate can offset the changes in phosphorylation induced by glutamate excitotoxicity.

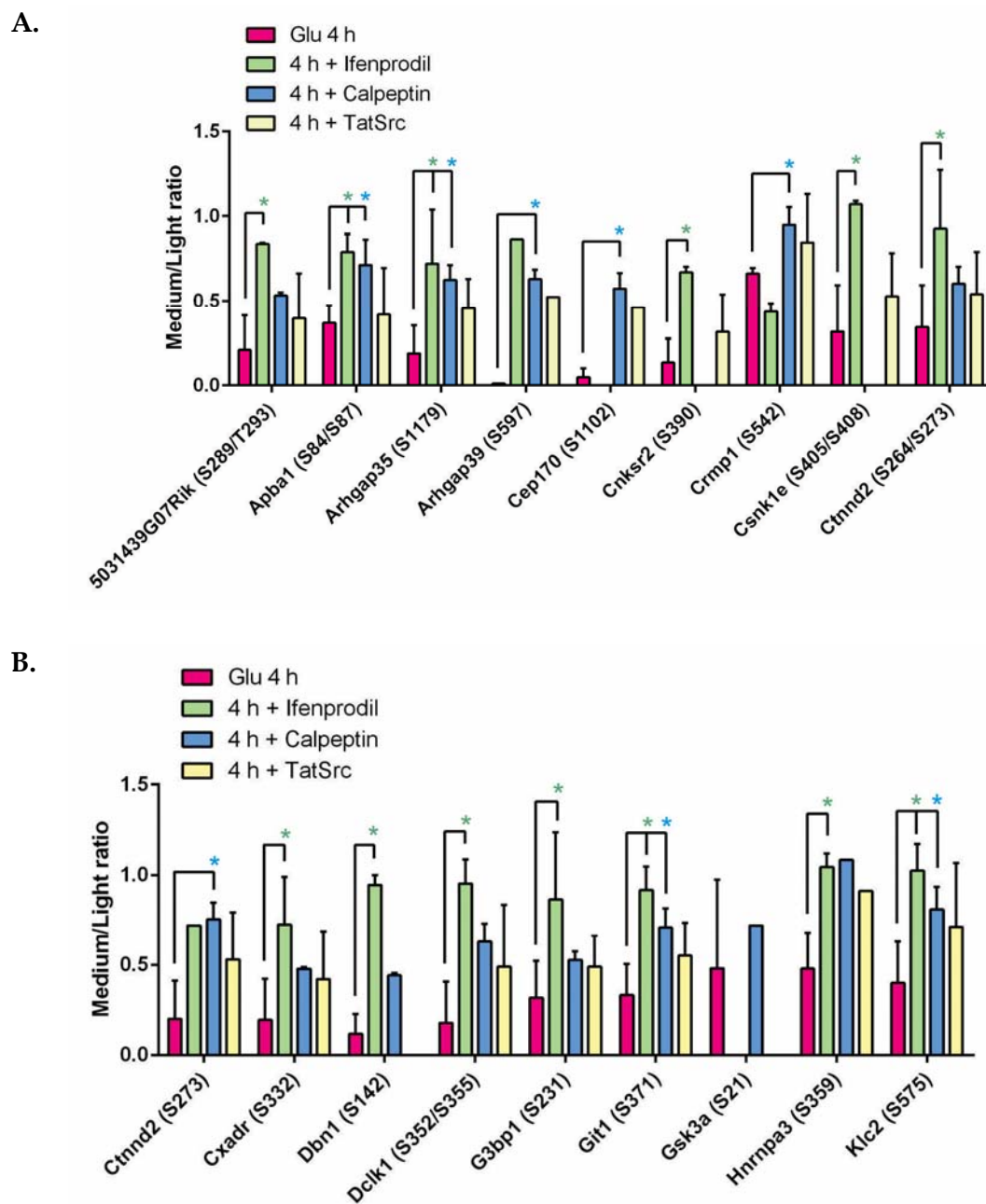


Figure 6.8

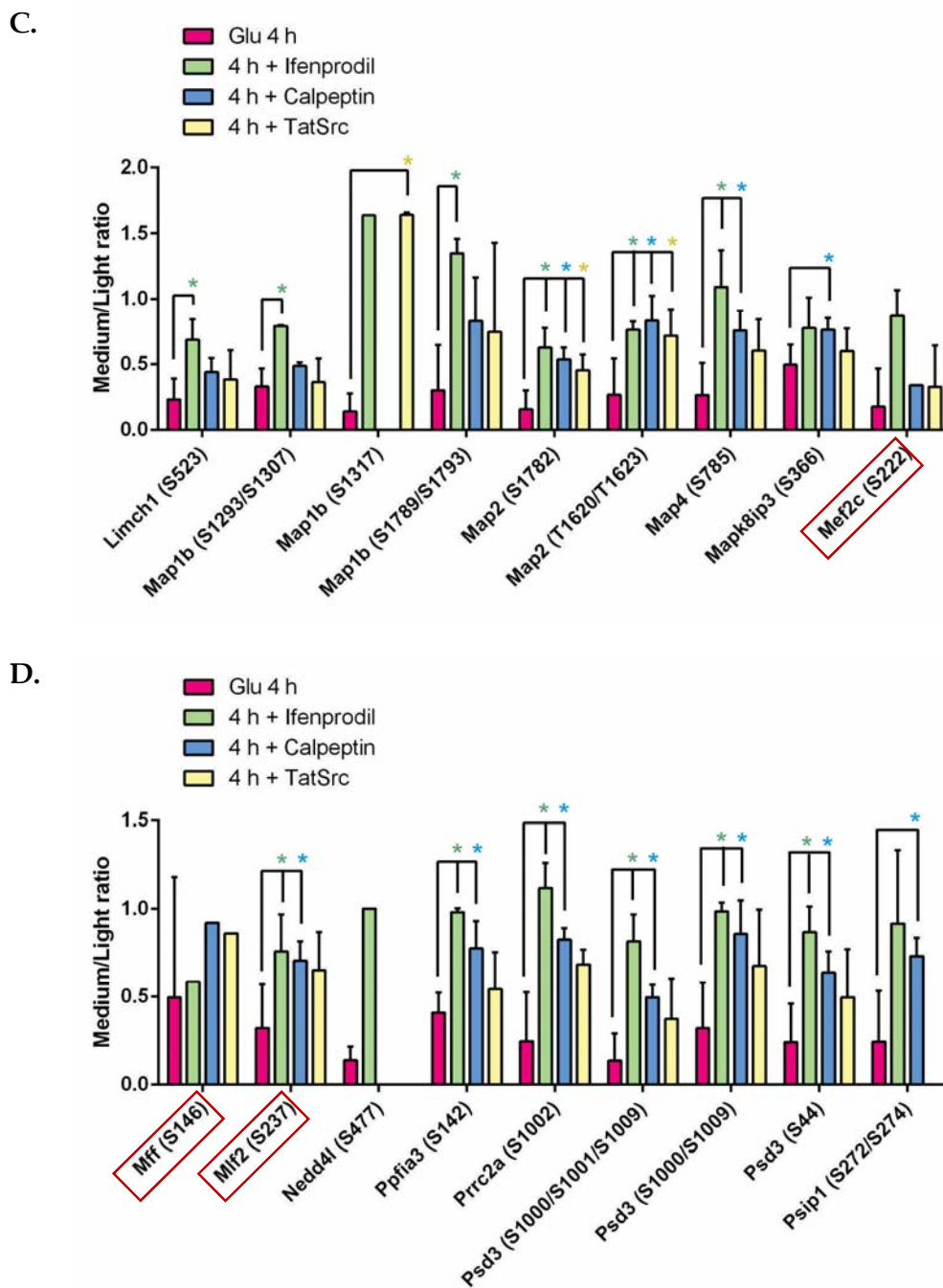


Figure 6.8

E.

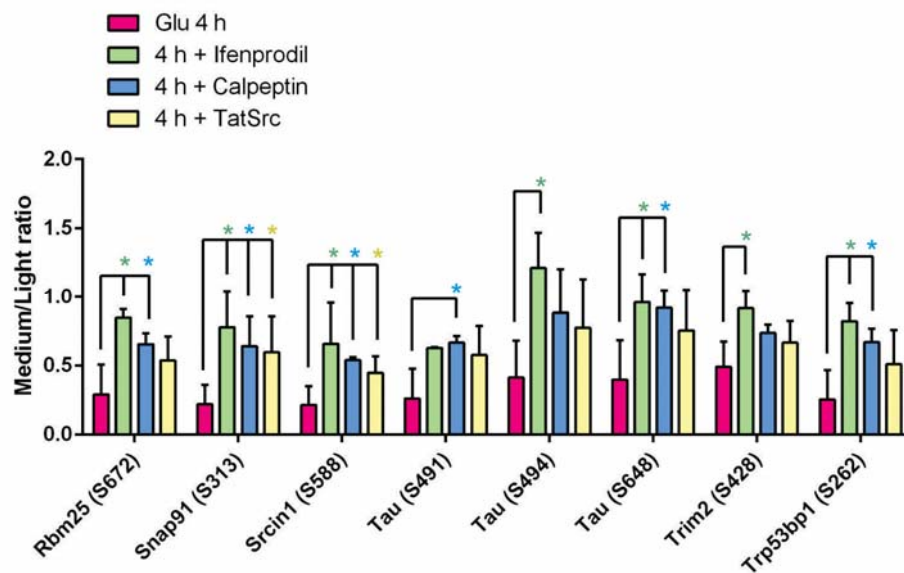


Figure 6.8 Identification of neuronal phosphoproteins that function downstream of the GluN2B-containing extrasynaptic NMDA receptors in glutamate-induced excitotoxicity. At day *in vitro* 7 (DIV7), cultured neurons were treated with glutamate for 4 h in presence or absence of Ifenprodil, calpeptin or Tat-Src. Quantitative phosphoproteomic analysis was performed using neuronal lysates derived from these treated and untreated control neurons. All of identified phosphopeptides showed a decrease in phosphorylation after 4 h of glutamate treatment and co-treatment with Ifenprodil, calpeptin or Tat-Src significantly offset the changes in phosphorylation induced by the glutamate treatment (**A**, **B**, **C**, **D&E**). Decreased phosphorylation of Mef2c (S222), Mff (S146) and Mlf2 (S237) [boxed (□) indicated] were confirmed by label-free quantitation method using synthetic phosphopeptide standards (described in section 6.3.6). Data are presented as average medium/light ratios \pm SD of the identified neuronal phosphoproteins with corresponding phosphorylation sites, $n = 6$ for 4 h of glutamate and $n = 3$ for 4 h glutamate + Ifenprodil/calpeptin/Tat-Src, Multiple t-tests, $*p \leq 0.05$.

6.3.5 Western blot analysis to confirm that enhanced dephosphorylation of Ser-21 and Ser-9 of Gsk3 α and Gsk3 β , respectively occurs as a result of over-stimulation of the GluN2B-containing NMDA receptors

Phosphoproteomic data of Gsk3 α phosphopeptide showed decreased phosphorylation at Ser-21 after 4 h of glutamate treatment (**Table 6.2**). Western blot analysis previously confirmed significant decrease in Ser-21 phosphorylation of Gsk3 α , which is an Akt phosphorylation site, at 4 h after glutamate treatment (**Figure 5.6**, Chapter 5). This phosphopeptide was identified from only one biological sample in phosphoproteome data after inhibitors/antagonist co-treatment with a medium to light ratio of 0.720 compare to 0.481 (average) for 4 h of glutamate treatment (**Table 6.2**). I therefore adopted another approach to ascertain if dephosphorylation of Gsk3 $\alpha\beta$ occurs as a consequence of over-stimulation of the extrasynaptic NMDA receptors. Western blot analysis confirmed that dephosphorylation of Gsk3 $\alpha\beta$ indeed occurred as a cellular event downstream of the GluN2B-containing extrasynaptic NMDA receptor signals (**Figure 6.9**). Treatment of the cultured neurons with cytotoxic level of glutamate (100 μ M) for 4 h in presence of Ifenprodil significantly offset the dephosphorylation of Ser-21 of Gsk3 α and Ser-9 of Gsk3 β induced by glutamate treatment (**Figure 6.9**). Relevant to this, Ifenprodil also offset Akt inactivation induced by glutamate treatment (**Figure 6.9**). These results confirm that over-stimulation of the GluN2B-containing extrasynaptic NMDA receptors contributes to inactivation of Akt and in turn downregulates its pro-survival activity. Gsk3 α and Gsk3 β are inactivated by phosphorylation of Ser-21 and Ser-9, respectively. The decrease in their phosphorylation likely contributes to their activation. Since Gsk3 α and Gsk3 β are neurotoxic kinases, their aberrant activation likely contributes to neuronal demise in glutamate-induced excitotoxicity.

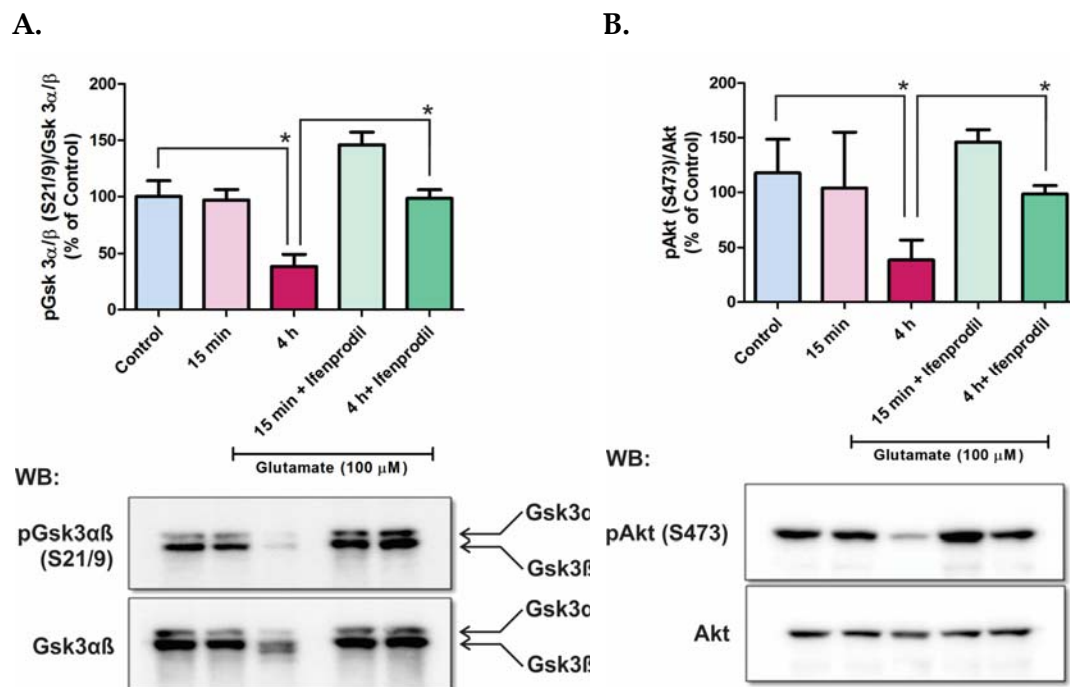


Figure 6.9 Blocking of the extrasynaptic NMDA receptor over-stimulation reduces dephosphorylation of Gsk3 α/β . At seventh days in culture (DIV7), cultured primary neurons were treated with cytotoxic level of glutamate (100 μ M). Glutamate treatment for 4 h significantly decreased phosphorylation of Ser-21 or Ser-9 of Gsk3 α and Gsk3 β , respectively. Co-treatment with Ifenprodil significantly offset dephosphorylation of Gsk3 α/β and its upstream kinase Akt. Data are presented as mean \pm SD, n = 3, * p < 0.05.

6.3.6 Label-free quantitation to confirm changes in phosphorylation of Mef2c, Mff, Mlf2 and Stmn1 induced by overstimulation of the GluN2B-containing extrasynaptic NMDA receptors

While changes in phosphorylation of Gsk3 $\alpha\beta$ and Akt can readily be monitored by Western blotting using phosphospecific antibodies, changes in phosphorylation of most of the targets listed in **Table 6.2** cannot be confirmed by Western blotting because of the lack of phosphospecific antibodies against these proteins. For example, phosphoproteomic analysis revealed decreased phosphorylation of Ser-222 of Mef2c, Ser-146 of Mff and Ser-237 of Mlf2 in glutamate-induced excitotoxicity (**Table 5.1** and **Table 6.2**). Since phosphospecific antibodies for these sites are not available, validation of the changes of these identified phosphorylation sites in these proteins was carried out using the label-free quantitation approach. This approach entails the use of isotopically labelled synthetic phosphopeptides (heavy) that correspond to the endogenous identified phosphopeptides (non-dimethyl labelled). The label-free quantitation method (as described in section 6.2.6) was then used to monitor the changes in phosphorylation levels of these proteins. The synthetic phosphopeptides NpSPGLLVSPGNLNK of Mef2c, NDpSIVTPSPPQAR of Mff, LAIQGPEDpSPSR of Mlf2 and ESVPDFPLpSPPK of Stmn1 (Ser-38 of Stmn1) contain either a heavy Proline or Leucine ($^{13}\text{C}^{15}\text{N}$) near the C-terminus (underlined). These peptide standards and the phosphopeptides derived from the endogenous neuronal proteins elute at the same HPLC retention time, have similar fragmentation efficiencies and patterns. The only difference is the extra mass of 6 Da of the heavy peptide standards, which can be easily differentiated from the endogenous phosphopeptides derived from the endogenous neuronal proteins by mass spectrometry. The label-free quantitation approach consists of four steps. First, equal amount of neuronal lysates from the untreated (control) and treatment (glutamate for 15 min and 4 h in presence or absence of Ifenprodil) experiments were digested with trypsin as described earlier and the digested tryptic peptides were purified using the solid phase extraction (SPE) clean-up cartridges and freeze-dried overnight. Second, each of the synthetic phosphopeptides were serially diluted with 3% ACN/0.1% formic acid and run on Agilent ESI-TOF for LC-MS analysis and searched for the precursor ions of these synthetic phosphopeptides in each of the dilutions. The dilution where the precursor ion intensity is similar to that of the endogenous phosphopeptide was selected for the spiking experiment (i.e. adding the synthetic peptide standard to the tryptic digests before LC-MS/MS analysis). Selected dilutions of the peptide standards were mixed

together to make the phosphopeptide standards mixture. Third, the freeze-dried tryptic digests were resuspended in DHB loading buffer and equal amount of the synthetic phosphopeptide standards mixture was spiked in and mixed with the tryptic peptides derived from the control and treated (15 min and 4 h of glutamate treatment in the presence or absence of Ifenprodil) neurons. The spiked samples were enriched for phosphopeptides using TiO₂ micro-columns as described in section 2.2.9 of Chapter 2. The enriched samples were run on a LTQ Orbitrap Elite (Thermo Scientific) mass spectrometer for LC-MS/MS analysis. This experiment was repeated before data analysis. Finally, data analysis was carried out using Proteome Discoverer 1.4 (PD 1.4), Xcalibur (Thermo Scientific 2.2) and Skyline software. PD 1.4 was used to identify the phosphopeptide based on MS2 spectra, Xcalibur and Skyline software applications were used to calculate the areas under the curve of the precursor ions chromatograms of the endogenous (light) and spiked (heavy) phosphopeptides. Light/heavy ratios among the samples (control vs. treatments) demonstrate the relative phosphorylation status of the identified phosphopeptides under different conditions. Indeed, there was a significant reduction in phosphorylation at Ser-222 of Mef2c, Ser-146 of Mff, Ser-237 of Mlf2 and Ser-38 of Stmn1 after 4 h of glutamate-induced excitotoxicity and co-treatment with Ifenprodil was able to offset dephosphorylation of Mef2c, Mff and Mlf2 and at least partially for Stmn1 (**Figure 6.10**). As a representative example, **Figure 6.11** shows the MS2 spectra and Skyline peptide trees used for quantitation to confirm the changes in phosphorylation at Ser-237 of Mlf2 after glutamate-induced excitotoxicity.

The results obtained in label-free quantitation demonstrate that dephosphorylation of Mef2c, Mff, Mlf2 and Stmn1 in glutamate-induced excitotoxicity is due to over-stimulation of the GluN2B-containing extrasynaptic NMDA receptors. Specifically, neuronal phosphatase(s) or protein kinase(s) targeting these phosphorylation sites operate downstream of the neurotoxic GluN2B-containing NMDA receptors.

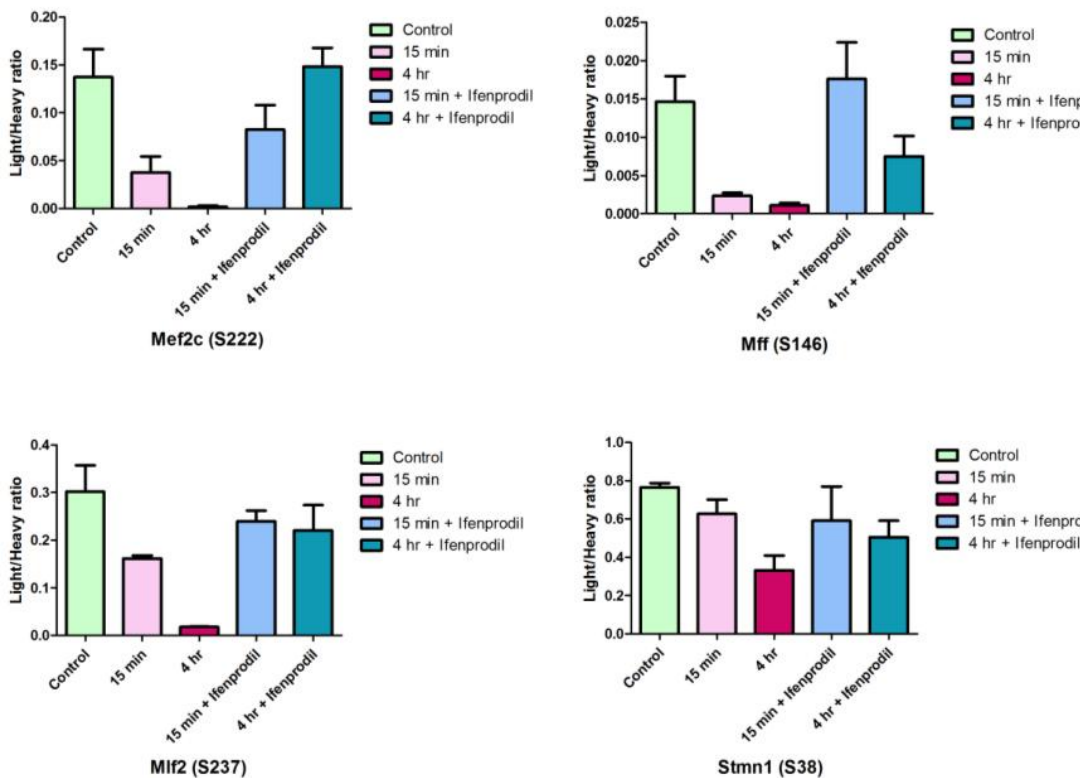


Figure 6.10 Label-free quantitation using synthetic phosphopeptides to confirm changes in phosphorylation of Mef2c, Mff, Mif2 and Stmn1 in glutamate-induced excitotoxicity. Equal amount of synthetic phosphopeptide standards with a heavy amino acid ($^{13}\text{C}^{15}\text{N}$ -Proline/Leucine) were spiked in with tryptic peptides derived from control and treated neuronal lysates. Phosphopeptides were enriched using TiO_2 micro-columns before LC-MS/MS analysis. Following label-free quantitation experiment, area under the curve of endogenous (light) and synthetic (heavy) phosphopeptides were calculated by full-scan MS1 filtering from the extracted ion chromatograms (XICs). The light/heavy ratios correspond to the relative phosphorylation status of these phosphopeptides under different conditions. Data are presented as mean \pm SD (n = 2).

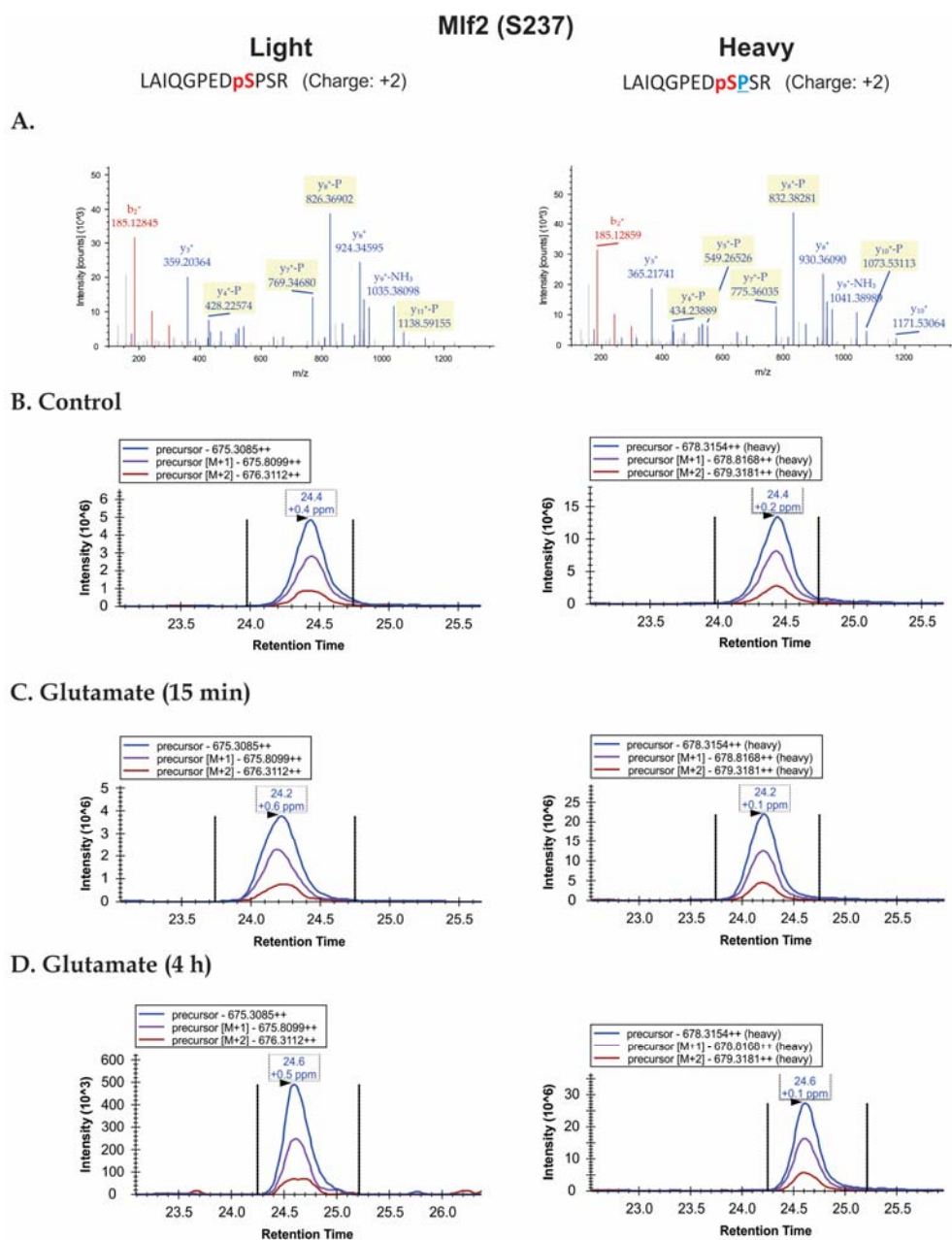


Figure 6.11

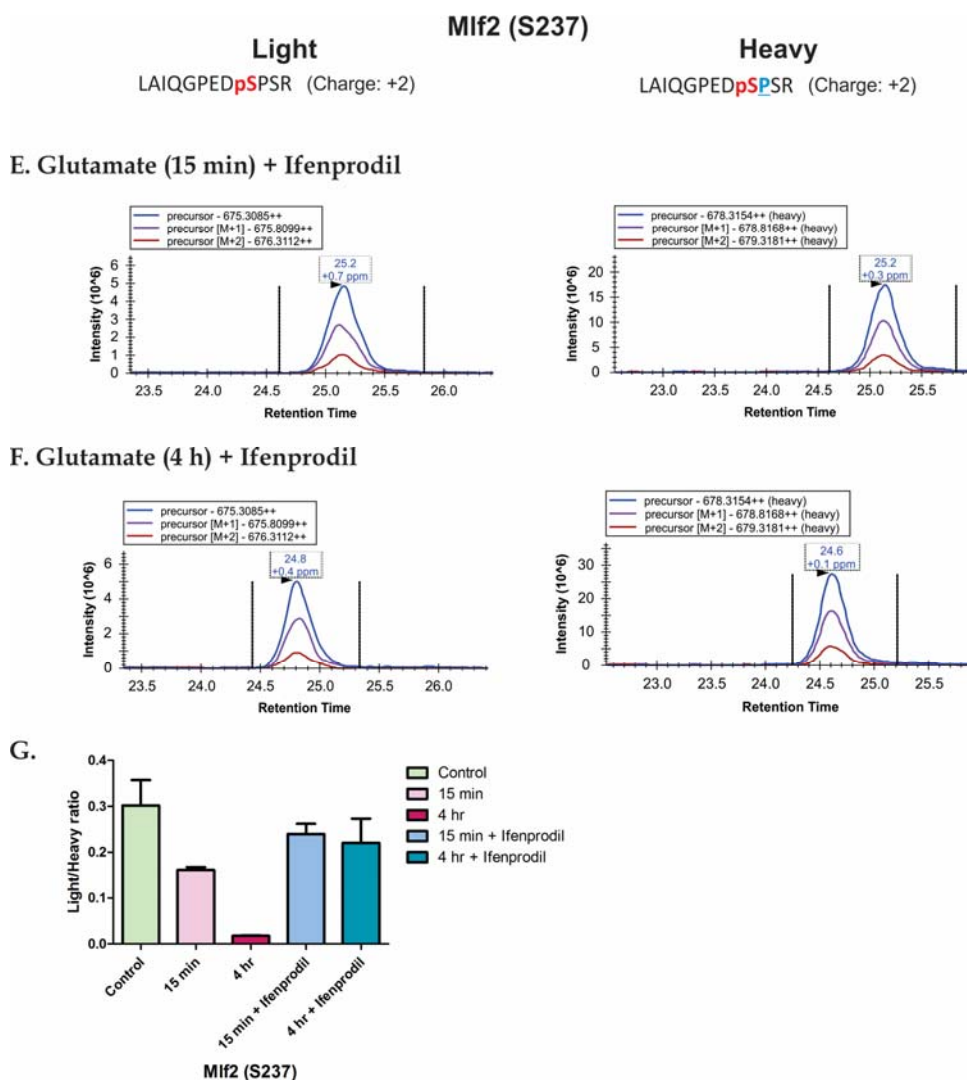


Figure 6.11 Label-free quantitation using synthetic phosphopeptide confirms change in phosphorylation of Ser-237 of Mif2 in glutamate-induced excitotoxicity. **A.** MS/MS spectra used for the identification of endogenous (light) and the spiked (heavy) synthetic heavy peptide ($^{13}\text{C}^{15}\text{N}$ -proline was used as heavy amino acid). **B, C, D, E & F.** Skyline peptide trees showing integrated chromatograms used for quantitation and the similar HPLC retention times and high mass accuracies (< 0.5 ppm). **G.** Bar graph showing relative abundance (area under the curve) of this phosphopeptide in control and treatment experiments. Data are presented as mean \pm SD ($n = 2$).

6.4 Discussion

Calpain mediated Src cleavage and generation of Src Δ N is one of the key events directing neuronal death in excitotoxicity, and previous study from our laboratory discovered that calpain cleaves neuronal Src in the unique domain to generate the neurotoxic Src Δ N in excitotoxicity (Hossain et al., 2013). The membrane-permeable Tat-Src peptide derived from a fragment containing Gly₄₉-Ala₇₉ of the unique domain of Src blocks calpain cleavage of Src and protects neuron against excitotoxic cell death (Hossain et al., 2013). However, the exact calpain cleavage site remained unknown. We therefore hypothesised that calpain cleavage site in Src resides in the Src fragment (Gly₄₉-Ala₇₉) of Tat-Src peptide and Tat-Src functions as a competitive inhibitor to restrict calpain cleavage of Src. To further define the exact calpain cleavage site in Src, I employed two mass spectrometric approaches namely (i) dimethyl labelling of the nascent-N-terminus of Src Δ N after *in vitro* calpain digestion and (ii) label-free MS1 quantitation of the selected tryptic peptides derived from both full-length and truncated Src. Following these two approaches we identified the Phe-63/Gly-64 peptide bond as the major calpain cleavage site in Src unique domain and as expected this site reside in the Gly₄₉-Ala₇₉ segment of Src (**Figure 6.5**). Identification of this site will help to design a shorter Tat-fusion peptide containing a shorter segment derived from the unique domain of Src for use as a neuroprotectant in future animal model studies.

The previous studies by my colleagues and other researchers have identified the extrasynaptic NMDA receptors, calpains and Src Δ N as the key components of the neurotoxic signalling network. These key components directly and/or indirectly modulate protein kinases and phosphatases to direct neuronal death (Hossain et al., 2013). To further single out the neurotoxic signalling events originating from the over-activated NMDA receptors, calpains and Src Δ N, mass spectrometry-based quantitative proteomic and phosphoproteomic analyses were performed using neuronal lysates after 4 h of glutamate treatment in the presence or absence of Ifenprodil, calpeptin and Tat-Src. This chapter describes the findings of these proteomic studies.

Table 6.1 shows that the decrease in the abundance of at least 12 cellular proteins in neurons treated with glutamate for 4 h were offset partially or completely by Ifenprodil co-treatment (**Table 6.1**). Decreased expression of these neuronal proteins could be caused by activation of specific proteases such as calpains and/or decreased protein synthesis resulting from over-stimulation of the extrasynaptic NMDA receptors. Phosphoproteomic analysis identified 31

neuronal proteins of which the changes in phosphorylation were offset by Ifenprodil co-treatment (**Table 6.2**). Again, the decreases in phosphorylation of these neuronal proteins were due to inactivation of the upstream kinases and/or activation of the phosphatases targeting these phosphorylation sites in neurons undergoing excitotoxicity.

Over-stimulated extrasynaptic NMDA receptors allow excessive Ca^{2+} influx inside the cytosol and in turn over-activate calpains that proteolyse neuronal proteins, irreversibly modifying their physiological functions to induce neuronal death (Liu et al., 2008). Similar to the previous set of data, decreased expression of 13 neuronal proteins were offset by glutamate and calpeptin co-treatment (**Table 6.1**). These proteins are likely neuronal proteins that are direct or indirect downstream substrates of over-activated calpains in neurons undergoing excitotoxic demise. Of these identified proteins, Map2 is a well-known calpain substrate implicated in neuronal loss in excitotoxicity and cerebral ischaemia (Blomgren et al., 1995; Siman and Noszek, 1988). One of the experimental strategies for further investigation to identify other potential calpain substrates in neurons and also their corresponding cleavage sites is explained in section 7.2.5 in the next chapter. Following the quantitative phosphoproteomic approach, the decrease in phosphorylation levels of 21 neuronal proteins was found to be offset by co-treatment of glutamate with calpeptin (**Table 6.2**). The results suggest that the changes in phosphorylation of these neuronal proteins are due to activation of neuronal phosphatases and/or inactivation of upstream kinases caused by over-activation of calpains in excitotoxicity.

Since the generation of the neurotoxic Src Δ N is downstream of over-activation of calpains, I used the same approach to define the downstream effectors of Src Δ N. Cultured neurons were co-treated with glutamate and Tat-Src. Quantitative proteomic analysis identified at least 5 neuronal proteins including Anp32a, Dync11l1, Hnrnpm, Hnrnpu and Rsp28 of which the decrease in abundance upon glutamate-induced excitotoxicity was partially or totally offset by Tat-Src co-treatment (**Table 6.1**). Thus, these neuronal proteins are downstream effector signalling molecules of Src Δ N. Somehow, phosphorylation of specific neuronal proteins by Src Δ N reduces their expression. Similarly, by blocking calpain mediated Src cleavage by Tat-Src, changes in phosphorylation of several neuronal phosphoproteins including Map1b (phosphorylation at Ser-1317), Map2 (phosphorylation at Thr-1620/Thr-1623 and Ser-1782), Snap91 (phosphorylation at Ser-313) and Srcin1 (phosphorylation at Ser-588) were partially or completely offset by co-treatment of Tat-Src with glutamate (**Table 6.2**). The changes in these serine or threonine sites are due to modulation of neuronal

SrcΔN substrates that are either upstream kinases or phosphatases targeting these sites. Further investigation should focus on delineating whether reduced phosphorylation of these neuronal proteins contributes to neuronal demise in excitotoxicity.

Western blot analysis confirmed that decrease in phosphorylation of Ser-21 and Ser-9 of Gsk3α and Gsk3β, respectively is a downstream signal of over-activated GluN2B-containing extrasynaptic NMDA receptors (**Figure 6.9**). Dephosphorylation and the consequential activation of the pro-death Gsk3α and Gsk3β were likely caused by inactivation of their upstream kinase - the pro-survival kinase Akt. Indeed, specific blockade of over-stimulation of the extra-synaptic NMDA receptors by Ifenprodil significantly offset the dephosphorylation of Gsk3αβ by 'reviving' the Akt pro-survival signalling pathway (**Figure 6.9**).

The label-free quantitation approach using isotopically labelled synthetic phosphopeptide standards was used to validate the changes in phosphorylation levels of Mef2c (at Ser-222), Mff (at Ser-146), Mlf2 (at Ser-237) and Stmn1 (at Ser-38). Decreases in phosphorylation of these neuronal proteins were caused by downstream signals originating from the over-stimulated GluN2B-containing NMDA receptors and co-treatment of Ifenprodil with glutamate treatment for 4 h was able to offset these phosphorylation changes (**Figure 6.10**).

Mef2c is a transcription factor implicated in regulation of neuronal survival (Cho et al., 2011; Lin et al., 1996; Lyons et al., 1995). Mef2c stimulates gene expression of peroxisome proliferator-activated receptor gamma coactivator 1-alpha (PGC-1α), which regulates mitochondrial biogenesis (Wu et al., 1999). Perturbation of Mef2c-PGC-1α signalling is implicated in neuronal death in excitotoxicity, where oxidative stress and increased NO production lead to S-nitrosylation of Mef2c and in turn inactivates the Mef2c-PGC-1α pro-survival signalling pathway (Ryan et al., 2013). The MAPK member p38 is an upstream kinase known to activate Mef2c that regulates *c-jun* expression in inflammation (Han et al., 1997). It is unclear if p38 phosphorylates Ser-222 of Mef2c. Based upon the sequence encompassing Ser-222, prediction analysis suggests Erk1/2 and JNK1/2/3 as the upstream kinases (<http://www.phosphonet.ca/>). Future experiments should aim to delineate how dephosphorylation of Mef2c (Ser-222) contributes to neuronal demise in excitotoxicity and define the upstream kinase(s) and phosphatase(s) targeting this site.

Mitochondrial outer membrane protein Mff controls mitochondrial fission by recruiting Drp1 to the mitochondrial outer membrane from the cytosol (Gandre-Babbe and van der

Blik, 2008). A recent study identified AMP-activated protein kinase (AMPK) as an upstream kinase for Mff targeting Ser-146, the identified site (Ducommun et al., 2015). But how the decreased phosphorylation of Mff contributes to neuronal death in glutamate-induced excitotoxicity has yet to be confirmed.

Stathmin 1 (Stmn1) is a microtubule destabilising protein and phosphorylation at Ser-38 by the upstream kinases such as Erk1 (Antonsson et al., 2001) or CDK1 (Luo et al., 1994) leads to its inactivation, and this in turn stabilises microtubules. Presumably, decrease in Ser-38 phosphorylation activates the protein to destabilise microtubules and ultimately leads to neuronal death.

Similarly, involvement of Mlf2 (dephosphorylation at Ser-237) in glutamate-induced excitotoxic neuronal demise has yet to be confirmed. Because of the lack of sequence homology with other proteins, biological function(s) of this protein is not well understood. A recent study has described Mlf2 as an upstream inhibitor of nitric oxide synthase pathway in breast cancer metastasis (Dave et al., 2014).

My PhD project identifies a number of potential neuronal targets showing perturbed expression and phosphorylation levels in excitotoxicity and their likely perturbation is pathologically associated as these molecules are downstream of over-activated GluN2B-containing extrasynaptic NMDA receptors, over-activated calpains and Src Δ N generation in excitotoxicity.

Chapter 7: Summary and future directions

7.1 Summary

Excitotoxicity, due to over-stimulation of ionotropic glutamate receptors is an early key event directing neuronal demise in acute neurological disorders such as ischaemic stroke and neurodegenerative diseases. Understanding the overall signalling mechanism of excitotoxicity is one of the best avenues for the development of neuroprotectants to reduce neuronal loss in these neurological disorders. In my PhD study, I employed the targeted biochemical and molecular approaches and mass spectrometry-based systems biology approaches to understand molecular mechanism of excitotoxic neuronal death.

Here, I present the data demonstrating that non-receptor Src protein tyrosine kinase plays dual function in governing neuronal survival. Intact Src under normal physiological conditions maintains neuronal survival in part by activating Erk1/2 (**Figure 3.8**). Previous study from our laboratory described that in excitotoxicity, Src is cleaved by the over-activated Ca²⁺-dependent cysteine protease calpain to generate the neurotoxic Src Δ N (Hossain et al., 2013). Using two mass spectrometric approaches I identified the Phe-63/Gly-64 peptide bond as the calpain cleavage site in Src unique domain (**Figure 6.5**).

Using unbiased quantitative proteomic and phosphoproteomic approaches, I identified a number a neuronal proteins showing perturbed expression and changes in phosphorylation levels in excitotoxicity (described in Chapters 4 and 5). Bioinformatics analysis was performed to identify the perturbed signalling pathways. PI3K/Akt and Erk/MAPK were two of the pro-survival pathways found to be dysregulated in excitotoxicity.

Again, using quantitative proteomic approach, I identified several neuronal proteins (listed in **Tables 6.1** and **6.2**) showing perturbed expression and phosphorylation changes that are downstream signals of NMDA receptors over-activation. Specifically, these perturbed expression and/or phosphorylation states are due to over-activation of the extrasynaptic GluN2B-containing NMDA receptors, over-activated calpains or Src Δ N generated in neurons undergoing excitotoxic cell death. The findings of my current study are summarised and depicted in **Figure 7.1**. The next few sections describe the future directions of my PhD project to better understand the molecular mechanism of excitotoxic neuronal death and how

delineating the mechanism facilitates development of neuroprotectants targeting the neuronal proteins potentially involved in excitotoxic neuronal death identified in my study.

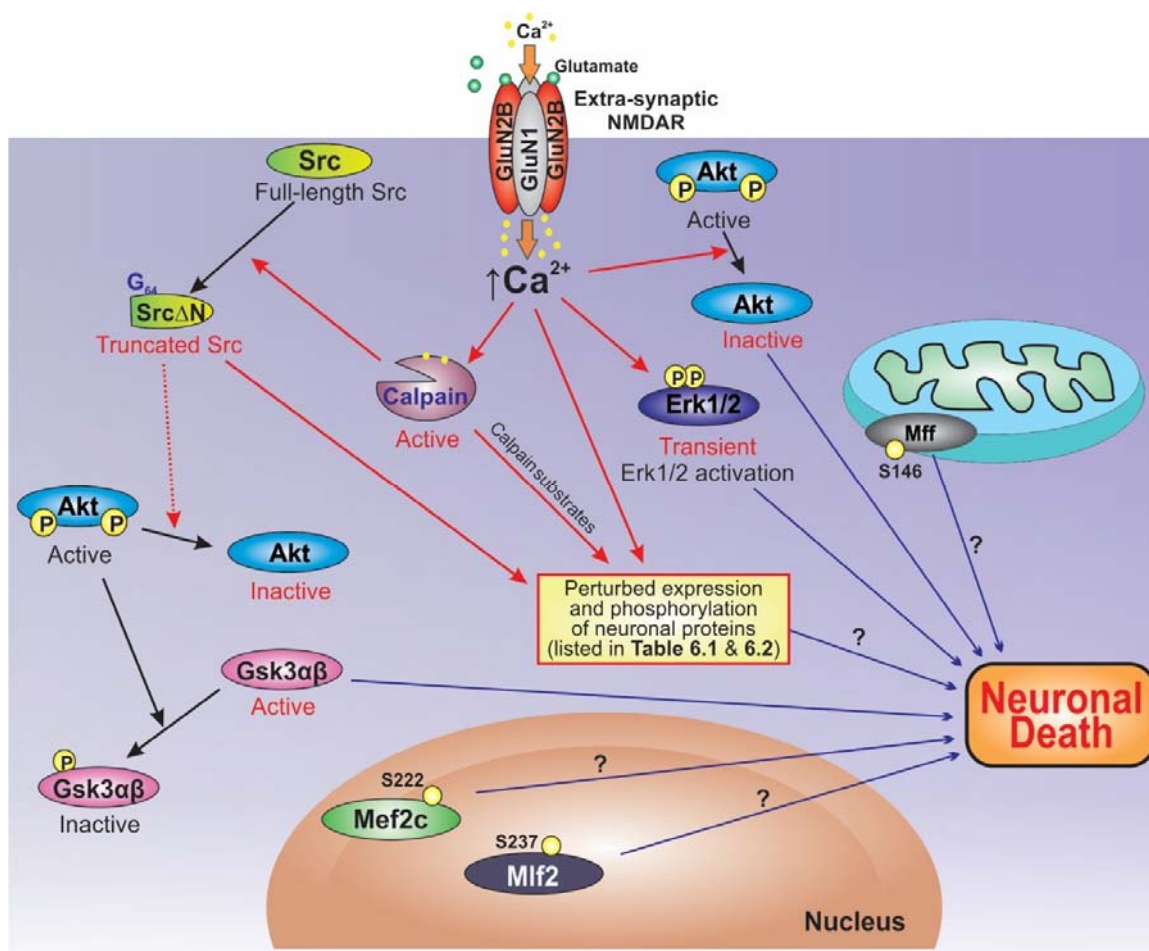


Figure 7.1 Neurotoxic signalling pathways leading to neuronal demise in glutamate-induced excitotoxicity. My study identifies a number of perturbed signalling pathways that interplay together to contribute to neuronal demise in glutamate-induced excitotoxicity. Question marks (?) indicate yet unknown mechanisms.

7.2 Future directions

7.2.1 Investigation of the mechanism by which calpain-mediated cleavage of c-Src causes neuronal loss in neurodegenerative diseases

Excitotoxic calpain activation and subsequent neuronal loss has been implicated in a number of chronic neurodegenerative diseases including Alzheimer's disease (AD) (Nixon et al., 1994; Saito et al., 1993), Huntington's disease (HD) (Panov et al., 2005) and Parkinson's disease (PD) (Crocker et al., 2003). Activated calpain is found to cleave common substrate for example α -fodrin (alpha-II spectrin) highlighting the shared mechanism of activation in these neurodegenerative diseases (Cardali and Maugeri, 2006; Lewis et al., 2007). To ascertain the neurotoxic signalling mechanism of calpain activation and aberrant Src regulation in AD model, I treated cultured primary cortical neurons with the neurotoxic amyloid beta oligomers ($A\beta$) (15 μ M) in presence or absence of calpeptin (20 μ M), MK801 (50 μ M) (an NMDA receptor antagonist) and Tat-Src (20 μ M). $A\beta$ treatment for 4 h generated the neurotoxic truncated Src (Src Δ N) fragment as like glutamate (4 h) treatment (**Figure 7.2**). Co-treatment of calpeptin, MK801 or Tat-Src with $A\beta$ blocked calpain mediated Src cleavage in this model (**Figure 7.2**). These preliminary results confirm that aberrant regulation and neurotoxic mechanism of Src kinase is intact in this model. Future experiments should focus on unveiling the common neurotoxic signalling mechanism of Src Δ N in these neurodegenerative diseases and how $A\beta$ treatment induces calpain cleavage of c-Src in neurons.

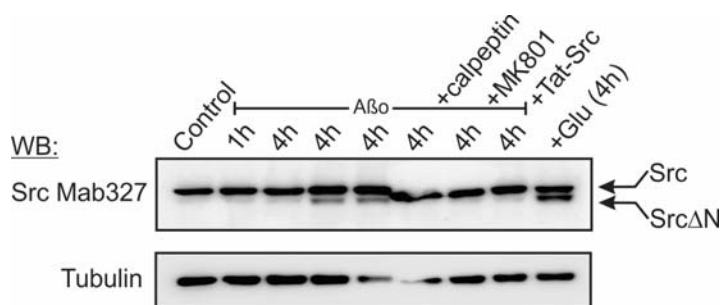


Figure 7.2 Amyloid beta oligomer ($A\beta$) treatment of cultured neurons induces calpain cleavage of Src. At DIV7, cultured primary cortical neurons were treated with $A\beta$ (15 μ M) in presence or absence of calpeptin, MK801 or Tat-Src peptide. Representative Western blot showing truncated Src (Src Δ N) fragment generation upon $A\beta$ treatment as like glutamate treatment (n = 2).

7.2.2 Identification of the direct protein substrates and downstream targets of Src Δ N in neurons undergoing excitotoxic cell death

Previous study demonstrated that Src Δ N generated by calpain cleavage of Src is a potent executor of neuronal death in excitotoxicity (Hossain et al., 2013). Preliminary study indicates that A β -induced neurotoxicity also causes calpain cleavage of Src in neurons (**Figure 7.2**). Thus we hypothesise that Src Δ N is a major mediator of the neurotoxic action of A β . Also to complement the findings of neuronal proteins Anp32a, Dync1li1, Hnrnpm, Hnrnpu, Rps28 (**Table 6.1**) and phosphoproteins Map1b/2, Snap91, Srcin1 (**Table 6.2**) as the potential downstream targets of Src Δ N, further studies to decipher how Src Δ N modulates the expression and phosphorylation states of these neuronal proteins and functional consequences of these perturbation are warranted. Since these neuronal proteins are serine and threonine-phosphoproteins, they are not direct substrates of Src Δ N. Thus, further studies will also aim to identify the direct substrates of Src Δ N in neurons undergoing excitotoxic cell death.

Doxycycline-inducible lentiviral expression of Src Δ N-GFP in neurons and subsequent quantitative proteomic or phosphoproteomic (TiO₂ micro-column chromatography and affinity column purification of phosphotyrosine-containing tryptic peptides) analysis will identify direct substrates and downstream targets of Src Δ N. Transduced neurons without induced expression of Src Δ N can be used as a control. The experimental workflow that can be followed is outlined in **Figure 7.3**. Tryptic peptides derived from the proteins of control neurons will be labelled with the dimethyl group (CH₂O, light label) while those of the neurons expressing Src Δ N-GFP will be labelled with the deuterated dimethyl group (CD₂O, medium label). After mixing, a small aliquot (15 μ l) will be run for LC-MS/MS for global proteome analysis and from the rest of the labelled peptide mixture the phosphotyrosine-(pY) containing peptides will be enriched using the anti-phosphotyrosine affinity magnetic beads. TiO₂-affinity micro-columns will be used to enrich mostly phosphoserine/phosphothreonine-containing peptides prior to LC-MS/MS analysis by the Orbitrap Elite mass spectrometer.

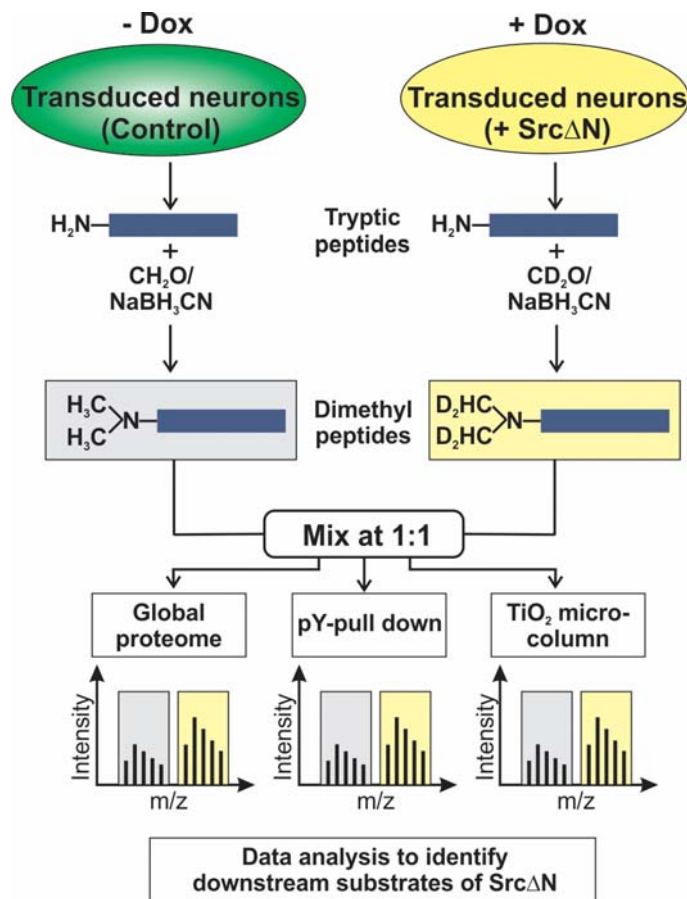


Figure 7.3 A general workflow to identify downstream substrates of Src Δ N. Inducible lentiviral system directed expression of Src Δ N-GFP under the control of doxycycline (+Dox) will be used to identify potential downstream substrates of Src Δ N. The anti-phosphotyrosine-(pY) affinity magnetic beads and TiO₂-affinity columns are used to enrich phosphotyrosine and phosphoserine/phosphothreonine-containing peptides, respectively from the mixed labelled peptide mixture.

7.2.3 Tat-Src as a potent neuroprotectant in animal models of stroke

Previous study from our lab demonstrated neuroprotective role of Tat-Src by blocking calpain cleavage of Src and restricting Src Δ N generation in cultured neurons undergoing excitotoxic cell death (Hossain et al., 2013). In line with this, my colleagues sought to ascertain neuroprotective function of Tat-Src *in vivo*. In an ongoing study, my colleagues have already demonstrated that Tat-Src can reduce neuronal death in a rat model of neurotoxicity (data not shown). In their study, Tat-Src was injected stereotaxically to 4 sites in the cortex and striatum of rats 1 h prior to injection of NMDA to the same sites to inflict excitotoxic damage. Tat-Src treatment reduced the number of damaged neurons caused by

over-stimulation of the NMDA receptor (data not shown). Owing to these promising experimental results, future investigation should focus on understanding if Tat-Src is a potent neuroprotectant *in vivo* in animal models of stroke when administered after the onset of stroke.

7.2.4 Co-treatment of Tat-Src and Tat-NR2B9c to reduce neuronal damage in acute ischaemic stroke

As described in section 1.5 of Chapter 1, the Tat-NR2B9c peptide inhibitor (also known as NA-1) can inhibit the nNOS neurotoxic signalling pathway by blocking the interaction between PSD95 and nNOS (Aarts et al., 2002). Tat-NR2B9c has so far been proven to be effective in reducing iatrogenic stroke-induced brain damage in a small subset of ischaemic stroke patients (Hill et al., 2012). It blocks the over-activation of nNOS and the production of excessive nitric oxide, which causes oxidative damages. Thus, Tat-NR2B9c inhibits one of the key pathologically activated cellular events of excitotoxic neuronal death. Over-activated calpain mediated Src cleavage is another pathologically activated cellular event directing neuronal death in excitotoxicity, and Tat-Src blocks this event and protects against excitotoxic cell death in neurons (Hossain et al., 2013) and *in vivo* in a rat model of NMDA-induced neurotoxicity (data not shown). Thus as a logical continuation, future study should aim to decipher whether combination therapy using both Tat-Src and Tat-NR2B9c is a much more neuroprotective strategy than that using Tat-Src or Tat-NR2B9c alone.

7.2.5 Quantitative protease proteomic approach to identify calpain or other protease substrates in neurons undergoing excitotoxic cell death

Over-activation of calpains is a major post-receptor event directing excitotoxic neuronal death [reviewed in (Carragher, 2006; Hara and Snyder, 2007)]. Multiple lines of evidence indicate that specific calpain substrates are key signalling molecules controlling neuronal survival. Some of these molecules such as CaN and Src acquire neurotoxic ability to initiate specific downstream signalling pathways to direct neuronal death (Hossain et al., 2015; Shioda et al., 2006). It is likely that these calpain-modified proteins cooperate among themselves as well as with other cellular proteins dysregulated in the nNOS and NADPH oxidase (NOX) signalling pathways to induce neuronal death (**Figure 1.2**). To study the mechanism of neuronal loss in neurological diseases, it is important to clearly define how

this network of calpain-modified proteins and dysregulated cellular proteins operate spatially and temporally to cause neuronal death. While calpain-2 acts as an executor of neuronal death, calpain-1 can perform both neurotoxic and neuroprotective functions in excitotoxicity (Badugu et al., 2008; Briz et al., 2013; Liu et al., 2008; Wang et al., 2013). Calpains can cleave and activate caspases (Sharma and Rohrer, 2004), which can potentially proteolyse and modulate the function of key cellular proteins in the neuronal death pathways. Besides calpain and caspases, cathepsins are also involved in neuronal death in neurological diseases (Kikuchi et al., 2003; Sun et al., 2010; Yamashima et al., 1998). We therefore need an unbiased systems biology approach to define how cellular proteins modified by the two calpains, caspases and cathepsins interplay to direct excitotoxic neuronal death.

Terminal Amine Isotopic Labelling of Substrates (TAILS) is a relatively new technique to identify protease substrates using mass spectrometry (Kleifeld et al., 2010). In this method, neuronal proteins that are proteolytically cleaved by calpains and other proteases in neurons after over-stimulation of glutamate receptors can be identified upon stable isotope dimethyl labelling. This method, outlined in **Figure 7.4**, involves five steps: (i) treatment of cultured neurons with excitotoxic level (100 μ M) of glutamate, (ii) differential dimethyl labelling of the free amino groups at the N-termini and side chain of Lys of cellular proteins isolated from untreated neurons (control) and glutamate-treated neurons with NaBH₃CN and CH₂O (light label for control) and deuterated CD₂O (medium label for glutamate treated), (iii) tryptic digestion of the proteins from both samples, (iv) depletion of the tryptic fragments with free amino termini by reaction with the hyper-branched polyglycerol and aldehyde (HPG-ALD) polymers developed by O. Kleifeld and his colleagues (Kleifeld et al., 2010), (v) LC-MS/MS analysis of the tryptic peptides derived from the blocked N-termini of neuronal proteins. For peptides derived from dimethyl labelling of the free N-termini present in both control and glutamate treated neurons, they will appear as doublets in the spectra. For dimethyl labelled peptides derived from the nascent free N-termini of truncated fragments generated by calpain cleavage, they will appear as singletons in the spectra (**Figure 7.4**). Co-treatment of calpeptin with glutamate and subsequent TAILS analysis will not only identify specific calpain substrates in neurons undergoing excitotoxic cell death but will also identify the calpain cleavage sites in those neuronal proteins. Inhibitors targeting those calpain cleavage sites will be potent neuroprotectants to reduce excitotoxic neuronal death in acute ischaemic stroke and neurodegenerative diseases.

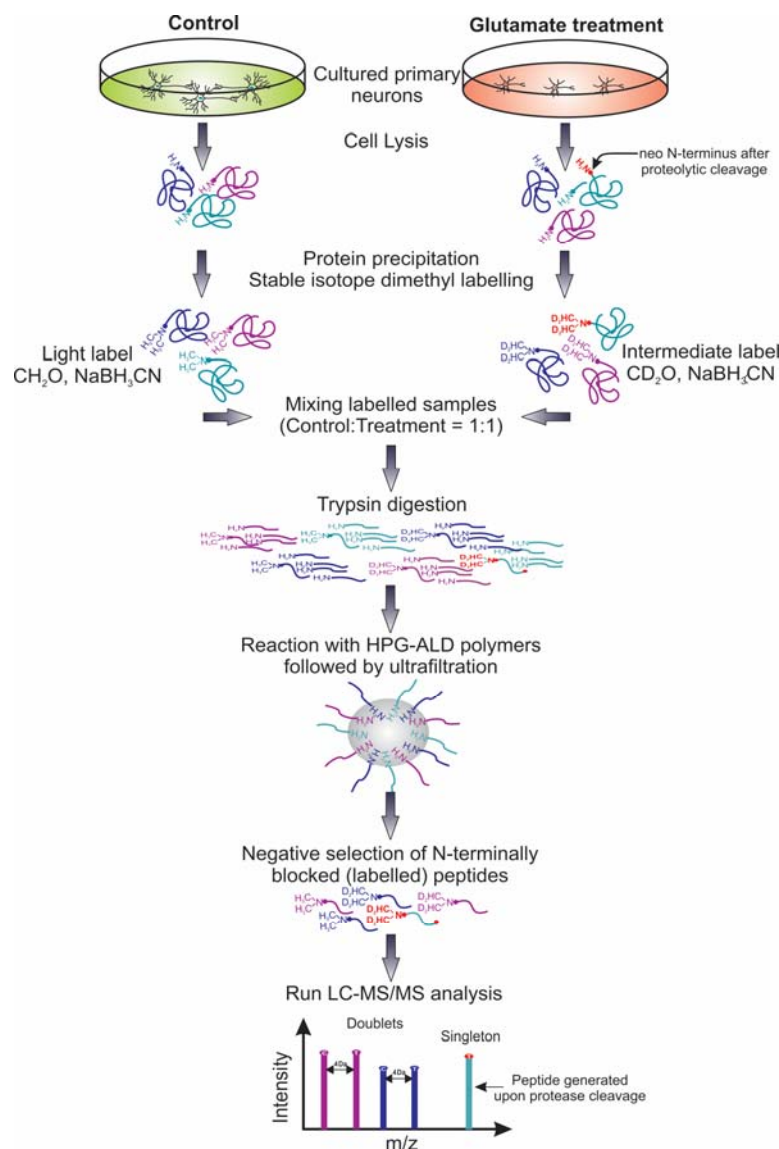


Figure 7.4 A general workflow for protease proteomics. Glutamate excitotoxicity triggers a number of cellular proteases including calpain to exacerbate neuronal death. To identify the protease substrates following glutamate excitotoxicity in cultured neurons terminal amine isotopic labelling of substrates (TAILS) method can be used. Equal amount of protein lysates are isotopically labelled in the free N-terminus with formaldehyde (CH_2O for control) or deuterated formaldehyde (CD_2O for treated sample) in presence of sodium cyanoborohydride (NaBH_3CN). Labelled peptides are mixed together before trypsin digestion. Digested tryptic peptides are mixed with hyper-branched polyglycerol and aldehyde (HPG-ALD) polymer that specifically binds the newly formed free N-terminus containing peptides leaving modified or labelled N-terminus containing peptides. By this negative selection and ultrafiltration N-terminally labelled peptides (from free N-terminus containing proteins or new N-terminus generated upon protease cleavage) are separated and analysed by mass spectrometry. New protease substrates and cleavage sites can be identified by this protease proteomic approach.

7.3 Concluding remarks

As discussed in Chapter 1, Stuart Lipton proposed the drug that interact with cellular targets during states of pathological activation only but not under physiological condition are clinically well tolerated (Lipton, 2007). The reason is that these drugs, referred to as pathologically activate therapeutic drugs would have no or little impact on the physiological functions of the targets. Over-stimulation of the extrasynaptic NMDA receptors is a pathologically activated cellular event occurring in excitotoxicity. Drugs that inhibit this event are expected to be clinically effective and exhibiting little or no side effect. Indeed, memantine, an antagonist of the extrasynaptic NMDA receptor is a pathologically activated drug used clinically to slow down neuronal loss in Alzheimer's disease patients. Some of the future investigations outlined in this chapter aim to define which of the neuronal proteins with perturbed expression and phosphorylation in excitotoxicity are also pathologically activated drug targets. Once identified, these neuronal proteins will be the targets for the development of new neuroprotectant drugs to slow down or prevent neuronal loss in patients suffering from ischaemic stroke and neurodegenerative diseases.

References

- Aarts M, Iihara K, Wei WL, Xiong ZG, Arundine M, Cerwinski W, MacDonald JF and Tymianski M (2003) A key role for TRPM7 channels in anoxic neuronal death. *Cell* **115**:863-877.
- Aarts M, Liu Y, Liu L, Besshoh S, Arundine M, Gurd JW, Wang YT, Salter MW and Tymianski M (2002) Treatment of ischemic brain damage by perturbing NMDA receptor- PSD-95 protein interactions. *Science* **298**:846-850.
- Aarts MM and Tymianski M (2005) TRPM7 and ischemic CNS injury. *Neuroscientist* **11**:116-123.
- Abel T and Zukin RS (2008) Epigenetic targets of HDAC inhibition in neurodegenerative and psychiatric disorders. *Current opinion in pharmacology* **8**:57-64.
- Akhand AA, Pu M, Senga T, Kato M, Suzuki H, Miyata T, Hamaguchi M and Nakashima I (1999) Nitric oxide controls src kinase activity through a sulfhydryl group modification-mediated Tyr-527-independent and Tyr-416-linked mechanism. *J Biol Chem* **274**:25821-25826.
- Alessandrini A, Namura S, Moskowitz MA and Bonventre JV (1999) MEK1 protein kinase inhibition protects against damage resulting from focal cerebral ischemia. *Proc Natl Acad Sci U S A* **96**:12866-12869.
- Alessi DR, Andjelkovic M, Caudwell B, Cron P, Morrice N, Cohen P and Hemmings BA (1996) Mechanism of activation of protein kinase B by insulin and IGF-1. *EMBO J* **15**:6541-6551.
- Amini M, Ma CL, Farazifard R, Zhu G, Zhang Y, Vanderluit J, Zoltewicz JS, Hage F, Savitt JM, Lagace DC, Slack RS, Beique JC, Baudry M, Greer PA, Bergeron R and Park DS (2013) Conditional disruption of calpain in the CNS alters dendrite morphology, impairs LTP, and promotes neuronal survival following injury. *J Neurosci* **33**:5773-5784.
- Andres ME, Burger C, Peral-Rubio MJ, Battaglioli E, Anderson ME, Grimes J, Dallman J, Ballas N and Mandel G (1999) CoREST: a functional corepressor required for regulation of neural-specific gene expression. *Proc Natl Acad Sci U S A* **96**:9873-9878.
- Ankarcrona M, Dypbukt JM, Bonfoco E, Zhivotovsky B, Orrenius S, Lipton SA and Nicotera P (1995) Glutamate-induced neuronal death: a succession of necrosis or apoptosis depending on mitochondrial function. *Neuron* **15**:961-973.
- Antonsson B, Kassel DB, Ruchti E and Grenningloh G (2001) Differences in phosphorylation of human and chicken stathmin by MAP kinase. *Journal of cellular biochemistry* **80**:346-352.
- Aronowski J, Strong R and Grotta JC (1997) Reperfusion injury: demonstration of brain damage produced by reperfusion after transient focal ischemia in rats. *J Cereb Blood Flow Metab* **17**:1048-1056.
- Arthur JS, Elce JS, Hegadorn C, Williams K and Greer PA (2000) Disruption

- of the murine calpain small subunit gene, *Capn4*: calpain is essential for embryonic development but not for cell growth and division. *Molecular and cellular biology* **20**:4474-4481.
- Asara JM, Christofk HR, Freimark LM and Cantley LC (2008) A label-free quantification method by MS/MS TIC compared to SILAC and spectral counting in a proteomics screen. *Proteomics* **8**:994-999.
- Astrup J, Siesjo BK and Symon L (1981) Thresholds in cerebral ischemia - the ischemic penumbra. *Stroke* **12**:723-725.
- Baba T, Kameda M, Yasuhara T, Morimoto T, Kondo A, Shingo T, Tajiri N, Wang F, Miyoshi Y, Borlongan CV, Matsumae M and Date I (2009) Electrical stimulation of the cerebral cortex exerts antiapoptotic, angiogenic, and anti-inflammatory effects in ischemic stroke rats through phosphoinositide 3-kinase/Akt signaling pathway. *Stroke* **40**:e598-605.
- Bading H (2013) Nuclear calcium signalling in the regulation of brain function. *Nat Rev Neurosci* **14**:593-608.
- Badugu R, Garcia M, Bondada V, Joshi A and Geddes JW (2008) N terminus of calpain 1 is a mitochondrial targeting sequence. *J Biol Chem* **283**:3409-3417.
- Bae ON, Rajanikant K, Min J, Smith J, Baek SH, Serfozo K, Hejabian S, Lee KY, Kassab M and Majid A (2012) Lymphocyte cell kinase activation mediates neuroprotection during ischemic preconditioning. *J Neurosci* **32**:7278-7286.
- Bain J, Plater L, Elliott M, Shpiro N, Hastie CJ, McLauchlan H, Klevernic I, Arthur JS, Alessi DR and Cohen P (2007) The selectivity of protein kinase inhibitors: a further update. *Biochem J* **408**:297-315.
- Bano D, Young KW, Guerin CJ, Lefevre R, Rothwell NJ, Naldini L, Rizzuto R, Carafoli E and Nicotera P (2005) Cleavage of the plasma membrane Na⁺/Ca²⁺ exchanger in excitotoxicity. *Cell* **120**:275-285.
- Bantscheff M, Schirle M, Sweetman G, Rick J and Kuster B (2007) Quantitative mass spectrometry in proteomics: a critical review. *Analytical and bioanalytical chemistry* **389**:1017-1031.
- Baxter PS, Bell KF, Hasel P, Kaindl AM, Fricker M, Thomson D, Cregan SP, Gillingwater TH and Hardingham GE (2015) Synaptic NMDA receptor activity is coupled to the transcriptional control of the glutathione system. *Nat Commun* **6**:6761.
- Beggs HE, Soriano P and Maness PF (1994) NCAM-dependent neurite outgrowth is inhibited in neurons from Fyn-minus mice. *J Cell Biol* **127**:825-833.
- Bellacosa A, Chan TO, Ahmed NN, Datta K, Malstrom S, Stokoe D, McCormick F, Feng J and Tsichlis P (1998) Akt activation by growth factors is a multiple-step process: the role of the PH domain. *Oncogene* **17**:313-325.
- Berg D, Holzmann C and Riess O (2003) 14-3-3 proteins in the nervous system. *Nat Rev Neurosci* **4**:752-762.
- Bernath E, Kupina N, Liu MC, Hayes RL, Meegan C and Wang KK (2006) Elevation of cytoskeletal protein

- breakdown in aged Wistar rat brain. *Neurobiol Aging* **27**:624-632.
- Beyers MB and Neumar RW (2008) Mechanistic role of calpains in postischemic neurodegeneration. *J Cereb Blood Flow Metab* **28**:655-673.
- Bijur GN, Davis RE and Jope RS (1999) Rapid activation of heat shock factor-1 DNA binding by H₂O₂ and modulation by glutathione in human neuroblastoma and Alzheimer's disease cybrid cells. *Brain research Molecular brain research* **71**:69-77.
- Blomgren K, McRae A, Bona E, Saido TC, Karlsson JO and Hagberg H (1995) Degradation of fodrin and MAP 2 after neonatal cerebral hypoxic-ischemia. *Brain Res* **684**:136-142.
- Boersema PJ, Raijmakers R, Lemeer S, Mohammed S and Heck AJ (2009) Multiplex peptide stable isotope dimethyl labeling for quantitative proteomics. *Nat Protoc* **4**:484-494.
- Bogoyevitch MA, Ngoei KR, Zhao TT, Yeap YY and Ng DC (2010) c-Jun N-terminal kinase (JNK) signaling: recent advances and challenges. *Biochim Biophys Acta* **1804**:463-475.
- Bonita R (1992) Epidemiology of stroke. *Lancet* **339**:342-344.
- Borsello T, Clarke PG, Hirt L, Vercelli A, Repici M, Schorderet DF, Bogousslavsky J and Bonny C (2003) A peptide inhibitor of c-Jun N-terminal kinase protects against excitotoxicity and cerebral ischemia. *Nat Med* **9**:1180-1186.
- Boston PF, Jackson P and Thompson RJ (1982) Human 14-3-3 protein: radioimmunoassay, tissue distribution, and cerebrospinal fluid levels in patients with neurological disorders. *J Neurochem* **38**:1475-1482.
- Braselmann S and McCormick F (1995) Bcr and Raf form a complex in vivo via 14-3-3 proteins. *EMBO J* **14**:4839-4848.
- Briz V, Hsu YT, Li Y, Lee E, Bi X and Baudry M (2013) Calpain-2-mediated PTEN degradation contributes to BDNF-induced stimulation of dendritic protein synthesis. *J Neurosci* **33**:4317-4328.
- Broughton BR, Reutens DC and Sobey CG (2009) Apoptotic mechanisms after cerebral ischemia. *Stroke* **40**:e331-339.
- Burnashev N, Monyer H, Seeburg PH and Sakmann B (1992) Divalent ion permeability of AMPA receptor channels is dominated by the edited form of a single subunit. *Neuron* **8**:189-198.
- Caccamo A, Maldonado MA, Bokov AF, Majumder S and Oddo S (2010) CBP gene transfer increases BDNF levels and ameliorates learning and memory deficits in a mouse model of Alzheimer's disease. *Proc Natl Acad Sci U S A* **107**:22687-22692.
- Campbell RL and Davies PL (2012) Structure-function relationships in calpains. *Biochem J* **447**:335-351.
- Cao G, Xing J, Xiao X, Liou AK, Gao Y, Yin XM, Clark RS, Graham SH and Chen J (2007) Critical role of calpain I in mitochondrial release of apoptosis-inducing factor in ischemic neuronal injury. *J Neurosci* **27**:9278-9293.
- Cao X, Kambe F, Yamauchi M and Seo H (2009) Thyroid-hormone-dependent activation of the

- phosphoinositide 3-kinase/Akt cascade requires Src and enhances neuronal survival. *Biochem J* **424**:201-209.
- Cardali S and Maugeri R (2006) Detection of alphaII-spectrin and breakdown products in humans after severe traumatic brain injury. *Journal of neurosurgical sciences* **50**:25-31.
- Carragher NO (2006) Calpain inhibition: a therapeutic strategy targeting multiple disease states. *Curr Pharm Des* **12**:615-638.
- Centeno C, Repici M, Chatton JY, Riederer BM, Bonny C, Nicod P, Price M, Clarke PG, Papa S, Franzoso G and Borsello T (2007) Role of the JNK pathway in NMDA-mediated excitotoxicity of cortical neurons. *Cell Death Differ* **14**:240-253.
- Chan PH (2001) Reactive oxygen radicals in signaling and damage in the ischemic brain. *J Cereb Blood Flow Metab* **21**:2-14.
- Chan TO, Rittenhouse SE and Tsichlis PN (1999) AKT/PKB and other D3 phosphoinositide-regulated kinases: kinase activation by phosphoinositide-dependent phosphorylation. *Annual review of biochemistry* **68**:965-1014.
- Charton JP, Herkert M, Becker CM and Schroder H (1999) Cellular and subcellular localization of the 2B-subunit of the NMDA receptor in the adult rat telencephalon. *Brain Res* **816**:609-617.
- Chateauvieux S, Morceau F, Dicato M and Diederich M (2010) Molecular and therapeutic potential and toxicity of valproic acid. *Journal of biomedicine & biotechnology* **2010**.
- Chen A, Liao WP, Lu Q, Wong WS and Wong PT (2007) Upregulation of dihydropyrimidinase-related protein 2, spectrin alpha II chain, heat shock cognate protein 70 pseudogene 1 and tropomodulin 2 after focal cerebral ischemia in rats--a proteomics approach. *Neurochemistry international* **50**:1078-1086.
- Chen D, Shah A, Nguyen H, Loo D, Inder KL and Hill MM (2014) Online quantitative proteomics p-value calculator for permutation-based statistical testing of peptide ratios. *J Proteome Res* **13**:4184-4191.
- Chen HS and Lipton SA (2005) Pharmacological implications of two distinct mechanisms of interaction of memantine with N-methyl-D-aspartate-gated channels. *J Pharmacol Exp Ther* **314**:961-971.
- Chen Y, Brennan-Minnella AM, Sheth S, El-Benna J and Swanson RA (2015) Tat-NR2B9c prevents excitotoxic neuronal superoxide production. *J Cereb Blood Flow Metab* **35**:739-742.
- Chen ZF, Paquette AJ and Anderson DJ (1998) NRSF/REST is required in vivo for repression of multiple neuronal target genes during embryogenesis. *Nature genetics* **20**:136-142.
- Cho EG, Zaremba JD, McKercher SR, Talantova M, Tu S, Masliah E, Chan SF, Nakanishi N, Terskikh A and Lipton SA (2011) MEF2C enhances dopaminergic neuron differentiation of human embryonic stem cells in a parkinsonian rat model. *PLoS One* **6**:e24027.
- Choi DW (1987) Ionic dependence of glutamate neurotoxicity. *J Neurosci* **7**:369-379.
- Choi DW (1988a) Calcium-mediated neurotoxicity: relationship to

- specific channel types and role in ischemic damage. *Trends Neurosci* **11**:465-469.
- Choi DW (1988b) Glutamate neurotoxicity and diseases of the nervous system. *Neuron* **1**:623-634.
- Choi DW, Maulucci-Gedde M and Kriegstein AR (1987) Glutamate neurotoxicity in cortical cell culture. *J Neurosci* **7**:357-368.
- Choi DW and Rothman SM (1990) The role of glutamate neurotoxicity in hypoxic-ischemic neuronal death. *Annual review of neuroscience* **13**:171-182.
- Choi WS, Lee EH, Chung CW, Jung YK, Jin BK, Kim SU, Oh TH, Saido TC and Oh YJ (2001) Cleavage of Bax is mediated by caspase-dependent or -independent calpain activation in dopaminergic neuronal cells: protective role of Bcl-2. *J Neurochem* **77**:1531-1541.
- Chong JA, Tapia-Ramirez J, Kim S, Toledo-Aral JJ, Zheng Y, Boutros MC, Altshuler YM, Frohman MA, Kraner SD and Mandel G (1995) REST: a mammalian silencer protein that restricts sodium channel gene expression to neurons. *Cell* **80**:949-957.
- Chow HM, Guo D, Zhou JC, Zhang GY, Li HF, Herrup K and Zhang J (2014) CDK5 activator protein p25 preferentially binds and activates GSK3beta. *Proc Natl Acad Sci U S A* **111**:E4887-4895.
- Chung JH and Eng C (2005) Nuclear-cytoplasmic partitioning of phosphatase and tensin homologue deleted on chromosome 10 (PTEN) differentially regulates the cell cycle and apoptosis. *Cancer research* **65**:8096-8100.
- Clements JD, Lester RA, Tong G, Jahr CE and Westbrook GL (1992) The time course of glutamate in the synaptic cleft. *Science* **258**:1498-1501.
- Coffey ET (2014) Nuclear and cytosolic JNK signalling in neurons. *Nat Rev Neurosci* **15**:285-299.
- Cohen P (2001) The role of protein phosphorylation in human health and disease. The Sir Hans Krebs Medal Lecture. *European journal of biochemistry / FEBS* **268**:5001-5010.
- Cook D, Brown D, Alexander R, March R, Morgan P, Satterthwaite G and Pangalos MN (2014) Lessons learned from the fate of AstraZeneca's drug pipeline: a five-dimensional framework. *Nat Rev Drug Discov* **13**:419-431.
- Courtney MJ, Lambert JJ and Nicholls DG (1990) The interactions between plasma membrane depolarization and glutamate receptor activation in the regulation of cytoplasmic free calcium in cultured cerebellar granule cells. *J Neurosci* **10**:3873-3879.
- Craft GE, Chen A and Nairn AC (2013) Recent advances in quantitative neuroproteomics. *Methods* **61**:186-218.
- Croall DE and Ersfeld K (2007) The calpains: modular designs and functional diversity. *Genome biology* **8**:218.
- Crocker SJ, Smith PD, Jackson-Lewis V, Lamba WR, Hayley SP, Grimm E, Callaghan SM, Slack RS, Melloni E, Przedborski S, Robertson GS, Anisman H, Merali Z and Park DS (2003) Inhibition of calpains prevents neuronal and behavioral deficits in an MPTP mouse model

- of Parkinson's disease. *J Neurosci* **23**:4081-4091.
- Cross DA, Alessi DR, Cohen P, Andjelkovich M and Hemmings BA (1995) Inhibition of glycogen synthase kinase-3 by insulin mediated by protein kinase B. *Nature* **378**:785-789.
- Cross DA, Culbert AA, Chalmers KA, Facci L, Skaper SD and Reith AD (2001) Selective small-molecule inhibitors of glycogen synthase kinase-3 activity protect primary neurones from death. *J Neurochem* **77**:94-102.
- Cuadrado E, Rosell A, Colome N, Hernandez-Guillamon M, Garcia-Berrocoso T, Ribo M, Alcazar A, Ortega-Aznar A, Salinas M, Canals F and Montaner J (2010) The proteome of human brain after ischemic stroke. *J Neuropathol Exp Neurol* **69**:1105-1115.
- Cuddihy AR and O'Connell MJ (2003) Cell-cycle responses to DNA damage in G2. *International review of cytology* **222**:99-140.
- Cull-Candy S, Brickley S and Farrant M (2001) NMDA receptor subunits: diversity, development and disease. *Current opinion in neurobiology* **11**:327-335.
- Cull-Candy S, Kelly L and Farrant M (2006) Regulation of Ca²⁺-permeable AMPA receptors: synaptic plasticity and beyond. *Current opinion in neurobiology* **16**:288-297.
- Cull-Candy SG and Leszkiewicz DN (2004) Role of distinct NMDA receptor subtypes at central synapses. *Science's STKE : signal transduction knowledge environment* **2004**:re16.
- Czyz A and Kiedrowski L (2002) In depolarized and glucose-deprived neurons, Na⁺ influx reverses plasmalemmal K⁺-dependent and K⁺-independent Na⁺/Ca²⁺ exchangers and contributes to NMDA excitotoxicity. *J Neurochem* **83**:1321-1328.
- D'Orsi B, Bonner H, Tuffy LP, Dussmann H, Woods I, Courtney MJ, Ward MW and Prehn JH (2012) Calpains are downstream effectors of bax-dependent excitotoxic apoptosis. *J Neurosci* **32**:1847-1858.
- Datta A, Jingru Q, Khor TH, Teo MT, Heese K and Sze SK (2011) Quantitative neuroproteomics of an in vivo rodent model of focal cerebral ischemia/reperfusion injury reveals a temporal regulation of novel pathophysiological molecular markers. *J Proteome Res* **10**:5199-5213.
- Datta K, Franke TF, Chan TO, Makris A, Yang SI, Kaplan DR, Morrison DK, Golemis EA and Tsichlis PN (1995) AH/PH domain-mediated interaction between Akt molecules and its potential role in Akt regulation. *Molecular and cellular biology* **15**:2304-2310.
- Datta SR, Dudek H, Tao X, Masters S, Fu H, Gotoh Y and Greenberg ME (1997) Akt phosphorylation of BAD couples survival signals to the cell-intrinsic death machinery. *Cell* **91**:231-241.
- Dave B, Granados-Principal S, Zhu R, Benz S, Rabizadeh S, Soon-Shiong P, Yu KD, Shao Z, Li X, Gilcrease M, Lai Z, Chen Y, Huang TH, Shen H, Liu X, Ferrari M, Zhan M, Wong ST, Kumaraswami M, Mittal V, Chen X, Gross SS and Chang JC (2014) Targeting RPL39 and MLF2

- reduces tumor initiation and metastasis in breast cancer by inhibiting nitric oxide synthase signaling. *Proc Natl Acad Sci U S A* **111**:8838-8843.
- Davila D, Connolly NM, Bonner H, Weisova P, Dussmann H, Concannon CG, Huber HJ and Prehn JH (2012) Two-step activation of FOXO3 by AMPK generates a coherent feed-forward loop determining excitotoxic cell fate. *Cell Death Differ* **19**:1677-1688.
- Deb I, Manhas N, Poddar R, Rajagopal S, Allan AM, Lombroso PJ, Rosenberg GA, Candelario-Jalil E and Paul S (2013) Neuroprotective role of a brain-enriched tyrosine phosphatase, STEP, in focal cerebral ischemia. *J Neurosci* **33**:17814-17826.
- Delavallee L, Cabon L, Galan-Malo P, Lorenzo HK and Susin SA (2011) AIF-mediated caspase-independent necroptosis: a new chance for targeted therapeutics. *IUBMB Life* **63**:221-232.
- Delmore JE, Issa GC, Lemieux ME, Rahl PB, Shi J, Jacobs HM, Kastritis E, Gilpatrick T, Paranal RM, Qi J, Chesi M, Schinzel AC, McKeown MR, Heffernan TP, Vakoc CR, Bergsagel PL, Ghobrial IM, Richardson PG, Young RA, Hahn WC, Anderson KC, Kung AL, Bradner JE and Mitsiades CS (2011) BET bromodomain inhibition as a therapeutic strategy to target c-Myc. *Cell* **146**:904-917.
- Dick O and Bading H (2010) Synaptic activity and nuclear calcium signaling protect hippocampal neurons from death signal-associated nuclear translocation of FoxO3a induced by extrasynaptic N-methyl-D-aspartate receptors. *J Biol Chem* **285**:19354-19361.
- Dirnagl U, Iadecola C and Moskowitz MA (1999) Pathobiology of ischaemic stroke: an integrated view. *Trends Neurosci* **22**:391-397.
- Doepfner TR, Doehring M, Bretschneider E, Zechariah A, Kaltwasser B, Muller B, Koch JC, Bahr M, Hermann DM and Michel U (2013) MicroRNA-124 protects against focal cerebral ischemia via mechanisms involving Usp14-dependent REST degradation. *Acta Neuropathol* **126**:251-265.
- Donnan GA, Fisher M, Macleod M and Davis SM (2008) Stroke. *Lancet* **371**:1612-1623.
- Drose S, Stepanova A and Galkin A (2016) Ischemic A/D transition of mitochondrial complex I and its role in ROS generation. *Biochim Biophys Acta*.
- Du W, Huang J, Yao H, Zhou K, Duan B and Wang Y (2010) Inhibition of TRPC6 degradation suppresses ischemic brain damage in rats. *J Clin Invest* **120**:3480-3492.
- Ducommun S, Deak M, Sumpton D, Ford RJ, Nunez Galindo A, Kussmann M, Viollet B, Steinberg GR, Foretz M, Dayon L, Morrice NA and Sakamoto K (2015) Motif affinity and mass spectrometry proteomic approach for the discovery of cellular AMPK targets: identification of mitochondrial fission factor as a new AMPK substrate. *Cell Signal* **27**:978-988.
- Dudek H, Datta SR, Franke TF, Birnbaum MJ, Yao R, Cooper GM, Segal RA, Kaplan DR and Greenberg ME (1997) Regulation of neuronal survival by the serine-threonine protein kinase Akt. *Science* **275**:661-665.

- Eisenberg-Lerner A and Kimchi A (2007) DAP kinase regulates JNK signaling by binding and activating protein kinase D under oxidative stress. *Cell Death Differ* **14**:1908-1915.
- Ellekjaer H, Holmen J, Indredavik B and Terent A (1997) Epidemiology of stroke in Innherred, Norway, 1994 to 1996. Incidence and 30-day case-fatality rate. *Stroke* **28**:2180-2184.
- Encinas M, Crowder RJ, Milbrandt J and Johnson EM, Jr. (2004) Tyrosine 981, a novel ret autophosphorylation site, binds c-Src to mediate neuronal survival. *J Biol Chem* **279**:18262-18269.
- Encinas M, Tansey MG, Tsui-Pierchala BA, Comella JX, Milbrandt J and Johnson EM, Jr. (2001) c-Src is required for glial cell line-derived neurotrophic factor (GDNF) family ligand-mediated neuronal survival via a phosphatidylinositol-3 kinase (PI-3K)-dependent pathway. *J Neurosci* **21**:1464-1472.
- Erreger K, Chen PE, Wyllie DJ and Traynelis SF (2004) Glutamate receptor gating. *Critical reviews in neurobiology* **16**:187-224.
- Fatokun AA, Dawson VL and Dawson TM (2014) Parthanatos: mitochondrial-linked mechanisms and therapeutic opportunities. *Br J Pharmacol* **171**:2000-2016.
- Feder D and Bishop JM (1990) Purification and enzymatic characterization of pp60c-src from human platelets. *J Biol Chem* **265**:8205-8211.
- Feng S, Ye M, Zhou H, Jiang X, Jiang X, Zou H and Gong B (2007) Immobilized zirconium ion affinity chromatography for specific enrichment of phosphopeptides in phosphoproteome analysis. *Molecular & cellular proteomics : MCP* **6**:1656-1665.
- Feng T, Wang H, Zhang X, Sun H and You Q (2014) The discovery of novel histone lysine methyltransferase G9a inhibitors (part 1): molecular design based on a series of substituted 2,4-diamino-7-aminoalkoxyquinazoline by molecular-docking-guided 3D quantitative structure-activity relationship studies. *Medicinal chemistry* **10**:426-440.
- Ferrarese CaB, M. F. Ed. (2004) *Excitotoxicity in Neurological Diseases: New Therapeutic Challenge*, Springer US.
- Ficarro SB, McClelland ML, Stukenberg PT, Burke DJ, Ross MM, Shabanowitz J, Hunt DF and White FM (2002) Phosphoproteome analysis by mass spectrometry and its application to *Saccharomyces cerevisiae*. *Nat Biotechnol* **20**:301-305.
- Filippakopoulos P and Knapp S (2014) Targeting bromodomains: epigenetic readers of lysine acetylation. *Nat Rev Drug Discov* **13**:337-356.
- Fisher M (2004) The ischemic penumbra: identification, evolution and treatment concepts. *Cerebrovasc Dis* **17 Suppl 1**:1-6.
- Flynn RW, MacWalter RS and Doney AS (2008) The cost of cerebral ischaemia. *Neuropharmacology* **55**:250-256.
- Franke TF, Kaplan DR, Cantley LC and Toker A (1997) Direct regulation of the Akt proto-oncogene product by phosphatidylinositol-3,4-

- bisphosphate. *Science* **275**:665-668.
- Franke TF, Yang SI, Chan TO, Datta K, Kazlauskas A, Morrison DK, Kaplan DR and Tsichlis PN (1995) The protein kinase encoded by the Akt proto-oncogene is a target of the PDGF-activated phosphatidylinositol 3-kinase. *Cell* **81**:727-736.
- Fu H, Subramanian RR and Masters SC (2000) 14-3-3 proteins: structure, function, and regulation. *Annu Rev Pharmacol Toxicol* **40**:617-647.
- Fujikawa DG (2015) The role of excitotoxic programmed necrosis in acute brain injury. *Comput Struct Biotechnol J* **13**:212-221.
- Gabbita SP, Lovell MA and Markesbery WR (1998) Increased nuclear DNA oxidation in the brain in Alzheimer's disease. *J Neurochem* **71**:2034-2040.
- Gamir-Morralla A, Lopez-Menendez C, Ayuso-Dolado S, Tejada GS, Montaner J, Rosell A, Iglesias T and Diaz-Guerra M (2015) Development of a neuroprotective peptide that preserves survival pathways by preventing Kidins220/ARMS calpain processing induced by excitotoxicity. *Cell Death Dis* **6**:e1939.
- Gan Q, Salussolia CL and Wollmuth LP (2015) Assembly of AMPA receptors: mechanisms and regulation. *J Physiol* **593**:39-48.
- Gandre-Babbe S and van der Blik AM (2008) The novel tail-anchored membrane protein Mff controls mitochondrial and peroxisomal fission in mammalian cells. *Mol Biol Cell* **19**:2402-2412.
- Gao X, Zhang H, Steinberg G and Zhao H (2010) The Akt pathway is involved in rapid ischemic tolerance in focal ischemia in Rats. *Transl Stroke Res* **1**:202-209.
- Gerstner T, Bell N and Konig S (2008) Oral valproic acid for epilepsy--long-term experience in therapy and side effects. *Expert opinion on pharmacotherapy* **9**:285-292.
- Ginsberg MD (1997) The new language of cerebral ischemia. *AJNR Am J Neuroradiol* **18**:1435-1445.
- Goll DE, Thompson VF, Li H, Wei W and Cong J (2003) The calpain system. *Physiol Rev* **83**:731-801.
- Graham SH and Chen J (2001) Programmed cell death in cerebral ischemia. *J Cereb Blood Flow Metab* **21**:99-109.
- Grant SG, O'Dell TJ, Karl KA, Stein PL, Soriano P and Kandel ER (1992) Impaired long-term potentiation, spatial learning, and hippocampal development in fyn mutant mice. *Science* **258**:1903-1910.
- Grimes JA, Nielsen SJ, Battaglioli E, Miska EA, Speh JC, Berry DL, Atouf F, Holdener BC, Mandel G and Kouzarides T (2000) The co-repressor mSin3A is a functional component of the REST-CoREST repressor complex. *J Biol Chem* **275**:9461-9467.
- Guroff G (1964) A Neutral, Calcium-Activated Proteinase from the Soluble Fraction of Rat Brain. *J Biol Chem* **239**:149-155.
- Gygi SP, Rist B, Gerber SA, Turecek F, Gelb MH and Aebersold R (1999) Quantitative analysis of complex protein mixtures using isotope-coded affinity tags. *Nat Biotechnol* **17**:994-999.
- Haass C and Mandelkow E (2010) Fyn-tau-amyloid: a toxic triad. *Cell* **142**:356-358.

- Han G, Ye M, Zhou H, Jiang X, Feng S, Jiang X, Tian R, Wan D, Zou H and Gu J (2008) Large-scale phosphoproteome analysis of human liver tissue by enrichment and fractionation of phosphopeptides with strong anion exchange chromatography. *Proteomics* **8**:1346-1361.
- Han J, Jiang Y, Li Z, Kravchenko VV and Ulevitch RJ (1997) Activation of the transcription factor MEF2C by the MAP kinase p38 in inflammation. *Nature* **386**:296-299.
- Hara MR, Agrawal N, Kim SF, Cascio MB, Fujimuro M, Ozeki Y, Takahashi M, Cheah JH, Tankou SK, Hester LD, Ferris CD, Hayward SD, Snyder SH and Sawa A (2005) S-nitrosylated GAPDH initiates apoptotic cell death by nuclear translocation following Siah1 binding. *Nature cell biology* **7**:665-674.
- Hara MR and Snyder SH (2007) Cell signaling and neuronal death. *Annu Rev Pharmacol Toxicol* **47**:117-141.
- Hara MR, Thomas B, Cascio MB, Bae BI, Hester LD, Dawson VL, Dawson TM, Sawa A and Snyder SH (2006) Neuroprotection by pharmacologic blockade of the GAPDH death cascade. *Proc Natl Acad Sci U S A* **103**:3887-3889.
- Hardingham GE (2006) Pro-survival signalling from the NMDA receptor. *Biochem Soc Trans* **34**:936-938.
- Hardingham GE, Arnold FJ and Bading H (2001) A calcium microdomain near NMDA receptors: on switch for ERK-dependent synapse-to-nucleus communication. *Nat Neurosci* **4**:565-566.
- Hardingham GE and Bading H (2002) Coupling of extrasynaptic NMDA receptors to a CREB shut-off pathway is developmentally regulated. *Biochim Biophys Acta* **1600**:148-153.
- Hardingham GE and Bading H (2010) Synaptic versus extrasynaptic NMDA receptor signalling: implications for neurodegenerative disorders. *Nat Rev Neurosci* **11**:682-696.
- Hardingham GE, Chawla S, Johnson CM and Bading H (1997) Distinct functions of nuclear and cytoplasmic calcium in the control of gene expression. *Nature* **385**:260-265.
- Hardingham GE, Fukunaga Y and Bading H (2002) Extrasynaptic NMDARs oppose synaptic NMDARs by triggering CREB shut-off and cell death pathways. *Nat Neurosci* **5**:405-414.
- Harris AZ and Pettit DL (2007) Extrasynaptic and synaptic NMDA receptors form stable and uniform pools in rat hippocampal slices. *J Physiol* **584**:509-519.
- Hegele RA and Dichgans M (2010) Advances in stroke 2009: update on the genetics of stroke and cerebrovascular disease 2009. *Stroke* **41**:e63-66.
- Heiss WD (2000) Ischemic penumbra: evidence from functional imaging in man. *J Cereb Blood Flow Metab* **20**:1276-1293.
- Hetman M and Gozdz A (2004) Role of extracellular signal regulated kinases 1 and 2 in neuronal survival. *European journal of biochemistry / FEBS* **271**:2050-2055.
- Hetman M and Kharebava G (2006) Survival signaling pathways

- activated by NMDA receptors. *Current topics in medicinal chemistry* **6**:787-799.
- Hill MD, Martin RH, Mikulis D, Wong JH, Silver FL, Terbrugge KG, Milot G, Clark WM, Macdonald RL, Kelly ME, Boulton M, Fleetwood I, McDougall C, Gunnarsson T, Chow M, Lum C, Dodd R, Poublanc J, Krings T, Demchuk AM, Goyal M, Anderson R, Bishop J, Garman D, Tymianski M and investigators Et (2012) Safety and efficacy of NA-1 in patients with iatrogenic stroke after endovascular aneurysm repair (ENACT): a phase 2, randomised, double-blind, placebo-controlled trial. *Lancet Neurol* **11**:942-950.
- Hollmann M and Heinemann S (1994) Cloned glutamate receptors. *Annual review of neuroscience* **17**:31-108.
- Horn J and Limburg M (2000) Calcium antagonists for acute ischemic stroke. *The Cochrane database of systematic reviews*:CD001928.
- Hossain IM, Hoque A, Lessene G, Aizuddin Kamaruddin M, Chu PW, Ng IH, Irtegun S, Ng DC, Bogoyevitch MA, Burgess AW, Hill AF and Cheng HC (2015) Dual role of Src kinase in governing neuronal survival. *Brain Res* **1594**:1-14.
- Hossain MI, Kamaruddin MA and Cheng HC (2012) Aberrant regulation and function of Src family tyrosine kinases: Their potential contributions to glutamate-induced neurotoxicity. *Clin Exp Pharmacol Physiol* **39**:684-691.
- Hossain MI, Roulston CL, Kamaruddin MA, Chu PW, Ng DC, Dusting GJ, Bjorge JD, Williamson NA, Fujita DJ, Cheung SN, Chan TO, Hill AF and Cheng HC (2013) A truncated fragment of Src protein kinase generated by calpain-mediated cleavage is a mediator of neuronal death in excitotoxicity. *J Biol Chem* **288**:9696-9709.
- Hou ST, Jiang SX, Aylsworth A, Cooke M and Zhou L (2013) Collapsin response mediator protein 3 deacetylates histone H4 to mediate nuclear condensation and neuronal death. *Sci Rep* **3**:1350.
- Hou ST, Jiang SX, Desbois A, Huang D, Kelly J, Tessier L, Karchewski L and Kappler J (2006) Calpain-cleaved collapsin response mediator protein-3 induces neuronal death after glutamate toxicity and cerebral ischemia. *J Neurosci* **26**:2241-2249.
- Hou XY, Liu Y and Zhang GY (2007) PP2, a potent inhibitor of Src family kinases, protects against hippocampal CA1 pyramidal cell death after transient global brain ischemia. *Neurosci Lett* **420**:235-239.
- Howard R, McShane R, Lindsay J, Ritchie C, Baldwin A, Barber R, Burns A, Dening T, Findlay D, Holmes C, Hughes A, Jacoby R, Jones R, Jones R, McKeith I, Macharouthu A, O'Brien J, Passmore P, Sheehan B, Juszcak E, Katona C, Hills R, Knapp M, Ballard C, Brown R, Banerjee S, Onions C, Griffin M, Adams J, Gray R, Johnson T, Bentham P and Phillips P (2012) Donepezil and memantine for moderate-to-severe Alzheimer's disease. *N Engl J Med* **366**:893-903.
- Howitt J, Lackovic J, Low LH, Naguib A, Macintyre A, Goh CP, Callaway JK, Hammond V, Thomas T, Dixon M, Putz U, Silke J, Bartlett P, Yang B, Kumar S, Trotman LC and Tan SS (2012) Ndfip1

- regulates nuclear Pten import in vivo to promote neuronal survival following cerebral ischemia. *J Cell Biol* **196**:29-36.
- Hsu JL, Huang SY, Chow NH and Chen SH (2003) Stable-isotope dimethyl labeling for quantitative proteomics. *Analytical chemistry* **75**:6843-6852.
- Hu SQ, Ye JS, Zong YY, Sun CC, Liu DH, Wu YP, Song T and Zhang GY (2012) S-nitrosylation of mixed lineage kinase 3 contributes to its activation after cerebral ischemia. *J Biol Chem* **287**:2364-2377.
- Husi H, Ward MA, Choudhary JS, Blackstock WP and Grant SG (2000) Proteomic analysis of NMDA receptor-adhesion protein signaling complexes. *Nat Neurosci* **3**:661-669.
- Hwang JY, Aromolaran KA and Zukin RS (2013) Epigenetic mechanisms in stroke and epilepsy. *Neuropsychopharmacology* **38**:167-182.
- Hwang JY, Kaneko N, Noh KM, Pontarelli F and Zukin RS (2014) The gene silencing transcription factor REST represses miR-132 expression in hippocampal neurons destined to die. *Journal of molecular biology* **426**:3454-3466.
- Ignelzi MA, Jr., Miller DR, Soriano P and Maness PF (1994) Impaired neurite outgrowth of src-minus cerebellar neurons on the cell adhesion molecule L1. *Neuron* **12**:873-884.
- Ingraham CA, Cox ME, Ward DC, Fults DW and Maness PF (1989) c-src and other proto-oncogenes implicated in neuronal differentiation. *Molecular and chemical neuropathology* / sponsored by the International Society for Neurochemistry and the World Federation of Neurology and research groups on neurochemistry and cerebrospinal fluid **10**:1-14.
- Ittner LM, Ke YD, Delerue F, Bi M, Gladbach A, van Eersel J, Wolfing H, Chieng BC, Christie MJ, Napier IA, Eckert A, Staufenbiel M, Hardeman E and Gotz J (2010) Dendritic function of tau mediates amyloid-beta toxicity in Alzheimer's disease mouse models. *Cell* **142**:387-397.
- Iwasaki Y, Negishi T, Inoue M, Tashiro T, Tabira T and Kimura N (2012) Sendai virus vector-mediated brain-derived neurotrophic factor expression ameliorates memory deficits and synaptic degeneration in a transgenic mouse model of Alzheimer's disease. *J Neurosci Res* **90**:981-989.
- Jackson TC, Verrier JD, Semple-Rowland S, Kumar A and Foster TC (2010) PHLPP1 splice variants differentially regulate AKT and PKCalpha signaling in hippocampal neurons: characterization of PHLPP proteins in the adult hippocampus. *J Neurochem* **115**:941-955.
- Jayanthi S, Deng X, Ladenheim B, McCoy MT, Cluster A, Cai NS and Cadet JL (2005) Calcineurin/NFAT-induced up-regulation of the Fas ligand/Fas death pathway is involved in methamphetamine-induced neuronal apoptosis. *Proc Natl Acad Sci U S A* **102**:868-873.
- Jeffs GJ, Meloni BP, Bakker AJ and Knuckey NW (2007) The role of the Na(+)/Ca(2+) exchanger (NCX) in neurons following ischaemia. *Journal of clinical neuroscience : official journal of*

- the Neurosurgical Society of Australasia* **14**:507-514.
- Johnson CE, Huang YY, Parrish AB, Smith MI, Vaughn AE, Zhang Q, Wright KM, Van Dyke T, Wechsler-Reya RJ, Kornbluth S and Deshmukh M (2007) Differential Apaf-1 levels allow cytochrome c to induce apoptosis in brain tumors but not in normal neural tissues. *Proc Natl Acad Sci U S A* **104**:20820-20825.
- Johnson GL and Lapadat R (2002) Mitogen-activated protein kinase pathways mediated by ERK, JNK, and p38 protein kinases. *Science* **298**:1911-1912.
- Jones R, Sheehan B, Phillips P, Juszczak E, Adams J, Baldwin A, Ballard C, Banerjee S, Barber B, Bentham P, Brown R, Burns A, Denning T, Findlay D, Gray R, Griffin M, Holmes C, Hughes A, Jacoby R, Johnson T, Jones R, Knapp M, Lindsay J, McKeith I, McShane R, Macharouthu A, O'Brien J, Onions C, Passmore P, Raftery J, Ritchie C, Howard R and team D-A (2009) DOMINO-AD protocol: donepezil and memantine in moderate to severe Alzheimer's disease - a multicentre RCT. *Trials* **10**:57.
- Jones RW (2010) A review comparing the safety and tolerability of memantine with the acetylcholinesterase inhibitors. *Int J Geriatr Psychiatry* **25**:547-553.
- Kakizawa T, Ota Y, Itoh Y, Tsumoto H and Suzuki T (2015) Histone H3 peptide based LSD1-selective inhibitors. *Bioorg Med Chem Lett* **25**:1925-1928.
- Kaneko N, Hwang JY, Gertner M, Pontarelli F and Zukin RS (2014) Casein kinase 1 suppresses activation of REST in insulted hippocampal neurons and halts ischemia-induced neuronal death. *J Neurosci* **34**:6030-6039.
- Kaneko S, Kawakami S, Hara Y, Wakamori M, Itoh E, Minami T, Takada Y, Kume T, Katsuki H, Mori Y and Akaike A (2006) A critical role of TRPM2 in neuronal cell death by hydrogen peroxide. *Journal of pharmacological sciences* **101**:66-76.
- Kang TH, Bae KH, Yu MJ, Kim WK, Hwang HR, Jung H, Lee PY, Kang S, Yoon TS, Park SG, Ryu SE and Lee SC (2007) Phosphoproteomic analysis of neuronal cell death by glutamate-induced oxidative stress. *Proteomics* **7**:2624-2635.
- Karpova A, Mikhaylova M, Bera S, Bar J, Reddy PP, Behnisch T, Rankovic V, Spilker C, Bethge P, Sahin J, Kaushik R, Zuschratter W, Kahne T, Naumann M, Gundelfinger ED and Kreutz MR (2013) Encoding and transducing the synaptic or extrasynaptic origin of NMDA receptor signals to the nucleus. *Cell* **152**:1119-1133.
- Kashiwagi K, Masuko T, Nguyen CD, Kuno T, Tanaka I, Igarashi K and Williams K (2002) Channel blockers acting at N-methyl-D-aspartate receptors: differential effects of mutations in the vestibule and ion channel pore. *Mol Pharmacol* **61**:533-545.
- Kaufman AM, Milnerwood AJ, Sepers MD, Coquinco A, She K, Wang L, Lee H, Craig AM, Cynader M and Raymond LA (2012) Opposing Roles of Synaptic and Extrasynaptic NMDA Receptor Signaling in Cocultured Striatal and Cortical Neurons. *J Neurosci* **32**:3992-4003.

- Khanna S, Roy S, Park HA and Sen CK (2007) Regulation of c-Src activity in glutamate-induced neurodegeneration. *J Biol Chem* **282**:23482-23490.
- Kieran D and Greensmith L (2004) Inhibition of calpains, by treatment with leupeptin, improves motoneuron survival and muscle function in models of motoneuron degeneration. *Neuroscience* **125**:427-439.
- Kikuchi H, Yamada T, Furuya H, Doh-ura K, Ohyagi Y, Iwaki T and Kira J (2003) Involvement of cathepsin B in the motor neuron degeneration of amyotrophic lateral sclerosis. *Acta Neuropathol* **105**:462-468.
- Kim MJ, Jo DG, Hong GS, Kim BJ, Lai M, Cho DH, Kim KW, Bandyopadhyay A, Hong YM, Kim DH, Cho C, Liu JO, Snyder SH and Jung YK (2002) Calpain-dependent cleavage of cain/cabin1 activates calcineurin to mediate calcium-triggered cell death. *Proc Natl Acad Sci U S A* **99**:9870-9875.
- Kim YS, Choi MY, Lee DH, Jeon BT, Roh GS, Kim HJ, Kang SS, Cho GJ and Choi WS (2014) Decreased interaction between FoxO3a and Akt correlates with seizure-induced neuronal death. *Epilepsy Res* **108**:367-378.
- Kirkpatrick DS, Gerber SA and Gygi SP (2005) The absolute quantification strategy: a general procedure for the quantification of proteins and post-translational modifications. *Methods* **35**:265-273.
- Kleifeld O, Doucet A, auf dem Keller U, Prudova A, Schilling O, Kainthan RK, Starr AE, Foster LJ, Kizhakkedathu JN and Overall CM (2010) Isotopic labeling of terminal amines in complex samples identifies protein N-termini and protease cleavage products. *Nat Biotechnol* **28**:281-288.
- Kleppe R, Martinez A, Doskeland SO and Haavik J (2011) The 14-3-3 proteins in regulation of cellular metabolism. *Seminars in cell & developmental biology* **22**:713-719.
- Koshiji M, Kageyama Y, Pete EA, Horikawa I, Barrett JC and Huang LE (2004) HIF-1alpha induces cell cycle arrest by functionally counteracting Myc. *EMBO J* **23**:1949-1956.
- Kotermanski SE, Wood JT and Johnson JW (2009) Memantine binding to a superficial site on NMDA receptors contributes to partial trapping. *J Physiol* **587**:4589-4604.
- Kovacina KS, Park GY, Bae SS, Guzzetta AW, Schaefer E, Birnbaum MJ and Roth RA (2003) Identification of a proline-rich Akt substrate as a 14-3-3 binding partner. *J Biol Chem* **278**:10189-10194.
- Kruger M, Moser M, Ussar S, Thievensen I, Luber CA, Forner F, Schmidt S, Zanivan S, Fassler R and Mann M (2008) SILAC mouse for quantitative proteomics uncovers kindlin-3 as an essential factor for red blood cell function. *Cell* **134**:353-364.
- Kumar J, Schuck P and Mayer ML (2011) Structure and assembly mechanism for heteromeric kainate receptors. *Neuron* **71**:319-331.
- Kwok RP, Lundblad JR, Chrivia JC, Richards JP, Bachinger HP, Brennan RG, Roberts SG, Green MR and Goodman RH (1994) Nuclear protein CBP is a

- coactivator for the transcription factor CREB. *Nature* **370**:223-226.
- Lai TW, Zhang S and Wang YT (2014) Excitotoxicity and stroke: identifying novel targets for neuroprotection. *Prog Neurobiol* **115**:157-188.
- Lalumiere M and Richardson CD (1995) Production of recombinant baculoviruses using rapid screening vectors that contain the gene for beta-galactosidase. *Methods Mol Biol* **39**:161-177.
- Larson M, Sherman MA, Amar F, Nuvolone M, Schneider JA, Bennett DA, Aguzzi A and Lesne SE (2012) The complex PrP(c)-Fyn couples human oligomeric Abeta with pathological tau changes in Alzheimer's disease. *J Neurosci* **32**:16857-16871a.
- Lau D and Bading H (2009) Synaptic activity-mediated suppression of p53 and induction of nuclear calcium-regulated neuroprotective genes promote survival through inhibition of mitochondrial permeability transition. *J Neurosci* **29**:4420-4429.
- Lau D, Bengtson CP, Buchthal B and Bading H (2015) BDNF Reduces Toxic Extrasynaptic NMDA Receptor Signaling via Synaptic NMDA Receptors and Nuclear-Calcium-Induced Transcription of inhba/Activin A. *Cell Rep* **12**:1353-1366.
- Lawler S, Fleming Y, Goedert M and Cohen P (1998) Synergistic activation of SAPK1/JNK1 by two MAP kinase kinases in vitro. *Curr Biol* **8**:1387-1390.
- Lee IH, Dinudom A, Sanchez-Perez A, Kumar S and Cook DI (2007) Akt mediates the effect of insulin on epithelial sodium channels by inhibiting Nedd4-2. *J Biol Chem* **282**:29866-29873.
- Lee MS, Kwon YT, Li M, Peng J, Friedlander RM and Tsai LH (2000) Neurotoxicity induces cleavage of p35 to p25 by calpain. *Nature* **405**:360-364.
- Leveille F, Papadia S, Fricker M, Bell KF, Soriano FX, Martel MA, Puddifoot C, Habel M, Wyllie DJ, Ikonomidou C, Tolkovsky AM and Hardingham GE (2010) Suppression of the intrinsic apoptosis pathway by synaptic activity. *J Neurosci* **30**:2623-2635.
- Lew J, Huang QQ, Qi Z, Winkfein RJ, Aebersold R, Hunt T and Wang JH (1994) A brain-specific activator of cyclin-dependent kinase 5. *Nature* **371**:423-426.
- Lew J and Wang JH (1995) Neuronal cdc2-like kinase. *Trends Biochem Sci* **20**:33-37.
- Lewis SB, Velat GJ, Miralia L, Papa L, Aikman JM, Wolper RA, Firment CS, Liu MC, Pineda JA, Wang KK and Hayes RL (2007) Alpha-II spectrin breakdown products in aneurysmal subarachnoid hemorrhage: a novel biomarker of proteolytic injury. *Journal of neurosurgery* **107**:792-796.
- Li AG, Piluso LG, Cai X, Wei G, Sellers WR and Liu X (2006) Mechanistic insights into maintenance of high p53 acetylation by PTEN. *Mol Cell* **23**:575-587.
- Li H, Huang J, Du W, Jia C, Yao H and Wang Y (2012) TRPC6 inhibited NMDA receptor activities and protected neurons from ischemic excitotoxicity. *J Neurochem* **123**:1010-1018.
- Li Y, Xu X, Qi D, Deng C, Yang P and Zhang X (2008) Novel

- Fe₃O₄@TiO₂ core-shell microspheres for selective enrichment of phosphopeptides in phosphoproteome analysis. *J Proteome Res* **7**:2526-2538.
- Liao L, Park SK, Xu T, Vanderklish P and Yates JR, 3rd (2008) Quantitative proteomic analysis of primary neurons reveals diverse changes in synaptic protein content in *fmr1* knockout mice. *Proc Natl Acad Sci U S A* **105**:15281-15286.
- Lin X, Shah S and Bulleit RF (1996) The expression of MEF2 genes is implicated in CNS neuronal differentiation. *Brain research Molecular brain research* **42**:307-316.
- Linseman DA, Butts BD, Precht TA, Phelps RA, Le SS, Laessig TA, Bouchard RJ, Florez-McClure ML and Heidenreich KA (2004) Glycogen synthase kinase-3 β phosphorylates Bax and promotes its mitochondrial localization during neuronal apoptosis. *J Neurosci* **24**:9993-10002.
- Lipton P (1999) Ischemic cell death in brain neurons. *Physiol Rev* **79**:1431-1568.
- Lipton SA (2007) Pathologically activated therapeutics for neuroprotection. *Nat Rev Neurosci* **8**:803-808.
- Liu DZ and Sharp FR (2011) The dual role of SRC kinases in intracerebral hemorrhage. *Acta Neurochir Suppl* **111**:77-81.
- Liu J, Liu MC and Wang KK (2008) Physiological and pathological actions of calpains in glutamatergic neurons. *Sci Signal* **1**:tr3.
- Liu J, Narasimhan P, Lee YS, Song YS, Endo H, Yu F and Chan PH (2006) Mild hypoxia promotes survival and proliferation of SOD2-deficient astrocytes via c-Myc activation. *J Neurosci* **26**:4329-4337.
- Liu XS, Chopp M, Wang XL, Zhang L, Hozeska-Solgot A, Tang T, Kassis H, Zhang RL, Chen C, Xu J and Zhang ZG (2013) MicroRNA-17-92 cluster mediates the proliferation and survival of neural progenitor cells after stroke. *J Biol Chem* **288**:12478-12488.
- Lo EH, Dalkara T and Moskowitz MA (2003) Mechanisms, challenges and opportunities in stroke. *Nat Rev Neurosci* **4**:399-415.
- Loeffler M, Daugas E, Susin SA, Zamzami N, Metivier D, Nieminen AL, Brothers G, Penninger JM and Kroemer G (2001) Dominant cell death induction by extramitochondrially targeted apoptosis-inducing factor. *FASEB J* **15**:758-767.
- Lopez de Armentia M, Leeson AH, Stebbing MJ, Urban L and McLachlan EM (2003) Responses to sympathomimetics in rat sensory neurones after nerve transection. *Neuroreport* **14**:9-13.
- Loroch S, Dickhut C, Zahedi RP and Sickmann A (2013) Phosphoproteomics--more than meets the eye. *Electrophoresis* **34**:1483-1492.
- Lowell CA and Soriano P (1996) Knockouts of Src-family kinases: stiff bones, wimpy T cells, and bad memories. *Genes & development* **10**:1845-1857.
- Lu T, Aron L, Zullo J, Pan Y, Kim H, Chen Y, Yang TH, Kim HM, Drake D, Liu XS, Bennett DA, Colaiacovo MP and Yankner BA (2014) REST and stress resistance

- in ageing and Alzheimer's disease. *Nature* **507**:448-454.
- Luo HR, Hattori H, Hossain MA, Hester L, Huang Y, Lee-Kwon W, Donowitz M, Nagata E and Snyder SH (2003) Akt as a mediator of cell death. *Proc Natl Acad Sci U S A* **100**:11712-11717.
- Luo XN, Mookerjee B, Ferrari A, Mistry S and Atweh GF (1994) Regulation of phosphoprotein p18 in leukemic cells. Cell cycle regulated phosphorylation by p34cdc2 kinase. *J Biol Chem* **269**:10312-10318.
- Lynch DR and Guttman RP (2001) NMDA receptor pharmacology: perspectives from molecular biology. *Current drug targets* **2**:215-231.
- Lyons GE, Micales BK, Schwarz J, Martin JF and Olson EN (1995) Expression of mef2 genes in the mouse central nervous system suggests a role in neuronal maturation. *J Neurosci* **15**:5727-5738.
- Ma H, Groth RD, Cohen SM, Emery JF, Li B, Hoedt E, Zhang G, Neubert TA and Tsien RW (2014) gammaCaMKII shuttles Ca(2+)(+)/CaM to the nucleus to trigger CREB phosphorylation and gene expression. *Cell* **159**:281-294.
- Ma LY, Zheng YC, Wang SQ, Wang B, Wang ZR, Pang LP, Zhang M, Wang JW, Ding L, Li J, Wang C, Hu B, Liu Y, Zhang XD, Wang JJ, Wang ZJ, Zhao W and Liu HM (2015) Design, synthesis, and structure-activity relationship of novel LSD1 inhibitors based on pyrimidine-thiourea hybrids as potent, orally active antitumor agents. *Journal of medicinal chemistry* **58**:1705-1716.
- MacLean B, Tomazela DM, Shulman N, Chambers M, Finney GL, Frewen B, Kern R, Tabb DL, Liebler DC and MacCoss MJ (2010) Skyline: an open source document editor for creating and analyzing targeted proteomics experiments. *Bioinformatics* **26**:966-968.
- Maehama T and Dixon JE (1998) The tumor suppressor, PTEN/MMAC1, dephosphorylates the lipid second messenger, phosphatidylinositol 3,4,5-trisphosphate. *J Biol Chem* **273**:13375-13378.
- Maehama T and Dixon JE (1999) PTEN: a tumour suppressor that functions as a phospholipid phosphatase. *Trends in cell biology* **9**:125-128.
- Mandic A, Viktorsson K, Strandberg L, Heiden T, Hansson J, Linder S and Shoshan MC (2002) Calpain-mediated Bid cleavage and calpain-independent Bak modulation: two separate pathways in cisplatin-induced apoptosis. *Molecular and cellular biology* **22**:3003-3013.
- Maness PF (1992) Nonreceptor protein tyrosine kinases associated with neuronal development. *Dev Neurosci* **14**:257-270.
- Maness PF, Shores CG and Ignelzi M (1990) Localization of the normal cellular src protein to the growth cone of differentiating neurons in brain and retina. *Advances in experimental medicine and biology* **265**:117-125.
- Manev H, Favaron M, Guidotti A and Costa E (1989) Delayed increase of Ca²⁺ influx elicited by glutamate: role in neuronal death. *Mol Pharmacol* **36**:106-112.
- Mann M, Hendrickson RC and Pandey A (2001) Analysis of proteins and proteomes by mass spectrometry.

- Annual review of biochemistry* **70**:437-473.
- Mann M and Jensen ON (2003) Proteomic analysis of post-translational modifications. *Nat Biotechnol* **21**:255-261.
- Manning G, Whyte DB, Martinez R, Hunter T and Sudarsanam S (2002) The protein kinase complement of the human genome. *Science* **298**:1912-1934.
- Marcoux FW, Probert AW, Jr. and Weber ML (1990) Hypoxic neuronal injury in tissue culture is associated with delayed calcium accumulation. *Stroke* **21**:III71-74.
- Martel MA, Ryan TJ, Bell KF, Fowler JH, McMahon A, Al-Mubarak B, Komiyama NH, Horsburgh K, Kind PC, Grant SG, Wyllie DJ and Hardingham GE (2012) The subtype of GluN2 C-terminal domain determines the response to excitotoxic insults. *Neuron* **74**:543-556.
- Mathers CD, Boerma T and Ma Fat D (2009) Global and regional causes of death. *Br Med Bull* **92**:7-32.
- Mattson MP (2000) Apoptosis in neurodegenerative disorders. *Nature reviews Molecular cell biology* **1**:120-129.
- Mattson MP (2003) Excitotoxic and excitoprotective mechanisms: abundant targets for the prevention and treatment of neurodegenerative disorders. *Neuromolecular Med* **3**:65-94.
- Mattson MP, Cheng B, Davis D, Bryant K, Lieberburg I and Rydel RE (1992) beta-Amyloid peptides destabilize calcium homeostasis and render human cortical neurons vulnerable to excitotoxicity. *J Neurosci* **12**:376-389.
- Mayr B and Montminy M (2001) Transcriptional regulation by the phosphorylation-dependent factor CREB. *Nature reviews Molecular cell biology* **2**:599-609.
- Mehta SL, Manhas N and Raghbir R (2007) Molecular targets in cerebral ischemia for developing novel therapeutics. *Brain Res Rev* **54**:34-66.
- Merali Z, Gao MM, Bowes T, Chen J, Evans K and Kassner A (2014) Neuroproteome changes after ischemia/reperfusion injury and tissue plasminogen activator administration in rats: a quantitative iTRAQ proteomics study. *PLoS One* **9**:e98706.
- Meyer DA, Torres-Altora MI, Tan Z, Tozzi A, Di Filippo M, DiNapoli V, Plattner F, Kansy JW, Benkovic SA, Huber JD, Miller DB, Greengard P, Calabresi P, Rosen CL and Bibb JA (2014) Ischemic stroke injury is mediated by aberrant Cdk5. *J Neurosci* **34**:8259-8267.
- Meyn MA, 3rd, Wilson MB, Abdi FA, Fahey N, Schiavone AP, Wu J, Hochrein JM, Engen JR and Smithgall TE (2006) Src family kinases phosphorylate the Bcr-Abl SH3-SH2 region and modulate Bcr-Abl transforming activity. *J Biol Chem* **281**:30907-30916.
- Miller DJ, Simpson JR and Silver B (2011) Safety of thrombolysis in acute ischemic stroke: a review of complications, risk factors, and newer technologies. *Neurohospitalist* **1**:138-147.
- Milnerwood AJ, Gladding CM, Pouladi MA, Kaufman AM, Hines RM, Boyd JD, Ko RW, Vasuta OC, Graham RK, Hayden MR, Murphy TH and Raymond LA (2010) Early increase in

- extrasynaptic NMDA receptor signaling and expression contributes to phenotype onset in Huntington's disease mice. *Neuron* **65**:178-190.
- Miyawaki T, Ofengeim D, Noh KM, Latuszek-Barrantes A, Hemmings BA, Follenzi A and Zukin RS (2009) The endogenous inhibitor of Akt, CTMP, is critical to ischemia-induced neuronal death. *Nat Neurosci* **12**:618-626.
- Mony L, Kew JN, Gunthorpe MJ and Paoletti P (2009) Allosteric modulators of NR2B-containing NMDA receptors: molecular mechanisms and therapeutic potential. *Br J Pharmacol* **157**:1301-1317.
- Morse WR, Whitesides JG, 3rd, LaMantia AS and Maness PF (1998) p59fyn and pp60c-src modulate axonal guidance in the developing mouse olfactory pathway. *Journal of neurobiology* **36**:53-63.
- Moskowitz MA, Lo EH and Iadecola C (2010) The science of stroke: mechanisms in search of treatments. *Neuron* **67**:181-198.
- Motoyama A, Xu T, Ruse CI, Wohlschlegel JA and Yates JR, 3rd (2007) Anion and cation mixed-bed ion exchange for enhanced multidimensional separations of peptides and phosphopeptides. *Analytical chemistry* **79**:3623-3634.
- Mukherjee A and Soto C (2011) Role of calcineurin in neurodegeneration produced by misfolded proteins and endoplasmic reticulum stress. *Curr Opin Cell Biol* **23**:223-230.
- Nakae J, Barr V and Accili D (2000) Differential regulation of gene expression by insulin and IGF-1 receptors correlates with phosphorylation of a single amino acid residue in the forkhead transcription factor FKHR. *EMBO J* **19**:989-996.
- Nakagawa K, Masumoto H, Sorimachi H and Suzuki K (2001) Dissociation of m-calpain subunits occurs after autolysis of the N-terminus of the catalytic subunit, and is not required for activation. *Journal of biochemistry* **130**:605-611.
- Nakamura T and Lipton SA (2016) Protein S-Nitrosylation as a Therapeutic Target for Neurodegenerative Diseases. *Trends Pharmacol Sci* **37**:73-84.
- Nakamura T, Tu S, Akhtar MW, Sunico CR, Okamoto S and Lipton SA (2013) Aberrant protein s-nitrosylation in neurodegenerative diseases. *Neuron* **78**:596-614.
- Nakka VP, Gusain A, Mehta SL and Raghuram R (2008) Molecular mechanisms of apoptosis in cerebral ischemia: multiple neuroprotective opportunities. *Mol Neurobiol* **37**:7-38.
- Namikawa K, Honma M, Abe K, Takeda M, Mansur K, Obata T, Miwa A, Okado H and Kiyama H (2000) Akt/protein kinase B prevents injury-induced motoneuron death and accelerates axonal regeneration. *J Neurosci* **20**:2875-2886.
- Newton AC and Trotman LC (2014) Turning off AKT: PHLPP as a drug target. *Annu Rev Pharmacol Toxicol* **54**:537-558.
- Nicotera P and Bano D (2003) The enemy at the gates. Ca²⁺ entry through TRPM7 channels and anoxic neuronal death. *Cell* **115**:768-770.
- NINDS.(rt-PA).SSG (1995) Tissue plasminogen activator for acute ischemic stroke. The National Institute of Neurological

- Disorders and Stroke rt-PA Stroke Study Group. *N Engl J Med* **333**:1581-1587.
- Nixon RA, Saito KI, Grynspan F, Griffin WR, Katayama S, Honda T, Mohan PS, Shea TB and Beermann M (1994) Calcium-activated neutral proteinase (calpain) system in aging and Alzheimer's disease. *Annals of the New York Academy of Sciences* **747**:77-91.
- Noh KM, Hwang JY, Follenzi A, Athanasiadou R, Miyawaki T, Grealley JM, Bennett MV and Zukin RS (2012) Repressor element-1 silencing transcription factor (REST)-dependent epigenetic remodeling is critical to ischemia-induced neuronal death. *Proc Natl Acad Sci U S A* **109**:E962-971.
- Norberg E, Gogvadze V, Ott M, Horn M, Uhlen P, Orrenius S and Zhivotovsky B (2008) An increase in intracellular Ca²⁺ is required for the activation of mitochondrial calpain to release AIF during cell death. *Cell Death Differ* **15**:1857-1864.
- Nowak L, Bregestovski P, Ascher P, Herbert A and Prochiantz A (1984) Magnesium gates glutamate-activated channels in mouse central neurones. *Nature* **307**:462-465.
- O'Collins VE, Macleod MR, Donnan GA, Horky LL, van der Worp BH and Howells DW (2006) 1,026 experimental treatments in acute stroke. *Ann Neurol* **59**:467-477.
- Obata T, Yaffe MB, Leparac GG, Piro ET, Maegawa H, Kashiwagi A, Kikkawa R and Cantley LC (2000) Peptide and protein library screening defines optimal substrate motifs for AKT/PKB. *J Biol Chem* **275**:36108-36115.
- Oda A, Druker BJ, Ariyoshi H, Smith M and Salzman EW (1993) pp60src is an endogenous substrate for calpain in human blood platelets. *J Biol Chem* **268**:12603-12608.
- Ogura M, Yamaki J, Homma MK and Homma Y (2012) Mitochondrial c-Src regulates cell survival through phosphorylation of respiratory chain components. *Biochem J* **447**:281-289.
- Okamoto S, Pouladi MA, Talantova M, Yao D, Xia P, Ehrnhoefer DE, Zaidi R, Clemente A, Kaul M, Graham RK, Zhang D, Vincent Chen HS, Tong G, Hayden MR and Lipton SA (2009) Balance between synaptic versus extrasynaptic NMDA receptor activity influences inclusions and neurotoxicity of mutant huntingtin. *Nat Med* **15**:1407-1413.
- Old WM, Meyer-Arendt K, Aveline-Wolf L, Pierce KG, Mendoza A, Sevinsky JR, Resing KA and Ahn NG (2005) Comparison of label-free methods for quantifying human proteins by shotgun proteomics. *Molecular & cellular proteomics : MCP* **4**:1487-1502.
- Ong SE, Blagoev B, Kratchmarova I, Kristensen DB, Steen H, Pandey A and Mann M (2002) Stable isotope labeling by amino acids in cell culture, SILAC, as a simple and accurate approach to expression proteomics. *Molecular & cellular proteomics : MCP* **1**:376-386.
- Ong SE and Mann M (2005) Mass spectrometry-based proteomics turns quantitative. *Nature chemical biology* **1**:252-262.

- Ong WY, Tanaka K, Dawe GS, Ittner LM and Farooqui AA (2013) Slow excitotoxicity in Alzheimer's disease. *J Alzheimers Dis* **35**:643-668.
- Ooi L and Wood IC (2007) Chromatin crosstalk in development and disease: lessons from REST. *Nature reviews Genetics* **8**:544-554.
- Osaki M, Oshimura M and Ito H (2004) PI3K-Akt pathway: its functions and alterations in human cancer. *Apoptosis : an international journal on programmed cell death* **9**:667-676.
- Ozlu N, Akten B, Timm W, Haseley N, Steen H and Steen JA (2010) Phosphoproteomics. *Wiley interdisciplinary reviews Systems biology and medicine* **2**:255-276.
- Panov AV, Lund S and Greenamyre JT (2005) Ca^{2+} -induced permeability transition in human lymphoblastoid cell mitochondria from normal and Huntington's disease individuals. *Molecular and cellular biochemistry* **269**:143-152.
- Paoletti P, Bellone C and Zhou Q (2013) NMDA receptor subunit diversity: impact on receptor properties, synaptic plasticity and disease. *Nat Rev Neurosci* **14**:383-400.
- Pap M and Cooper GM (1998) Role of glycogen synthase kinase-3 in the phosphatidylinositol 3-Kinase/Akt cell survival pathway. *J Biol Chem* **273**:19929-19932.
- Papadia S, Soriano FX, Leveille F, Martel MA, Dakin KA, Hansen HH, Kaindl A, Siffringer M, Fowler J, Stefovskaja V, McKenzie G, Craigon M, Corriveau R, Ghazal P, Horsburgh K, Yankner BA, Wyllie DJ, Ikonomidou C and Hardingham GE (2008) Synaptic NMDA receptor activity boosts intrinsic antioxidant defenses. *Nat Neurosci* **11**:476-487.
- Parsons MP and Raymond LA (2014) Extrasynaptic NMDA receptor involvement in central nervous system disorders. *Neuron* **82**:279-293.
- Parsons SJ and Parsons JT (2004) Src family kinases, key regulators of signal transduction. *Oncogene* **23**:7906-7909.
- Pathan M, Keerthikumar S, Ang CS, Gangoda L, Quek CY, Williamson NA, Mouradov D, Sieber OM, Simpson RJ, Salim A, Bacic A, Hill AF, Stroud DA, Ryan MT, Agbinya JI, Mariadason JM, Burgess AW and Mathivanan S (2015) FunRich: An open access standalone functional enrichment and interaction network analysis tool. *Proteomics* **15**:2597-2601.
- Paul R, Zhang ZG, Eliceiri BP, Jiang Q, Boccia AD, Zhang RL, Chopp M and Cheresch DA (2001) Src deficiency or blockade of Src activity in mice provides cerebral protection following stroke. *Nat Med* **7**:222-227.
- Pene-Dumitrescu T, Peterson LF, Donato NJ and Smithgall TE (2008) An inhibitor-resistant mutant of Hck protects CML cells against the antiproliferative and apoptotic effects of the broad-spectrum Src family kinase inhibitor A-419259. *Oncogene* **27**:7055-7069.
- Pettigrew LC, Holtz ML, Craddock SD, Minger SL, Hall N and Geddes JW (1996) Microtubular proteolysis in focal cerebral ischemia. *J Cereb Blood Flow Metab* **16**:1189-1202.
- Piatkov KI, Oh JH, Liu Y and Varshavsky A (2014) Calpain-generated natural protein fragments as short-

- lived substrates of the N-end rule pathway. *Proc Natl Acad Sci U S A* **111**:E817-826.
- Pinkse MW, Uitto PM, Hilhorst MJ, Ooms B and Heck AJ (2004) Selective isolation at the femtomole level of phosphopeptides from proteolytic digests using 2D-NanoLC-ESI-MS/MS and titanium oxide precolumns. *Analytical chemistry* **76**:3935-3943.
- Pirianov G, Brywe KG, Mallard C, Edwards AD, Flavell RA, Hagberg H and Mehmet H (2007) Deletion of the c-Jun N-terminal kinase 3 gene protects neonatal mice against cerebral hypoxic-ischaemic injury. *J Cereb Blood Flow Metab* **27**:1022-1032.
- Plum S, Steinbach S, Abel L, Marcus K, Helling S and May C (2015) Proteomics in neurodegenerative diseases: Methods for obtaining a closer look at the neuronal proteome. *Proteomics Clinical applications* **9**:848-871.
- Polat AN, Kraiczek K, Heck AJ, Rajmakers R and Mohammed S (2012) Fully automated isotopic dimethyl labeling and phosphopeptide enrichment using a microfluidic HPLC phosphochip. *Analytical and bioanalytical chemistry* **404**:2507-2512.
- Polat AN and Ozlu N (2014) Towards single-cell LC-MS phosphoproteomics. *The Analyst* **139**:4733-4749.
- Polster BM, Basanez G, Etxebarria A, Hardwick JM and Nicholls DG (2005) Calpain I induces cleavage and release of apoptosis-inducing factor from isolated mitochondria. *J Biol Chem* **280**:6447-6454.
- Pottorf WJ, 2nd, Johanns TM, Derrington SM, Strehler EE, Enyedi A and Thayer SA (2006) Glutamate-induced protease-mediated loss of plasma membrane Ca²⁺ pump activity in rat hippocampal neurons. *J Neurochem* **98**:1646-1656.
- Potts PR, Singh S, Knezek M, Thompson CB and Deshmukh M (2003) Critical function of endogenous XIAP in regulating caspase activation during sympathetic neuronal apoptosis. *J Cell Biol* **163**:789-799.
- Pozniak CD, Sengupta Ghosh A, Gogineni A, Hanson JE, Lee SH, Larson JL, Solanoy H, Bustos D, Li H, Ngu H, Jubb AM, Ayalon G, Wu J, Scarce-Levie K, Zhou Q, Weimer RM, Kirkpatrick DS and Lewcock JW (2013) Dual leucine zipper kinase is required for excitotoxicity-induced neuronal degeneration. *J Exp Med* **210**:2553-2567.
- Prusevich P, Kalin JH, Ming SA, Basso M, Givens J, Li X, Hu J, Taylor MS, Cieniewicz AM, Hsiao PY, Huang R, Roberson H, Adejola N, Avery LB, Casero RA, Jr., Taverna SD, Qian J, Tackett AJ, Ratan RR, McDonald OG, Feinberg AP and Cole PA (2014) A selective phenelzine analogue inhibitor of histone demethylase LSD1. *ACS chemical biology* **9**:1284-1293.
- Rahman MA, Senga T, Ito S, Hyodo T, Hasegawa H and Hamaguchi M (2010) S-nitrosylation at cysteine 498 of c-Src tyrosine kinase regulates nitric oxide-mediated cell invasion. *J Biol Chem* **285**:3806-3814.
- Renner M, Lacor PN, Velasco PT, Xu J, Contractor A, Klein WL and Triller A (2010) Deleterious

- effects of amyloid beta oligomers acting as an extracellular scaffold for mGluR5. *Neuron* **66**:739-754.
- Reynolds IJ and Miller RJ (1989) Ifenprodil is a novel type of N-methyl-D-aspartate receptor antagonist: interaction with polyamines. *Mol Pharmacol* **36**:758-765.
- Ritter LS, Orozco JA, Coull BM, McDonagh PF and Rosenblum WI (2000) Leukocyte accumulation and hemodynamic changes in the cerebral microcirculation during early reperfusion after stroke. *Stroke* **31**:1153-1161.
- Rodenas-Ruano A, Chavez AE, Cossio MJ, Castillo PE and Zukin RS (2012) REST-dependent epigenetic remodeling promotes the developmental switch in synaptic NMDA receptors. *Nat Neurosci* **15**:1382-1390.
- Ross PL, Huang YN, Marchese JN, Williamson B, Parker K, Hattan S, Khainovski N, Pillai S, Dey S, Daniels S, Purkayastha S, Juhasz P, Martin S, Bartlett-Jones M, He F, Jacobson A and Pappin DJ (2004) Multiplexed protein quantitation in *Saccharomyces cerevisiae* using amine-reactive isobaric tagging reagents. *Molecular & cellular proteomics : MCP* **3**:1154-1169.
- Rusconi L, Kilstrup-Nielsen C and Landsberger N (2011) Extrasynaptic N-methyl-D-aspartate (NMDA) receptor stimulation induces cytoplasmic translocation of the CDKL5 kinase and its proteasomal degradation. *J Biol Chem* **286**:36550-36558.
- Ryan SD, Dolatabadi N, Chan SF, Zhang X, Akhtar MW, Parker J, Soldner F, Sunico CR, Nagar S, Talantova M, Lee B, Lopez K, Nutter A, Shan B, Molokanova E, Zhang Y, Han X, Nakamura T, Masliah E, Yates JR, 3rd, Nakanishi N, Andreyev AY, Okamoto S, Jaenisch R, Ambasudhan R and Lipton SA (2013) Isogenic human iPSC Parkinson's model shows nitrosative stress-induced dysfunction in MEF2-PGC1alpha transcription. *Cell* **155**:1351-1364.
- Sahota P and Savitz SI (2011) Investigational therapies for ischemic stroke: neuroprotection and neurorecovery. *Neurotherapeutics* **8**:434-451.
- Saito K, Elce JS, Hamos JE and Nixon RA (1993) Widespread activation of calcium-activated neutral proteinase (calpain) in the brain in Alzheimer disease: a potential molecular basis for neuronal degeneration. *Proc Natl Acad Sci U S A* **90**:2628-2632.
- Salter MW and Kalia LV (2004) Src kinases: a hub for NMDA receptor regulation. *Nat Rev Neurosci* **5**:317-328.
- Sandilands E, Cans C, Fincham VJ, Brunton VG, Mellor H, Prendergast GC, Norman JC, Superti-Furga G and Frame MC (2004) RhoB and actin polymerization coordinate Src activation with endosome-mediated delivery to the membrane. *Dev Cell* **7**:855-869.
- Sattler R, Charlton MP, Hafner M and Tymianski M (1998) Distinct influx pathways, not calcium load, determine neuronal vulnerability to calcium neurotoxicity. *J Neurochem* **71**:2349-2364.
- Savitz SI and Fisher M (2007) Future of neuroprotection for acute stroke:

- in the aftermath of the SAINT trials. *Ann Neurol* **61**:396-402.
- Schilling B, Rardin MJ, MacLean BX, Zawadzka AM, Frewen BE, Cusack MP, Sorensen DJ, Bereman MS, Jing E, Wu CC, Verdin E, Kahn CR, Maccoss MJ and Gibson BW (2012) Platform-independent and label-free quantitation of proteomic data using MS1 extracted ion chromatograms in skyline: application to protein acetylation and phosphorylation. *Molecular & cellular proteomics : MCP* **11**:202-214.
- Schoenherr CJ and Anderson DJ (1995) The neuron-restrictive silencer factor (NRSF): a coordinate repressor of multiple neuron-specific genes. *Science* **267**:1360-1363.
- Sharma AK and Rohrer B (2004) Calcium-induced calpain mediates apoptosis via caspase-3 in a mouse photoreceptor cell line. *J Biol Chem* **279**:35564-35572.
- Shen WH, Balajee AS, Wang J, Wu H, Eng C, Pandolfi PP and Yin Y (2007) Essential role for nuclear PTEN in maintaining chromosomal integrity. *Cell* **128**:157-170.
- Shinoda S, Schindler CK, Meller R, So NK, Araki T, Yamamoto A, Lan JQ, Taki W, Simon RP and Henshall DC (2004) Bim regulation may determine hippocampal vulnerability after injurious seizures and in temporal lobe epilepsy. *J Clin Invest* **113**:1059-1068.
- Shioda N, Han F, Moriguchi S and Fukunaga K (2007) Constitutively active calcineurin mediates delayed neuronal death through Fas-ligand expression via activation of NFAT and FKHR transcriptional activities in mouse brain ischemia. *J Neurochem* **102**:1506-1517.
- Shioda N, Moriguchi S, Shirasaki Y and Fukunaga K (2006) Generation of constitutively active calcineurin by calpain contributes to delayed neuronal death following mouse brain ischemia. *J Neurochem* **98**:310-320.
- Shuaib A and Hachinski VC (1991) Mechanisms and management of stroke in the elderly. *CMAJ* **145**:433-443.
- Shukla V, Zheng YL, Mishra SK, Amin ND, Steiner J, Grant P, Kesavapany S and Pant HC (2013) A truncated peptide from p35, a Cdk5 activator, prevents Alzheimer's disease phenotypes in model mice. *FASEB J* **27**:174-186.
- Siman R and Noszek JC (1988) Excitatory amino acids activate calpain I and induce structural protein breakdown in vivo. *Neuron* **1**:279-287.
- Slupe AM, Merrill RA, Flippo KH, Lobas MA, Houtman JC and Strack S (2013) A calcineurin docking motif (LXVP) in dynamin-related protein 1 contributes to mitochondrial fragmentation and ischemic neuronal injury. *J Biol Chem* **288**:12353-12365.
- Small DL, Morley P and Buchan AM (1999) Biology of ischemic cerebral cell death. *Prog Cardiovasc Dis* **42**:185-207.
- Small DL, Morley, P. and Buchan, A.M. (2002) Current and Experimental Treatment of Stroke, in *Neuropsychopharmacology - 5th Generation of Progress* (Davis KL, Charney, D., Coyle, J.T. and Nemeroff, C. ed) pp 1327-1338, Lippincott, Williams, & Wilkins.

- Sommer B, Kohler M, Sprengel R and Seeburg PH (1991) RNA editing in brain controls a determinant of ion flow in glutamate-gated channels. *Cell* **67**:11-19.
- Soriano FX, Martel MA, Papadia S, Vaslin A, Baxter P, Rickman C, Forder J, Tymianski M, Duncan R, Aarts M, Clarke P, Wyllie DJ and Hardingham GE (2008) Specific targeting of pro-death NMDA receptor signals with differing reliance on the NR2B PDZ ligand. *J Neurosci* **28**:10696-10710.
- Soriano P, Montgomery C, Geske R and Bradley A (1991) Targeted disruption of the c-src proto-oncogene leads to osteopetrosis in mice. *Cell* **64**:693-702.
- Spellman DS, Deinhardt K, Darie CC, Chao MV and Neubert TA (2008) Stable isotopic labeling by amino acids in cultured primary neurons: application to brain-derived neurotrophic factor-dependent phosphotyrosine-associated signaling. *Molecular & cellular proteomics : MCP* **7**:1067-1076.
- Stam J (2005) Thrombosis of the cerebral veins and sinuses. *N Engl J Med* **352**:1791-1798.
- Stefanis L (2005) Caspase-dependent and -independent neuronal death: two distinct pathways to neuronal injury. *Neuroscientist* **11**:50-62.
- Stephens L, Anderson K, Stokoe D, Erdjument-Bromage H, Painter GF, Holmes AB, Gaffney PR, Reese CB, McCormick F, Tempst P, Coadwell J and Hawkins PT (1998) Protein kinase B kinases that mediate phosphatidylinositol 3,4,5-trisphosphate-dependent activation of protein kinase B. *Science* **279**:710-714.
- Stokoe D, Stephens LR, Copeland T, Gaffney PR, Reese CB, Painter GF, Holmes AB, McCormick F and Hawkins PT (1997) Dual role of phosphatidylinositol-3,4,5-trisphosphate in the activation of protein kinase B. *Science* **277**:567-570.
- Subramaniam S and Unsicker K (2010) ERK and cell death: ERK1/2 in neuronal death. *FEBS J* **277**:22-29.
- Summy JM, Sudol M, Eck MJ, Monteiro AN, Gatesman A and Flynn DC (2003) Specificity in signaling by c-Yes. *Front Biosci* **8**:s185-205.
- Sun HS, Jackson MF, Martin LJ, Jansen K, Teves L, Cui H, Kiyonaka S, Mori Y, Jones M, Forder JP, Golde TE, Orser BA, Macdonald JF and Tymianski M (2009) Suppression of hippocampal TRPM7 protein prevents delayed neuronal death in brain ischemia. *Nat Neurosci* **12**:1300-1307.
- Sun L, Wu Z, Baba M, Peters C, Uchiyama Y and Nakanishi H (2010) Cathepsin B-dependent motor neuron death after nerve injury in the adult mouse. *Biochem Biophys Res Commun* **399**:391-395.
- Susin SA, Zamzami N, Castedo M, Hirsch T, Marchetti P, Macho A, Daugas E, Geuskens M and Kroemer G (1996) Bcl-2 inhibits the mitochondrial release of an apoptogenic protease. *J Exp Med* **184**:1331-1341.
- Sweis RF, Pliushchev M, Brown PJ, Guo J, Li F, Maag D, Petros AM, Soni NB, Tse C, Vedadi M, Michaelides MR, Chiang GG and Pappano WN (2014) Discovery and development of potent and selective inhibitors of histone methyltransferase g9a. *ACS medicinal chemistry letters* **5**:205-209.

- Sykora C, Hoffmann R and Hoffmann P (2007) Enrichment of multiphosphorylated peptides by immobilized metal affinity chromatography using Ga(III)- and Fe(III)-complexes. *Protein and peptide letters* **14**:489-496.
- Szydlowska K and Tymianski M (2010) Calcium, ischemia and excitotoxicity. *Cell Calcium* **47**:122-129.
- Takadera T, Fujibayashi M, Koriyama Y and Kato S (2012) Apoptosis Induced by Src-Family Tyrosine Kinase Inhibitors in Cultured Rat Cortical Cells. *Neurotox Res* **21**:309-316.
- Takahashi H, Shin Y, Cho SJ, Zago WM, Nakamura T, Gu Z, Ma Y, Furukawa H, Liddington R, Zhang D, Tong G, Chen HS and Lipton SA (2007) Hypoxia enhances S-nitrosylation-mediated NMDA receptor inhibition via a thiol oxygen sensor motif. *Neuron* **53**:53-64.
- Takahashi H, Xia P, Cui J, Talantova M, Bodhinathan K, Li W, Holland EA, Tong G, Pina-Crespo J, Zhang D, Nakanishi N, Larrick JW, McKercher SR, Nakamura T, Wang Y and Lipton SA (2015) Pharmacologically targeted NMDA receptor antagonism by NitroMemantine for cerebrovascular disease. *Sci Rep* **5**:14781.
- Takasu MA, Dalva MB, Zigmond RE and Greenberg ME (2002) Modulation of NMDA receptor-dependent calcium influx and gene expression through EphB receptors. *Science* **295**:491-495.
- Talantova M, Sanz-Blasco S, Zhang X, Xia P, Akhtar MW, Okamoto S, Dziewczapolski G, Nakamura T, Cao G, Pratt AE, Kang YJ, Tu S, Molokanova E, McKercher SR, Hires SA, Sason H, Stouffer DG, Buczynski MW, Solomon JP, Michael S, Powers ET, Kelly JW, Roberts A, Tong G, Fang-Newmeyer T, Parker J, Holland EA, Zhang D, Nakanishi N, Chen HS, Wolosker H, Wang Y, Parsons LH, Ambasudhan R, Masliah E, Heinemann SF, Pina-Crespo JC and Lipton SA (2013) Abeta induces astrocytic glutamate release, extrasynaptic NMDA receptor activation, and synaptic loss. *Proc Natl Acad Sci U S A* **110**:E2518-2527.
- Tan YW, Zhang SJ, Hoffmann T and Bading H (2012) Increasing levels of wild-type CREB up-regulates several activity-regulated inhibitor of death (AID) genes and promotes neuronal survival. *BMC Neurosci* **13**:48.
- Tang LJ, Li C, Hu SQ, Wu YP, Zong YY, Sun CC, Zhang F and Zhang GY (2012) S-nitrosylation of c-Src via NMDAR-nNOS module promotes c-Src activation and NR2A phosphorylation in cerebral ischemia/reperfusion. *Molecular and cellular biochemistry* **365**:363-377.
- Taus T, Kocher T, Pichler P, Paschke C, Schmidt A, Henrich C and Mechtler K (2011) Universal and confident phosphorylation site localization using phosphoRS. *J Proteome Res* **10**:5354-5362.
- Thingholm TE, Jensen ON and Larsen MR (2009) Analytical strategies for phosphoproteomics. *Proteomics* **9**:1451-1468.
- Thingholm TE, Jorgensen TJ, Jensen ON and Larsen MR (2006) Highly selective enrichment of phosphorylated peptides using titanium dioxide. *Nat Protoc* **1**:1929-1935.

- Thompson A, Schafer J, Kuhn K, Kienle S, Schwarz J, Schmidt G, Neumann T, Johnstone R, Mohammed AK and Hamon C (2003) Tandem mass tags: a novel quantification strategy for comparative analysis of complex protein mixtures by MS/MS. *Analytical chemistry* **75**:1895-1904.
- Tremper-Wells B and Vallano ML (2005) Nuclear calpain regulates Ca²⁺-dependent signaling via proteolysis of nuclear Ca²⁺/calmodulin-dependent protein kinase type IV in cultured neurons. *J Biol Chem* **280**:2165-2175.
- Trotman LC, Wang X, Alimonti A, Chen Z, Teruya-Feldstein J, Yang H, Pavletich NP, Carver BS, Cordon-Cardo C, Erdjument-Bromage H, Tempst P, Chi SG, Kim HJ, Misteli T, Jiang X and Pandolfi PP (2007) Ubiquitination regulates PTEN nuclear import and tumor suppression. *Cell* **128**:141-156.
- Tsujinaka T, Kajiwara Y, Kambayashi J, Sakon M, Higuchi N, Tanaka T and Mori T (1988) Synthesis of a new cell penetrating calpain inhibitor (calpeptin). *Biochem Biophys Res Commun* **153**:1201-1208.
- Tu W, Xu X, Peng L, Zhong X, Zhang W, Soundarapandian MM, Balel C, Wang M, Jia N, Lew F, Chan SL, Chen Y and Lu Y (2010) DAPK1 interaction with NMDA receptor NR2B subunits mediates brain damage in stroke. *Cell* **140**:222-234.
- Tymianski M, Charlton MP, Carlen PL and Tator CH (1993) Source specificity of early calcium neurotoxicity in cultured embryonic spinal neurons. *J Neurosci* **13**:2085-2104.
- Um JW, Kaufman AC, Kostylev M, Heiss JK, Stagi M, Takahashi H, Kerrisk ME, Vortmeyer A, Wisniewski T, Koleske AJ, Gunther EC, Nygaard HB and Strittmatter SM (2013) Metabotropic glutamate receptor 5 is a coreceptor for Alzheimer abeta oligomer bound to cellular prion protein. *Neuron* **79**:887-902.
- Um JW and Strittmatter SM (2013) Amyloid-beta induced signaling by cellular prion protein and Fyn kinase in Alzheimer disease. *Prion* **7**:37-41.
- Umemori H, Ogura H, Tozawa N, Mikoshiba K, Nishizumi H and Yamamoto T (2003) Impairment of N-methyl-D-aspartate receptor-controlled motor activity in LYN-deficient mice. *Neuroscience* **118**:709-713.
- Vauzour D, Pinto JT, Cooper AJ and Spencer JP (2014) The neurotoxicity of 5-S-cysteinyldopamine is mediated by the early activation of ERK1/2 followed by the subsequent activation of ASK1/JNK1/2 proapoptotic signalling. *Biochem J* **463**:41-52.
- Vivanco I and Sawyers CL (2002) The phosphatidylinositol 3-Kinase AKT pathway in human cancer. *Nature reviews Cancer* **2**:489-501.
- Vosler PS, Brennan CS and Chen J (2008) Calpain-mediated signaling mechanisms in neuronal injury and neurodegeneration. *Mol Neurobiol* **38**:78-100.
- Wada T, Nakagawa K, Watanabe T, Nishitai G, Seo J, Kishimoto H, Kitagawa D, Sasaki T, Penninger JM, Nishina H and Katada T (2001) Impaired synergistic activation of stress-activated protein kinase SAPK/JNK in mouse embryonic stem cells

- lacking SEK1/MKK4: different contribution of SEK2/MKK7 isoforms to the synergistic activation. *J Biol Chem* **276**:30892-30897.
- Wang HG, Pathan N, Ethell IM, Krajewski S, Yamaguchi Y, Shibasaki F, McKeon F, Bobo T, Franke TF and Reed JC (1999) Ca²⁺-induced apoptosis through calcineurin dephosphorylation of BAD. *Science* **284**:339-343.
- Wang J, Liu S, Fu Y, Wang JH and Lu Y (2003) Cdk5 activation induces hippocampal CA1 cell death by directly phosphorylating NMDA receptors. *Nat Neurosci* **6**:1039-1047.
- Wang Y, Briz V, Chishti A, Bi X and Baudry M (2013) Distinct roles for mu-calpain and m-calpain in synaptic NMDAR-mediated neuroprotection and extrasynaptic NMDAR-mediated neurodegeneration. *J Neurosci* **33**:18880-18892.
- Wang Y, Dawson VL and Dawson TM (2009a) Poly(ADP-ribose) signals to mitochondrial AIF: a key event in parthanatos. *Exp Neurol* **218**:193-202.
- Wang Y, Kim NS, Haince JF, Kang HC, David KK, Andrabi SA, Poirier GG, Dawson VL and Dawson TM (2011) Poly(ADP-ribose) (PAR) binding to apoptosis-inducing factor is critical for PAR polymerase-1-dependent cell death (parthanatos). *Sci Signal* **4**:ra20.
- Wang Y, Kim NS, Li X, Greer PA, Koehler RC, Dawson VL and Dawson TM (2009b) Calpain activation is not required for AIF translocation in PARP-1-dependent cell death (parthanatos). *J Neurochem* **110**:687-696.
- White BC, Sullivan JM, DeGracia DJ, O'Neil BJ, Neumar RW, Grossman LI, Rafols JA and Krause GS (2000) Brain ischemia and reperfusion: molecular mechanisms of neuronal injury. *Journal of the neurological sciences* **179**:1-33.
- Wilson MB, Schreiner SJ, Choi HJ, Kamens J and Smithgall TE (2002) Selective pyrrolo-pyrimidine inhibitors reveal a necessary role for Src family kinases in Bcr-Abl signal transduction and oncogenesis. *Oncogene* **21**:8075-8088.
- Wu GY, Deisseroth K and Tsien RW (2001) Activity-dependent CREB phosphorylation: convergence of a fast, sensitive calmodulin kinase pathway and a slow, less sensitive mitogen-activated protein kinase pathway. *Proc Natl Acad Sci U S A* **98**:2808-2813.
- Wu HY, Tomizawa K, Oda Y, Wei FY, Lu YF, Matsushita M, Li ST, Moriwaki A and Matsui H (2004) Critical role of calpain-mediated cleavage of calcineurin in excitotoxic neurodegeneration. *J Biol Chem* **279**:4929-4940.
- Wu PR, Tsai PI, Chen GC, Chou HJ, Huang YP, Chen YH, Lin MY, Kimchi A, Chien CT and Chen RH (2011) DAPK activates MARK1/2 to regulate microtubule assembly, neuronal differentiation, and tau toxicity. *Cell Death Differ* **18**:1507-1520.
- Wu Z, Puigserver P, Andersson U, Zhang C, Adelmant G, Mootha V, Troy A, Cinti S, Lowell B, Scarpulla RC and Spiegelman BM (1999) Mechanisms controlling mitochondrial biogenesis and

- respiration through the thermogenic coactivator PGC-1. *Cell* **98**:115-124.
- Xing H, Kornfeld K and Muslin AJ (1997) The protein kinase KSR interacts with 14-3-3 protein and Raf. *Curr Biol* **7**:294-300.
- Xiong ZG, Zhu XM, Chu XP, Minami M, Hey J, Wei WL, MacDonald JF, Wemmie JA, Price MP, Welsh MJ and Simon RP (2004) Neuroprotection in ischemia: blocking calcium-permeable acid-sensing ion channels. *Cell* **118**:687-698.
- Xu J, Kurup P, Zhang Y, Goebel-Goody SM, Wu PH, Hawasli AH, Baum ML, Bibb JA and Lombroso PJ (2009) Extrasynaptic NMDA receptors couple preferentially to excitotoxicity via calpain-mediated cleavage of STEP. *J Neurosci* **29**:9330-9343.
- Xu W, Wong TP, Chery N, Gaertner T, Wang YT and Baudry M (2007) Calpain-mediated mGluR1alpha truncation: a key step in excitotoxicity. *Neuron* **53**:399-412.
- Yaffe MB (2002) How do 14-3-3 proteins work?-- Gatekeeper phosphorylation and the molecular anvil hypothesis. *FEBS letters* **513**:53-57.
- Yamada KH, Kozlowski DA, Seidl SE, Lance S, Wieschhaus AJ, Sundivakkam P, Tiruppathi C, Chishti I, Herman IM, Kuchay SM and Chishti AH (2012) Targeted gene inactivation of calpain-1 suppresses cortical degeneration due to traumatic brain injury and neuronal apoptosis induced by oxidative stress. *J Biol Chem* **287**:13182-13193.
- Yamaguchi A, Tamatani M, Matsuzaki H, Namikawa K, Kiyama H, Vitek MP, Mitsuda N and Tohyama M (2001) Akt activation protects hippocampal neurons from apoptosis by inhibiting transcriptional activity of p53. *J Biol Chem* **276**:5256-5264.
- Yamashima T, Kohda Y, Tsuchiya K, Ueno T, Yamashita J, Yoshioka T and Kominami E (1998) Inhibition of ischaemic hippocampal neuronal death in primates with cathepsin B inhibitor CA-074: a novel strategy for neuroprotection based on 'calpain-cathepsin hypothesis'. *Eur J Neurosci* **10**:1723-1733.
- Yang DD, Kuan CY, Whitmarsh AJ, Rincon M, Zheng TS, Davis RJ, Rakic P and Flavell RA (1997) Absence of excitotoxicity-induced apoptosis in the hippocampus of mice lacking the Jnk3 gene. *Nature* **389**:865-870.
- Yano S, Tokumitsu H and Soderling TR (1998) Calcium promotes cell survival through CaM-K kinase activation of the protein-kinase-B pathway. *Nature* **396**:584-587.
- Yip-Schneider MT, Miao W, Lin A, Barnard DS, Tzivion G and Marshall MS (2000) Regulation of the Raf-1 kinase domain by phosphorylation and 14-3-3 association. *Biochem J* **351**:151-159.
- Yu SW, Wang Y, Frydenlund DS, Ottersen OP, Dawson VL and Dawson TM (2009) Outer mitochondrial membrane localization of apoptosis-inducing factor: mechanistic implications for release. *ASN Neuro* **1**.
- Zerangue N and Kavanaugh MP (1996) Flux coupling in a neuronal glutamate transporter. *Nature* **383**:634-637.

- Zhang S, Taghibiglou C, Girling K, Dong Z, Lin SZ, Lee W, Shyu WC and Wang YT (2013) Critical role of increased PTEN nuclear translocation in excitotoxic and ischemic neuronal injuries. *J Neurosci* **33**:7997-8008.
- Zhang SJ, Buchthal B, Lau D, Hayer S, Dick O, Schwaninger M, Veltkamp R, Zou M, Weiss U and Bading H (2011) A signaling cascade of nuclear calcium-CREB-ATF3 activated by synaptic NMDA receptors defines a gene repression module that protects against extrasynaptic NMDA receptor-induced neuronal cell death and ischemic brain damage. *J Neurosci* **31**:4978-4990.
- Zhang SJ, Steijaert MN, Lau D, Schutz G, Delucinge-Vivier C, Descombes P and Bading H (2007) Decoding NMDA receptor signaling: identification of genomic programs specifying neuronal survival and death. *Neuron* **53**:549-562.
- Zhang SJ, Zou M, Lu L, Lau D, Ditzel DA, Delucinge-Vivier C, Aso Y, Descombes P and Bading H (2009) Nuclear calcium signaling controls expression of a large gene pool: identification of a gene program for acquired neuroprotection induced by synaptic activity. *PLoS Genet* **5**:e1000604.
- Zhao H, Shimohata T, Wang JQ, Sun G, Schaal DW, Sapolsky RM and Steinberg GK (2005) Akt contributes to neuroprotection by hypothermia against cerebral ischemia in rats. *J Neurosci* **25**:9794-9806.
- Zhao W, Cavallaro S, Gusev P and Alkon DL (2000) Nonreceptor tyrosine protein kinase pp60c-src in spatial learning: synapse-specific changes in its gene expression, tyrosine phosphorylation, and protein-protein interactions. *Proc Natl Acad Sci U S A* **97**:8098-8103.
- Zhao Y, Yang CY and Wang S (2013) The making of I-BET762, a BET bromodomain inhibitor now in clinical development. *Journal of medicinal chemistry* **56**:7498-7500.
- Zheng YL, Amin ND, Hu YF, Rudrabhatla P, Shukla V, Kanungo J, Kesavapany S, Grant P, Albers W and Pant HC (2010) A 24-residue peptide (p5), derived from p35, the Cdk5 neuronal activator, specifically inhibits Cdk5-p25 hyperactivity and tau hyperphosphorylation. *J Biol Chem* **285**:34202-34212.
- Zheng Z and Yenari MA (2004) Post-ischemic inflammation: molecular mechanisms and therapeutic implications. *Neurol Res* **26**:884-892.
- Zhou H, Tian R, Ye M, Xu S, Feng S, Pan C, Jiang X, Li X and Zou H (2007) Highly specific enrichment of phosphopeptides by zirconium dioxide nanoparticles for phosphoproteome analysis. *Electrophoresis* **28**:2201-2215.
- Zhou X, Hollern D, Liao J, Andrechek E and Wang H (2013) NMDA receptor-mediated excitotoxicity depends on the coactivation of synaptic and extrasynaptic receptors. *Cell Death Dis* **4**:e560.
- Zhuang S and Schnellmann RG (2006) A death-promoting role for extracellular signal-regulated kinase. *J Pharmacol Exp Ther* **319**:991-997.















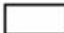



















Appendix I

IPA legends for molecule shapes and relationship types

These legends are copied and reproduced from the following link

<http://www.biolreprod.org/content/suppl/2010/09/29/biolreprod.110.085910.DC1/biolreprod.110.085910-3.pdf>

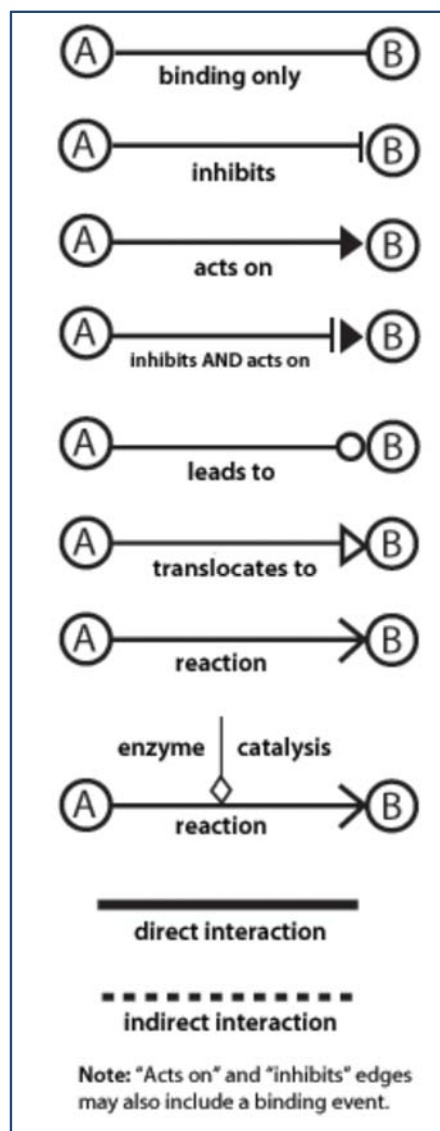
Molecule shapes

Network Shapes	Path Designer Shapes
 Cytokine	 Cytokine / Growth Factor
 Growth Factor	 Drug
 Chemical / Drug/ Toxicant	 Chemical / Toxicant
 Enzyme	 Enzyme
 G-protein Coupled Receptor	 G-protein Coupled Receptor
 Ion Channel	 Ion Channel
 Kinase	 Kinase
 Ligand-dependent Nuclear Receptor	 Ligand-dependent Nuclear Receptor
 Peptidase	 Peptidase
 Phosphatase	 Phosphatase
 Transcription Regulator	 Transcription Regulator
 Translation Regulator	 Translation Regulator
 Transmembrane Receptor	 Transmembrane Receptor
 Transporter	 Transporter
 microRNA	 microRNA
 Complex / Group	 Complex / Group
 Other	 Other

Relationship labels

A Activation
 B Binding
 C Causes/Leads to
 CC Chemical-Chemical interaction
 CP Chemical-Protein interaction
 E Expression (includes metabolism/ synthesis for chemicals)
 EC Enzyme Catalysis
 I Inhibition
 L ProteoLysis (includes degradation for Chemicals)
 LO Localization
 M Biochemical Modification
 MB Group/complex Membership
 P Phosphorylation/Dephosphorylation
 PD Protein-DNA binding
 PP Protein-Protein binding
 PR Protein-RNA binding
 RB Regulation of Binding
 RE Reaction
 RR RNA-RNA Binding
 T Transcription
 TR Translocation

Relationships





Minerva Access is the Institutional Repository of The University of Melbourne

Author/s:

HOQUE, MD ASHFAQUL

Title:

Exploring the signalling mechanism of excitotoxic neuronal injury by molecular and quantitative proteomic approaches

Date:

2016

Persistent Link:

<http://hdl.handle.net/11343/113673>

File Description:

Exploring the signalling mechanism of excitotoxic neuronal injury by molecular and quantitative proteomic approaches